CELL THERAPY FOR ACUTE LIVER INJURY- *IN VIVO* EFFICACY OF MESENCHYMAL STROMAL CELLS IN TOXIC AND IMMUNE-MEDIATED MURINE HEPATITIS

By

MOHAMMED ALFAIFI

A thesis submitted to
The University of Birmingham
for the degree of
DOCTOR OF PHILOSOPHY

Centre of Liver Research
Institute of Immunology and Immunotherapy
School of Medical and Dental Sciences
University of Birmingham
April 2018

Abstract

The ability of umbilical cord-derived mesenchymal stromal cells (UC-MSCs) to immunomodulate offers therapeutic potential in liver injury but the inherent heterogeneity of unsorted MSC populations may explain varied/reduced function as well as posing regulatory challenges. Thus, we aimed to evaluate the therapeutic potential of purified CD362+ MSC infusion in murine models of acute liver injury. UC-MSCs were injected intravenously into mice injured by single dose of Carbon tetrachloride (CCl_4) & OVA-BIL mice. MSC used were either unsorted or sorted CD362+. The extent of liver damage was determined by liver histology, serum analysis, gene expression and FACS analysis 3 or 5 days after cell infusion. Homing and bio-distribution of stem cells was determined by whole mouse cryo-imaging of Q-dot labelled MSC following infusion of UC-MSC into injured mice. $CD362^+$ MSC were as effective as unsorted MSC in ameliorating liver injury, with reductions in serum ALT seen in both models. In contrast heat-inactivated MSC had no effect on liver injury. MSC also led to a reduction in $CD45^+$staining on liver sections in both models of liver injury corroborated by an accompanying reduction in hepatic $CD45^+$ cells in (FACS analysis of liver digest). In addition, there was a significant reduction in hepatic CD19+ B cells in digested liver in CCl_4 injury. $CD362^+$ MSCs were found to have the ability to reduce the level of adhesion molecules (ICAM and VCAM) in Ova-Bil mice. Cryo-imaging of time-course in both animal models indicated that MSC had migrated to the lung within 1 hour and were then cleared rapidly, although there was a liver-specific increase in MSC 2-3 day in Ova-Bil mice. $CD362^+$ human MSC exert potent anti-inflammatory activity in toxic and immune-mediated murine liver injury with demonstrable reductions in infiltrating inflammatory leucocytes and B cells.

This thesis is dedicated to my role models, my father and mother, who always continuously support and encouraging me during the past years in my PhD

Acknowledgments

Thanks to almighty ALLAH for his uncountable blessing and for giving me the strength and patience to complete my thesis successfully, after all the challenges and difficulties.

First and foremost, I would like to express my special thanks to my supervisor professor Philip Newsome, for his supervision, guidance, and for helping me throughout my PhD project. I will always grateful for having the opportunity to study under his supervision. I would also like to thank my second supervisor professor Jon Frampton for his support and giving such thoughtful feedback.

I would like to express my warmest and deepest thanks to my wife, and my kids for their love and support over the past years. They have always been there for me and I am thankful for everything they have made for helping achieved my dreams.

This project would not have been completed without support and motivation from my colleagues at the centre for liver research for their help and assistance. A special thanks to Dr. Vasanthy Vigneswara for her help, training, and friendship throughout my PhD. I would also like to acknowledge other colleagues including Dr. Ngyyet-Thin Luu, Dr. Chris Weston, and Dr. Evaggelia Liaskou for their ideas, help, and good humour.

Lastly, a thank you to the government of Saudi Arabia, the Saudi Arabian Cultural Bureau in UK, and King Khalid University for offering me the scholarship to continue my studies and supporting me morally and materially.

Publications

Alfaifi, M., Eom, Y.W., Newsome, P.N., et al. (2018) Mesenchymal stromal cell therapy for liver diseases. *Journal of hepatology*.

Table of Contents

List of Figures

INTRODUCTION

MATERIALS AND METHODS

CHARACTERIZATION OF MESENCHYMAL STROMAL CELLS DERIVED FROM UMBILICAL CORD TISSUE

TIME COURSE OF LIVER INJURY AFTER ACUTE HEPATOTOXIN EXPOSURE TO CCL_4

THE ANTI-INFLAMMATORY ROLE OF UMBILICAL CORD-DERIVED MESENCHYMAL STROMAL CELLS IN MICE WITH ACUTE LIVER INJURY

IN VIVO EFFICACY OF HUMAN UMBILICAL CORD MSCS IN THE OVA-BIL MOUSE MODEL OF ALLOIMMUNE LIVER INJURY

IN VIVO TRACKING AND MONITORING OF THE HOMING OF INTRAVENOUS UMBILICAL CORD MESENCHYMAL STROMAL CELLS

List of Tables

INTRODUCTION

MATERIALS AND METHODS

CHARACTERIZATION OF MESENCHYMAL STROMAL CELLS DERIVED FROM UMBILICAL CORD TISSUE

Abbreviations

MSC	Mesenchymal Stem Cell
UC	Umbilical cord
UCB	Umbilical cord blood
SYN	Synovium
AT	Adipose tissue
AP	Umbilical perivascular
α-MEM	α-modified Minimum Essential Media
ACI	Autologous chondrocyte implantation
AIH	Autoimmune hepatitis
LFT	Liver function test
ALP	Alkaline phosphatase
ALT	Alanine transaminase
APC	Antigen presenting cell
HBV	Hepatitis B virus
BCV	Hepatitis C virus
HCC	Hepatocellular carcinoma
PBC	Primary biliary cirrhosis
BM	Bone marrow
CCl_4	Carbon tetrachloride
CFU-F	Colony forming unit-fibroblastic
CM	Conditioned medium
Col1	Collagen type I
Col2	Collagen type II
ConA	Concanavalin A
DAB	3,3'--Diaminobenzidine
DMB	Dimethyl methylene blue
DMEM	Dulbecco’s Modified Eagle Medium
ECM	Extracellular matrix
EGF	Epidermal growth factor
ELISA	Enzyme--linked immunosorbent assay
FACS	Fluorescence activated cell sorting
FBS	Fetal bovine serum
FC	Flow Cytometry
FFPE	Formalin-fixed Paraffin-embedded tissue
FGF	Fibroblast growth factor
GF	Growth factor
GvHD	Graft-versus-host disease
HBSS	Hank’s Balanced Salt Solution
HGF	Hepatocyte growth factor
HLA	Human Leukocyte Antigen

HRP	Horse radish peroxidase
HSC	Haematopoietic stem cell
IDO	Indoleamine 2,3 dioxygenase
IFNγ	Interferon-γ
IGF	Insulin-like growth factor
IHC	Immunohistochemistry
IL	Interleukin
IMC	Isotype matched control
iNOS	Inducible nitric oxide synthase
IP	Intraperitoneal infusion
IV	Intravenous infusion
SC	Subcutaneous
ISCT	International Society for Cellular Therapy
LPS	Lipopolysaccharide
MACS	Magnetic activated cell sorting
MHC	Major histocompatibility antigens
MI	Myocardial infarction
MMP	Matrix metalloproteinase
NK	Natural killer
NO	Nitric oxide
OVA	Ovalbumin
P	Passage number
PBC	Primary biliary cirrhosis
PSC	Primary sclerosing cholangitis
PBS-T	PBS+0.05% Tween
PGE2	Prostaglandin E2
PSG	Penicillin/Streptomycin/Glutamine
RPMI	Roswell Park Memorial Institute medium
Sca-1	Stem cell antigen 1
SDF-1	Stromal derived factor 1
TBS-T	Tris-buffered saline + 0.1% Tween20
TGF-β	Transforming growth factor beta
TNFα	Tumour necrosis factor alpha
Treg	Regulatory T cells
VEGF	Vascular endothelial growth factor
RPM	Round per minute
RCF	Relative centrifugal force
ITS	insulin-transferrin-selenium
BMSU	Biomedical Service Unit
TBARS	Thiobarbituric acid reactive substances
PCR	Polymerase chain reactions
ROS	Reactive oxygen species
NOS2	Nitric oxide synthase

GSS	Glutathione synthetase
HO-1	Heme oxygenase 1
HIF1-α	Hypoxia-inducible factor 1-alpha
SOD	Super oxide dismutase
CAT	Catalase
MRI	Magnetic resonance imaging
IVIS	*In vivo* imaging system
Qdots	Quantum dots
OCT	Optimal cutting temperature
ALDH	Aldehyde dehydrogenase
Sro-1	Stromal precursor antigen-1
EDTA	Ethylenediaminetetraacetic acid
TBS	Tris buffered saline
TUNEL	deoxynucleotidyl transferase-mediated biotinylated- dUTP nick-end labeling
cDNA	Complementary DNA
Ct	Cycle threshold

CHAPTER 1

INTRODUCTION

1.1 The Liver

1.1.1 Introduction to the human liver

The liver is the largest internal organ and plays a significant role in many of the metabolic processes in the body. The human liver consists of several lobes and weighs about 2% of the total body weight, and about 5% in the case of a mouse (Arias et al., 2009). The liver is located on the right side of the abdominal cavity under the right lower rib, and has two separate blood supplies (Iwakiri et al., 2008), consisting of both arterial and venous hepatic blood vessels. The hepatic artery supplies and provides oxygenated blood to the liver and the hepatic portal vein provides blood rich in nutrients from the intestine, stomach, and spleen to the liver (Arias et al., 2009).

1.1.2 Liver structure and function

The human liver is composed of several types of cells, the majority of which are hepatocytes, which represent about 90% of the total weight of the liver. The other cells that are present in the liver are stellate and endothelial cells, blood vessels, bile duct epithelial cells, Kupffer cells, macrophages, and different phenotypes of lymphocyte cells (Szabo and Petrasek, 2015). At the microscopic level, hepatic lobules represent the functional unit of the liver (Braet and Wisse, 2002). Hepatic lobules have a vein at the center of each lobule, with a portal area at the borders. The portal area of the liver consists of a portal vein, hepatic artery and a bile duct (Figure 1-1). As mentioned above, the liver plays a vital role in many of the metabolic functions in the human body. The main functions are: 1) Metabolism of amino acids, proteins, carbohydrates, hormones,

bilirubin, bile acid, and lipids, and the synthesis of serum proteins, such as albumin, coagulation factors, and growth factors; 2) Storage of glycogen and some essential nutrients, such as vitamins and minerals; and 3) Breakdown and detoxification of xenobiotic substances and ammonia (Taub, 2004).

A

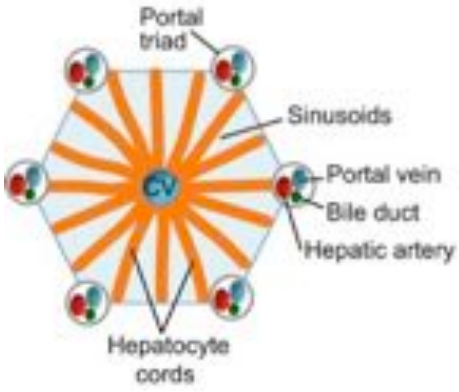

B

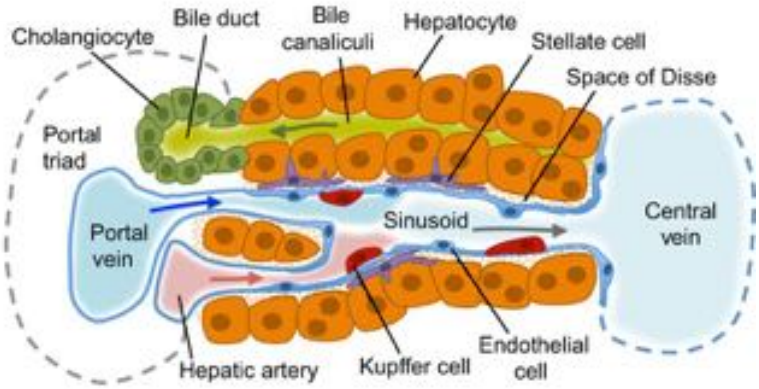

Figure 1-1 Schematic overview of hepatic architecture. A) Representative image of hepatic lobules, which are the functional unit of the liver. B) Overview of the content of the cells between each lobule. Blood flows through the hepatic vein and hepatic arteries towards the central vein. Bile produced by the hepatocytes collects in the bile duct, which is surrounded by cell cholangiocytes. Liver macrophage cells line the sinusoid area and are known as Kupffer cells. Stellate cells are fibroblast-like cells located between hepatocytes and sinusoids. (Figure taken from Gordillo et al., 2015).

1.1.3 Liver immunology

The liver represents one of the most complex systems in both normal and pathological conditions. In addition to its main metabolic function, the liver is also responsible for several immunological functions, such as producing chemokines and cytokines, which are essential in liver homeostasis (Racanelli and Rehermann, 2006).

From anatomical point of view, liver is continuously exposed to nutrients and microbial antigen derived from the gut microbiota, which therefore trigger the immune system through formation of bacterial endotoxin. Thus, the liver microenvironment showed to have more risk of immune activation comparing with other organs in the body and must have capacity to tolerate this immunogenic load. The liver is the only organ in the body with unique function in terms of antigen presentations. The liver immune response can be triggered by different resident cells with specialized function such as the sinusoidal endothelial cells as well as kupffer cells (intravascular liver resident macrophages). Both cells were able to produce different cytokine and chemokines and more importantly capable of antigen presentation. On the other hand, the hepatic parenchymal cells, mainly hepatocyte and cholangiocytes have reported to expressed different Toll-like receptor which make them act as primary sensor for activation the immune system (Heymann and Tacke, 2016).

Local resident macrophages in the liver (kupffer cells) have found to have potential function in liver homeostasis, they represent the major source of secretion IL-10 cytokines following LPA activations as well as express of PD-L1. In addition, hepatic resident kupffer cells have potential role in respond to the bacterial endotoxin derived

from the gut microbiota by releasing IL-10 and prostaglandins (Callery et al., 1991). They also capable of recruit more monocyte into the liver, which later formed or polarized into more regulatory dendritic cells. Moreover, during homeostasis kupffer cells have shown to induce regulatory T cells (Treg) in a mouse model following systemic induction of particular antigen. Kupffer cells specifically interact with T cells antigen and expand IL10 expressing T reg cells which therefore enhance the tissue protective function (Heymann et al., 2015). Additionally, in an *in vitro* experiment, purified kupffer cells have the ability to induce the Treg by secretion of prostaglandin (PG) E_2 (You et al., 2008).

Dendritic cells (DCs) are normally located in the portal area and around the central vein in the heathy liver and believed to form immunomodulatory function rather than immunogenic (Eckert et al., 2015). In a steady state condition, these cells have the ability to migrated from the liver tissue to the lymphoid organs where they act to present the antigens to T cells. More interestingly, it has been shown that the DCs isolated from the liver have immature phenotype as they found to have low expression profile of MHC-11 and some so-stimulatory molecules such as CD40 and CD80 (Tiegs and Lohse, 2010). This feature of hepatic DCs make them different from other DCs in other organs with unique immune tolerogenic function. One primary function of hepatic CDs is stimulate production of IL-10 which have a direct effect to generate regulatory T cells (Bamboat et al., 2009). In addition, Natural killer T (NKT) cells show sign of contribution in liver homeostasis by interacting with the hepatic endothelium. NKT cells function in the liver found to be directed by CXCL16 which secreted from the sinusoidal endothelial cells and kupffer cells (Geissmann et al., 2005).

In general, hepatic homeostasis and inflammation are regulated within the cells from different liver microenvironment.

The inflammation system, for example, is triggered through different pathogens, viruses or toxic products, and subsequently enhances the response from the immune system. In addition, damaged cells in the liver can stimulate inflammatory cytokines, which can initiate and recruit more immune cells to protect injured cells and initiate a regenerative process (Tilg et al., 2006). However, the liver has limited ability to clear toxicity and other dangerous triggers, which leads to the development of pathological inflammation and causes damage to liver homeostasis (Robinson et al., 2016).

Following the development of hepatic inflammation, macrophages from the liver secrete various chemokines and cytokines, which contribute to the activation of other signalling pathways and recruit more immune cells (Tacke and Zimmermann, 2014). For example, hepatic macrophages secrete CXC16, which is correlated with enhanced recruitment of natural killer (NK) cells and, markedly, with the activation of more pro-inflammatory activities (Wehr et al., 2013). Activated hepatic macrophages have also been proposed to increase the expression of matrix metalloproteinases, in particular, MMP-9 and MMP12, which have been found to be involved in matrix degradation. In experimental models of liver injury, two distinct populations were reported in mouse liver with different effects in response to liver inflammation: M1 macrophages were found to mediate the liver injury, whereas M2 had superior therapeutic functions in reducing liver inflammation (Possamai et al., 2014). In general, infiltrating monocytes and hepatic macrophages have not only demonstrated an essential role in liver homeostasis and immunity, but also have

an effect on liver pathological inflammation. Accordingly, more intervention strategies regarding their origins and further potential functions are in need of further investigation.

The adaptive immune system has been shown to have a vital role in the regulation of liver inflammation. Different types of T lymphocytes have been studied in the literature, including CD4, CD8 and regulatory T cells (Tregs). In particular, CD4 cells are characterized and been found to have several populations with different biological functions. Tregs were found to suppress inflammation, but other CD4 subsets, such as type 1 helper T cells (Th1), Th2 and Th17, tend to stimulate the adaptive and innate immune responses (Shuai et al., 2016). In addition, CD8 T cells were found to show some protective immune response. However, the same cells were also found to be activated in the local microenvironment by antigen-presenting cells (APCs) and to mediate the autoimmune process in the liver (Derkow et al., 2007). In general, the adaptive immune response has a very important role in liver inflammation and is mediated by different factors that are related to the pathology of the specific conditions of liver diseases.

1.1.4 Oxidative stress and liver diseases

Oxidative stress has been reported to play a critical role in the pathogenesis of many conditions due to the overproduction of reactive oxygen species (ROS) (Poli, 2000). Free radicals may have a beneficial role in normal metabolism, as they attach to foreign molecules, such as bacteria and pathogens, and have been reported to activate signalling pathways (Li et al., 2015). However, the balance between ROS and antioxidants is essential for normal physiological function. Under different conditions, such as hypoxia and inflammation, ROS levels can exceed the level of antioxidants, leading to an

imbalance in tissue levels in terms of oxidative stress and consequently generate tissue injury (Shimizu et al., 2012).

Several studies have implicated ROS in liver disease. For example, the accumulation of ROS represents the main cause of alcoholic liver disease (ALD) (Li et al., 2015). Chronic consumption of ethanol can induce early damage in mitochondria due to the formation of ROS (Mantena et al., 2008; Bailey and Cunningham, 2002). The same finding was reported *in vivo* in rats fed long term with ethanol; hepatocytes from the control and treated groups were isolated and ROS levels increased in the treatment group, with hepatocyte damage and apoptosis (Nassir and Ibdah, 2014). These findings indicate that the free radicals formed during oxidative stress may play a significant role in liver injury. Many studies have illustrated the ability of mesenchymal stromal cells (MSCs) to modulate the immune system but the mechanism behind the effect of MSC on immune cells remains unclear, particularly their action in liver damage. Moreover, the impact of MSCs on oxidative stress is unclear.

1.2 Animal Models for the Study of Acute Liver Injury

Various investigations have developed different animal models for the study of liver diseases. Animal models have an important role in the study of biology, as well as the effectiveness of different treatments of various conditions related to human diseases. However, due to some limitations in various animal models of liver disease, a process has been undertaken to develop more reliable and accurate animal models to reflect the pathological features of human diseases.

In acute liver injury, most animal models are based on injecting hepatotoxic chemicals or through surgery to induce hepatic ischemia (Tuñón et al., 2009). Hepatotoxic chemicals have been intensively reported in the literature in investigations of acute liver injury, as well as chronic liver injury. The main chemical agents used in animal models of liver injury are acetaminophen (paracetamol), carbon tetrachloride (CCl_4), thioacetamide (TAA), and concanavalin A (Con A) (Rahman and Hodgson, 2000). Acetaminophen has been shown to develop hepatotoxicity in humans as well as in experimental animals following the consumption of high doses (Bajt et al., 2003). This hepatotoxicity results in mitochondrial dysfunction, the formation of ROS, and a reduction in antioxidant enzymes (Rivera et al., 2017). It has been shown that toxicity caused by acetaminophen is mediated by the activation of P450 enzymes and c-Jun N-terminal kinases (JNK), which induce apoptosis in liver hepatocytes (Hur et al., 2012).

CCl_4 is another hepatotoxic substance that is used to induce liver injury in mice. CCl_4 is metabolized in the liver and activated by cytochrome P450 (Noguchi et al., 1982). This step causes reduction in one electron from the CCL_4 and forms a highly reactive radical known as trichloromethylperoxyl (CCl_3*) (Packer et al., 1978). These free radicals cause lipid peroxidation and consequently exacerbate cell membrane damage (Basu, 2003). CCl_4 can also induce liver inflammation by activating macrophages to produce inflammatory cytokines, such as interleukin (IL)-6 and IL-10 (Kovalovich et al., 2000). CCl_4 can also cause mitochondrial dysfunction *in vivo* - this finding was observed after chronic treatment of CCl_4 for 6 weeks, which resulted in mitochondrial DNA damage with a reduction in glutathione level (Mitchell et al., 2009b). In addition, a recent study reported that a single dose of CCl_4 can induce early alteration in mitochondrial DNA with

elevation in lipid peroxidation in mouse liver (Knockaert et al., 2012). The induction of rat hepatocyte apoptosis has also been reported after the administration of CCl_4, which augments the necrosis of hepatocytes (Shi et al., 1998a).

Injecting Con A has also been used to induce acute liver injury in several preclinical studies and was consequently found to enhance the destruction of hepatocytes and develop liver injury. The mechanism which caused this injury is related to increased activity of macrophages and $CD4^+$ cells in the liver microenvironment (Tuñón et al., 2009). Consistent with the previous finding, another study has clearly shown that, following induction with Con A, mice were found to have increased activity of T lymphocytes, which released different cytokines to induce hepatic inflammation (Rahman and Hodgson, 2000).

1.3 Mesenchymal Stromal Cells: Definition, Biology, and Origins

MSCs were initially described in 1968 (Friedenstein et al., 1968) and are a subtype of adult fibroblast-like cells that have the capacity to self-renew with high proliferative ability. MSCs can undergo tri-lineage differentiation both *in vivo* and *in vitro* down connective tissue lineages to become osteoblasts, chondrocytes and adipocytes.

MSCs are plastic adherent cells originally identified and isolated from bone marrow but, due to their limited number (0.01 to 0.001% of total bone marrow cells) (Gronthos et al., 2003) and the invasive nature of their isolation from bone marrow, researchers have explored alternative sources. Several studies have reported the successful isolation of MSCs from different tissues with similar *in vitro* properties, including synovial

membrane (De Bari et al., 2001), adipose tissue (AT) (Zuk et al., 2001), umbilical cord blood (UCB) (Lee et al., 2004b), amniotic fluid (AF) (Antonucci et al., 2011) and placenta (He et al., 2017). Umbilical cord (UC) tissue has been a particularly promising source of MSCs, as the cells can be isolated from several compartments within the UC, including the umbilical vein, arteries, and perivascular tissue, Wharton's jelly (WJ) and sub-amniotic tissue. Furthermore, MSCs isolated from UC tissue are believed to be more primitive than other cells isolated from other tissues and are found in higher numbers, ensuring this source is now gaining prominence. Notably, MSCs from various sources display a similar expression profile to MSC surface markers and have similar morphological features in culture. However, MSCs from different sources have demonstrated different levels of tri-lineage differentiation potential (Baksh et al., 2007).

In addition, differences have been reported with regard to culture conditions, particularly in the isolation procedure and culturing protocols, as well as the experiment protocol used (Bara et al., 2014). Thus, variations in studies have resulted in significant differences in the functional capabilities of MSCs found *in vivo* and *in vitro*. Direct comparisons of MSCs from different sources have been shown in a variety of studies and these cells have been demonstrated to share similar biological properties (Najar et al., 2010; Mattar and Bieback, 2015). Other authors have demonstrated differences in immunomodulatory properties between menstrual blood (MB)-MSCs, UC-MSCs, and AT-MSCs (Melief et al., 2013b; Chao et al., 2014). In addition to the biological variations between different sources of MSCs, UC-MSCs exhibit more proliferation capacity in comparison with some MSC populations obtained from other sources (Baksh et al., 2007). Despite the controversy in defining MSCs from different sources, these cells have shown great

potential in regenerative medicine. To fulfil the roles of MSCs in tissue regeneration, further progress in understanding the immunomodulatory mechanisms and heterogeneity of MSCs from different sources may provide clues in the future.

1.4 Human Umbilical Cord MSCs (hUC-MSC)

hUC-MSCs represent an attractive source of MSCs for use in clinical studies, as the isolation and collection of cells from umbilical cord does not require an invasive procedure. There are minimal ethical concerns, as UC is a postnatal organ that is usually disposed of as a waste product after delivery (Weiss et al., 2008).

1.5 Anatomy of Umbilical Cord Tissue

In order to understand the differences between MSCs derived from UC tissue and other sources, it is important to understand the anatomical and histological structure of umbilical cord. The UC represents a connection between the mother and the foetus during pregnancy, and its main function is to circulate blood from the placenta to the embryo. The UC is covered by a membrane known as the amniotic epithelium (amnion) and a sub-amniotic zone that grows closely into the central connective tissue of the cord. This connective tissue of the cord is known as Wharton's jelly and has been described in the literature as a cord matrix. Umbilical cord is composed of two arteries and one vein; a zone called the umbilical perivascular region surrounds these vessels (Nanaev et al., 1997). Figure ***1-2*** represents a cross section of human umbilical cord.

Human UC is formed at day 26 of embryonic development and in the fifth week of gestation. Human UC is usually 1–2 cm in diameter and 30–90 cm in length, with an

average of 55 cm (Sarugaser et al., 2005). When the amniotic cavity has expanded and surrounded the embryo, it causes the connective stalk and yolk sac to compress together to form the umbilical cord, which is then covered by the amniotic epithelial membrane and forms the outer layer of the umbilical cord (Baergen, 2013).

As referred to above, the inner tissue structure of the umbilical cord contains two arteries and one vein and is surrounded by Wharton's jelly. The two umbilical arteries carry deoxygenated blood from the foetus to the placenta, while the umbilical vein carries oxygenated blood from the placenta to the foetus (Kellow and Feldstein, 2011). Human umbilical vessels have different characteristics compared with the other major vessels of the human body (Ferguson and Dodson, 2009), having fewer organelles in their endothelial cells compared with the endothelium of other vessels. Moreover, umbilical arteries have no internal elastic membrane and less elastin than other arteries, whilst the vein, by contrast, has an elastic sub-intimal layer (Anthony Armson et al., 2015). Each umbilical vessel is surrounded by bunches of collagen fibers that form a type of adventitia: an elastic muscle-like tissue consisting of muscle cells to support the blood vessels (Jeschke et al., 2011).

Wharton's jelly is the connective tissue of the cord and is derived from the extra-embryonic myoblast which surrounds the embryoblast, lying between the amniotic epithelium and umbilical perivascular region. The main function of WJ is to maintain umbilical vessel strength and flexibility, thus preventing any compression or torsion in the vessels (Can and Karahuseyinoglu, 2007; Troyer and Weiss, 2008).

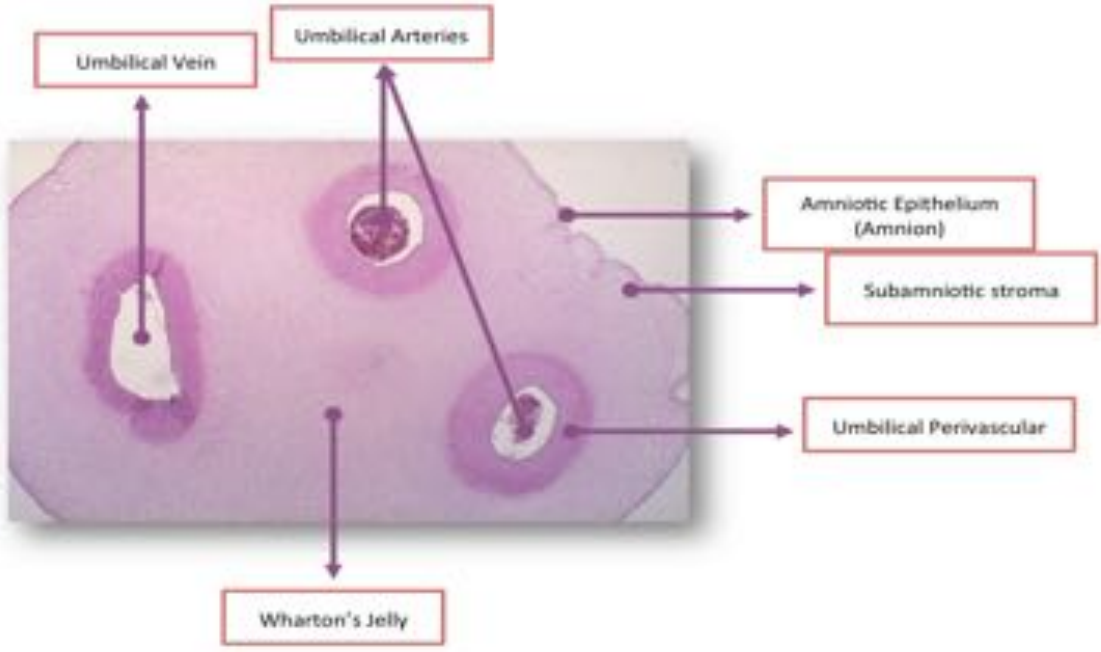

Figure 1-2 Cross section representing the anatomical structure of umbilical cord tissue.

1.6 Isolation of hUC-MSC

MSCs can be isolated from several sources within the UC, such as the umbilical vein, umbilical arteries, umbilical cord perivascular tissue, WJ and sub-amnion layer. The amniotic membrane (amniotic epithelia) is not a source of MSCs, but represents a good source of epithelial cells. However, it has been reported that multipotent epithelial stem cells can be isolated from amniotic membrane isolated from human placenta, but not the umbilical cord (Miki et al., 2005).

MSCs from umbilical cord can be obtained or isolated by different methods. There are two methods for isolating MSCs from UC tissue: (1) the enzymatic digestion method and (2) the explant culture method. The enzymatic digestion method has been used by many groups and uses collagenase either alone or in combination with other enzymes, such as trypsin or hyaluronidase. The other approach, which has been shown to be simpler and

more efficient, is the explant culture method, whereby UC is minced then placed in culture and seeded regularly on a tissue culture flask (Table ***1-1***).

Table 1-1 Human MSC derived from different umbilical cord tissues

Tissue	Source	Method of isolation	Description	References
hUC	Whole UC (No vessels removal or mincing the cord)	Enzymatic	Used an enzymatic cocktail contains collagenase type 1 and hyaluronidase.	*(Tsagias, N. et al, 2011)*
	Wharton's Jelly	Enzymatic & explant	Collagenase and Culture in (DMEM – low glucose +20%FBS+P/S Antibody)	(*Secunda, R. et al, 2014)*
		Enzymatic	Collagenase	*(Wang, H. et al, 2004)*
		Explant	Culture in (∝MEM+10%FBS+P/S Antibody)	*(Ishige, I. et al, 2009)*
	Umbilical Cord Vein	Enzymatic	Collagenase IV	*(Covas, D. et al, 2003)*
		Explant	Culture in (∝MEM+10%FBS+P/S Antibody)	*(Ishige, I. et al, 2009)*
	Umbilical cord Artery	Explant	Culture in (∝MEM+10%FBS+P/S Antibody)	*(Ishige, I. et al, 2009)*
	Perivascular	Enzymatic	Collagenase	*(Sarugaser, R. et al 2005)*

1.7 Phenotypic Characterization of MSCs Isolated from UC Tissue

As described previously, investigators have used different protocols for both the isolation and characterization of human MSCs. As a result, the International Society for Cellular Therapy (ISCT) established minimal criteria for defining human MSCs (Dominici et al., 2006). Dominici et al. summarized three main criteria for defining such cells: (1) MSCs must be adherent in plastic culture using tissue culture flasks; (2) MSCs exhibit surface antigen expression of CD105, CD73, and CD90 by flow cytometric analysis. In addition, these cells should lack expression of CD45, CD34, CD14, CD11b, CD79a, CD19 and HLA class II; and (3) MSCs must be capable of differentiation to adipogenic, osteogenic, and chondrogenic lineages (Dominici et al., 2006). UC-MSCs have been reported widely as being plastic adherent in culture, have the ability to differentiate into chondrogenic, adipogenic, and osteogenic lineages, and express the following surface antigen markers: CD90, CD73, and CD 105 whilst lacking expression of CD45, HLA class II, and CD34

(Secco et al., 2008). Figure 1-3 represents a diagram of the general characteristics of human MSCs.

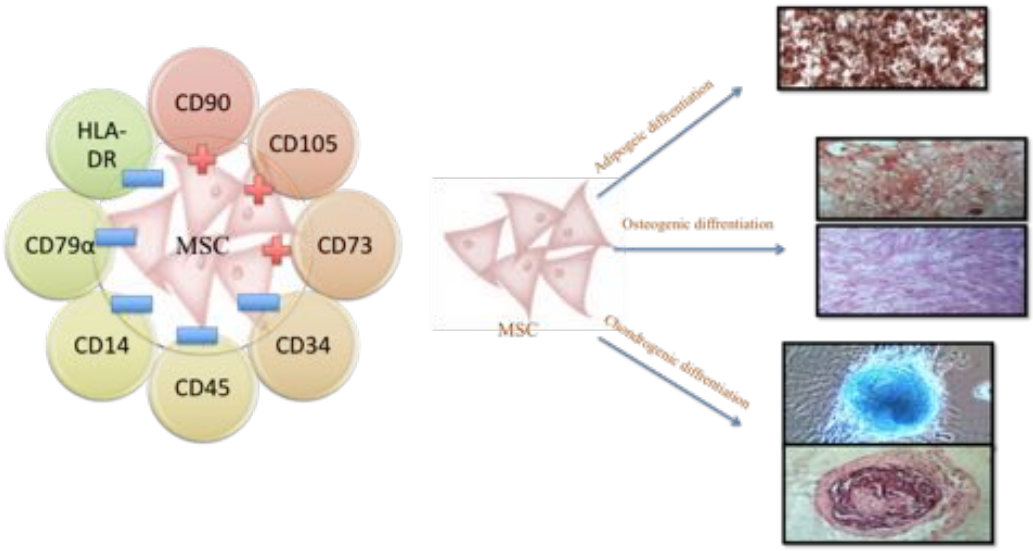

Figure 1-3 Different cell surface antigens expressed on human umbilical cord-derived MSCs.

1.8 UC-MSCs for the Treatment of Liver Diseases

Liver disease is a major cause of mortality and morbidity that is rising globally (Shiels et al., 2017; Williams et al., 2017). There remain many inflammatory liver conditions for which treatments are not effective and such patients will often progress to end-stage liver disease and require liver transplantation. To prevent progression to end-stage liver disease and to treat those with advanced fibrosis, MSC therapies have been considered and shown to have potential in this regard (Zhang and Wang, 2013; Haldar et al., 2016).

MSCs have been shown to have beneficial effects in a range of clinical settings, including heart failure (Ji et al., 2017), lung injury (Matthay et al., 2017), graft-versus-host diseases (GVHD) (Chen et al., 2015), and stroke (Honmou et al., 2012), as well as being reported to ameliorate liver injury in both acute and chronic liver damage (Volarevic et al., 2014; Kuo et al., 2008). The pleiotropic effects of MSCs represent a potential advantage over pharmacological therapies and principally focus on their ability to modulate different components of the immune system, either directly or by the release of paracrine factors. In addition to these immunomodulatory effects, MSCs have been shown to reduce liver injury by ameliorating oxidative stress through the release of antioxidants (Kuo et al., 2008) and through anti-fibrotic effects (Haldar et al., 2016). In addition, MSCs have been reported to have an ability to differentiate to hepatocyte-like cells, which may show promise in augmenting liver regeneration (Xingwei et al., 2009; Campard et al., 2008). Encouraging preclinical data have resulted in a number of clinical trials (Wang et al., 2013b; Zhang et al., 2012b) and it is, therefore, timely to review the data underpinning these effects and address the important scientific questions remaining in order to establish MSC therapy for patients with liver disease.

1.9 Clinical Trials

Several clinical trials were found in literature that related to the treatment of liver disease using MSCs, focusing on the study design, cell sources, injection route, patient groups, and efficacy of the therapies. Table 1-2 summarizes various studies that used MSC-based therapy for liver disease for the 10 years until 15 July 2017. All the studies reported in this section have shown heterogeneity in the dosage of the injected cells, MSC source, and route of injection. Various liver disease conditions were also reported, including

acute-on-chronic liver failure (ACLF), liver failure including cirrhosis due to alcohol, hepatitis B virus (HBV) or hepatitis C virus (HCV), and primary biliary cirrhosis (PBC). Of the clinical studies considered (Peng et al., 2011), the majority used MSCs derived from bone marrow (BM) (14 studies), whereas UC-MSCs were used in only three studies. Among the studies reported, five used allogenic MSCs, which are derived from different sources (BM and UC) to treat liver disease. The functional ability of MSCs to reduce liver injury was also investigated using single or multiple doses, with different therapeutic efficacies reported in the literature. The efficacy of infused repeated dosage of MSCs at 4 and 8 weeks was also investigated and found improvement in the liver function of patients with alcoholic liver cirrhosis (Jang et al., 2014). In this pilot study, hepatic fibrosis was found to be reduced following MSC infusion (54.5%) in six patients compared with the total of 11 patients involved in the phase ll clinical trial (Jang et al., 2014). In contrast, a comparison study found that infusing two doses of BM-MSCs did not result in improvement in fibrosis over a single transplantation (Suk et al., 2016a). The routes of injection were reported in different clinical trials and it was found that peripheral vein (PV) was the most commonly used, followed by hepatic artery (HA), intrasplenic (IS), intrahepatic (IH), and portal vein. Interestingly, the route of injection has not been reported as having a potential impact on MSC efficacy in different liver diseases, based on the use of different routes, such as PV, IS, portal vein or IH (Mohamadnejad et al., 2007a; Kharaziha et al., 2009).

Table 1-2 Clinical trials using MSCs in liver diseases. Table taken from (Alfaifi et al., 2018).

Study	Year	Design, F/U (month)	Patient cohort	Source of MSC	Injection route	Primary endpoint	Main improvement
(Mohamadnejad et al., 2007)	2007	Case series 12	Decompensated liver cirrhosis (n=4)	Autologous BM	Peripheral vein	Safety and feasibility	Creatinine and MELD score
(Kharaziha et al., 2009)	2009	Cohort 6	Liver cirrhosis (n=8)	Autologous BM	Portal vein (n=6) Peripheral vein (n=2)	Feasibility, safety, and efficacy (LFT and MELD score)	Creatinine, prothrombin time and MELD score
(El-Ansary et al. 2010)	2010	Case control 6	Decompensated liver cirrhosis due to HCV or HBV (n=12)	Autologous BM	Intrasplenic (n=6) Peripheral vein (n=6)	LFT and MELD score improvement	Creatinine, prothrombin time, albumin, bilirubin and MELD score
(Amer et al., 2011)	2011	Case control 6	Decompensated liver cirrhosis due to HCV (n=40)	Autologous BM	Intrasplenic (n=10) Intrahepatic (n=10)	Safety and short-term efficacy (LFT, MELD improvement)	Ascites, peripheral oedema, albumin, MELD score, and Child-Pugh score

(Peng et al., 2011)	2011	Case control 1, 48	ACLF caused by HBV (n=158)	Autologous BM	Hepatic artery	Improvement of MELD and LFT (short term) or development of HCC and mortality (long term)	Prothrombin time, albumin, bilirubin and MELD score
(El-Ansary et al., 2012)	2012	Case control 6	Decompensated liver cirrhosis due to HCV (n=25)	Autologous BM	Peripheral vein	Improvement of MELD and LFT	Albumin and MELD score
(Shi et al., 2012a)	2012	Case control 12 or 18	ACLF associated HBV (n=43)	Allogeneic UC	Peripheral vein	LFT and MELD improvement, adverse events, and survival rates	Albumin, prothrombin time, bilirubin, ALT, survival rates and MELD score
(Amin et al., 2013)	2013	Cohort 6	Post-HCV (n=20)	Autologous BM	Intrasplenic	Safety and efficacy	Albumin, prothrombin time, bilirubin, AST, ALT and MELD score
(Mohamadnejad et al., 2013)	2013	RCT 12	Decompensated liver cirrhosis (n=25)	Autologous BM	Peripheral vein	Safety and efficacy	None
(Wang et al., 2013b)	2013	Cohort 12	UDCA-resistant PBC (n=7)	Allogeneic UC	Peripheral vein	Safety and efficacy	Alkaline phosphatase and γ-GGT levels

(Jang et al., 2014)	2014	Cohort 6	Alcohol-related liver cirrhosis (n=11)	Autologous BM	Hepatic artery	Safety and efficacy	MELD score and liver histology
(Salama et al., 2014)	2014	RCT 6	Post-HCV end-stage liver disease (n=40)	Autologous BM	Peripheral vein	Safety and efficacy	MELD score and Child-Pugh score
(Wang et al., 2014)	2014	Cohort 12	UDCA-resistant PBC (n=10)	Allogeneic BM	Peripheral vein	Safety and efficacy	ALT, AST, GGT and IgM
(Suk et al., 2016a)	2016	RCT 12	Alcohol-related liver cirrhosis (n=72)	Autologous BM	Hepatic artery	Safety and efficacy	Histologic fibrosis and Child-Pugh score
(Lanthier et al., 2017)	2017	RCT 1	Decompensated alcoholic hepatitis (n=58)	Autologous BM	Hepatic artery	Safety and efficacy	None
(Lin et al., 2017)	2017	RCT 6	ACLF associated HBV (n=110)	Allogeneic BM	Peripheral vein	Safety and efficacy	Bilirubin, MELD score and survival rates

Note: acute-on-chronic liver failure (ACLF); alanine aminotransferase (ALT); aspartate aminotransferase (AST); bone marrow (BM); follow-up (F/U); gamma-glutamyltransferase (γ-GGT); hepatitis B virus (HBV); hepatocellular carcinoma (HCC); hepatitis C virus (HCV); immunoglobulin M (IgM); liver function test (LFT); Model for End-Stage Liver Disease (MELD); primary biliary cirrhosis (PBC); randomized controlled trial (RCT); ursodeoxycholic acid (UDCA).

1.10 Immunomodulatory Properties of MSCs Derived from UC Tissue Compared with Other Sources

MSCs can modulate and repair injured tissue by modulating injurious immune responses through a range of mechanisms, including direct cell-to-cell interaction or remotely by the secretion of paracrine and/or endocrine factors (Figure 1-4) (Christ et al., 2015). It is worth noting that MSCs have reduced immunogenicity due to a lack of expression of class II major histocompatibility complex (MHC) antigens when unprimed and do not express many of the molecules required for immune recognition, such as CD80, CD86n and CD40 (Klyushnenkova et al., 2005).

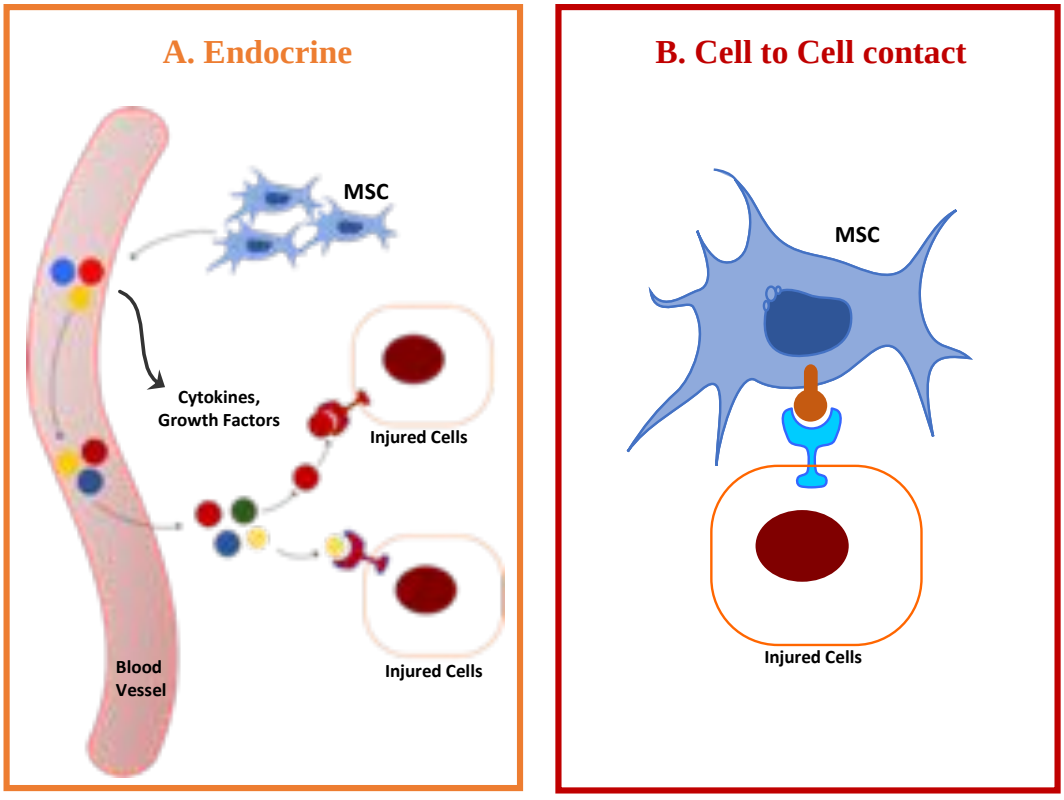

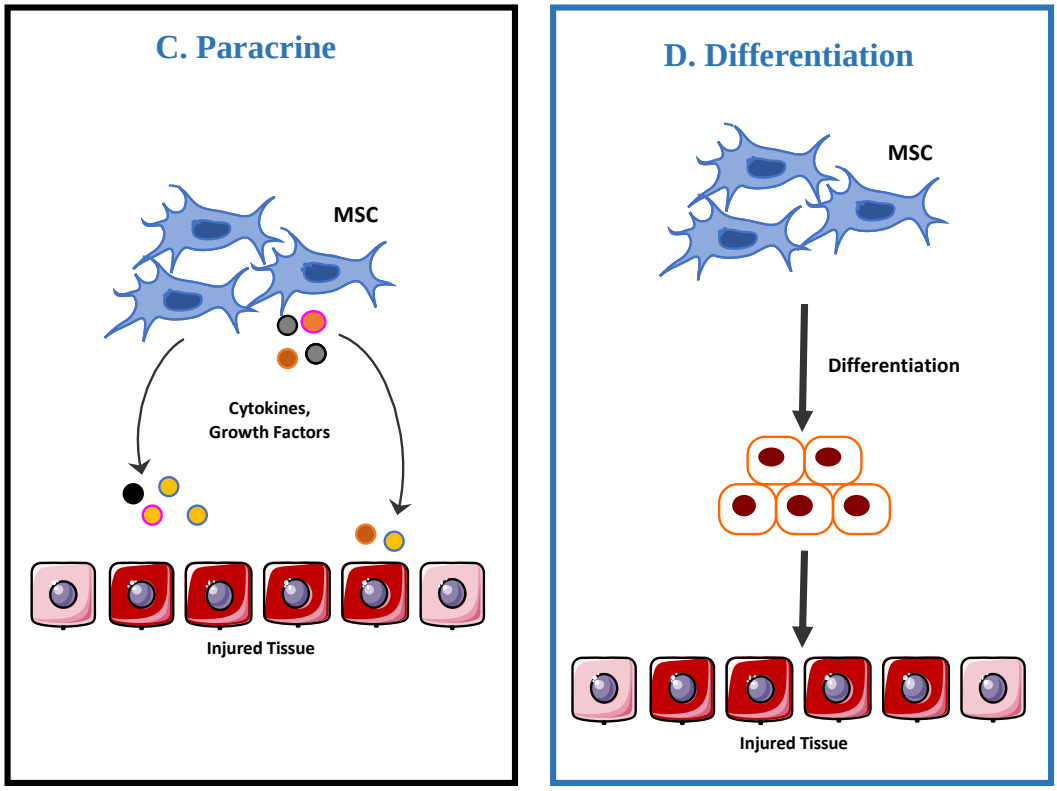

Figure 1-4 Modes of MSC-based therapy. MSC-based therapy could be used to treat diseases through several mechanisms of action. A) Upon transplantation, MSCs can respond to the injury environment through endocrine mechanism by releasing factors in circulation that can stimulate the repair process via different therapeutic properties. B) Another therapeutic potential of MSCs relies on some of which require direct cell-to-cell contact mechanism. MSCs can modulate injury through expressing a number of molecules on their surface, which can subsequently enhance the regeneration process. C) MSCs can repair the injury via paracrine mechanism and secret trophic factors that mediate the terapuetic effect in the injured cells. D) As a result of the ability of MSCs to differentiate into multiple lineages, they can be recruited to the site of injury and are believed to differentiate into a new functional cell to replace injured tissue (cell replacement therapy). Figure modified from (Alfaifi et al., 2018).

1.10.1 Immunomodulatory effect of MSCs on adaptive immunity

MSCs can inhibit the proliferation of T cells *in vitro* either by the secretion of soluble factors or by direct interaction with T lymphocytes (Figure ***1-5***) (Nicola et al., 2002).

Several different molecules secreted by MSCs have been reported to have an immunomodulatory effect on T-cell activities, including transforming growth factor-beta (TGF-β), hepatocyte growth factor (HGF) (Nicola et al., 2002), prostaglandin E2 (PGE2) (Aggarwal and Pittenger, 2005), and indoleamine 2,3-dioxygenase (IDO) (Meisel et al., 2004). Notably, the production of these immunomodulatory molecules differs according to the source of the MSCs; for example, WJ-MSCs produce higher amounts of TGF-β than BM-MSCs (Meisel et al., 2004).

The inflammatory environment is known to have an essential role during the interaction between MSCs and T cells; for example, the immunosuppressive capacity of MSCs is induced by treatment involving a combination of cytokines (interferon-gamma [IFN-γ], IL-1α, tumour necrosis factor-alpha [TNF-α], and IL-1β) (Ren et al., 2008). These cytokines can enhance some chemokines and other immune cells to ease contact with MSCs and mediate the immune reaction. Another mechanism by which MSCs can suppress the proliferation of T cells is via the secretion of nitric oxide (NO), which causes inhibition of signal transducer and activator of transcription 5 (STAT5) pathways (Sato et al., 2007). Another study demonstrated that MSCs can secrete matrix metalloproteinases (MMPs), such as MMP-2 and MMP-9, which suppress T-cell activation by cleaving surface CD25 from T cells (Ding et al., 2009).

MSCs have also been shown to promote the generation and development of Tregs, which can positively influence the balance of immune damage during tissue injury (Prevosto et al., 2007). For example, the induction of CD4+ CD25+ FOXP3+ Tregs is mediated by the secretion of TGF-β (Melief et al., 2013a) and is accompanied by inhibition of the

proliferation and differentiation of Th1 and Th17, which can further trigger the activation of Tregs. This mechanism has been associated with an increased production of IL-10 by MSCs (Luz-Crawford et al., 2013).

MSCs can also inhibit the proliferation of B cells and reduce their production of immunoglobulin. CD40 and IL-4 were used to increase the proliferation rate of murine B cells and it was demonstrated that subsequent co-culture with MSCs significantly inhibited their proliferation (Glennie et al., 2005). In addition, MSCs have resulted in the significant stimulation of immunoglobulin production after co-culture of B cells in a Transwell experiment (Rasmusson et al., 2007). MSCs may also alter the surface expression of chemokine receptors on B cells; co-culture with MSCs in a 1:1 ratio resulted in a significant reduction of the expression of CXCR4, CCR7 and CXCR5 on B cells (Corcione et al., 2006a). CXCR4 was found to have been significantly reduced even with a 1:10 ratio when cultured with MSCs, suggesting that MSCs can specifically target CXCR4, which has a role in the homing and fate of MSCs (Nitzsche et al., 2017).

NK cells represent a critical component in the immune response to viral infections and tumour cells (Sotiropoulou et al., 2006). Sotiropoulou et al. (2006) demonstrated that MSCs reduced IL-15 secretion from IL-2-induced NK cells. This reduction was presumed to be due either to cell-to-cell interaction or the release of soluble factors, such as PGE2 and TGF-β (Klyushnenkova et al., 2005). Another group reported that MSCs can suppress NK cells after stimulation with IL-5 (Sotiropoulou et al., 2006). In models of acute liver injury, MSCs have ameliorated the hepatotoxicity of natural killer T (NKT) cells in an IDO-dependent manner, by reducing the number of IL-17 cells and stimulating FOXP3

and IL-10 resulting from increased numbers of NK Tregs in the injured liver (Milosavljevic et al., 2017a).

1.10.2 Immunomodulatory effect of MSCs in innate immunity

Macrophages can be classified into classical pro-inflammatory macrophages (M1) or alternative macrophages (M2) that secret anti-inflammatory cytokines (Figure ***1-5***) (Milosavljevic et al., 2017a). MSCs have been reported to trigger polarization of M1 towards M2 both *in vivo* and *in vitro*. The polarization is driven by the ability of MSCs to secrete soluble factors, such as IL-10 and IL-1Ra, which have been shown to attenuate liver injury by promoting the number of M2 macrophages (Lee et al., 2015). In addition to the IL-10-mediated ability of MSCs to promote the switching of phenotype macrophages from M1 to M2, MSCs can also help promote the survival of monocytes through upregulation of CCL18, which is found indirectly to mediate MSCs to induce Tregs formation (Melief et al., 2013a), as demonstrated in animal models of sepsis and colitis (Anderson et al., 2013). In this study, murine adipose-derived MSCs significantly increased the proportion of M2-like cells by increased production of IL-10 and arginase-1 activities (Anderson et al., 2013).

MSCs can also regulate, and interact with, dendritic cell (DC) function by blocking differentiation of APCs to monocytes and decreasing their expression of anti-inflammatory molecules, such as IL-12, TNF-α, and IFN-γ, whilst also enhancing their secretion of IL-10, which may induce regulatory T-cell numbers (Figure ***1-5***) (Beyth et al., 2005). Notably, WJ-MSC can also inhibit the differentiation of monocytes to mature DCs when cultured with CD14+ monocytes, indicating an indirect effect of WJ-MSCs on

the allogeneic response of T cells (Tipnis et al., 2010). There is now, therefore, a greater recognition of the importance of the microenvironment in the immunomodulatory capacity of MSCs (Ren et al., 2008), prompting a need for better understanding of the microenvironments associated with specific diseases in order to develop a more effective therapeutic efficacy for MSCs.

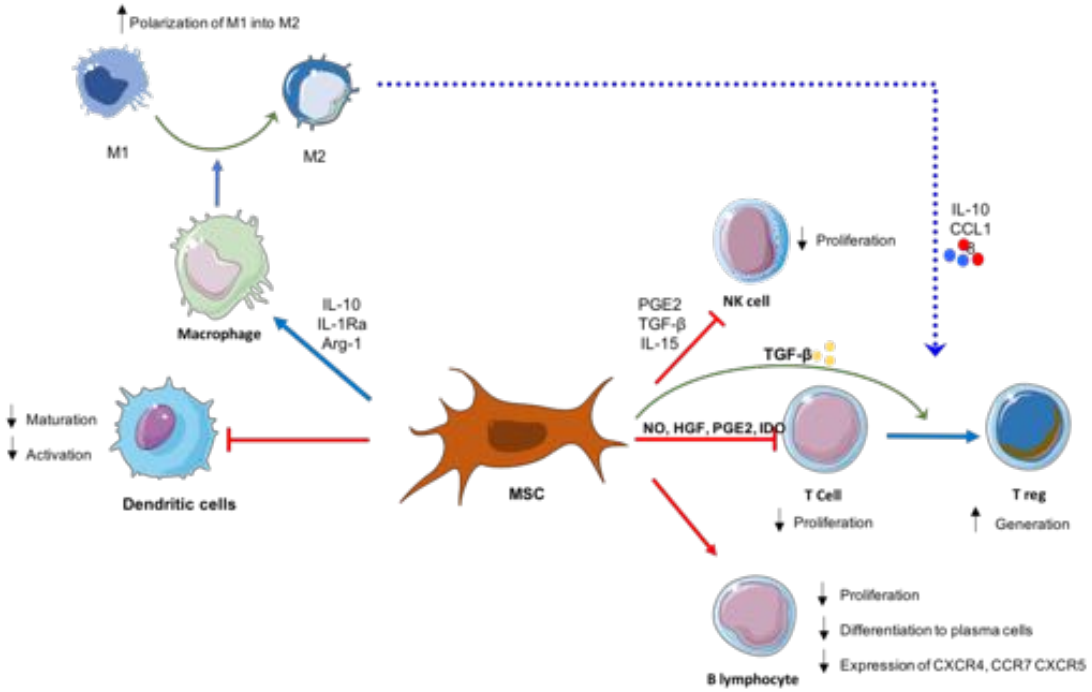

Figure 1-5 Potential mechanisms of MSC interaction with immune cells. MSCs may regulate immune responses through interaction with different types of immune cell, such as T lymphocytes, B lymphocytes, NK cells, macrophages, and DCs. This immunosuppressive property of MSCs is due to their production and secretion of soluble factors and/or by direct interaction with immune cells. MSCs have an immunomodulatory effect on T-cell activities by releasing molecules, such as TGF-β, HGF, PGE2, IDO and NO. MSCs have also been shown to promote the generation and development of Tregs by the secretion of TGF-β. MSCs can also inhibit the proliferation of B cells and reduce the expression of CXCR4, CCR7 and CXCR5. MSCs supress NK cell activities by reducing IL-15 secretion; this reduction is due either to cell-to-cell interaction or the release of soluble factors, such as PGE2 and TGF-β. MSCs interact with macrophages and trigger the polarization of pro-inflammatory macrophages (M1)

towards alternative macrophages (M2), which is driven by the ability of MSCs to secrete soluble factors such as IL-10 and IL-1Ra. M2-polarized macrophages produce anti-inflammatory cytokines, such as IL-10, which can further trigger the activation of Tregs. MSCs can also regulate and interact with DC function by blocking the differentiation of APCs to monocytes. Figure taken from (Alfaifi et al., 2018).

1.10.3 Antioxidant activities of MSCs

MSCs have been proposed as producing or releasing local systemic molecules which help have a protective effect on injured tissue. Many studies have hypothesized that this effect could be associated with enhanced expression of antioxidants from MSCs, which is linked to the regenerative process in different disease conditions. MSCs have been shown to have potential therapeutic effect by the overexpression of superoxide dismutase 3 (SDO3), which is reported to have immunosuppressive properties through the inhibition of Th17 (Sah et al., 2016). Another research group found that MSCs can mediate the suppression of neutrophils, which can be mediated through the upregulation of SOD3 (Jiang et al., 2016). In addition, MSCs have been identified as upregulating the catalase enzyme in mice with CCl_4 injury, resulting in improvement in liver injury following 8 days of MSC treatment (Burra et al., 2012). Interestingly, this study confirmed that MSCs were able to influence the antioxidant enzyme in the hepatic microenvironment without engraftment to the liver. Although MSCs from bone marrow enhance the viability of neural cells as well as promoting survival in murine models of neural injury, these findings resulted from antioxidant and anti-apoptotic functions reported in response to MSC injection.

1.11 Tracking and Monitoring the Homing of Transplanted UC-MSCs

The homing of infused stem cells has been reported in several studies but accurate quantification of the location of the cells has not been undertaken. Researchers have reported different methods in studying the homing of transplanted stem cells *in vivo*. For example, Shenghong Ju et al. studied the migration of infused labelled BM-MSCs to the liver using magnetic resonance imaging (MRI) and found the cells in the liver after 3 hours with a gradual reduction after 3, 7, and 14 days (Ju et al., 2007).

Another technique that has been used in animals is the *in vivo* imaging system (IVIS), which represents a reliable optical means of detecting the migration of infused cells (Eisenblätter et al., 2009). It has also been shown that MSCs can be detected in a number of organs, such as the lung, heart, liver, and kidney, from the first hour to 7 days after the intravenous injection of MSCs (Gao et al., 2001). In a similar finding, UC matrix stem cells were detected after 2 days but no cells were observed 6 and 12 days after infusion (Weiss et al., 2006). Another study determined the homing of MSCs administered by intravenous (IV) injection by testing the DNA expression of human albumin by using quantitative polymerase chain reaction (qPCR). They reported different expressions among different tissues, with the greatest expression in the lung (Briquet et al., 2014).

More recently, an advanced system was developed that provided very high-resolution images for a whole mouse using CryoViz™ technology. This device is a fully automatic machine which has the sensitivity to detect a single live cell, and can provide a 3D structure for the whole animal or a specific organ of interest (Roy et al., 2009). In addition, one unique feature of this technique is the ability to quantify the number of live cells *in vivo* after fluorescent labelling of cells prior to injection. Using the CryoViz™ imaging

system, it was shown that 80% of hMSCs were detected within different organs 1 hour after systemic infusion and this dropped to 0.06% within 2 days post infusion (Schmuck et al., 2016). Generally, there are still limitations and complexity with regard to accurate techniques for studying the homing of MSCs in different preclinical experiments, and this will surely be more difficult in a human clinical study.

1.12 Dosage and Route of Administration

With regard to the important role of tracking MSCs *in vivo*, the number of MSCs injected as well as the route of administration have a strong impact on enhancing the therapeutic potential of these cells in the treatment of different disease conditions. Several research groups have reported various doses of MSCs in different animal experiments with different potential effects in response to the dose of injected cells. For example, in a mouse model with brain injury, an injection of a low dose of MSCs was reported to have more effective therapeutic outcomes compared with a high dose (Wu et al., 2008). In addition, several studies have reported different routes of MSC administration, such as intravascular (IV), intraperitoneal (IP), and intra-articular injection. In a murine model with arthritis, MSCs were shown to have a great effect in reducing inflammation following intra-articular injection of MSCs, with more engraftment ability to the site of the injury (Kehoe et al., 2014). Recent work has shown that intramuscular injection was found to support the prolonged survival of MSCs compared with other routes of injection (Braid et al., 2017). Systemic administration of MSCs was the most common route of injection reported in the literature, with conflicting findings in the engraftment potential in different preclinical settings. However, it has been shown that IV injections have less engraftment potential compared with other routes, such as intra-cardiac and intra-arterial

routes of injection (Freyman et al., 2006). A study in a rat model with heart disease found that systemically injected MSCs migrated to the site of injury and had differentiation potential towards myocytes (Wu et al., 2003). The same finding was reported in lung injury and it was noted that MSCs were trapped in the lung and reduced inflammation, as well as collagen composition (Ortiz et al., 2003). In contrast with the previous findings, data from a liver injury murine model found that most MSCs were trapped in the lung and cleared from the body after 24 hours, and no MSCs were found to have engrafted to the injured site (De Witte et al., 2017). In addition, MSCs have shown significant improvement in mice with myocardial infarction via the secretion of TSG-6 from MSCs after activation following being trapped in the lung; these data suggest that MSCs have the ability to enhance treatment without engraftment to injured tissue (Lee et al., 2009).

1.13 Future perspectives

Whilst conventional unmanipulated MSC have been the mainstay of therapeutic studies thus far there have been extensive efforts to try and enhance their efficacy. This section will review some of the key strategies which include sorting MSC to enrich for greater functionality, priming of MSC with factors such as cytokines and finally genetic engineering of cells (Figure ***1-6***). The main driver for these approaches is to enhance efficacy and/or organ homing although there is also often a need to create/protect intellectual property so as to generate a viable business model. The challenge therefore is to balance the additional costs and potential logistical/safety concerns associated with such perturbations against improvements in efficacy.

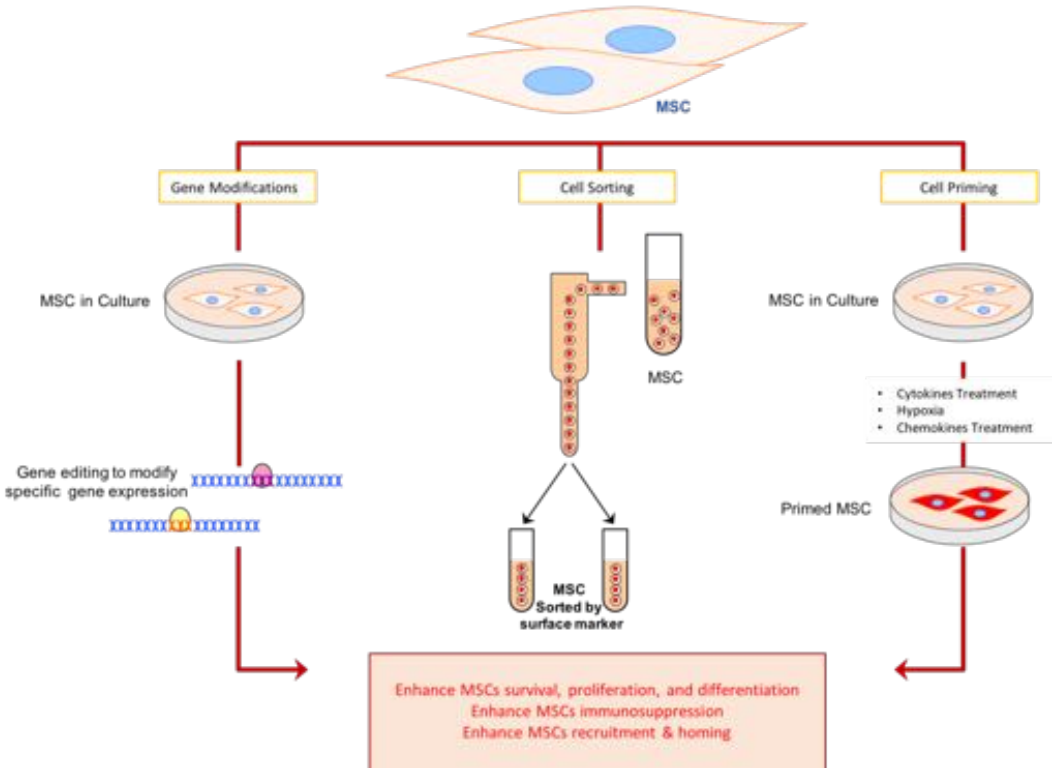

Figure 1-6 Schematic diagram illustrating therapeutic strategies to enhance MSCs functions. Number of techniques are available to manipulate the MSCs for more functional therapeutic features, including MSC sorting or using enriched MSCs based on surface marker expression to achieve homogenous populations resulting in enriched subsets for greater functionality. Priming MSCs by pre-treating cells with factors such as cytokines or chemokines can improve their function within injured environment. Another approach can be applied is to modify MSCs by gene modification via editing or engineering specific gene expression for improving the therapeutic benefits of the MSCs. Figure taken from (Alfaifi et al., 2018).

1.13.1 MSCs enrichment

MSC represent heterogeneous populations of cells, therefore, sorting approaches are highly considered to achieve homogenous populations of MSC, resulting in enriched

subsets which could crucially produce various selected populations with different therapeutic functions and open new strategies for the modification of MSC for more beneficial effects.

MSC are phenotypically diverse both morphologically and functionally and thus sorting cells based on marker expression may allow for the selection of cells with greater efficacy. This does require definition of which function is being focused on, and often markers of stemness or proliferation are reported, whereas immunomodulatory action may be the most important.

Sorting of cells for pre-clinical studies is relatively straightforward and can use a range of modalities including flow cell sorting which should result in high purity yields. It is more challenging however when such approaches are attempted in clinical practice as they need to adhere more closely to good manufacturing practice (GMP) which can restrict the modality used. Clinically approved modalities such as the CliniMACS are clinically accredited but may not result in high purities of rare populations and thus the use of GMP fluorescence cell sorting analysis is encouraging.

$CD146^+$ is expressed on various cells types including endothelia cells (Baksh et al., 2007b) and can contribute to biological functions such as cell migration, proliferation and differentiation (Tsang et al., 2013; Ulrich et al., 2015) CD146 expression is correlated with cellular senescence of MSC and markedly affects the proliferation, differentiation, and stemness of hUCB-MSC. Sorted $CD146^+$ MSC have delayed cellular senescence which is mediated by regulation of Bmi-1, id1, and Twist1 expression, which can regulate the cellular senescence process (Jin et al., 2016). This suggested that $CD146^+$ could be a novel marker that control the senescence of MSCs and improve the therapeutic efficacy

of MSCs. In a recent study, sorting MSC sub-populations based on $CD73^+$ expression has demonstrated greater self-renewal and differentiation properties (Suto et al., 2017). These sorted cells ($CD73^+$) exhibited high levels of colony forming unit ability in contrast with an absence observed with $CD73^-$ cells.

Another study has characterized populations of MSC using several markers, including $CD271^+$, known as nerve growth factor receptor and proposed as a marker of BM stromal cells, adhesion molecule (CD56), and MSCA-1^+ (mesenchymal stem cell antigen-1) (Battula et al., 2009). Sorted dual-positive MSCA-1^+ and $CD56^+$ MSC were reported to have 2-4 greater clonal efficiency than MSCA-1^+ $CD56^-$. However, MSCA-1^+ $CD56^-$ were shown to have potential ability to differentiate into adipocytes, whereas MSCA-1^+ $CD56^+$ were restricted to chondrogenic and pancreatic like cells differentiation. Similarly, other reports indicate that enrichment of synovium-derived-MSC using CD271 in combination with THY-1 (CD90) results in greater chondrogenic differentiation ability and colony forming potential in the CFU-F assay compared to $CD271^+$ $CD90^+$ BM-MSC. Thus, this combination could be a good candidate for the isolation of MSC from different tissue sources for cartilage regeneration (Ogata et al., 2015).

Sherman et al. (Sherman et al., 2017) have proposed aldehyde dehydrogenase (ALDH) as a marker for MSC which defines an enhanced ability to contribute to revascularization. MSC isolated from human bone marrow and purified into $ALDH^{hi}$ and $ALDH^{lo}$ populations had identical expression of MSC surface makers and ability to differentiate into adipocytes, osteoblasts, and chondroblasts *in vitro*. Notably though conditioned medium from $ALDH^{hi}$ MSC was shown to promote endothelial cell expansion *in vitro* and enhance recruitment of endogenous vascular cells after subcutaneously implanted in NOD/SCID mice, which was mediated by up-regulation of lectin (Sherman et al., 2017).

Positive selection on the basis of expression of the Stro-1 specific marker has also been proposed and such MSC are enriched with respect to CFU-F progenitors (Dennis et al., 2002). Stro-1^+ expanded MSC were reported to have better migratory capacity in various tissues when compare to Stro-1^- (Bensidhoum et al., 2004). Other research groups were able to increase expression of cytokines related cardiovascular which can be mediated through using Stro-1^+ enriched MSC (Hiwase et al., 2009).

Expression of CD200 has also been used to purify MSCs (Delorme et al., 2008), with its expression inhibiting osteoclast formation via inhibition of RANKL signalling pathways, which consequently reduce expression of osteoclast associated genes such as tartrate resistance acid phosphatase (TRAP) and nuclear factor of activated T cells cytoplasmic 1 (NFARC1) (Varin et al., 2013). Another study has clearly shown that $CD200^+$ BM-MSC can modulate the immune response of macrophages by inhibition of TNF-alpha secretion when compared to $CD200^{low}$ BM-MSC (Pietilä et al., 2012). Consisting with its role in immunomodulation, MSC have been identified to drive the expression of CD200 in T cell subsets following co-culture with MSC (Najar et al., 2012). This upregulation was reported in both $CD4^+$ and $CD8^+$ T lymphocyte.

More recently, $CD362^+$ (Syndecan-2) marker has been identified as a novel marker to select a homogeneous population of MSC with enhanced immunomodulatory properties (patent number WO 20131177661 A1). This marker has recently investigated for its ability to reduce immunogenicity and enhance the immunomodulatory ability in liver inflammation (De Witte et al., 2017; de Witte et al., 2015) Syndecan-2 found to be expressed in hematopoietic cells and myeloid cells (Teixé et al., 2008). And Functionally reported to upregulate upon T cell activation and play significance role in CD3 downregulation through degradation of T-cell receptor (TCR) (Rovira-Clavé et al., 2012).

These findings strongly suggest that enrichment of syndecan-2 expression in MSC could play an essential role in immune modulation in injured tissue. The potential benefits of the various markers that have been used to select/enrich MSC are detailed in Table ***1-3***.

Table 1-3 Reported selection and purification makers of Mesenchymal stromal cells for tissue repair. Table taken from (Alfaifi et al., 2018).

MSCs Source	Species	Markers expressed	Purification/ selection methods	Experimental Models	Target/ Mechanism	References
BM	Human	$CD271^+$ and $CD56^+$	Cell Sorting	In-vitro	Increase clonogenic and proliferation potential. Increase chondrocyte and pancreatic like cells differentiation.	(Battula et al., 2009)
BM	Rate	$CD73^+$	Cell Sorting	In-vitro Lewis rates	Enhance self-renewal and differentiation. Increase engraftment.	(Suto et al., 2017).
BM	Human	$CD200^+$	Magnetic separation	In-vitro	Enhance regulation of bone resorption. Inhibit osteoclast formation via inhibition of RANKL signaling pathway.	(Delorme et al., 2008).
BM	Human	$CD200^+$	Cell Sorting	In-vitro	Suppress TNF-α secretion in macrophage like cells (Immunosuppressive activity)	(Pietilä et al., 2012).
UP, AT, and BM	Human	αSMA+	FACS	In vitro	Improve MSC fate through regulation of YAP/TAZ activation.	(Talele et al., 2015)
PAM	Human	CD34+	FACS	TAA (liver fibrosis model)	Reduce hepatic fibrosis and restore liver function by reduce collagen level and deactivate the hepatic stellate cells.	(Lee et al., 2016)
BM	Human	CD271+	Magnetic separation	In vitro (model of wound healing)	Significant potential in wound healing	(Latifi-pupovci et al., 2015)
UCB	Human	CD 146+	FACS	In vitro	Reduce MSCs senescence.	(Jin et al., 2016)
SYN	Human	LNGFR and THY-1	FACS	In vitro	Shown to have more chondrogenic differentiation ability	56

BM	Human	ALDH	FACS	In vitro and in vivo (NOD/SCID mice)	Promote endothelial cell expansion. Enhance recruitment of endogenous vascular cells in vivo by upregulation of lectin.	(Sherman et al., 2017).
SYN and BM	Human	LNGFR and THY-1	FACS	In vitro	Greater chondrogenic differentiation ability and colony forming potential than BM-MSC.	(Ogata et al., 2015).
UC	Human	C362+ (Syndecan-2)	FACS	ALF	Improve immunomodulatory properties and clonogenicity.	(De Witte et al., 2017)
BM	Human	STRO-1	FACS	In vitro	Increase expression of cardiovascular relate cytokines.	(Hiwase et al., 2009).

Note: Bone Marrow (BM), Umbilical cord (UC), Umbilical cord blood (UCB), Synovium (SYN), Placenta amnion membrane (PAM), Adipose tissue (AT), Umbilical perivascular (AP), Aldehyde dehydrogenase (ALDH). Stromal Precursor antigen-1 (Stro-1), Acute liver failure (ALF), Receptor activator of nuclear factor kappa-B ligand (RANKL)

1.13.2 MSCs priming

As with selection of MSC, priming of cells before use is intended to enhance their biological properties for whichever clinical indication is being considered (Table ***1-4***). This may include improvements in MSC immunomodulatory effects, homing to injured organs and/or greater expansion of cells.

1.13.2.1 Enhancing immunomodulatory properties of MSC

Pre-treatment of MSC with the pro-inflammatory cytokines IL-1β, IL-23 and IL-6 for 96 hours (Pourgholaminejad et al., 2016) was found to enhance secretion of TGF-β and reduce production of IL-4 by MSC, although notably no changes were reported in production of IFN-γ and TNF-α. In addition, cytokine-treated MSC exhibited superior multi-lineage differentiation capacity compared to untreated MSC, with no associated

changes in their morphology. IL-1 appears to be important for pre-conditioning of MSC, as combined treatment with IL-1α and IL-1β increases production of granulocyte-colony stimulating factor (G-CSF) and secretion of anti-inflammatory mediators such as IL-10. Moreover, microglial cells incubated with conditioned medium from IL-1 primed MSC increase expression of anti-inflammatory cytokines such as IL10 and decrease secretion of pro-inflammatory cytokines as reported in TNF-α and IL-6 (Redondo-Castro et al., 2017).

Duijvestein et al. (Duijvestein et al., 2011) showed that stimulation MSC with IFN-γ enhanced the anti-inflammatory response of MCS in experiment colitis animal model. In addition, IFN-γ primed MSC exhibit a significant reduction in TNF-α and IL-6 in colon homogenates, while normal MSC had no effect. In the same model, activation of MSC with IFN-γ further promote the immunomodulation via enhance production of IL-17 and Il-4, which therefore inhibit the Th1 and reduce T cell activation (Duijvestein et al., 2011). Under similar conditions, pre-stimulation of BM-MSC with IFN-γ and TNF-α stimulate production of IL-6, HGF, TGF-β (Linero and Chaparro, 2014). More interestingly, an in vivo GVDH model, administration of MSC pre-treated with IFN-γ have the capability to enhance survival rates of mice with GVHD, resulted in 100% survival (Polchert et al., 2008).

More recently, data from de Witte and colleagues have demonstrated that pre-treatment of UC-MSC with different treatments such as TGF-β, IFN-γ, IFN-β or in combinations (TGF-β, IFN-γ and retinoic acid) suppress expression of CD107a on NK cells, enhancing MSC immunomodulation. In addition, MSC treated with IFN-γ and the multiple cytokine combination were found to significantly upregulate IDO activities which subsequently

suppressed CD4 and CD8 proliferation when compare to untreated MSC. Notably, following infusion into mice injured with a single dose of CCl_4, a higher percentage of TGF-β treated MSC homed to the injured liver (25%) compared with untreated MSC (13%) (De Witte et al., 2017).

In another liver injury studies, IL-7 treated MSC had a superior therapeutic effect on liver injury mediated in part through increased activation of iNOS. IL-17 down-regulates gene expression of ARE/poly(U)-binding/ degradation factor 1 (AUF-1) in MSC which is a protein known to regulate immune related molecules (Han et al., 2014) and has a key role in regulation stromal cell fate (Chenette et al., 2016). Thus, AUF1 could have a novel role to enhance the effect of IL-17 on immunosuppression. Similarly, IL-17a modified MSC have been reported to suppress proliferation of T cell *in vitro* via mechanisms such as inhibition of Th1 cytokines (IFN-γ, TNF-α, IL-10, and IL-2), enhance production of IL-6 and induction of regulatory T cells (Sivanathan et al., 2015).

IL-6 priming of MSC infused into an acute model of CCl_4 injury resulted in improved viability of isolated hepatocytes as well as a reduction in expression of pro-apoptotic markers such as BAX, Caspase-3 and LDH activities. This finding was not observed when MSC or IL-6 treatment were applied alone (Nasir et al., 2013). In addition, administration of IL-6 with MSC was found to enhance repair of liver injury in a mouse model of liver fibrosis with reductions in fibrosis, improvements in liver synthetic function, promote hepatocyte survival, and decrease apoptosis in fibrotic liver (Nasir et al., 2013).

1.13.2.2 Enhancing homing of MSC

A study demonstrated that adhesion molecules such as ICAM and VCAM can be highly expressed on MSC following priming with a combination of IFN-γ, TNF-α and IL-1. This upregulation of expression of ICAM and VCAM led to increased recruiting of MSC to vascular endothelium, this close contact of MSC with immune cells could enhance the immunosuppressive properties of MSC (Ren et al., 2010, 2011) Similarly, MSC pre-treated with IFN-γ, TNF-α can induced regulatory T cells more efficiently than non-treated MSC. Furthermore, MSC pre-incubated with IFN-γ, TNF-α induced secretion of CCR6 and therefore increase the adhesion of Th17 cells to MSC, resulting in promote the generation of regulatory T cells ($FOXP3^+$ cell) from Th17 cells and consequently improve their immunosuppressive properties (Luz-Crawford et al., 2013).

Priming with CXCL9 has also been shown to enhance adherence of MSC to endothelial cells as well as increase spreading of MSC on the endothelial cells as characterized by the extension of pseudopodia in multiple directions (Chamberlain et al., 2011). Further characterization of the beneficial effect of chemokines on MSC behaviour was reported in the same study using trans-well migration experiments, in which MSC migrated across endothelial layers in the presence of chemokines such as CXCL9, CXCL16, and CXCL20, and CXCL25. Of note no migration was observed in the presence of TNF-α alone.

MSC are commonly maintained in culture at an oxygen concentration of about 21% (Nitzsche et al., 2017), whereas *in vivo* they are exposed to oxygen tensions in the range of 0.4 to 2%. Under hypoxic condition, hBM-MSC significantly increase their expression

of chemotactic and angiogenic mediators such as VEGF-A, VEGF-C, IL-8, and MCP-1(Mylotte et al., 2008), and also result in activation of Akt signaling pathways and expression of cMET (a major receptor for HFG)(Rosova et al., 2008), all of which are involved in homing and tissue repair ability of MSCs. Oxygen tensions as low as 0.1-0.3% appears to stimulate expression of CXCR4, MMP-2 and MMP-9, which have been associated with enhanced cell migration(Wei et al., 2013). This maybe mediated by hypoxia inducible factor (HIF-1α) which is also activated under conditions of hypoxia and has been reported to drive expression of CXCR4 and CX3R1 (Hung et al., n.d.; Schioppa et al., 2003). Culture of MSC under hypoxic conditions appears to maintain their state of pluripotency and increase their proliferative capacity, resulting in an approximately 30-fold increase in cell number in compare to normal oxygen tension (Das et al., 2010). In a mouse model of liver injury, hypoxia preconditioned MSC significantly improved liver regeneration which was mediated by up regulation of VEGF secretion, the peak of VEGF expression (72 hours) was reported to be correlated with the proliferations of the sinusoidal endothelia cells in the liver, this finding showed that MSCs derived VEGF promote liver generation through regeneration of sinusoidal endothelia cells (Yu et al., 2013). Similarly, another study reported that hypoxia led to activation of MT1-MMB in MSC which in turn was correlated with activation level of VEGF (Promotes et al., 2003). Notably, other studies have shown that whilst there is a decrease in differentiation of MSC into adipogenic and osteogenic lineages under low oxygen conditions (1%) when compared to normoxic condition, there is an up-regulation of both CXCR4 and CX3R1 (Hung et al., 2007).

Table 1-4 Reported factors and their effect in PRIMING of Mesenchymal stromal cells for tissue repair. Table taken from (Alfaifi et al., 2018).

MSC source	Molecule name	Time of treatment	Biological Function	Reference
Human BM Human AT	IL1β, IL23, IL-6	96 hours	• Enhance secretion of TGF-β. • Reduce production of IL-4. • Exhibit significance multi-lineage. differentiation capacity.	(Pourgholaminejad et al., 2016)
Human BM	IL-1	24 hours	• Increase production of G-CSF. • Increase production of IL-10.	(Redondo-Castro et al., 2017).
Human UC	INF-γ, TGF-β, or multiple cytokine cocktail (INF-γ, TGF-β, and retinoic acid)	72 hours	• Multiple cytokines cocktails improve the immunomodulatory properties of MSCs. • TGF-β treated MSCs increased recruitment of MSCs to the liver injury *in-vivo.*	(De Witte et al., 2017).
Mouse BM	INF-γ + TNF-α with IL-17	12 hours	• Mediate liver injury through activation of iNOS.	(Han et al., 2014)
Human BM	IL-17	24, 48, and 120 hours.	• Induction regulatory T cells. • Inhibition of Th1 cytokines. • Enhance production of IL-6.	(Sivanathan et al., 2015).
Mouse BM	IL-6	24 hours	• Improve viability of hepatocytes treated with CCL_4. • Decreased expression of pro-apoptotic markers (BAX, caspase-3, and LDH). • Reduced liver fibrosis in vivo.	(Nasir et al., 2013).
Mouse BM	INF-γ or (TNF-α and IL-1)	Not sure	• Increase upregulation of ICAM and VCAM.	(Ren et al., 2010, 2011)
Mouse BM	(INF-γ + TNF-α + IL-1α) or (IL-1β + INF-γ)	24 hours	• Increase ability of MSC to inhibit T cell proliferations. • Enhance secretion of chemokines such as CXCl-9 and CXCL-10.	(Kusuma et al., n.d.)
Mouse BM	CXCL9	30 minutes	• Ameliorate the adhesion of MSC to murine endothelial cells.	(Chamberlain et al., 2011).

Human BM	O_2 (1-3%)	16 hours	• Increase expression of HGF receptor (cMET) on MSCs. • Regulate survival, migration, and proliferation of MSC through regulation of Akt and Erk signalling pathway.	(Rosova et al., 2008).
Rat MB	O_2 (0.1-0.3%)	24 hours	• Stimulate expression of CXCR4, MMP-2, and MMP-9.	(Wei et al., 2013).
Rat MB	O_2 (1%)	24 hours	• Significant improvement in liver injury by upregulation of VEGF.	(Yu et al., 2013).
Mouse BM	O_2 (1%)	4 hours	• Increase activation of MT1-MMB in MSC.	(Promotes et al., 2003).
Human BM	O_2 (1%)	7 days	• Increases expression of CXCR4 and CX3CR1.	(Hung et al., 2007).

1.13.3 Genetic modification of MSC (Gene editing)

Beside enrichment and priming MSC *in vitro*, transplantation of MSC after genetic correction or modification (gene editing) represents a powerful approach to use of MSC in regenerative medicine (Table ***1-5***). This section will review progress with genetic engineering approaches that have reported with MSC, including viral and non-viral manipulations. Viral transfection of MSC can be achieved with several approaches including lentivirus, adenovirus and retrovirus (Park et al., 2015).

Overexpression of Oct4 and Nanog in MSC can increase level of Dnmt1, a methyltrasferase known to have an essential role in maintaining DNA replication, through a direct binding to its promoters (Tsai et al., 2012), resulting in increased proliferation and differentiation of MSC *in vitro*. Similarly, another research group reported that MSC

transfected with Oct-4 have enhanced expression of Sox-2 and Nanog (Wang et al., 2015), thus potentially leading to enhanced pluripotency of MSC and possibly also function.

MSC have also been genetically modified to increase expression of CXCR4, thereby improving their homing to the injured liver and reducing liver damage (Ma et al., 2014). Similarly, the same finding was reported in a rat model of lung injury, with increased expression of CXCR4 on MSC resulting in enhanced hepatic migration and improvement of their immunomodulatory properties mediated by increased production of IL-10 and reduction in TNF-α. Notably, these findings suggest that overexpression of CXCR4 not only enhanced MSC homing but also increased their immunosuppressive effects (Yang et al., 2015).

Further examination of the beneficial effects of genetic modified MSC was reported in a mouse model of liver fibrosis, following overexpression of insulin growth factor like-1 (IGF-1) (Sobrevals et al., 2016). After systemic administration, IGF-1 modified MSC were able to significantly reduce the degree of fibrosis, likely through the down regulation of α-SMA, TGF-β and COL1A2 in animal treated with IGF-1 MSC when compare with animal treated with normal MSC (Fiore et al., 2015). Over-expression of HGF in MSC was also found to reduce liver fibrosis, seemingly mediated by a reduction in TFG-β, platelet-derived growth factor-bb (PDGF-bb), and metalloprotease-14 (MMP-14) (Kim et al., 2014). HGF overexpressed MSC also act on hepatic stellate cells to reduce α-SMA and desmin expression, indicating that MSC that overexpress HGF decreased both the activation and number of hepatic stellate cells more greater level than MSC. This could have therapeutic effect to prevent diseases progression and foster liver restoration.

Another reprogramming approach showed that over-expression of miR-27b in adipose tissue derived MSC resulted in reduction in a rat model of ischemic liver injury in rat with improvements in ALT, AST, TNF-α, and IL-6 as well as significance suppression in TGF-β (Chen et al., 2016). Moreover, these transfected cells were shown to have anti-fibrotic ability with suppression of MMP-2 and MMP-9 in liver tissue.

Further study linked between the genetic modified MSC and their capacity to express endothelial cell (EC) markers with similar function. For example, silencing MMP-2 and MMP-14 with endothelial growth medium can induce the MSC differentiation into EC by enhance production of endothelial markers, such as PECAM and VE-cadherin. These markers were increase from 4 to 15% and from 4 to 30% after silencing MMP-2 and MMP-12, respectively. This observation was in comparison with MSC that treated with endothelial growth medium only (Almalki et al., 2017).

In other work, the expression level of HO-1 was genetically modified in MSC and shown to have resistance to cell death under oxidative stress condition and enhance their anti-apoptotic properties (Hamedi-Asl et al., 2012). Moreover, HO-1 overexpressed MSC have shown to have more surviving cells following exposure to H_2O_2 and hypoxia, indicating that HO-1 may shape the stress responsive and cytoprotective properties of MSC. Notably, in the murine model of myocardial infarction, overexpression of HO-1 resulted in diminished oxidative stress and apoptosis as well as an enhanced effect on angiogenesis. This was associated with a 2.1-fold up-regulation of VEGF levels compared to normal MSC (Tsubokawa et al., 2010).

Table 1-5 example molecules to genetically modified mesenchymal stem cells (MSCs).

Table taken from (Alfaifi et al., 2018).

MSC source	Example of associated genes	Condition	Viral vector	Representative biological activities	Reference
Mouse BM	IGF-1 overexpression	Liver cirrhosis	Adenovirus	Ameliorate liver fibrosis by significant reduction in α-SMA, collagen deposition, and TGF-β1.	(Fiore et al., 2015)
Mouse BM	Let-7a Knockdown	IBD and GVHD	siRNA	Significant improvement in both models, by suppress T cell proliferation (decreased in $CD3^+$), increase MCP-1 secretion, and enhancing expression of Fasl/Fas.	(Yu et al., 2017)
Human BM	CXCR5 overexpression	CHS	Lentiviral	Increase migration and engraftment of MSC to the site of injury. Enhance immunomodulatory effects of MSCs *in vivo* through inhibit of T cell proliferation and supress production of INF-γ and IL-17.	(Zhang et al., 2017b)
Human BM	CXCR4 overexpression	ALF	Lentiviral	Enhance migration and improve liver regeneration.	(Ma et al., 2014).
Rat BM	CXCR4 overexpression	Lung injury	Lentiviral	Improve migration and suppress inflammation of lung tissue by upregulation of IL-10 and downregulation of TNF-α.	(Yang et al., 2015)
Rat AT	miR-27b overexpression	Partial hepatectomy	Micro RNA	Enhance liver regeneration through reduction in ALT, TNF-α, and IL-6 in serum. Reduce expression of TGF-β, MMP2, and MMP9.	(Chen et al., 2016).
Human BM	Oct4 and Nano over expression	In vitro	Lentiviral	Increase MSC proliferation and differentiation capacity by upregulation of Dnmt1 protein.	(Tsai et al., 2012)
Human BM	Oct4 and Nano Knockdown	In vitro	Lentiviral	Reduce MSC proliferation rate and differentiation ability.	(Tsai et al., 2012)
Human AF	Oct4 over expression	In-vitro	Plasmid	Increase expression of Oct-4, Nanog, and Sox-2. Increase colony forming ability.	(Wang et al., 2015)
Rat MB	CAMKK1 over expression	AMI	siRNA	Reduce scar formation and improve cardiac function *in vivo.*	(Dong et al., 2017)
Porcine AT	MMP-2 and MMP-14 knockdown	In-vitro	siRNA	Enhance differentiation of MSC into endothelia cells by production of PECAM and V-caderen. Increase the formation of capillary like cells and Sc-LDL uptake.	(Almalki et al., 2017).
Human BM	HO-1 overexpression	In-vitro	Adenovirus	Enhance MSC survival and resistant to oxidative stress. Enhanced anti-apoptotic and anti-oxidative capabilities of MSCs	(Tsubokawa et al., 2010).

Rat BM	HO-1 overexpression	MI	Plasmid	Enhanced anti-apoptotic and anti-oxidative properties and improved angiogenesis level.	(Hamedi-Asl et al., 2012).
Human BM	HGF overexpression	Liver Fibrosis (MDN model)	Adenovirs	Promote liver function and reduce liver fibrosis via significant reuction in TGF-β and PDGF-bb.	(Kim et al., 2014)
Mouse BM	COUP-TF1 knockdown	Streptozotocin-induced diabetic mice	siRNA	Increase ability of BM-MSCs to differentiate into IPCs.	(Zhang et al., 2017a)
Rat BM	Aqp1 overexpression	Tibia fracture Model	Lentiviral	Enhance MSCs migration *in vitro* and *in vivo* through modulation expression of FAK and β-catenin.	(Meng et al., n.d.)
Human BM	Apoptin overexpression	HCC	Adenovirus	Inhibit the proliferation of liver carcinoma cells *in vitro* and tumour growth *in vivo*.	(Zhang et al., n.d.)

1.14 Aims and Objectives

The ability of UC-MSCs to immunomodulate offers therapeutic potential in liver injury but the inherent heterogeneity of unsorted MSC populations may explain varied/reduced function, as well as posing regulatory challenges. Thus, I set out to evaluate the therapeutic potential of purified CD362+ MSC infusion in murine models of acute liver injury.

In this study, two different cell subsets were used: unsorted UC-MSCs and sorted UC-MSCs based on the expression of CD362. The main aims of the project were as follows:

1) Phenotypic characterization of unsorted UC-MSCs and sorted UC-MSCs based on the expression of CD362 by measuring the expression of surface markers using flow cytometry and analysing their ability to differentiate into adipocyte, chondrocyte and osteocyte lineages.

2) To investigate and evaluate the effects of CCl_4 treatment in mice. The hepatotoxicity of CCl_4 was evaluated at different time points by measuring hepatic injury, inflammatory response, cell proliferation, DNA damage, antioxidants, and the level of autophagy.

3) Comparison of the immunomodulatory properties of unsorted UC-MSCs and $CD362^+$ sorted UC-MSCs *in vivo*. The efficacy of unsorted/purified UC-MSCs in the CCl_4 model was determined by measuring serum alanine aminotransferase (ALT) and inflammatory cytokines. The efficacy of sorted UC-MSCs in modulating the numbers of hepatic infiltrating lymphocytes and monocytes was studied using flow cytometric analysis.

4) To investigate the immunosuppressive potential of unsorted/purified hUC-MSCs *in vivo* using an OVA-BIL model of acute liver injury.

5) To study the distribution of infused UC-MSCs *in vivo* using the Cryo-Imaging System.

CHAPTER 2

MATERIALS & METHODS

2.1 Isolation of human mesenchymal stromal cells from umbilical cord tissue.

Orbsen Therapeutics Ltd developed a research protocol for the isolation of MSC from umbilical cord tissue using enzymatic digestion. Briefly, umbilical cord (5-6 cm) was washed in 70% ethanol and then washed again using PBS (Figure ***2-1***).

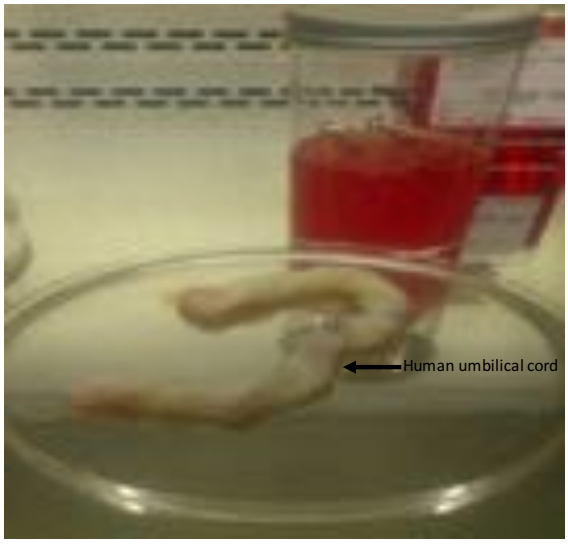

Figure 2-1 Human umbilical cord.

The cord was dissected into 1 cm^3 pieces and washed free of contaminating blood with PBS throughout the process. For digestion, the cord was immersed in a 5 ml (x2 2.5ml in each 50ml Falcon tube) enzymatic mixture (α-MEM, Collagenase I, Hyaluronidase I and DNase) and incubated for 1 hour at 37°C with gentle agitation. After incubation, digested tissues were removed by squeezing with forceps to release cells into solution. The action of enzymes was stopped by addition of α-MEM media containing 10% FBS and the cell suspension was kept on ice. Cell suspensions were further diluted to reduce the viscosity of the suspension and passed through a 100-µm filter. All digested explants were split

between two 10cm dishes and cultured in α-MEM media with fibroblast growth factor (FGF) and placed in a hypoxic incubator. The filtered cell suspension was centrifuged at 400 relative centrifugal force (RCF) for 5 minutes. Viable cells were counted using by Trypan blue dye exclusion on hemocytometer. Cells were washed and resuspended in sort buffer for staining (1:50, αCD362 – APC for 30 minutes at 4 °C). Cells were washed and centrifuged at 400 RCF for 5 minutes at 4 °C. Cells were resuspended at a density of 80µl/10^7cells. αAPC beads were added at a concentration of 20µl/10^7cells and incubated at 4 °C for 15 minutes. Cells were washed in MACS buffer at a concentration of 1-2mls/10^7cells and cells resuspended in 500µl of MACS buffer. MACS column was prepared by adding 500µl of MACS buffer before addition of labelled cells. Column was then washed three times with 500µl of MACS buffer, and cells flushed from column (x2 1ml CD362+ cells into 15ml tube). Cells were then counted and cultured in αMEM media (+FGF) and placed in CO_2 in a 37°C incubator.

2.2 Characterisation of MSC derived from UC by flow cytometry.

After the MSC were isolated from umbilical cord, cells from passage 2 or 3 were seeded in a 175cm2 culture flask containing 30 ml of complete media, which was prepared by adding 50ml of fetal bovine serum (FBS, F9665; Sigma-Aldrich, UK) to 445 ml of minimum essential medium Eagle alpha modification (MEM-α, 32561029; Gibco, UK) with 5ml of penicillin/streptomycin solution (P/S, 10,000 U/mL, 15140122; Gibco, UK), and 10µl of 1 ng/ml basic human recombinant fibroblast growth factor (rhFGF, 100-18B; Peprotech, UK). Cells were fed every two to three days until the cells reached 70-80% confluent. Next, medium was discarded and the adherent cells were gently washed with sterile PBS. Finally, cells were detached by incubation with pre-warmed TrypLE™

Express (12605010; Gibco,UK) for 3-5 minutes at 37 °C, and then diluted with complete media. Cells were centrifuged at 400 g for 5 minutes and resuspended at a concentration of $1x10^7$ cells/ml in FACS buffer (2ml FBS with 98ml cold PBS). Tubes were labelled, and the amount of each antibody was added as per the following table (Table 2-1). 100µl of cell suspension was added into each tube and tubes were then incubated in the dark for 30 minutes (all tubes were wrapped in foil to prevent exposure of samples to the light). After incubation, cells were washed twice with FACS buffer by adding 2 ml cold FACS buffer, vortexed, and centrifuged at 400 g for 5 minutes. Supernatant was discarded, and the pellet resuspended in 300-500µl of FACS Buffer (FBS). The cell suspension was filtered for each tube using a yellow strainer, and cells were analyzed using a flow cytometer (Cyan, ADP Flow cytometer analyzer).

Table 2-1 A) hMSC analysis kit contents (BD). B) This table presented labelled tubes and the amount of antibody added to each tube.

A	
Product	**Contents**
Positive Marker Cocktail	CD105 PerCP-Cy5.5, CD73 APC, and CD90 FITC.
Additional Positive Drop-In Marker	CD44 PE.
Negative Marker Cocktail	CD45, CD34, CD11b, CD19, and HLA-DR PE.
Isotype Controls	mIgG1 PerCP-Cy5.5, mIgG1 APC, and mIgG1 FITC for positive cocktail
	IgG1 and IgG2b PE for negative cocktail
	IgG2b PE for CD44 drop in.
Compensation controls	CD105 PerCP-Cy5.5
	CD73 APC
	CD90 FITC
	CD44 PE

B		
Tube No	Add	Size
1	FITC Mouse Anti-Human CD90	5µl
2	PE Mouse Anti-Human CD44	5µl
3	PerCP-Cy™5.5 Mouse Anti-Human CD105	5µl
4	APC Mouse Anti-Human CD73	5µl
5	Nothing	
6	hMSC Positive Isotype Control Cocktail + PE hMSC Negative Isotype Control Cocktail	20µl 20µl
7	hMSC Positive Cocktail + PE hMSC Negative Cocktail	20µl + 20µl
And/or		
8	hMSC Positive Isotype Control Cocktail + Drop in isotype control (i.e. PE Mouse IgG2b)	20µl 5 µl
9	hMSC Positive Cocktail (20µl) + PE Drop in (i.e. PE Mouse Anti-Human CD44) (5µl)	20µl 5 µl

2.3 *In vitro* differentiation of UC-MSC.

2.3.1 Adipogenic differentiation.

Cells from passage 3 were cultured in a 12-well plate at a seeding density of $1x10^4$ cells/cm^2 and incubated at 37°C in a humidified atmosphere of 5% CO_2. Culture medium was replaced every three days using complete AMEM medium until the cells reached confluence (60-80%). At 80% confluence, media was replaced with pre-warmed adipogenesis differentiation medium consisting of 90 ml adipocyte differentiation medium, 10 ml of adipogenesis supplement, and 50ul of Gentamicin (10mg/ml) (*Invitrogen Inc*) and culture continued. MSC continued to undergo limited expansion as they differentiated under adipogenic conditions, with the medium being changed every 3 to 4 days. Normal complete media AMEM was used as a negative control. Adipogenesis was assessed using Oil red-O staining.

For Oil Red O staining, media was aspirated after 14 days and each well washed with 2ml of PBS. Cells were fixed with 10% formalin for 30 minutes. Formalin were aspirated from each well and rinsed again with PBS. Cells were stained with Oil red-O solution (15ml of stock oil red with 10ml distilled water). Stock solution was prepared by dissolving 300 mg of oil red-O powder (Sigma-Aldrich) in 100 ml of 99% isopropanol. 2ml of the oil red-O working solution was added along the side of each well and left for 15 minutes, before counterstaining with Mayer's hematoxylin (Sigma-Aldrich) for 5 minutes. Under the microscope, adipogenesis was assessed by staining for lipid droplets with red and the nuclei seen in blue.

2.3.2 Osteogenic differentiation.

Osteogenic differentiation was undertaken as described in the adipogeneic differentiation method, with a few modifications. Cells from passage 3 were cultured in a 12 well plate at a seeding density of $1x10^4$ cells/cm^2 and cells incubated at 37°C in a humidified atmosphere of 5% CO_2. Cells were fed every three days using complete AMEM medium until the cells reached confluence (70-80%). At 80% confluence, medium was replaced with pre-warmed osteogenic differentiation medium consisting of 90 ml Osteocyte Differentiation Basal Medium, 10 ml of osteogenesis supplement, and 50ul of Penicillin and Streptomycin (10mg/ml) (*Invitrogen Inc*) and culture continued. MSC continued to undergo limited expansion with the media changed every 3 to 4 days. Normal complete media AMEM was used as a negative control for undifferentiated cells. Osteogenesis was assessed using 1% Alizarin Red S staining.

Calcium deposition of osteogenic differentiation was analyzed by 1% Alizarin Red S

staining. In order to prepare 1% of Alizarin Red S, I dissolved 1g of Alizarin Red S powder (Sigma) with 100 ml of ionized distilled water. The pH was monitored to be between 4.1 to 4.3. Cells were fixed with 10% formalin for 30 minutes and stained with 1% of Alizarin Red S staining for 20 minutes. After incubation with Alizarin staining, cells were washed with deionized water and then examined using a light microscope.

2.3.3 Chondrogenic differentiation

To induce chondrogenic differentiation, a pellet system was used. Cells were transferred into 15 ml Polypropylene tube and cells centrifuged at 150g for 5 minutes. Supernatant was discarded, and cells resuspended in 1 ml incomplete chondrogenic medium (mixture of 185ml differentiation basal chondrogenic medium with dexamethasone, ascorbate, insulin-transferrin-selenium (ITS) supplement, GA-1000, sodium pyruvate, proline, and L-glutamine) per 7.5 x 10^5 cells, centrifuged again at 150g for 5 minutes. MSC were resuspended in complete chondrogenic medium (2.5 µl of TGF-b3 was used to convert 5 ml of incomplete media to complete media) to a concentration of 5.0 x 10^5 cells per ml. Cells were centrifuged at 150g for 5 minutes, and the tubes then incubated at 37°C in a humidified atmosphere of 5% CO_2. Pellets were left undisturbed for 24 hours, after which 0.5ml of freshly prepared complete chondrogenic medium was added to each tube. After 21 days, pellets were snap frozen and kept in frozen medium at -20 °C. For histological analysis, sections were taking from each pellet and stained with 0.1% toluidine blue staining. This staining was prepared as follows: 0.1g of Toluidine Blue O powder was weighed out and suspended into 100ml of 0.1 Sodium Acetate buffer (1.36g of sodium acetate buffer with 100ml D.W, pH 4). Staining was performed on frozen sections; slides were defrosted for 30 minutes and 200µl of toluidine blue we added onto each section and

incubated for 2 minutes. Slides were washed in tap water and dehydrated, sections were mounted using DPX mounting (Leica 08600E) and examined under the light microscope.

2.4 Preparation of hUC-MSCs for perfusion

Cryopreserved human umbilical cord (UC) MSC from passages 2-3 were supplied by Orbsen Therapeutics Ltd (Galway, Ireland). Passage three to four UC-MSCs were used in all experiments. To expand a culture, a frozen vial of MSCs ($1x10^6$ cells) was plated in 175-cm^2 cell culture flask containing 30 ml complete minimum essential medium Eagle alpha modification (MEM-α, 32561029; Gibco, UK) supplemented with 1% penicillin/streptomycin solution (P/S, 10,000 U/mL, 15140122; Gibco, UK), 10% heat inactivated fetal bovine serum (FBS, F9665; Sigma-Aldrich, UK) and 1 ng/ml basic human recombinant fibroblast growth factor (rhFGF, 100-18B; Peprotech, UK). Cells were incubated at 37 °C, 5% CO_2 and 20% O_2 in humidified atmosphere. After 2-3 days, non-adherent cells were removed, and culture growth medium was replaced until they reached approximately 70-80% confluence. Finally, medium was discarded and the adherent cells were gently washed with sterile PBS and the MSC monolayer detached using 5 ml of pre-warmed TrypLE™ Express (12605010; Gibco,UK) following incubation for 3-5 minutes at 37 °C. Cells were then washed twice with sterile PBS, counted and checked for viability via trypan blue.

2.5 *In vivo* transplantation of hUC-MSCs

For intravenous delivery of MSC, mice were warmed in a thermal cage for 5-10 minutes to dilate their tail vein and make it more visible so as to perform the injection more easily.

Mice were held in a tail vein injection restrainer which can help to easily rotate the mice to position their tail for injection. MSCs (About 250 or 500 X 10^5) was suspended in 200 µl of normal saline (PA931/1/1; Maco Pharma Ltd, UK) and were infused with a 29-gauge needle through a tail vein. Control mice received normal saline via tail vein injection alone at the same time as MSC treated animals. Prior to infusion, the cell suspension was filtered through a 50 µm Cell Tricks filter (04-004-2327; Sysmex, USA). The cells were maintained at 4° C, and they were gently mixed with a pipette to ensure they were not aggregated before infusion.

2.6 Pre-clinical murine models of acute liver injury

2.6.1 Animal breeding

All the animals used in this study were bred and used under standard conditions in the BioMedical Services Unit (BMSU) at the University of Birmingham in accordance with the guidelines for animal care in compliance with UK Animals (Scientific Procedures) Act 1986. All protocols and procedures performed under Home Office Project license number 70/7707.

Experimental mice (up to 5 mice/cage) were bred and maintained in a temperature-controlled sterile animal facility with 12-hour light/dark cycles at 23°C and permitted *ad libitum* consumption of water and a standard laboratory chow diet. C57/BL6 mice were purchased from Charles River Laboratories (London, UK) whereas transgenic mice strains used for this study were bred in-house at the BMSU of the University of Birmingham. In all the animal experiments, mice were randomly allocated to control or experimental groups.

2.6.2 CCl_4 model (induced acute liver injury)

To induce acute liver injury, male C57/BL6 mice at 8-10 weeks of age were injected intra-peritoneally with a single dose of carbon tetrachloride (CCl_4) (Sigma-Aldrich, product number 289116, MW=153.82g/mol, 99.95% concentration) 1 mg/kg diluted in mineral oil (Sigma-Aldrich). Mineral oil alone was used for control mice. Male C57Bl/6 mice were purchased from Charles River Laboratories (London, UK) and used at an average age of 8 to 10 weeks. Five hours after CCl_4 injection, animals were infused intravenously via tail vein with either 250K or 1M unsorted and sorted $CD362^+$hUC-MSCs in 200 µl normal saline, whilst control mice received normal saline. Three days after infusion of MSC, animals were sacrificed to collect blood and liver samples for further analyses as described above.

2.6.3 Transgenic OVA-BIL (a model of antigen specific induction of hepatobiliary inflammation)

OVA-BIL mouse model was previously developed by Buxbaum et al (2006)(Buxbaum et al., 2006). Ordinarily, OVA-BIL transgenic mice are tolerant of the over expression of ovalbumin (OVA) antigen on their biliary epithelium without any hepatic injury. However, adoptive transfer of OVA-specific $CD8^+$ (OT-l) and OVA-specific $CD4^+$(OT-ll) T cells isolated from spleens of OT-l and OT-ll transgenic mice into naïve OVA-BIL mice leads to dose-dependent biliary-centered necro-inflammation.

In this animal model, the author reported an increase in the serum ALT following adaptive transferred of OT-1 and OT-ll into Ova-Bil mice at different time and found to peak at 10 days. In addition, liver histological sections showed bile duct damage with inflammation

around the portal area increasing across time points to a maximum level at day 10 and resolved by day 28.

The inflammation response in this animal model is CD8 dependent, but the CD4 required to initiate more pathogenesis. CD4 alone have not shown to have any sign of inflammation or injury upon transferred to the OVA-BIL mice and the mechanism of CD4 in this animal model are not well defined. The immune cells were characterized in the liver during inflammation and found that the largest population was in the CD8+ cells (Most CD8+ cells were Vα2+) and small increase was reported in the CD4+ cells.

In addition, NK T cells were found to increase in the liver more than 6-fold after adaptive transfer for OT-1 and OT-11 solenocytes at day 10. Due to the heterogamous population of NKT cells in the liver, this animal model lacks the definition of the functional subsets of the NKT cells which is an area of feature study. The author also reported an increase in the inflammatory cytokines INFγ and TNFα during the hepatobiliary inflammation.

OVA-BIL mice strain used for this study were inbred and maintained as heterozygotes on a C57BL/6 background. Routine genotyping for heterozygous apical sodium-dependent bile acid transporter (ASBT)-membrane-bound ovalbumin (mOVA) in animals was carried out using real time PCR (Transnetyx, Inc. Tennessee, USA).

In this experiment, Induction of hepatobiliary injury was achieved by adaptive transfer of splenocytes from OT-l and OT-ll transgenic mice into male OVA-BIL mice. 10-12 weeks old male OT-l & OT-ll mice were sacrificed by schedule 1 method (cervical dislocation) and spleens from each animal were harvested and stored in cold RPMI medium. The harvested spleens were minced into small pieces and mashed through a 40μm cell

strainer. Cell suspensions were washed with cold 5% FBS/RPMI and the pellets were resuspended in 3 ml of red blood cell lysis buffer (Sigma-Aldrich) for 5-10 minutes. Samples were washed in PBS and centrifuged at 2000 rpm for 5 minutes. Cell pellets were resuspended in normal saline and an aliquot containing of $1x10^7$ OT-l and $1x10^7$ OT-ll splenocytes was injected intra-peritoneally into male OVA-BIL mice at 8-12 weeks of age. Control mice were injected with sterile PBS alone. At day 4 post injury, animals were infused again with 250K, 500K or 1M unsorted and sorted $CD362^+$hUC-MSC via tail vein. Animals were sacrificed 6 days after the administration of MSC to collect blood and liver samples for further analyses. Figure **2-2** briefly described the design of this experiment.

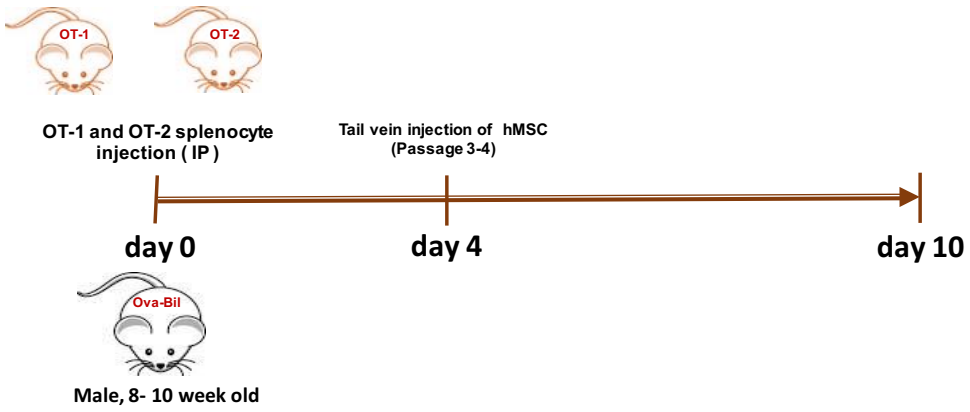

Figure 2-2 Experimental design. OVA-BIL mice were I.P. injected with $1x10^7$ OT-l and $1x10^7$ OT-ll splenocytes, followed by I.V. injection with MSCs, or with PBS four days later. At day 6 following the administration of MSCs, mice were sacrificed for harvesting the specimens.

2.7 Study of the time course of carbon tetrachloride (CCl_4) induced hepatotoxicity in mince.

In this experiment, acute liver injury was induced in mice by administration of a single intra-peritoneal (IP) dose of CCl_4. At different time points (12, 24, 48, 72, and 96 hours) after CCl_4 administration mice were anaesthetized using isopropanol and 0.6-1ml of blood collected by cardiac puncture and liver was harvested for further analyses. Blood was allowed to clot and then centrifuged at 10000 rpm for 10 minutes. After centrifugation, serum was separated and place in an Eppendorf tube for measurement of biochemical markers. The experimental design is illustrated in Figure 2-3.

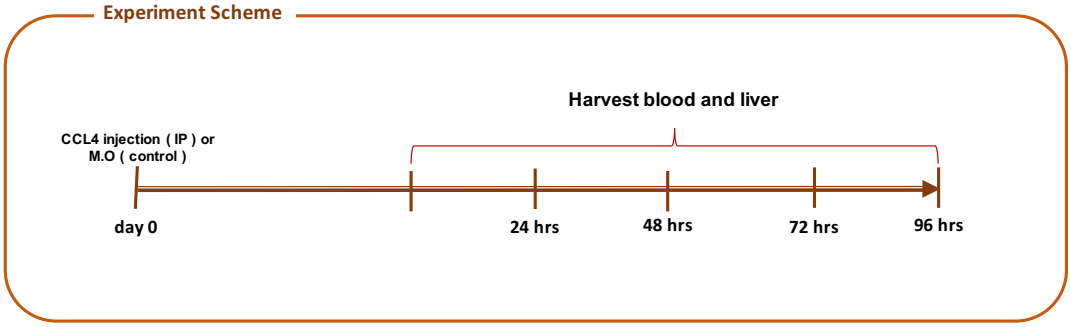

Figure 2-3 Overview of experimental design of time course study of CCl_4

2.8 Mouse immune cell isolation

2.8.1 Isolation of liver-infiltrating murine immune cells using OPTIPEP

To isolate lymphocytes and monocytes from mice, the largest liver lobe was harvested from each mouse, weighed and kept in a 7ml tube containing cold RPMI on ice. Livers were transferred into gentle MACS "C" tubes with 3 ml of cold plain RPMI and homogenized using a Gentle MACS Dissociator. The homogenized suspension was passed through a 70µm strainer into a 50ml Falcon tube. The MACS tube and the strainer were washed with RPMI to remove all the cells and topped up with RPMI up to 30 ml. This wash filtrate was transferred to 2x 15 ml tubes and was centrifuged at 2000rpm for 5 minutes with a brake. The pellet in each tube was resuspended in 5 ml RPMI (each sample has two separate tubes with 5 ml in each).

For each tube, 7ml of mouse OptiPrep Density Gradient Medium (Sigma-Aldrich, product number, D1556) was added to a new 15 ml Falcon tube, and in the same tube I layered 5 ml of the cell suspension on top of the Optiprep medium and centrifuged it at 1000g (with no break) for 25 minutes at room temperature. Following incubation, I carefully removed 2/3 of the medium using a plastic pipette and transferred the isolated layer from each tube into new 15 ml Falcon tubes. Isolated cells were washed with cold RPMI and centrifuged at 2000 rpm for 5 minutes. Cell pellets were washed again with MACS buffer (PBS+1mMEDTA+2% FCS), and then resuspended in 750µl of cold PBS (phosphate buffered saline) for flow cytometry analysis. For an overview of this method see (Figure ***2-4*** A).

2.8.2 Spleen mononuclear cell isolation

To isolate splenocytes, spleens were harvested from animals and collected on cold 5% FBS/RPMI medium for further processing. The harvested spleens were minced into small pieces and mashed through a 40µm cell strainer. The cell suspensions were washed with cold 5% FBS/RPMI and the pellets were resuspended in 3 ml of red blood cell lysis buffer (Sigma-Aldrich), for 5-10 minutes. Following cell lysis, cell suspensions were then washed two times with cold 5% FBS/RPMI medium before staining. Cells were washed twice with flow cytometry buffer and further analyzed by flow cytometry.

2.8.3 Isolation of circulating mononuclear cells

At the indicated time points after MSC administration, mice were anesthetized with isoflurane and blood collected by cardiac puncture. Blood was immediately placed in 200µl of EDTA blood tubes (459036; Greiner Bio-One Ltd). To lyse erythrocytes, blood was incubated at room temperature with 500 µl RBC lysis buffer (00-4333-57; eBioscience, UK) for 5 minutes, and then centrifuged at 2000 rpm for 5 minutes (Figure ***2-4*** B). The pellet was washed twice with cold RPMI, and cells were then resuspended in FACS buffer and used later for flow cytometry analysis. A schematic of the protocol used is shown in (Figure ***2-4*** B).

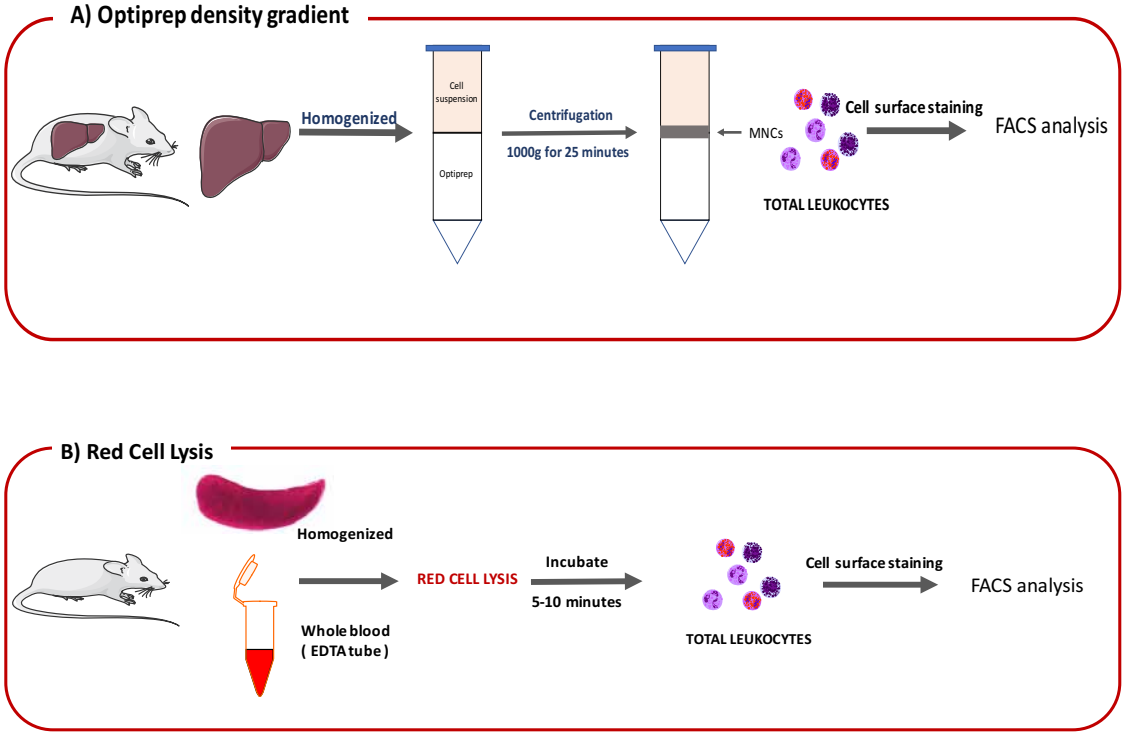

Figure 2-4 Preparation scheme for the isolation of total leukocytes from liver, spleen and blood: A) Liver were harvested and homogenized to obtained liver cell suspensions. Cell suspension from liver were pelleted using Optiprep medium, and centrifuged (1000g, 25 minutes, RT) to separate the MNCs layer. B) Blood was collected in EDTA tube and spleen was harvested and dissociated into single cell suspensions in PBS. Red blood cells lysis was performed using RBC lysis buffer.

2.9 Antibody staining and flow cytometry analysis

Cells from different sources were isolated and prepared as described earlier. Live dead staining (Fixable viability dye) was undertaken by addition of 0.5 µl of APC-CY7 viability dye to all samples, vortexing and incubation at 4°C for 30 minutes. Negative controls (unstained cells) and isotype matched controls (IMC) for each panel were prepared by transfer of 50 µl from each sample into separate tubes labelled as unstained

cells, live/dead and IMC (lymphoid & myeloid). Following incubation, 2ml of FACS buffer were added and centrifuged at 2000 rpm for 5 minutes. Cells were resuspended in a total of 200µl cold FACS buffer. The 200µl cell suspension was divided into two clean-labeled FACS tubes (100µl/tube) for flow cytometric analysis for both lymphocyte and monocyte panels.

The master mix of primary antibodies for both lymphoid and myeloid panel (for cell surface markers only) was prepared and added to each sample and incubated in a cold room for 30-45 minutes (Table ***2-2***). After incubation with primary antibodies, 2ml of FACS buffer was added to all the tubes, which were then vortexed and centrifuged at 2000 rpm for 5 minutes. Cells from the myeloid panel and unstained cells were resuspended in 400 µl FACS buffer and fixed by adding 100µl of 3% formalin (37% formaldehyde (sigma, Cat # F1635) and sterile PBS). Cells were then incubated at RT for 10 minutes and washed with 2 ml FACS buffer and then resuspended in 400µl of FACS buffer. All the tubes were kept in the cold room and were analyzed on the flow cytometer (Cyan, ADP Flow cytometer analyzer).

After staining cells with lymphoid antibodies specific for surface markers, I performed fixation and permeabilization procedure to detect the intracellular staining cells. The fixation and permeabilization working solution was prepared by diluting 1 part of fix and perm concentrate (ebioscience, Cat. 00-5123) with 3 parts of diluent (ebioscience, Cat. 00-5223). Permeabilization buffer (X10) was diluted to 1X with deionized water. 100µl of fixation and permeabilization working solution were added to each sample, vortexed and incubated in the dark for 30 minutes in a cold room. Following incubation, 1 ml of

permeabilization buffer was added to each tube and centrifuged at 2000 rpm for 5 minutes. The supernatant was discarded, and the pellet resuspended in 100µl FACS buffer. After fixation and permeabilization steps, we added the required amount of FoxP3 antibody to each tube of lymphoid panel and FoxP3 isotype to the IMC tube (lymphoid panel only). The tubes were incubated in the cold room for 30 minutes and washed twice with 2 ml of FACS buffer. Finally, the pellets were resuspended in 400µl FACS buffer and were filtered using a yellow filter before running them in Flow cytometer (Cyan, ADP Flow cytometer analyzer). 7 µl of AccuCheck counting beads (Invitrogen, PCB 100) were added to each sample just before running them on the flow cytometer. A single-cell suspension was prepared from each sample by passing the cells through a 40 µm cell strainer (08-771-1; Fisher Scientific, UK) and analyzed using a CyAn ADP flow cytometer (Beckman Coulter). All data were analyzed using FlowJo software version 8.7. The absolute cell count of cells was finally count according to this formula (***Absolute cell count (cell/µl) = (number of cell counted/total number of beads counted) X number of counting beads per µl),*** and the final calculation was normalized to the total tissue weight.

Table 2-2 Panels used in flow cytometer analysis for different lymphoid and myeloid markers

A) Lymphoid Panel					
CD marker	Fluorochrome	Isotype	Volume required/ test (µl)	Master mix (55 sample) (55X60)/DF	Volume of IMC (µl)
CD19	Brilliant violet (421)	Rat IgG2a	1(1:200)	16.5	0.5
CD3	Brilliant violet (510)	Rat IgG2b	5(1:40)	82.5	2.5
CD49b	Alexa Fluor (488)	Rat IgM	0.5 (1:400)	8.3	0.5

Foxp3 (Treg)	PE	Rat IgG2a	5 (1:40)	82.5	2.5
CD25	PE/Dazzle (594)	Rat IgG1	2.5 (1:80)	41.3	1.3
CD8a	PreCP-Cyanine 5.5	Rat IgG2a	1(1:200)	16.5	0.5
CD69	PE/Cy7	Armenian Hamster IgG	5 (1:40)	82.5	2.5

B) Myeloid Panel					
CD marker	Fluorochrome	Isotype	Volume required/ test (µl)	Master mix (55 sample)	Volume of IMC 100µl
Ly-6C	Brilliant violet (421)	Rat IgG2c	5 (1:40)	82.3	2.5
LY-6G	Brilliant violet (510)	Rat IgG2a	5 (1:40)	82.3	2.5
CD11b	Alexa Fluor (488)	Rat IgG2b	1 (1:200)	16.5	0.5
F4/80	PE	Rat IgG2a	5 (1:40)	82.3	2.5
CD45	PerCP-Cyanine5.5	Rat IgG2b	0.5 (1:400)	8.3	0.5
Gr-1 (Ly-6G/Ly-6C)	APC	Rat IgG2b	1 (1:200)	16.5	0.5
CD11c	PE/CY7	Armenian Hamster IgH	1 (1:200)	16.5	0.5

2.10 Flow cytometric gating strategy for analysis of intra-hepatic immune cell subsets.

Hepatic infiltrating immune cell subsets (lymphocytes and monocytes) were isolated from mouse liver using OPTIPREP gradient medium (as described previously). All antibodies, including the isotype controls used in this study are listed in (Table ***2-2***). All data were analyzed using the Flow Jo software (http://www.flowjo.com). Flow cytometric gating strategy for analysis of monocytes and lymphocytes population is shown in (Figure ***2-5*** and Figure ***2-6***).

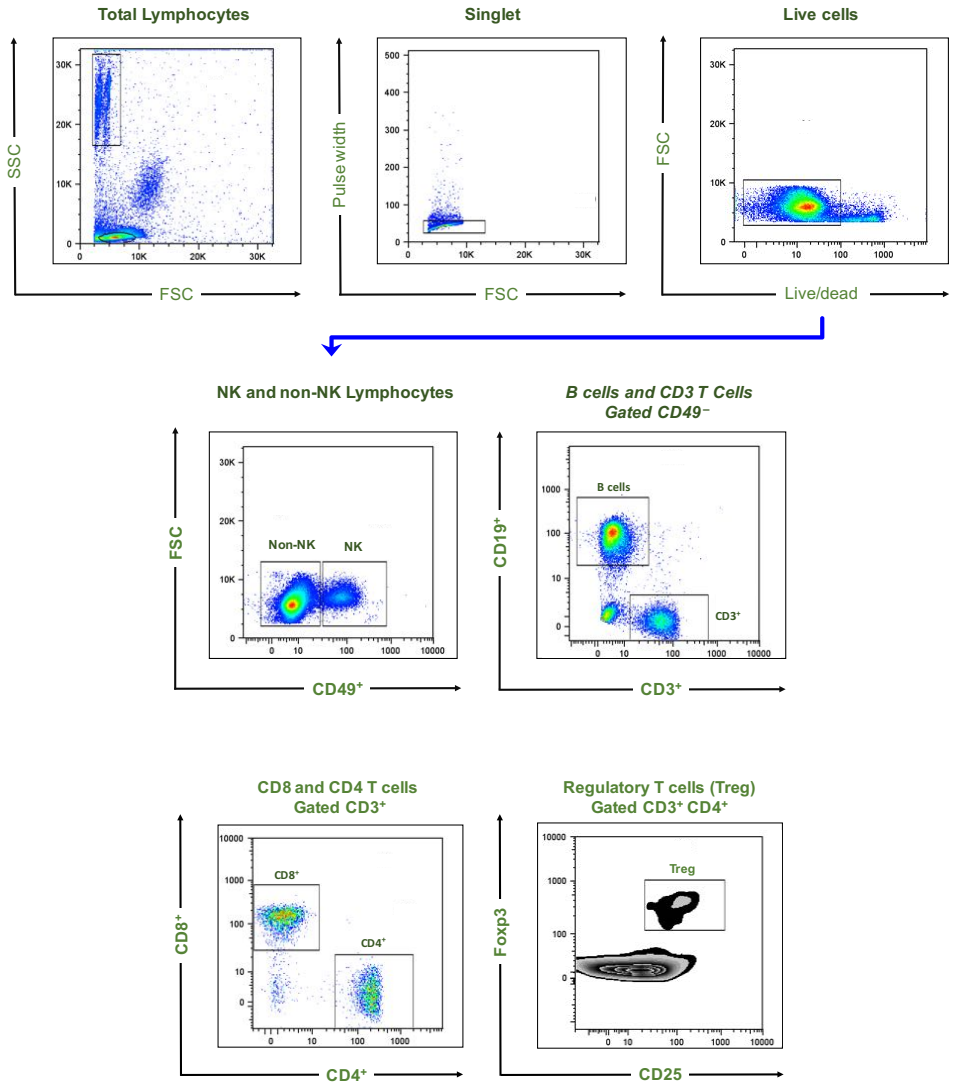

Figure 2-5 Flow cytometer analysis of lymphocyte sub-populations in mouse liver. Lymphocyte populations were gated on the side scatter and forward scatter. Debris and dead cells were determined and excluded. From the total live cells NK cells were excluded by CD49b+ expression. From the CD49b^{-} population, two distinct populations were gated based on CD19+ (B cells) and CD3+ expression. From the CD3+ population, I gated CD4+ and CDB+ cells. Finally, the CD4+ cells were gated for further analysis of the expression of Treg population (Foxp3+ CD25+).

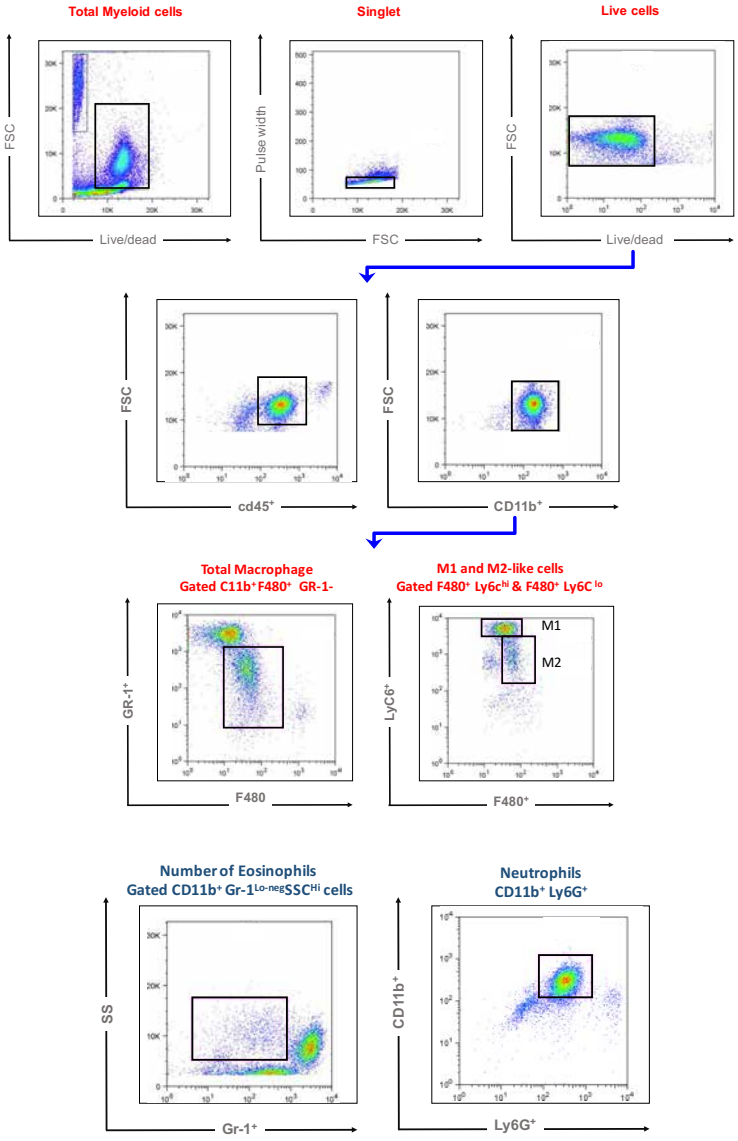

Figure 2-6 Flow cytometer analysis of monocytes in mouse liver. Monocyte populations were gated as follows. Debris and dead cells were determined and excluded. I identified several populations after gating the live cells with CD11b+. A) F4/80+ cells (total macrophage), B) Gr-1 + cells (neutrophil). Total macrophages were divided into classic (M1) and alternative macrophages (M2), as shown in C and D respectively. Both cells stained with (C11b+, F480+, Ly6c). Eosinophil populations of myeloid cells were gating on (CD11b+ and Gr-$^{1lo\text{-}neg}$ SSC^{Hi}).

2.11 Tracking of hUC-MSCs *in vivo* after infusion.

2.11.1 Cryo-imaging of UC-MSCs labeled with Quantum Dots

In order to label MSCs for *in vivo* cell tracking, I used Qtracker Cell Labeling Kits (Qtracker® 625 Cell Labeling Kit, Invitrogen, A10198) and the labelling procedure was performed according to the manufacturer's instructions. I prepared a 10 nM labeling solution by mixing 1 µL each of Qtracker Component A and Component B in a 1.5 mL micro-centrifuge tube (1 µL of each component/1X10^6 cells). Both compounds were mixed and incubated for 5 minutes at room temperature. For each 1x10^6 cells, 0.2 mL of fresh complete growth medium was added to the tube and vortexed for 30 seconds. The cell suspension was then added to the tube containing the labelling solution. The samples were incubated at 37 °C for 45–60 minutes in dark. After incubation, labeled cells were washed twice with complete growth medium and resuspended in normal saline for infusion. Cells were kept on ice until ready for injection. Injections were performed intravenously via tail vein using standard techniques. Following cell injection, mice were culled by CO_2 at various time points and whole mice were embedded in fresh mounting medium (O.C.T. compound; VWR Chemicals, UK) and kept on dry ice until frozen. The whole mice were then stored at -80 °C until shipment for analysis. All mice were analyzed by BioInVision Inc, Cleveland, USA. BioInVision's CryoViz™ cryo-imaging system was used to study bio distribution of QD labelled-MSCs in organs and in the whole mouse by serial sectioning and imaging. The CryoViz™ technology picked up the signal of clusters of Qtracker 605 quantum particles, which were internalized in the hUC-MSC. Labelled cells were analyzed by co-registration of bright field and confocal images to generate three-dimensional anatomical and molecular fluorescence videos of the frozen

whole mice samples. Cell counts in organs and whole mouse were quantified using imaging algorithms. Figure ***2-7*** illustrated the protocol used for cell labelling.

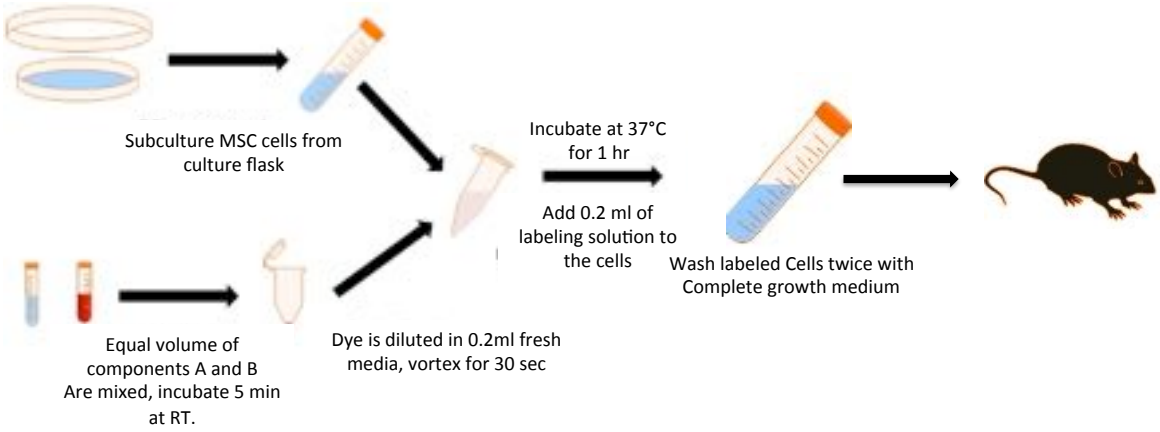

Figure 2-7 A schematic representation of the protocol used for labeling MSCs with Qdots.

2.12 Liver histology: Haematoxylin and Eosin (H&E).

After culling mice, mice liver lobes were harvested and fixed in 10% formaldehyde for a few days, then embedded in paraffin, and liver sections cut at 4μm thickness. For histological examination and to assess changes in liver structure, liver sections were rinsed three times in xylene (to dissolve all the wax away) and then dehydrated with serial dilution of alcohol (99%, 95%, and 70%) for 5 minutes periods. Slides were washed twice and sections were stained with haematoxylin and eosin (VWR International, UK). Following H&E staining, slides were passed through different dilutions of alcohol and then rinsed in different baths of xylene. Finally, slides were mounted using DPX

mounting medium and left for few hours to dry. Liver sections were scanned at ×20 magnification using an automated fashion and identical settings on an AxioScan Z1 (Zeiss) slide scanner.

2.13 Immunohistochemistry (IHC).

All slides used were paraffin sections. Slides were de-waxed and rehydrated as described previously. I carefully drew a ring around the section using a wax pen and then placed the slides in a humidified plastic chamber. To block endogenous peroxidase activity 150µl of Dako peroxidase blocking solution was added to each section and incubated for a further 40 minutes on a rocker. After incubation, slides were washed twice with TBS+0.1 Tween for 5 minutes. Ttris buffered saline (TBS) was prepared by dissolving 1 tablet of TBS (pH 7.6, sigma) in 500ml of deionized water. Antigen retrieval was performed to unmask antigen epitope by mixing 10ml of concentrated antigen unmasking solution (EDTA-NAOH, pH 8.0) with 990ml of distilled water in plastic bucket and microwaved at high power for 5 minutes to heat the solution. Slides were transferred into a plastic bucket and heated for 15 minutes. After heating, slides were washed two times with TBS+0.1 Tween for 5 minutes. Non-specific staining was blocked by addition of 150µl of casein buffer (diluted x10 stock in DW) to each section and incubation of the slides on a rocker for 30 minutes. Sections were incubated with primary antibody (diluted in TBS) for 1 hour (Table ***2-3***). After washing two times with TBS+T, sections were incubated with anti-rat IgG (Vector impress, peroxidase) for a further 30 minutes. After washing again with TBS+T, sections were incubated with 200µl of DAP substrate (prepared by adding 1 drop of chromagen to 1ml of DAP buffer) for 2-3 minutes and then slides gently rinsed in tap water. Finally, haematoxylin stain was added to each section

and incubated for 20 seconds; slides were then washed with tap water. Slides were passed through different dilutions of alcohol and then rinsed in different bath of xylene. Finally, slides were mounted using DPX mounting medium and left for a few hours to dry. Liver sections were scanned at ×20 magnification using an AxioScan Z1 (Zeiss) slide scanner. Depending on the size of the sections, more than 10 random non-overlapping fields of view per liver lobe were selected to measure the positive areas of these markers using ImageJ software.

Quantification analysis of histological staining using ImageJ program

In order to turn our imaging into quantifiable data, we used ImageJ program to measure the intensity of the immunohistochemistry staining in the liver sections. Image needs to be opened in the imageJ program and the following steps applied: (1) select (image-split channel), this will split the image into black and white which help to clearly distinguished between the positive and the negative staining. (2) select (image-adjust-threshold), and then moved the sliders manually until all the staining areas become red, the red colour indicate the positive area of staining. (3) click on “set” to see the threshold of the image followed by selectin (analyse-measure), % of the area will be displayed in the results window and can be saved as the intensity measurement of the positive staining in the tissue section. Figure (2-8) below illustrate how to quantify the histological staining using ImageJ program.

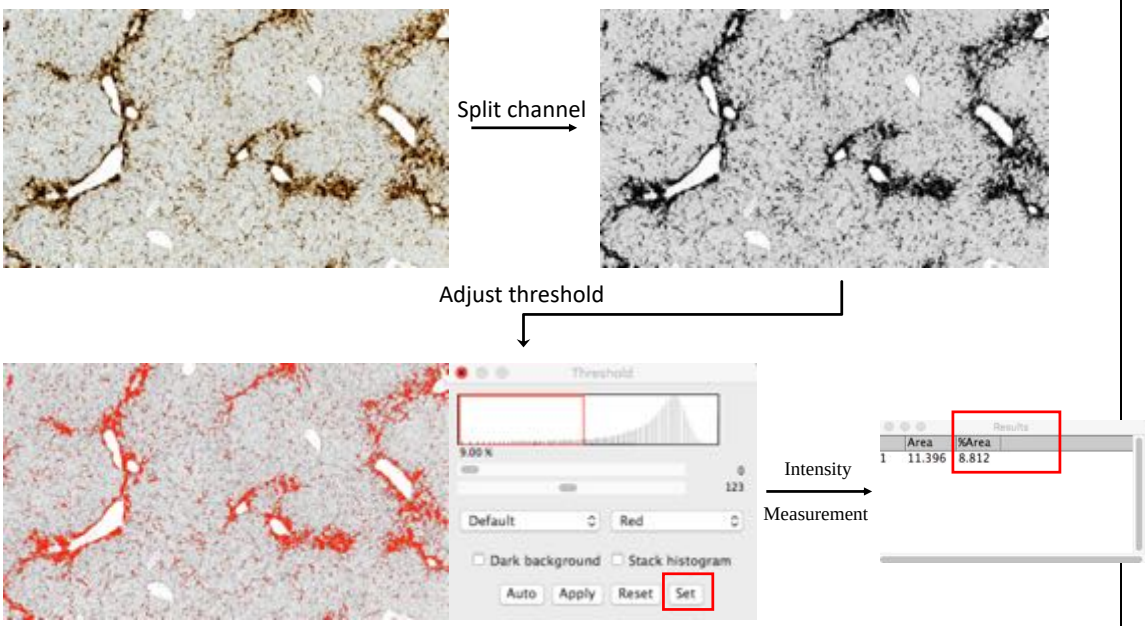

Figure 2-8 overview of the analytical process of the quantification analysis of histological staining using ImageJ program.

Table 2-3 Antibodies and the dilutions used in IHC.

Antibody	Host	Secondary antibody	Dilution	Specificity	Isotype
CD45	Rat	Anti-rat	1:200	Mouse	IgG2b
F480	Rat	Anti-rate	1:200	Mouse	IgG2b
ICAM	Rat	Anti-rat	1:200	Mouse	IgG2b
VCAM	Rabbit	Anti-rabbit	1:400	Mouse	IgG2b
Anti-Ki67	Rabbit	Anti-rabbit	1:200	Mouse	IgG
Beclin 1	Rabbit	Anti-rabbit	1:200	Mouse	IgG
H2A.X	Rabbit	Anti-rabbit	1:200	Mouse	IgG

2.14 Apoptosis Staining (TUNEL assay)

Liver DNA damage of apoptotic cells was verified using terminal deoxynucleotidyl transferase-mediated biotinylated- dUTP nick-end labeling (TUNEL) staining. Apoptotic cells in liver sections were identified by using the In-Situ Cell Death Detection Kit Fluorescence (Roche Applied Science, UK), following the manufacturer's instructions. Paraffin sections were de-waxed and rehydrated as described previously. Sections were then rinsed with PBS for 5 minutes and antigen retrieval was performed to unmask antigen epitope. This was done by microwaving the solution at high power for 10 minutes. Non-specific staining was blocked by adding casein buffer to each section and incubated for 30 minutes. Sections were washed in PBS for 5 min and 50 µl of TUNEL reaction mixture were added to each slide and incubated for 60 min at 37 °C. The sections were washed three times with PBS and the nuclei were stained with DAPI staining. Finally, slides were mounted with coverslips using DPX and imaging for each slide was taking using light microscopy (Carl Zeiss AG).

2.15 RNA Isolation and Quantitative Polymerase Chain Reaction (qPCR) Analysis

Liver tissues were immediately snap frozen in liquid nitrogen and then stored at -80°C until mRNA extraction. Tissue samples were thawed on ice and mRNA extraction was carried out using an RNeasy mini kit in accordance with the manufacturer's instructions (74104; QIAGEN). RNA was also extracted from freshly cultured MSCs using an RNeasy micro kit in accordance with the manufacturer's instructions (74004; QIAGEN). Briefly, liver tissue (~30 mg) was transferred into gentle MACS "M" tube with 600 µl of

RLT buffer and homogenized using a Gentle MACS Dissociator. 600 µl of 70% ethanol was added to the lysate and mixed well by pipetting. The samples were transferred to an RNeasy spin column and placed in a 2-ml collection tube, centrifuged at 13.000 rpm for 15 seconds, the supernatant was then discarded. Samples were washed with 600 µl RW1 buffer then centrifuged at 13.000 rpm for 15 seconds. Samples were washed again twice with 500 µl and centrifuged at 13.000 rpm for 15 seconds. The RNeasy spin column was replaced with new collection tubes and the old collection tubes discarded. They were then centrifuged at 13.000 rpm for 1 min. Finally, the RNeasy spin column was placed in an Eppendorf and 40 µl RNase free water was added directly to the spin column membrane. The column was centrifuged at 13.000 for 1 min to elute the RNA, this step repeated twice to yield 80 µl of RNA. Following RNA extraction, mRNA concentration and purity of each sample was measured using a Nanophotometer (Gene flow Ltd).

A total of 5 µg of mRNA was transcribed to complementary DNA (cDNA) using Superscript II reverse transcriptase kit (18064014; Invitrogen, UK) using a standard protocol. In brief, the final reaction was incubated for 10 minutes at 25°C, followed by 50 minutes at 45°C, and finally by heating at 70°C for 15 minutes. The cDNA was then amplified by qPCR for each sample in triplicates using probes listed in (Table 2-4) and TaqMan Universal master mix ii kit (4304437; Applied Biosystems, UK). PCR was performed using a Roche Light cycler 480 machine (Roche, UK). Initially reactions were incubated at 95°C for 10 minutes, followed by 50 cycles at 95°C for 10 seconds, 55–60°C for 50 seconds and 72°C for 1 second. Cycle thresh hold (Ct) for relative quantification of genes of interest were normalized to the appropriate housekeeping gene, GAPDH (Mm99999915_g1; Applied biosystems, UK). Relative expression levels were shown as fold change compared with the appropriate untreated control samples. Quantification of

the gene expression was calculated using the ΔΔCt method. For each sample, the average of Ct values was taken, and the average Ct value for GAPDH was subtracted from the Ct value for the gene of interest to give ΔCt **(Ct (gene of interest- Ct control (GAPDH)).** The ΔΔCt value was calculated by subtract the ΔCt for the treated sample from the ΔCt of untreated. Then the relative quantification (RQ) values for each sample were determined using the following formula: **QR= ($2^{-\Delta\Delta Ct}$).**

Table 2-4 Primer sets for qPCR analysis

Gene Symbol	Gene description	Species	TaqMan assay ID
SOD1	superoxide dismutase 1	Mouse	Mm01344233_g1
SOD2	superoxide dismutase 2	Mouse	Mm01313000_m1
SOD3	superoxide dismutase 3	Mouse	Mm01213380_s1
GSS	glutathione synthetase	Mouse	Mm00515065_m1
CAT	Catalase	Mouse	Mm00437992_m1
IHD-1	isocitrate dehydrogenase 1	Mouse	Mm00516030_m1
HO-1	heme oxygenase 1	Mouse	Mm00516005_m1
NOS2	nitric oxide synthase 2	Mouse	Mm00440502_m1
P62	sequestosome 1 (P62)	Mouse	Mm00448091_m1
Bcl-2	Bcl-2	Mouse	Mm00477631_m1
Cyp2e1	Cyp2e1 (cytochrome P450)	Mouse	Mm00491127_m1
ICAM-1	intercellular adhesion molecule 1	Mouse	Mm00516023_m1
VCAM-1	vascular cell adhesion molecule 1	Mouse	Mm01320970_m1
Pecam1	platelet/endothelial cell adhesion molecule 1	Mouse	Mm01242576_m1
Bcl2l1	BCL2-like 1	Mouse	Mm00437783_m1
Birc5	baculoviral IAP repeat-containing 5	Mouse	Mm01261895_m1
GAPDH	glyceraldehyde-3-phosphate dehydrogenase	Mouse	Mm99999915_g1

2.16 Assessment of liver function

At the indicated time points after MSC administration, mice were anesthetized with isoflurane in 100% oxygen for 3-5 minutes. Blood was collected by cardiac puncture and blood was placed in a tube until further processing. Blood was then centrifuged at 10000 rpm for 10 minutes to separate the serum which was placed into a new Eppendorf for evaluation of biochemical markers. The levels of serum alanine transaminase (ALT) and aspartate transaminase (AST) were measured by an Olympus AU400 analyzer (Beckman Coulter, Brea, CA) at the clinical biochemistry laboratory of the Women's Hospital Birmingham (Birmingham, United Kingdom).

2.17 Inflammatory cytokine detection by multiplex immunoassay

Blood samples were collected from each mouse and serum was obtained by centrifugation at 10000 rpm for 10 minutes. Serum samples were stored at -80 until the analysis day. Mouse Cytokine / Chemokine Magnetic Bead Panel kit (Merck Millipore, MCYTOMAG-70K-PMX) were used in this study to measure different cytokines and chemokines in mouse serum. This assay was performed according to the manufacturer's instructions. Cytokines measured in this assay were granulocyte colony stimulating factor (G-CSF), Eotaxin, granulocyte monocyte colony stimulating factor (GM-CSF), INFg, IL1b, IL6, IL7, IL10, LIX, IP10, keratinocyte chemoattractant (KC), monocyte chemoattractant protein (MCP1), macrophage inflammatory protein (MIP1a), and TNF-a. This assay was performed by colleagues at the Erasmus Medical Center, Netherlands.

2.18 Cytokine Treatment of MSC

MSCs were seeded in six-well plates at a density of 4,000 cells per square and cultured until 70–80% confluency. Fresh MSC media contained recombinant human TNF-α or IFN-γ (R&D Systems UK) at a final, concentration of 10 or 20 ng/ml. After 24 and 48 hours of treatment, cytokines were washed with PBS buffer and MSCs were detached and used for gene expression analysis.

2.19 Statistical analysis.

Statistical analysis of all data was performed using Prism 7.00 software (GraphPad, CA). Normality tests were applied by using D'Agostino-Pearson omnibus or Shapiro-Wilk normality tests. For parametric data, statistical significance was analysed using unpaired Student t-test. If the data were non-parametric, the Mann-Whitney U test was applied to test for significance. One-way ANOVA was used to compare between two different groups or Kruskal-Wallis test, if the data were non-parametric. The results were reported as the mean ± SEM unless otherwise noted. Differences were considered statistically significant when P value < 0.05. Significance was reported as: *$\leq$0.05; **$\leq$0.01; ***$\leq$0.001.

CHAPTER 3

CHARACTERIZATION OF MESENCHYMAL STROMAL CELLS DERIVED FROM UMBILICAL CORD TISSUE

3.1 Introduction

Mesenchymal stromal cells (MSCs) are a subtype of adult fibroblast-like cells that have the capacity of self-renewal with high proliferative ability. They can undergo tri-lineage differentiation both *in vivo* and *in vitro* down connective tissue lineages to become osteoblasts, chondrocytes and adipocytes. Furthermore, MSCs have been defined on the basis of their surface antigen expression of CD105, CD73 and CD90 by flow cytometric analysis. Additionally, these cells should lack expression of CD11b, CD79a, CD19, and HLA class II, and should not express haematopoietic markers such as CD45, CD34, and CD14. (Kim et al., 1994)

These cells are found in various human tissue, including synovial membrane(Ogata et al., 2015), adipose tissue (AT)(Melief et al., 2013b), umbilical cord blood (UCB)(Lee et al., 2004a), amniotic fluid (AF)(Zagoura et al., 2012) and placenta(LI et al., 2005). Umbilical cord tissue (UC) has been a particularly promising source of MSC - cells can be isolated from several compartments within UC including umbilical vein, umbilical arteries, umbilical cord perivascular tissue, Wharton's jelly and sub-amniotic tissue. Furthermore, MSCs isolated from UC tissue are believed to have more proliferation potential than other cells isolated from other tissues and are found in higher numbers, ensuring this source is gaining prominence.

MSCs are a heterogeneous population of cells that are phenotypically diverse both morphologically and functionally, therefore, sorting of cells based on marker expression has been considered to achieve a more homogenous population of cells. This could potentially resul in enriched subsets with different therapeutic effects. This does require definition of which function is being focused on, and often markers of stem-ness or proliferation are reported, whereas immunomodulatory actions may be more important.

Sorting of cells for pre-clinical studies is relatively straightforward and can use a range of modalities including flow cell sorting which can result in high purity cell yields.

A recent novel marker, $CD362^{+}$ (Syndecan-2), has been reported to select a homogeneous population of MSCs with superior immunomodulatory properties. This marker was under patent number (WO 20131177661 A1) and is owned by Orbsen Therapeutics, Ireland. Syndecan-2 is a transmembrane heparin sulphate proteoglycan, which contributes to several biological functions; it can contribute to zebrafish vascular development (Chen et al., 2004a), cellular adhesion (Canosa et al., 2017), control apoptosis in osteoblastic cells(Modrowski et al., 2005) and is involved in T cell biology (Teixé et al., 2008). Syndecan-2 is expressed in different cells throughout the body, which have different expression profile under normal or pathological conditions. It is expressed primarily on endothelial cells and fibroblasts, although it is also reported to expressed on human monocytes and monocyte-derived macrophages (Clasper et al. 1999). Furthermore, PCR data reveal that monocyte can produce syndecan-2 in culture upon stimulated with cytokines (TNF-α and LPS), interestingly, LPS stimulated monocytes have more expression potential than TNF-α stimulated cells. Additionally, syndecan-2 was also reported in monocyte derived macrophages (Clasper et al. 1999). Similarly, activated CD4 T cells were found to enhance secretion of syndecan-2 (Teixé et al., 2008). More recently, This marker was found to have the ability to reduce immunogenicity and play a role in immune regulation (De Witte et al., 2017; de Witte et al., 2015). For example, Syndecan-2 has also linked to contribute to modulate T cell biology through regulation of the T- cell receptor (TCR/CD3) complex expression, which can enhance the ability of T cell to response to any stimuli (Rovira-Clavé et al., 2012). Although Syndecan-2 was

reported to have possible role to control fibrosis by modulate expression of TGF-β in fibroblast cells (Chen et al., 2004b).

3.2 Chapter Aims

Human umbilical cord MSCs were provided by an industrial collaborator (Orbsen Therapeutics, Ireland). Two different cells subsets have been used in this study; unsorted UC-MSC and sorted UC-MSC based on expression of CD362. In this chapter, I focused on investigating the following:

- To analyze the phenotypic characteristics of both populations of UC-MSCs by characterising the expression of MSC surface markers using flow cytometry.
- Study the multi-lineage differentiation capacity of both populations of UC-MSC with regards to adipocyte, chondrocyte and osteocyte lineages.
- Evaluate the expression of CD362 among MSCs isolated from different donors and the potential stability of CD362 expression when cultured over later passage.

3.3 Results

3.3.1 Phenotypic characterization of mesenchymal stromal cells in umbilical cord (UC-MSC)

To determine whether UC-MSC had the ability to expand in culture and form a fibroblast like cells (spindle shape), they were cultured in AMEM and 10% FBS. The cells demonstrated a fibroblast-like appearance as showed in Figure ***3-1*** and reached confluence after 4 days (UC-MSCs with passage 2).

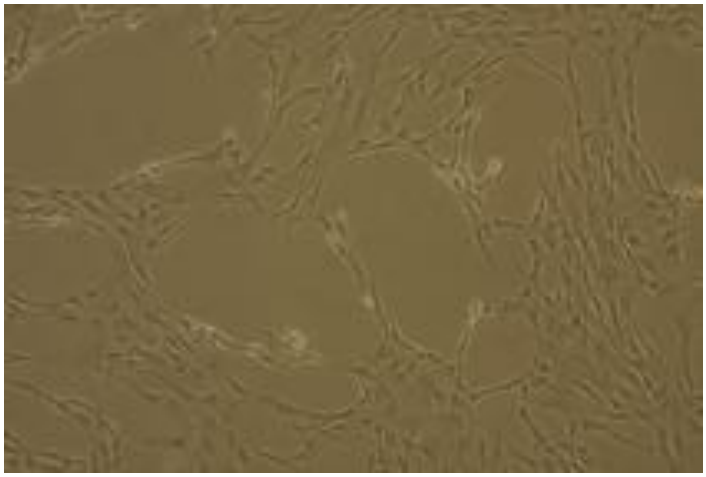

Figure 3-1 UC-MSCs display fibroblast like cells (spindle shape) morphology (one day after culture in AMEM at passage 2).

The presence of positive (CD105 PerCP-Cy™5.5/CD73 APC/CD90 FITC) and negative (CD45/CD34/CD11b/CD19/HLA-DR PE) surface antigen markers of UC-MSC was determined by flow cytometry. At passage 3 both unsorted (US) and $CD362^{+}$ sorted UC-

MSC expressed positive markers (CD90, CD105, CD73, and CD44) and were negative for (CD45, CD34, CD11b, CD19, and HLA-DR). There were no significance differences in the expression of these antigens between the two cell populations. Figure **3-2** and Figure **3-3** represent all the histograms for these markers on unsorted and $CD362^{+}$ UC-MSC, respectively. Percentage expression and median fluorescence intensity (MFI) of the two populations are presented in Table ***3-1***.

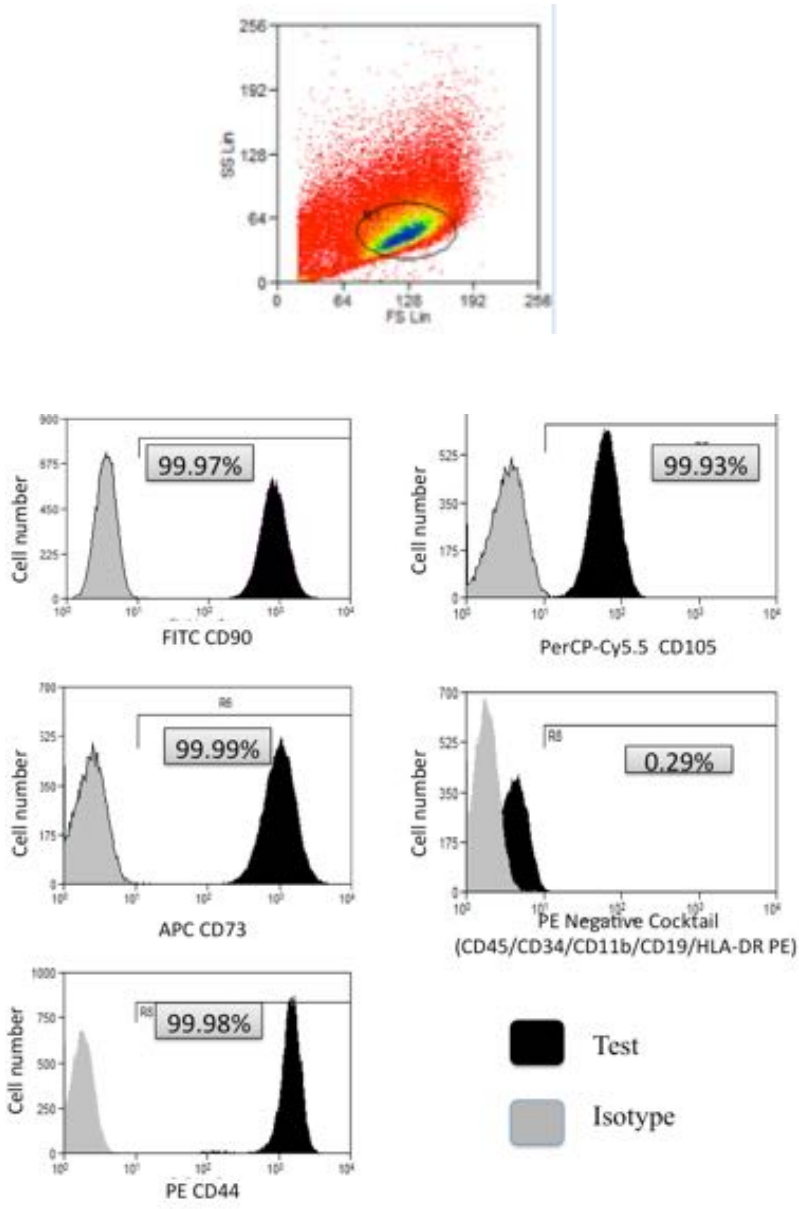

Figure 3-2 Flow cytometric analysis of positive and negative markers expressed on unsorted UC-MSCs. Cells were positive for CD90, CD105, CD73 and CD44, but negative for CD45, CD34, CD11b, CD19 and HLA-DR.

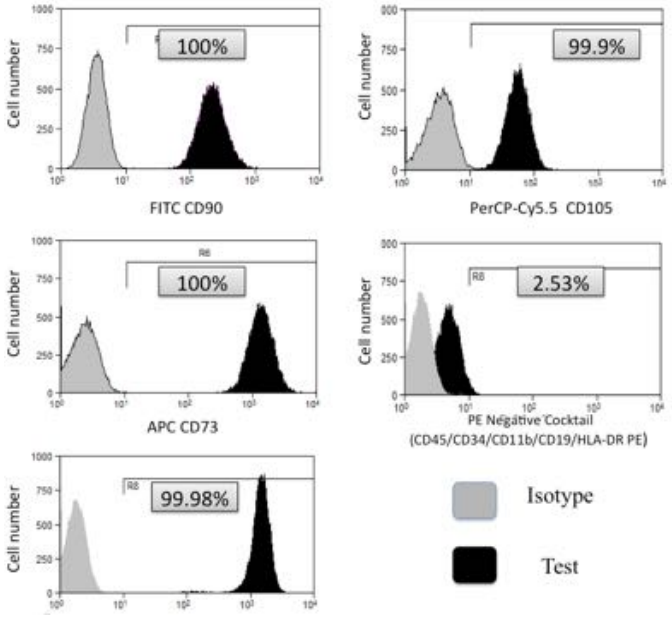

Figure 3-3 Flow cytometric analysis of positive and negative markers expressed on CD362^{+} sorted UC-MSCs. Cells were positive for CD90, CD105, CD73 and CD44, but negative for CD45, CD34, CD11b, CD19 and HLA-DR.

Table 3-1 Comparison between percent of expression and median fluorescence intensity (MFI) of all the positive and negative markers of UC-MSCs (US and CD362+)

		Markers	Expression (%)	Median Fluorescence intensity (MFI)
UC-MSCs	Unsorted cells	CD90	99.97	936.60
		CD105	99.93	67.64
		CD73	99.99	1152.20
		Negative cocktail (D45, CD34, CD11b, CD19, and HLA-DR)	0.29	12.04
		CD44	99.98	1566.52
	CD 362 sorted cells	CD90	100	149.19
		CD105	99.99	60.90
		CD73	100	1530.70
		Negative cocktail (D45, CD34, CD11b, CD19, and HLA-DR)	2.53	11.47
		CD44	99.98	1566.52

3.3.2 Unsorted and CD362 sorted UC-MSCs demonstrated multipotent differentiation potential *in vitro*.

To investigate the tri-lineage differentiation potential of UC-MSCs, unsorted and CD362+ cells were cultured under standard adipogenic, chondrogenic and osteogenic differentiation conditions.

Adipogenesis: Cells from passage 3 were cultured in 12 well-plates for 14 days in adipogenic medium. Lipid vacuoles were observed microscopically in cells along with positive Oil Red staining for both cell types, as shown in Figure ***3-4***.

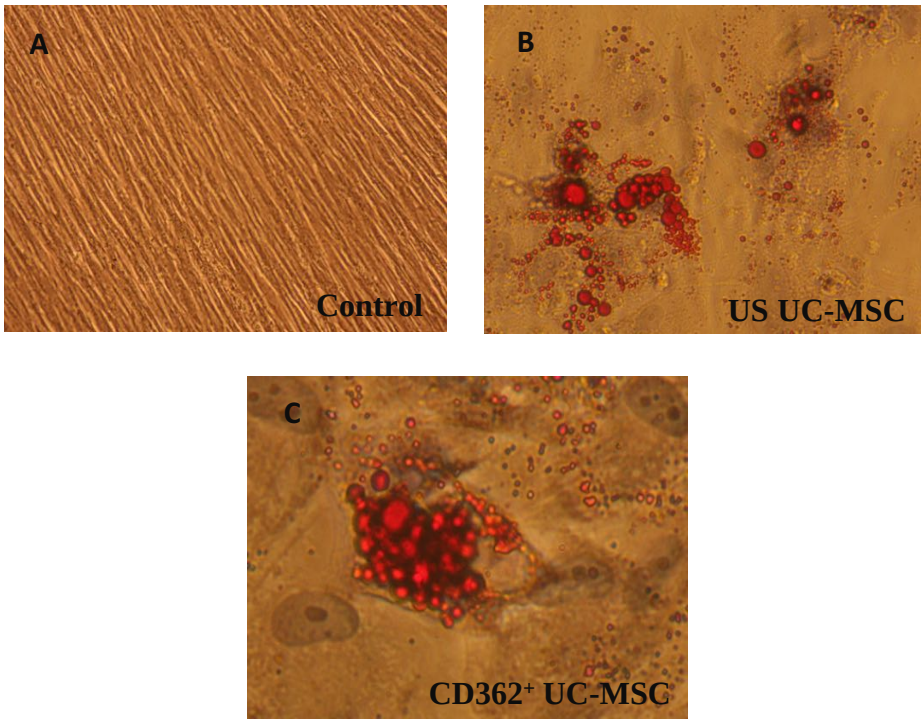

Figure 3-4 Adipogenic differentiation of mesenchymal stromal cells derived from umbilical cord tissue. Oil red staining was used to visualize lipid deposition cells. A) Control cells. B) US UC-MSCs in adipogenic condition showing some differentiated cells after 14 days of culture. C) CD362+ UC-MSCs represent clear adipocyte cells stained by Oil red.

Chondrogenic differentiation: 2.5 x 10^5 MSCs were cultured as a pellet and placed in chondrogenic differentiation medium. After 21 days, the pellets were snap frozen and prepared for frozen sections. The presence of proteoglycans and glycosaminoglycan was examined by toluidine blue staining (Figure ***3-5***). Passage 3 cells were cultured under osteogenic differentiation medium, and after 21 days of incubation, cells were stained with 1% Alizarin red staining to assess the level of calcium deposition. US and $CD362^+$ UC-MSCs represent low level of calcium formation (Figure ***3-6***).

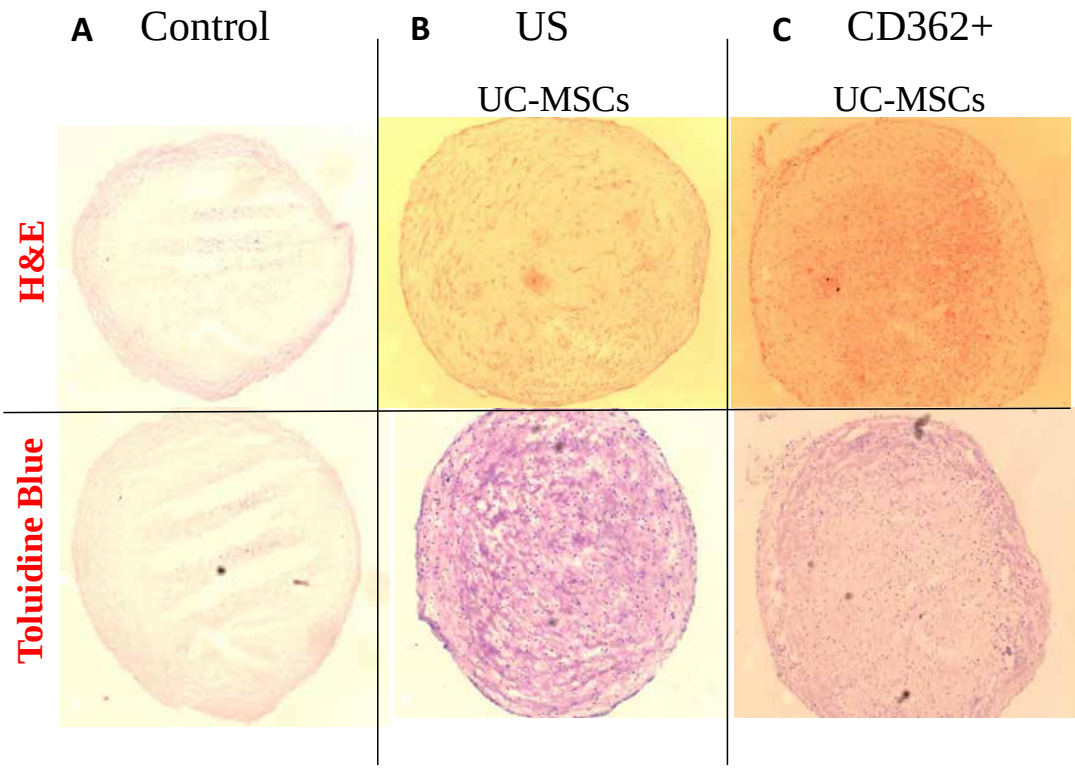

Figure 3-5 Chondrogenic differentiation of umbilical cord tissue derived mesenchymal stromal cells (US vs CD362+ MSCs). A) Control cells. B-C) UC-MSCs (US) and ($CD362^+$) cells stained with toluidine blue after chondrogenic induction for 21 days, also the same cells were stained with H&E. The entire picture was taking using lower magnification (X10).

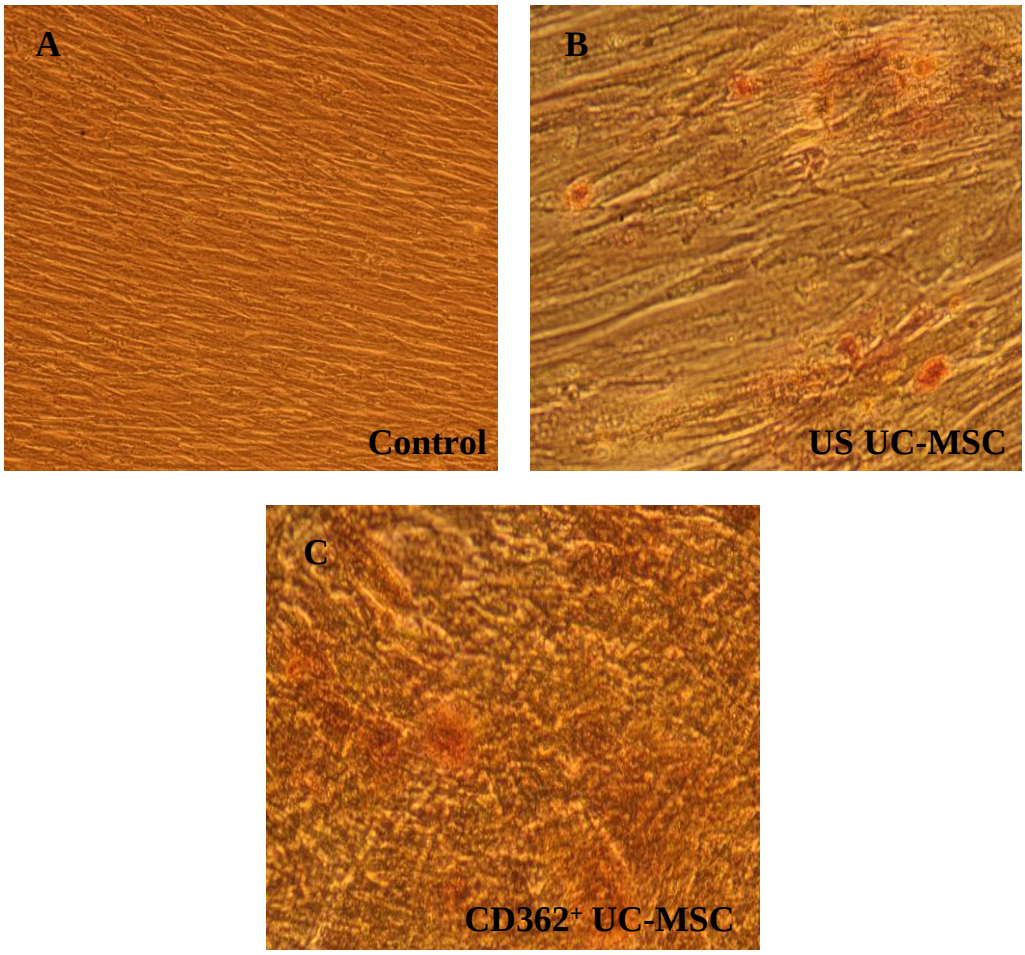

Figure 3-6 . Osteogenic differentiation of mesenchymal stromal cells derived from umbilical cord tissue. Alizarin red staining was used to visualize calcium deposition cells. A) Control cells. B) UC-MSCs (US) in adipogenic condition showing low level of differentiated cells after 21 days of culture. C) CD362+ UC-MSCs represent trace number of osteocyte-differentiated cells stained by Alizarin red.

3.3.3 Source and selection of UC-MSCs

Using flow cytometry, we investigate the expression of CD362 of MSCs derived from different sources, Bone Marrow (BM) and umbilical cord (UC). Notably, MSCs derived from BM and UC have different profiles of CD362 expression. Notably, CD362 was

found to downregulated in BM-MSCs as the number of passage number increase to passage 3. However, we observed a stable expression of CD362 in UC-MSCs at the same passage number. These results suggested that UC-MSCs have the capacity to express CD362 at different passage numbers, whereas BM-MSCs have no expression ability after passage 2. Figure *3-7* displays CD362 expression between bone marrow and umbilical cord across different passage numbers, P2 and P3.

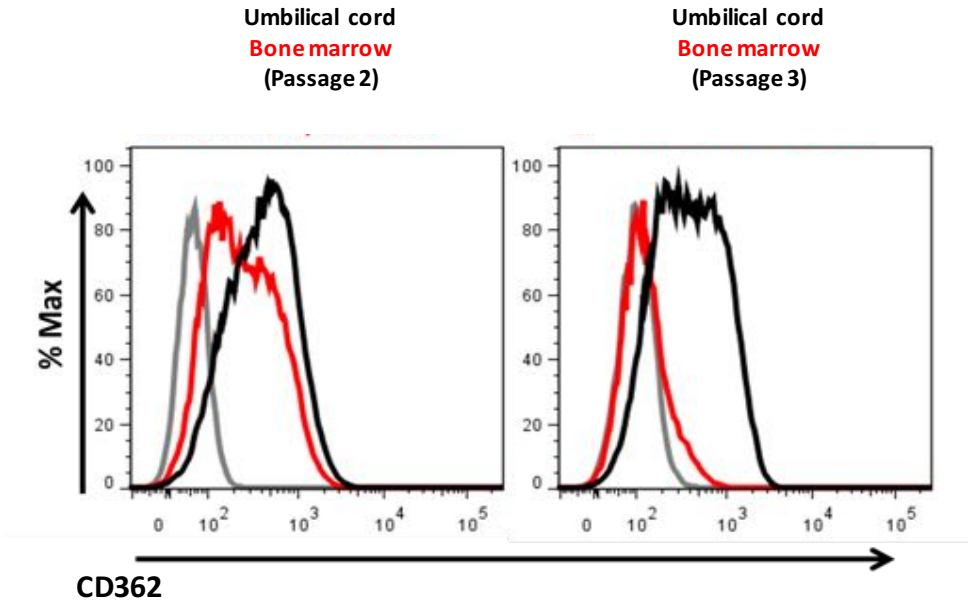

Figure 3-7 Respresentative histogram of CD362 expression on MSCs by flow cytometry. Expression of CD362 derived from bone marrow (red line) and umbilical cord (black line) was assessed from different passage number (P2 and P3). The gray line indicates isotype control staining. This figure was provided from *Orbsen Therapeutics.*

3.3.4 CD362 expression pattern differences in UC-MSC donors

To confirm the expression of CD362 from different donors, we performed flow cytometry analysis on three donors at different passage numbers (P3 and P4). Based on flow cytometric analysis of CD362, I found some differences in the expression of CD362 between different donors as reported in Figure ***3-8***. MSCs from donor 1, 2, and 3 expressed different levels of CD362 (25.4%, 54.1%, and 41.2%, respectively). Similarly, the same observation of CD362 expression was also variable between donors at passage 4 MSCs. The highest expression in all three donors was in donor 2 (49%), whereas donor 1 and 3 expressed 34.6% and 44.5%, respectively, as shown in Figure ***3-8***.

A

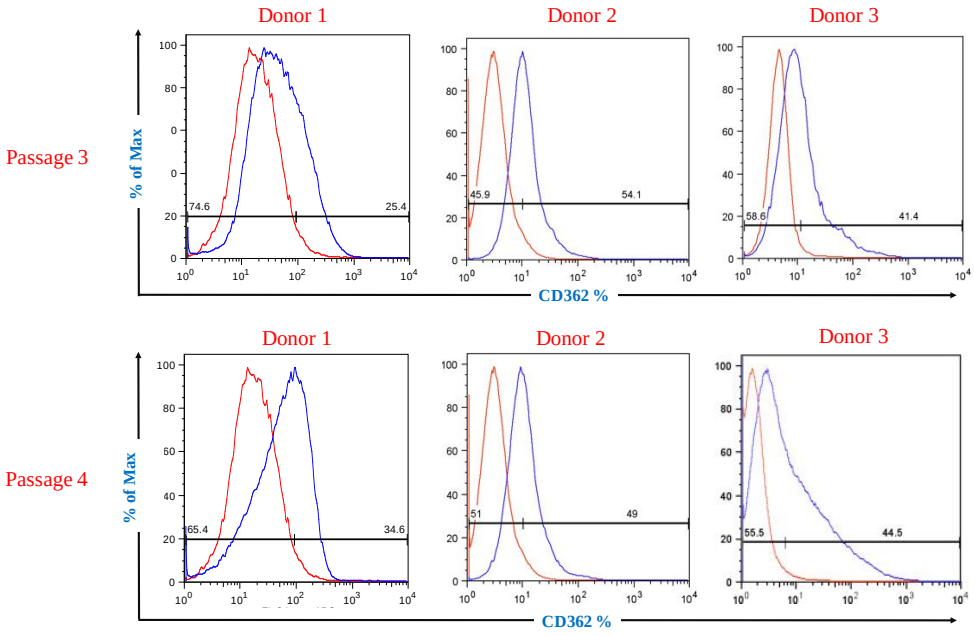

B

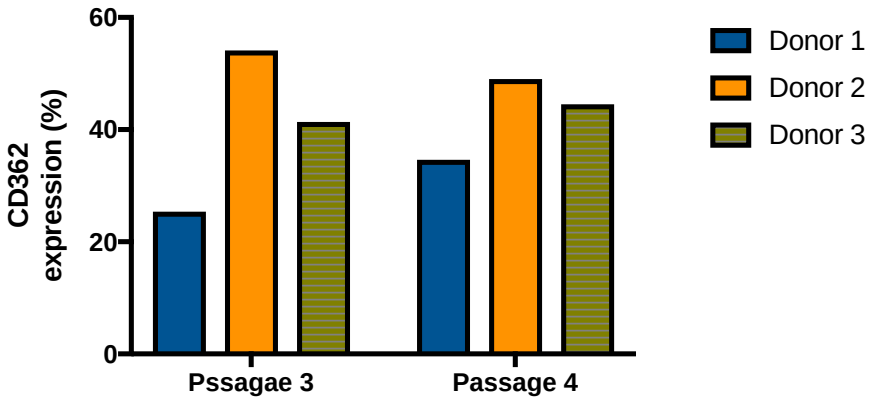

Figure 3-8 Screening of CD362 expression in umbilical cord derived mesenchymal stromal cells (hUC-MSCs) in different donors. A) a histogram of flow cytometry analysis of CD362 expression from different donors (1,2, and 3) at different passages (P3 and P4). B) Graph represents the amount of CD362 expressions in UC-MSCs from different donors at different passages.

3.3.5 Passaging of hUC-MSCs downregulated the expression of CD362 in culture.

To see whether culturing has effects on CD362 expression, I then determined the correlation between CD362 expression and the culture passage number. I used different passage numbers from different donors and the expression of CD362 was investigated using flow cytometry. As a result, no changes in CD362 expression were reported in MSCs between P3 and P4. In contrast, as shown by Figure ***3-9***, I determined a significant reduction in CD362 between P4 and P5. Percentage expression of CD362 at different passages of MSCs is presented in Table ***3-2***.

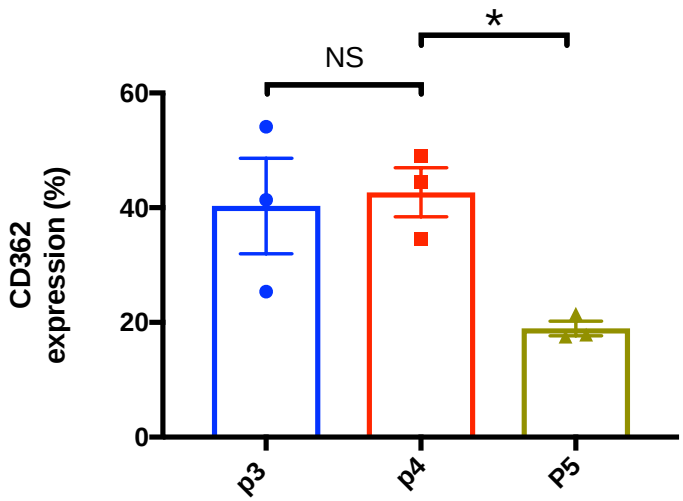

Figure 3-9 Flow cytometry analysis of CD362 expression at the indicated passages (Mean±SEM; n=3; *,p<0.05).

Table 3-2 Flow cytometry analysis of CD362 expression in UC-MSCs from different donors and different passages.

CD362 expression %			
	P3	P4	P5
Donor 1	25.4	34.6	21.5
Donor 2	54.1	49	17.9
Donor 3	41.4	44.5	17.5

3.4 Discussion

Human mesenchymal stromal cells are a sub-type of adult stem cell which was first described from bone marrow by Friedenstein et al, in 1968(Friedenstein et al., 1968), and which have the capacity for self-renewal with high proliferative ability and ability to

differentiate into several specialized cells with specific functions. Several studies have reported the successful isolation of MSC from different tissues, including synovial membrane(Ogata et al., n.d.), adipose tissue(Yañez et al., 2006), umbilical cord blood (Bieback et al., 2004), amniotic fluid (Antonucci et al., 2011), and placenta(Fukuchi et al., 2004). Mesenchymal stromal cells were successfully isolated from human umbilical cord and represent an attractive source of MSCs for use in clinical studies. Here, I studied two different cells subsets; unsorted UC-MSC and sorted UC-MSC based on expression of CD362 (syndecan-2), and the phenotypic characteristics were investigated according to the ISCT minimal criteria (Dominici et al., 2006). The morphology of these cells was fibroblast-like with spindle shape, resembling MSCs isolated from bone marrow. Flow cytometric analysis of expression markers on UC-MSCs in both cells population (unsorted and $CD362^{+}$) confirmed that they expressed (CD90, CD73, CD105, and CD44), but did not express hematopoietic markers (CD45, CD34), and some other markers such as CD11b, CD19, and HLA-DR. Thus, these findings confirmed that MSCs isolated from umbilical cord tissue are similar to other sources of MSCs.

The potential of UC-MSC to differentiate into the adipogenic, chondrogenic, osteogenic lineages was investigated. Under chondrogenic culture conditions, hUC-MSC also had the ability to form cartilage cells. Osteogenic differentiation of WJ-MSCs was found to be not effective with only a small number of cells differentiating under osteogenic medium conditions. These findings confirmed a previous study by Ishige et al, that indicated that mesenchymal stromal cells derived from hUC demonstrated low level of osteogenic differentiation and expressed low level of alkaline phosphatase (ALP), which found to have strong correlations with calcifications (Ishige et al., 2009). This finding

confirmed that MSCs from different origin could exhibit different level of osteogenic differentiation capacity. In addition, I believe we need to increase the time period of the osteogenic differentiation *in vitro* for more than two weeks as the UC-MSCs may have slower osteogenic differentiation ability.

Karahuseyinoglu *et al.* reported that umbilical cord stromal cells could form adipocytes (Karahuseyinoglu et al., 2007). In comparison with MSC from BM-MSCs, UC-MSC exhibited more significant adipocyte forming cells after 21 days in culture(Baksh et al., 2007b). In keeping with this, my results also demonstrate that UC-MSCs have adipogenic differentiative capacity after 14 days in culture, with lipid vacuoles clearly observed as Oil red positive cells.

Cultured MSCs are a heterogeneous population of cells, therefore, sorting is considered to achieve homogenous populations of MSC. Several studies have been reported that some surface markers have a potential impact in biological function of the MSCs (Sherman et al., 2017; Pietilä et al., 2012). However, there are few surface markers that are functionally related to immunomodulatory properties of the MSCs. A recent novel marker, $CD362^{+}$ (Syndecan-2), has been reported to select a homogeneous population of MSCs with superior immunomodulatory properties. This marker was under patent number (WO 20131177661 A1) and is owned by Orbsen Therapeutics, Ireland. As a functional marker for enrichment of MSCs, CD362 has been suggested as a novel marker for purifying and sorting MSCs from umbilical cord tissue as it may have potential immunosuppressive properties to modulate inflammation in different clinical settings (De Witte et al., 2017). Interestingly, CD362 was reported to have possible role to control

fibrosis by modulate expression of TGF-β in fibroblast cells (Chen et al., 2004b). Although, it was found to upregulated after T cells activation and reported to completely related to p38 MAP kinase pathway. This study indicates that CD362 expressions are involved in the regulation of T cells proliferation and TNF-α regulation, which therefore play a role in immune regulation (Teixé et al., 2008).

Using flow cytometry, I investigated the expression of CD362 across different MSCs sources (BM and UC). Both populations were shown to express CD362 at different levels. I also found that MSCs from different origins also expressed CD362 at different levels. At early passage number (P2), UC-MSCs and BM-MSCs displayed similar expression of CD362, although UC-MSCs had more CD362 expression than BM-MSCs after passage 3. This observation is in line with another study which reported that CD200 was expressed predominantly in UC as compared to other different tissue origin of MSCs (Pietilä et al., 2012).

Additionally, and because MSCs from different donors may have possible variation in CD362 expression, I evaluated the expression of CD362 from different donors at the same passage number. After validation, I found that MSCs at passage 3 expressed different levels of CD362. Moreover, the results from passage four indicated that CD362 level varied between different donors used in this study. These differences of CD362 expression could be due to the difference in the age of donors and the level of CD362 could be influenced by human aging. My observation was in agreement with studies that indicate donor age has an effect on some biological characteristics of MSCs isolated from bone marrow(Alves et al., 2012). This finding was also reported in another stem cells,

such as hematopoietic stem cells (HSCs)(Chambers et al., 2007). Hence, my observations of CD362 expression could have an impact and maintaining expression of CD362 may be desirable to improve the quality of MSCs for therapeutic use.

Similarly, some studies have reported that late passage cells may not be functionally suitable for transplantation due to the lack expression of relevant cell surface markers. Whilst no significant differences were reported in CD362 expression between MSCs from passage 3 and 4, my results show a significant decrease in the expression of CD362 by passage 5. In general, my results are similar to those reported by Hye Jin *et al*, who reported that CD146 expression markedly decreased in hUC-MSCs by late passage. Their marker was reported to have an essential impact on senescence in MSCs(Jin et al., 2016). In this respect, and due to the significant reduction of CD362 expression by passage 5, I decided that using late passage hUC-MSCs was not appropriate for their therapeutic use.

In summary, this study has clarified that unsorted and CD362 sorted UC-MSCs show similar expression of MSCs markers as well as the capacity to undergo tri-lineage differentiation *in vitro*. I also demonstrated that UC-MSCs and BM-MSCs have a different expression profile of CD362 expression. Although I have observed a variation in CD362 expression, this depends on MSCs passage number, and is markedly reduced during longer term passage of hUC-MSCs in culture. Because this chapter was only focused on the study of the general characterization of the MSCs in both population, we believe that further characterizations of human umbilical cord from both populations are required for future work. In addition, investigate the effect of the cells sorting on cellular function and the impact of cells sorting techniques in clinical applications.

CHAPTER 4

TIME COURSE OF LIVER INJURY AFTER ACUTE HEPATOTOXIN EXPOSURE USING CCl_4

4.1 Introduction

Carbon tetrachloride (CCl_4) is a well-known hepatotoxin, which is used to induce liver injury in mice. CCl_4 is metabolized in the liver and activated by cytochrome P450 (Noguchi et al., 1982). This step causes reduction in one electron from the CCl_4 and forms a highly reactive radical known as trichloromethylperoxyl (CCl_3*) (Slater1 et al., 1985). These free radicals cause lipid peroxidation and exacerbate cell membrane damage (Basu, 2003). A single dose of CCl_4 has been used to induce acute liver injury (Tuñón et al., 2009). However, the same treatment can be used for a long time, up to 8 weeks with two injections per week, to develop liver fibrosis, and further dose repetition can lead to cirrhosis and, finally, hepatocellular carcinoma (HCC) (Liu et al., 2013).

CCl_4 can also induce liver inflammation by activating macrophages (Kovalovich et al., 2000; Basu, 2003) and can produce mitochondrial dysfunction (Mitchell et al., 2009a), mitochondrial DNA damage, and hepatocyte apoptosis (Shi et al., 1998b). In addition to the many aforementioned factors that relate to CCl_4 acute liver injury, hypoxia levels were also elevated in some studies (Szabo and Petrasek, 2015).

A number of preclinical studies have used different animal models of acute liver injury to investigate the therapeutic efficacy of mesenchymal stromal cell (MSC) therapy. However, few studies have taken into consideration the variation observed in animal models following liver injury, including time to apply the stem cell injection, and the study endpoints in order to evaluate the therapeutic efficacy against liver injury. These variations could create some difficulties in drawing conclusions regarding the positive impact or efficacy of stem cell therapy. For example, cytokines could not be detected in

some animal models after MSC treatment, which could be due to the cytokines reaching a peak at an early time point after the injury was induced (He et al., 2016).

In addition, because the time course of acute liver injury is very short and the regeneration process happens quickly, some markers are difficult to detect. I believe that the endpoint of liver assessment is crucial and needs to be adjusted according to the stage of the injury. It is, therefore, valuable to assess the efficacy of MSCs after infusion according to the peak of the biological parameters that need to be investigated.

4.2 Chapter Aims

In this chapter, I will examine the hepatic injury caused by the administration of CCl_4 treatment in mice. The hepatotoxicity of CCl_4 was evaluated at different time points (12 h, 24 h, 48 h, 72 h and 96 h) by measuring hepatic injury, inflammatory response, oxidative stress and antioxidants. Other aspects are also briefly discussed with respect to CCl_4-induced liver injury. The main aims of this chapter are to:

- Assess the level of liver injury over a four-day period post-CCl_4 administration, including the quantitative measurement of liver enzymes as well as histological damage in the liver tissue.
- Discuss chemokine and cytokine responses following liver injury, as well as the infiltration of immune cells during the course of the liver damage.
- Measure the gene expression of some biological parameters, including cell proliferation, apoptosis, and autophagy along the time course of the injury, for up to three days.
- Determine the dynamic changes in antioxidants and oxidative stress markers during the course of the injury.

4.3 Results

4.3.1 Induction of CCl_4 hepatotoxicity (acute liver injury)

Acute liver injury was induced in mice using a single dose of CCl_4. At different time points (12 h, 24 h, 48 h, 72 h and 96 h) following CCl_4 administration, the mice were sacrificed and blood was collected by cardiac puncture to evaluate the level of liver enzymes. I observed a significant increase in the serum level of alanine aminotransferase (ALT) enzymes after 24 hours and 48 hours, which recovered after 72 hours. ALT activity returned to normal levels after 96 hours (Figure **4-1**).

A

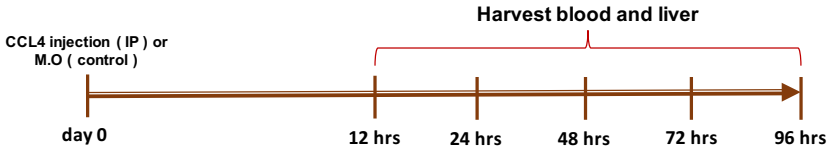

B

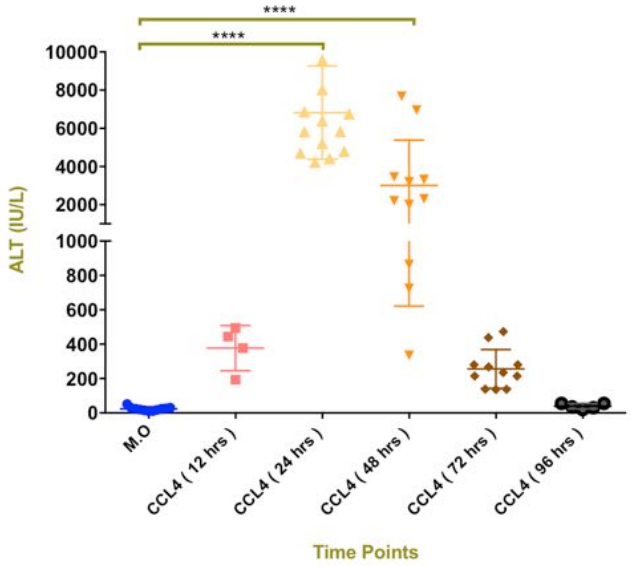

Figure 4-1 Male C57BL/6 mice show variation in liver enzyme activity at different time points after a single dose of CCl_4. A) Design of the study: mice received a single intraperitoneal injection of CCl_4 and liver injury was evaluated at different time points. B) Serum ALT was elevated after 12 h and improved with time. Representative data (> 10 mice for each time point, except for 5 mice at the 12 h and 96 h time points) from three independent experiments are shown. Each value is represented by the mean ± SD. * $P < 0.05$, ** $P < 0.01$, *** $P < 0.001$, and **** $P < 0.0001$.

4.3.2 Histological examination of liver injury after injection with CCl_4

For the histological examination of liver damage, liver sections from the mice were stained with haematoxylin and eosin (H&E). The stained tissue showed massive necrosis 24 hours after treatment with CCl_4 but less necrotic damage was seen after 48 hours (as shown by the red arrow in Figure ***4-2***). Compared with the liver histology in the control group (M.O), the greatest amount of infiltration of inflammatory cells was observed 72 hours after injury (the blue arrows in the figure represent the inflammatory cells).

Cytochrome P450 (Cyp2e1) has been reported to be involved in CCl_4 metabolism and has an essential role in the development of CCl_4 hepatotoxicity in mice (Khan et al., 2012). At the beginning of investigating the role of Cyp2e1 in this injury, I found that CCl_4 caused a significant downregulation in P450 at various stages (12–72 h), as reported in Figure ***4-3***.

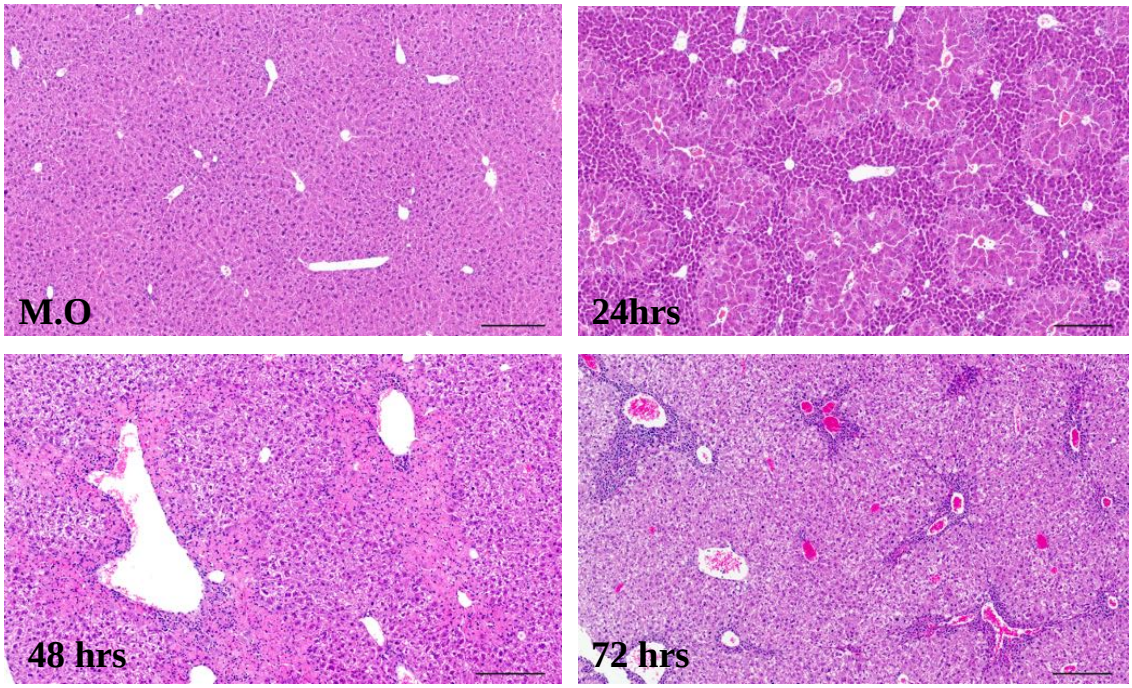

Figure 4-2 H&E staining of liver sections following treatment with CCl_4. Normal hepatic histology of the liver is seen from the control mice (M.O). Severe hepatic necrosis around the lobular and portal area was reported after 24 h. Liver tissue showed hepatic necrosis with a few inflammatory cells in the lobular area 48 h following injury. Massive infiltration of inflammatory cells to the portal area is shown 72 h after injury. Scale bars: 200 μm.

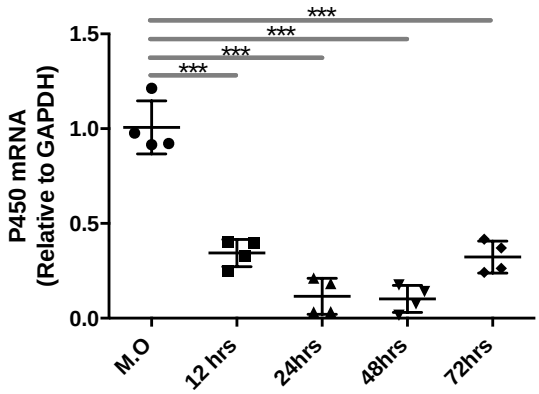

Figure 4-3 Gene expression of cytochrome P450 in the liver after CCl_4 administration as measured by qPCR and normalized to GAPDH; *n* = 4 per group. Data are presented as the mean ± SD. * P < 0.05, ** P < 0.01, *** P < 0.001, and **** P < 0.0001.

4.3.3 Assessment of hepatic inflammatory cell infiltration after a single dose of CCl_4 by injection

To investigate the changes in hepatic cell infiltration following CCl_4 injury, the immunohistochemical detection of CD45 was performed in liver sections across the time course of CCl_4-induced liver injury in C57BL/6 mice. At different time points, the infiltration of hepatic leucocytes significantly increased following CCl_4 injury, although it was most marked 48 and 72 hours after injury (Figure ***4-4***). The intrahepatic leucocyte count was found to have declined by 96 hours.

A

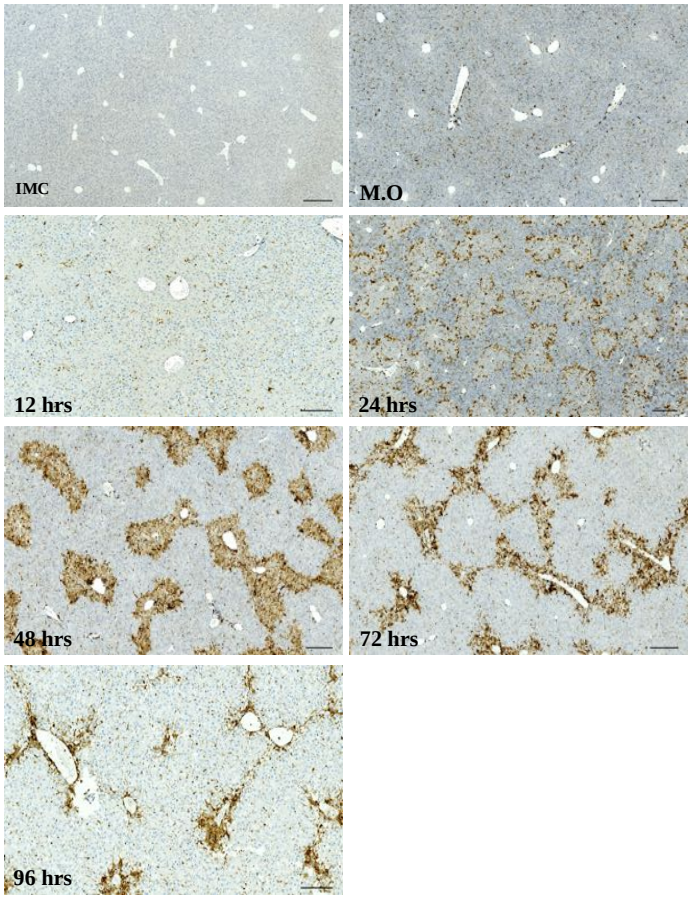

B

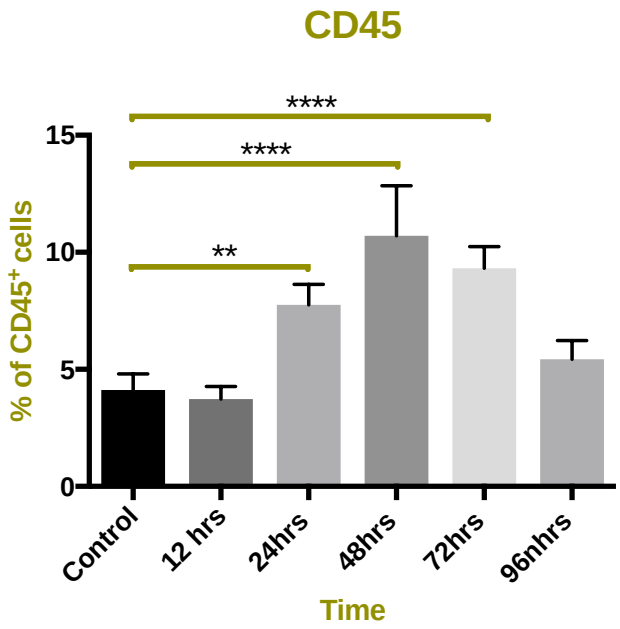

Figure 4-4 Expression of CD45 in CCl_4-injured mouse liver, as determined by immunohistochemistry. (A) Representative images of CD45-positive cell stained liver sections at 12 h, 24 h, 48 h, 72 h and 96 h following CCl_4 administration. In the injured group, CD45 expression increased at 24 h, 48 h, and 72 h after administration with CCl_4. (B) Percentage of CD45 immuno-positive cells increased over the different time points (24 h, 48 h and 72 h) and recovered by 96 h; n = 5 per group. Data are presented as the mean ± SD. * P < 0.05, ** P < 0.01, *** P < 0.001, and **** P < 0.0001. Scale bars: 200 μm.

In order to address whether macrophages also infiltrate during injury, I used immunohistochemistry (IHC) for F4/80, a specific marker for mouse macrophages, which revealed that the percentage of macrophages peaked 72 hours after CCl_4 treatment (Figure ***4-5***), with a clear reduction after 96 hours. In comparison with the control group, similar expression of F4/80 was seen in the injured group at 24 hours and 48 hours, whereas a great number of macrophages infiltrated to the portal area 72 hours after CCl_4 treatment, as shown in Figure ***4-5***.

A

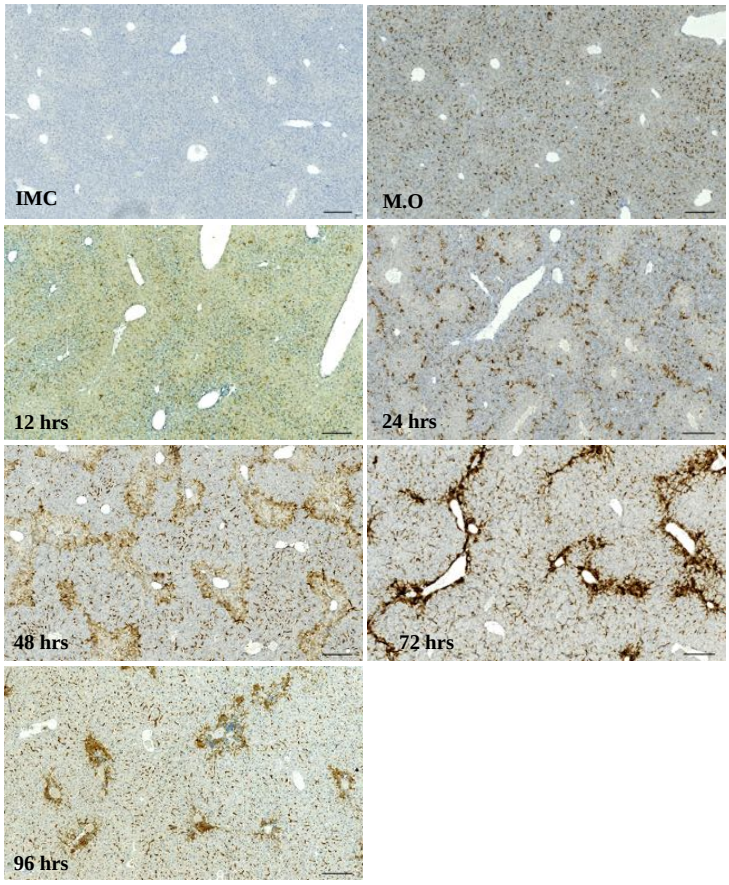

B

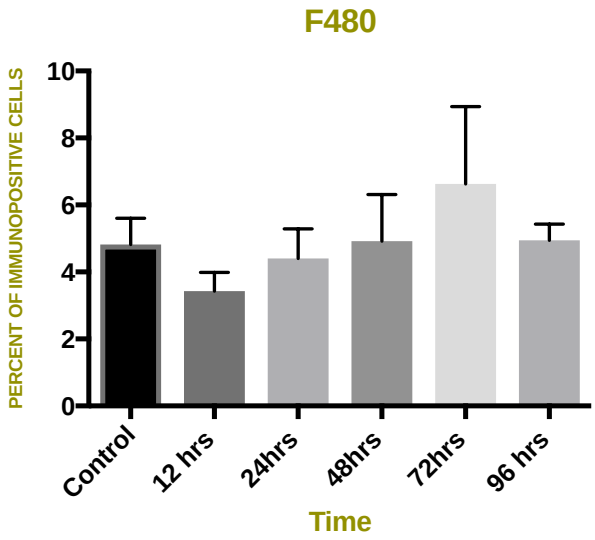

Figure 4-5 Time course of macrophage (F4/80) infiltration in the liver as measured by immunohistochemistry. (A) Representative images of F4/80-positive cell stained liver

sections at 12 h, 24 h, 48 h,72 h and 96 h following CCl_4 administration. (B) Infiltration of hepatic macrophages after CCl_4 peaked at 72 h; $n = 5$ per group. Data are presented as the mean ± SD. Scale bars: 200 μm.

4.3.4 Effect of acute CCl_4 on the circulating level of cytokines and chemokines at different time points

Different studies have reported that leukocyte infiltration is essential for the induction of liver injury and depends on cytokine and chemokine expression at an early time point (Saiman and Friedman, 2012). In order to determine the level of different pro-inflammatory and anti-inflammatory cytokines in CCl_4-induced liver injury, I performed a time course study to observe the level of expression in serum at different time points using multiplex immunoassay. Three different pro-inflammatory cytokines were measured in this study (tumour necrosis factor alpha [TNFα], interleukin 1 beta [IL-1β], and interferon gamma [IFNγ]).

Anti-inflammatory cytokines were also measured in this study. IL-10 was found to have modestly increased after 24 hours, but failed to reach statistical significance, and IL-10 expression gradually decreased with time. Figure ***4-6*** shows all the cytokines measured in this study. IFNγ has been reported to have massive variation between animals and in some mice levels were not detected in the serum using multiplex immunoassay. Similarly, TNFα was found to have variation in expression across the time points tested. Accordingly, I performed enzyme-linked immunosorbent assay (ELISA) as a confirmatory test to detect the TNFα level in serum. The TNFα level was significantly increased 24 and 48 hours after the CCl_4-induced liver injury, as shown in Figure ***4-7***.

To further define the relative contributions of chemokines to liver injury related to CCl_4 hepatotoxicity, I found a significant overexpression of monocyte chemoattractant protein 1 (MCP-1) and interferon-gamma-inducible protein 10 (IP-10) 24 hours after CCl_4 injection, followed by a reduction over subsequent time points. Macrophage inflammatory protein 1 alpha (MIP-1α) and endotoxin showed modest upregulation after 24 hours but failed to reach statistical significance.

A) Pro-inflammatory

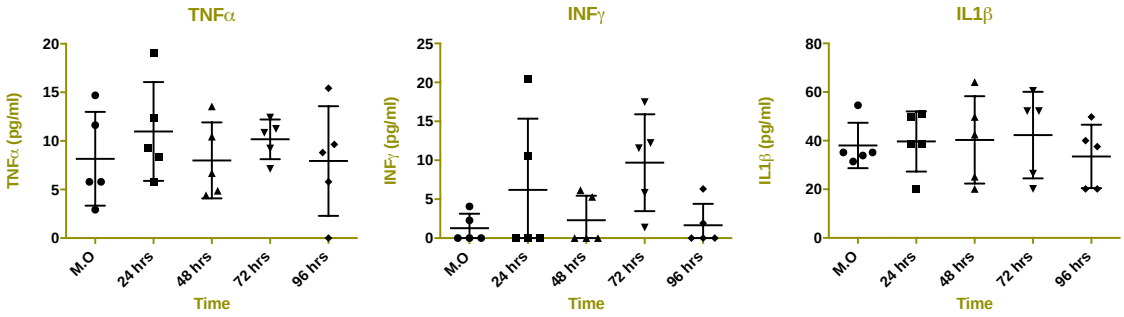

B) Anti-inflammatory

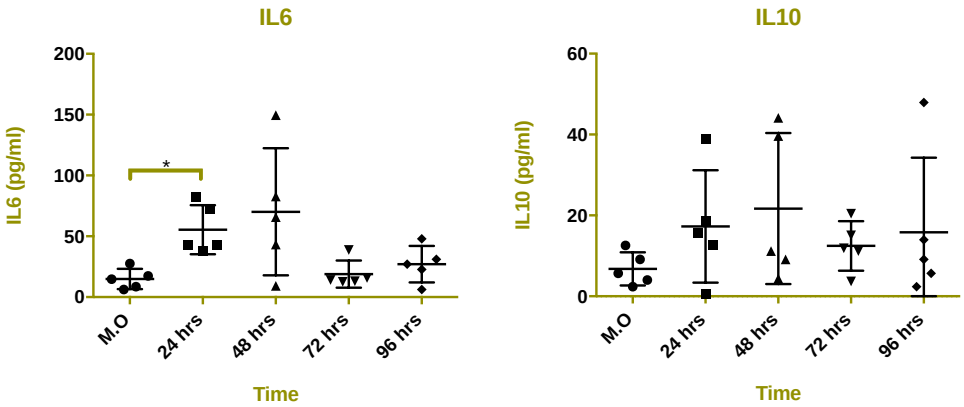

C) Chemokines

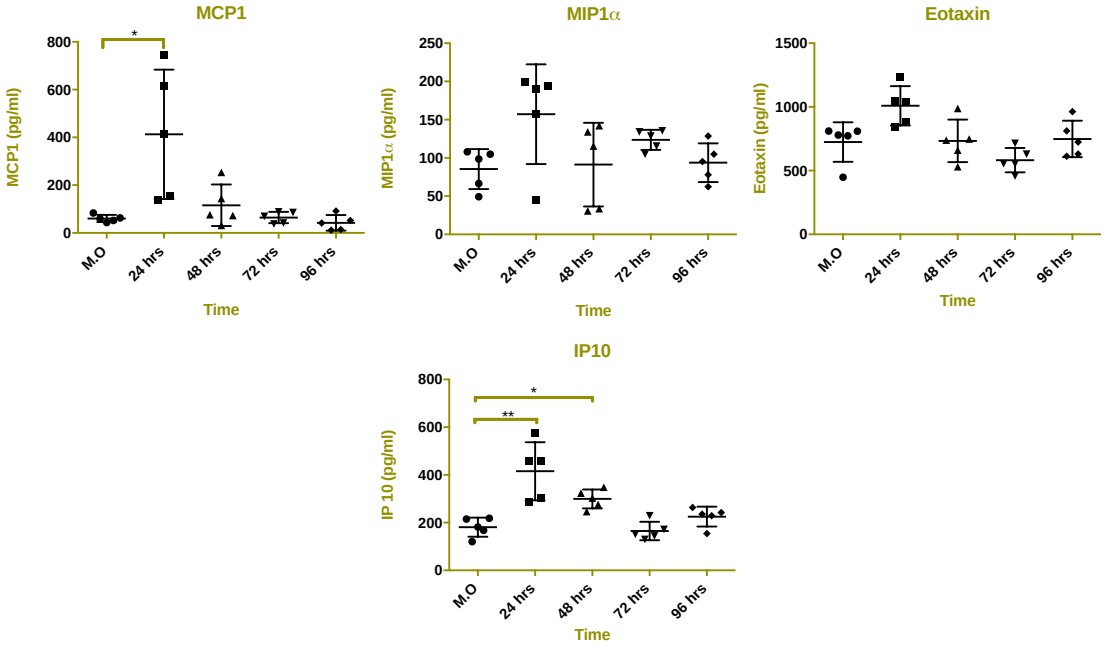

Figure 4-6 Serum cytokine time course following a single dose of CCl_4 treatment. Serum concentrations were measured using multiplex immunoassay. The mean ± SD was used to represent the data and five mice were used at each time point. * P < 0.05, ** P < 0.01, *** P < 0.001, and **** P < 0.0001; *n* = 5 per group.

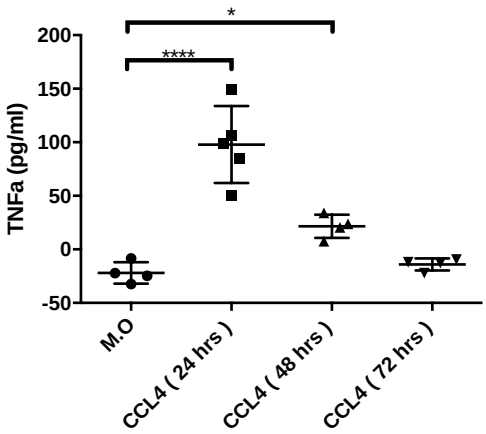

Figure 4-7 TNFα concentration was determined in the serum using ELISA. Each value is represented by the mean ± SD. * P < 0.05, ** P < 0.01, *** P < 0.001, and **** P < 0.0001; *n* = 5 per group.

4.3.5 Evaluation of cell proliferation, autophagy, and DNA damage in the CCl_4-injured mice using immunohistochemistry

In order to assess the amount of hepatocyte proliferation after liver injury, I quantified the expression of Ki-67 using immunohistochemistry. There was a clear increase in cell proliferation over time (Figure ***4-8***).

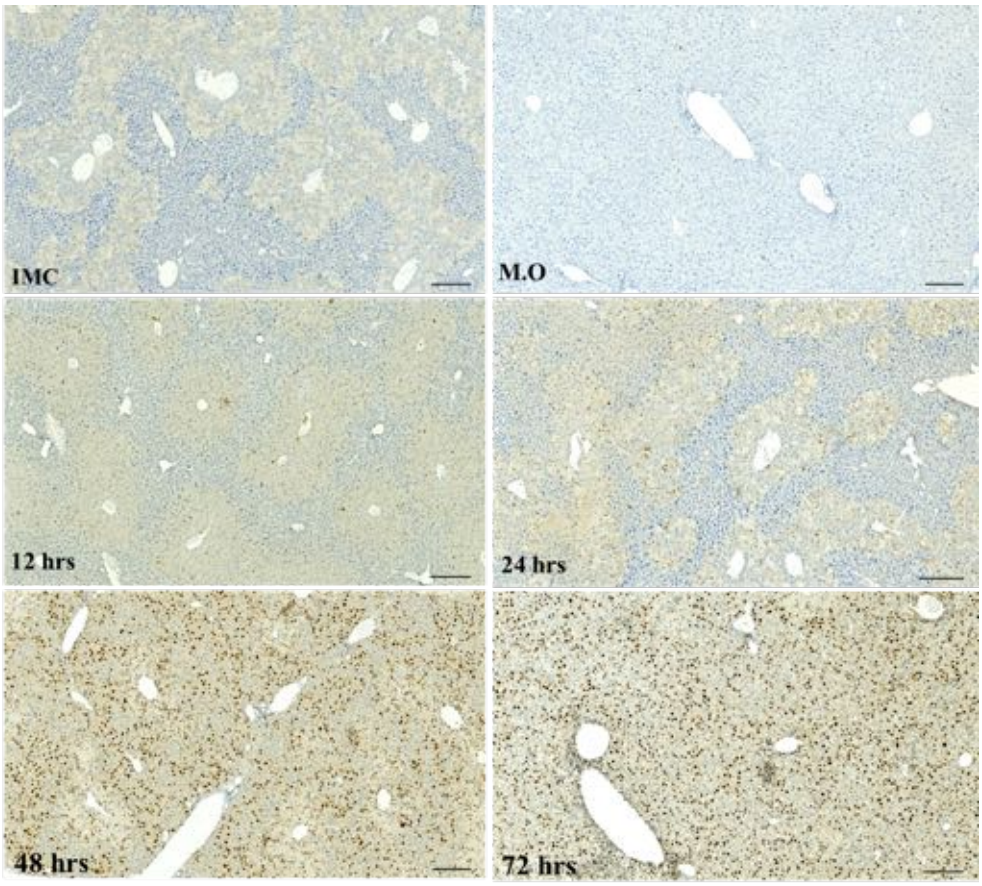

Figure 4-8 Cell proliferation in CCl_4-injured mice at different time points. Immunohistochemistry of Ki-67 was used to indicate the number of proliferated cells in the liver. The proliferated cells are stained with DAB (dark brown). Scale bars: 200 μm.

To assess whether autophagy was responsible for the hepatic injury induced by CCl_4, the level of autophagy was also investigated in injured liver across the time points. I evaluated the gene expression level of different autophagy markers, such as P62, LC3B and Becl-2, which play a pivotal role in autophagy progression. LC3B and Becl-2 were highly expressed after 24 hours and 48 hours, and LC3B was significantly increased at a later time point (72 h). More interestingly, I found that increased expression of P62 was reported at an early time point (12 h), as shown in Figure ***4-9***A. Furthermore, I stained liver sections using Beclin-2 to study the autophagy level in the liver tissue. There appeared to be an early increase in autophagy after 12 hours, with a peak observed after 24 hours. Clear reductions were subsequently seen after 48 and 72 hours (Figure ***4-9***b).

A)

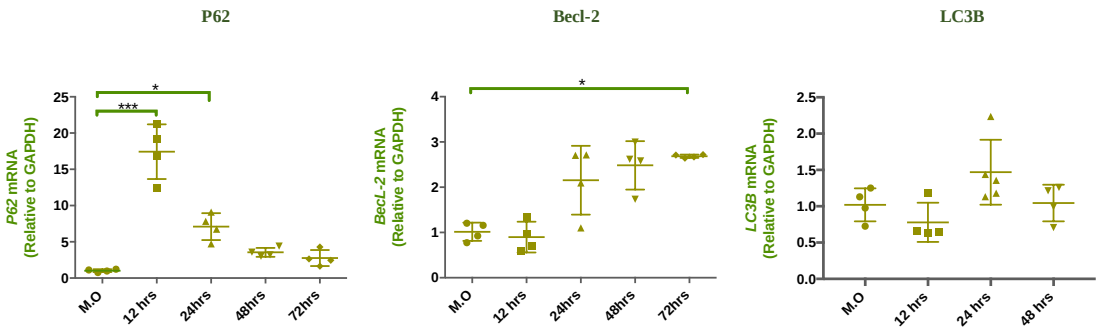

B)

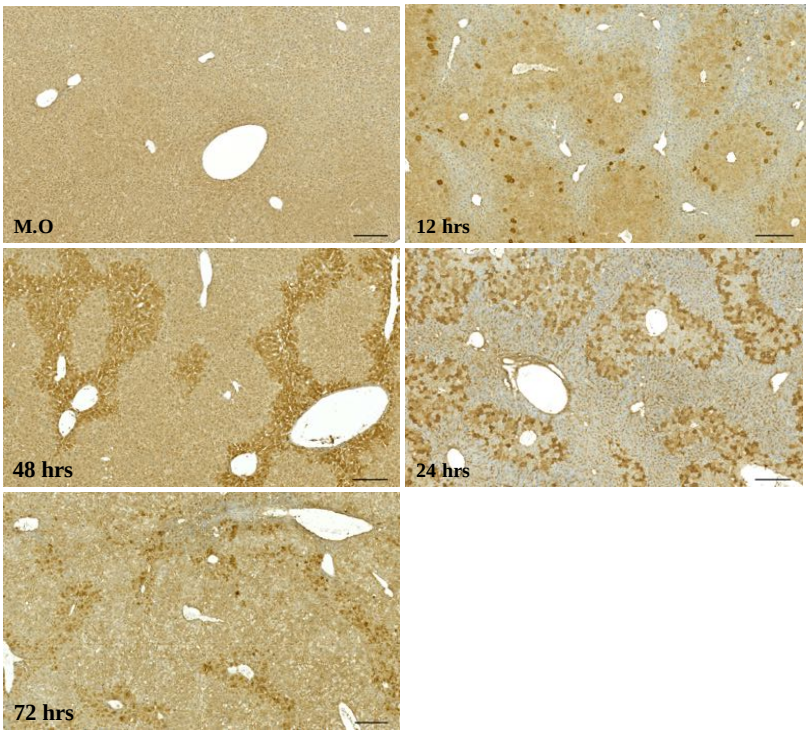

Figure 4-9 Autophagy expression in mouse liver after CCl_4 administration at different time points. A) Gene expression of P62, LC3B, and Becl-2 in the liver after CCl_4 administration, as measured by qPCR and normalized to GAPDH; n = 4 per group. Data are presented as the mean ± SD. * P < 0.05, ** P < 0.01, *** P < 0.001, and **** P < 0.0001. B) The Beclin-2 level was used to assess the level of autophagy in the liver using IHC. Scale bars: 200 μm.

Furthermore, I examined the level of DNA damage in the injured liver using IHC with Phospho-Histone H2A.X antibody. DNA damage developed early within the cells after 12 hours, with more cells reported to have DNA damage after 24 hours. Very few cells were detected after 48 hours, with no DNA damage after 72 hours. The DNA damage at the different time points is shown in Figure ***4-10***. Similarly, the same observation was reported in liver sections using TUNEL assay, also shown in Figure ***4-10***.

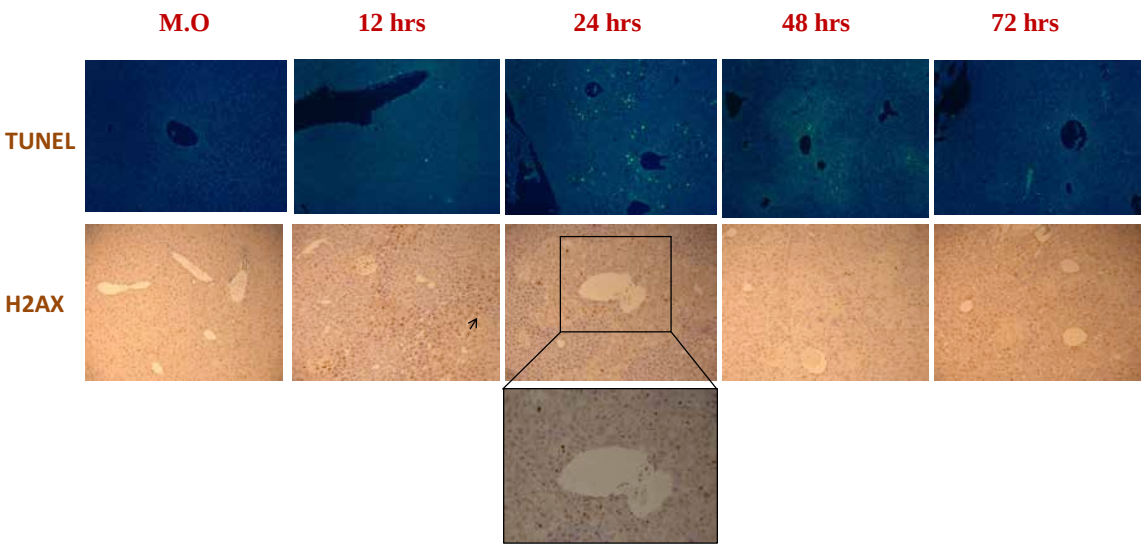

Figure 4-10 Phospho-Histone H2A.X and TUNEL assay were used to measure the level of DNA damage in the liver. Immunohistochemical staining of Phospho-Histone H2A. Arrows indicate the positive cells undergoing DNA damage.

4.3.6 Upregulation in antioxidant activities in the liver after CCl_4 injection

I investigated the expression of different antioxidant enzymes in the liver following a single dose of CCl_4. qPCR was performed using primers for five selected genes to assess the different antioxidants and the time course of changes in the liver. Among them, catalase and isocitrate dehydrogenase (IDH-1) were reported to have a significant reduction in liver tissue 24 hours after the CCl_4 liver injury (Figure ***4-11***). I also observed a significant upregulation in the catalase and IDH-1 antioxidant across time points,

mainly after 48 hours and 72 hours, respectively. In addition, superoxidase dismutase (SOD) enzymes, including cytoplasmic superoxidase dismutase (SOD1), mitochondrial superoxidase dismutase (SOD2), and extracellular superoxidase dismutase (SOD3), are also important antioxidant enzymes which protect against oxidative stress. Here, I show that SOD1 and SOD2 significantly increased after 24 hours, with no change reported in SOD3 at the same point. However, all the superoxide dismutase enzymes were found to be highly expressed 48 hours following CCl_4 injury (Figure ***4-11***). GAPDH was used as a reference gene.

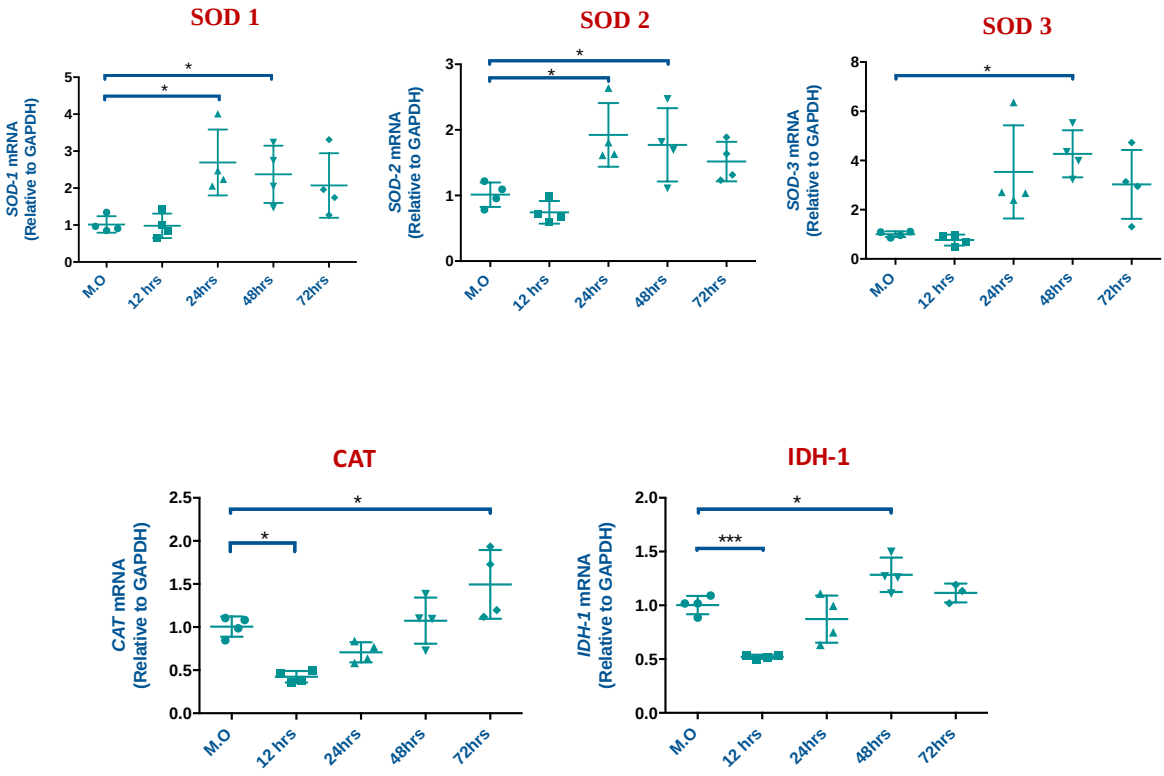

Figure 4-11 Liver antioxidant activities. Gene expression of antioxidant enzymes (SOD1, SOD2, SOD3, CAT, and IDH-1) in the liver after CCl_4 administration, as measured by qPCR

and normalized to GAPDH; *n* = 4 per group. Data are presented as the mean ± SD. * P < 0.05, ** P < 0.01, *** P < 0.001, and **** P < 0.0001.

4.3.7 Gene expression profiles of GSS, HO-1, NOS2, and HIF1-α during liver injury after CCl_4 injection

As several studies have shown that oxidative stress and reactive oxygen species (ROS) production are related to the liver damage associated with the induction of CCl_4 in mice, I determined the levels of GSS, HO-1, NOS2, and HIF1-α during liver injury after CCl_4 injection using qPCR. Remarkably, GSS, NOS2, and HIF1-α showed no expression at the early time point (12 h) following CCl_4, whereas HO-1 expression significantly increased and reached a peak at 12 hours. Hepatic GSS level increased in a time-dependent manner and significantly increased at 24 hours, 48 hours and 72 hours after CCl_4 administration (Figure *4-12*A). I further analysed the dynamic changes in hypoxia level as reported using HIF1-α, which represents the most prevalent marker during hypoxia. Following CCl_4 induction, I observed a markedly increased HIF1-α level at 24 hours and 48 hours, as shown in Figure *4-12*D.

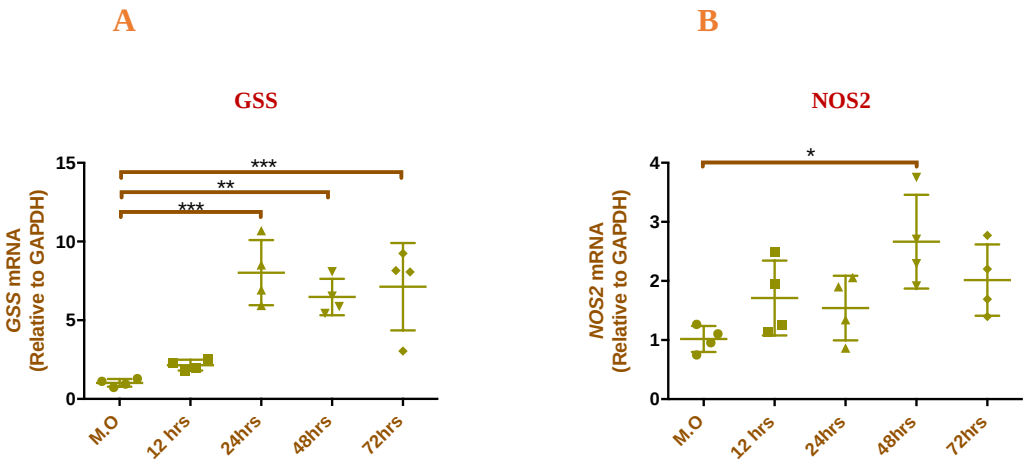

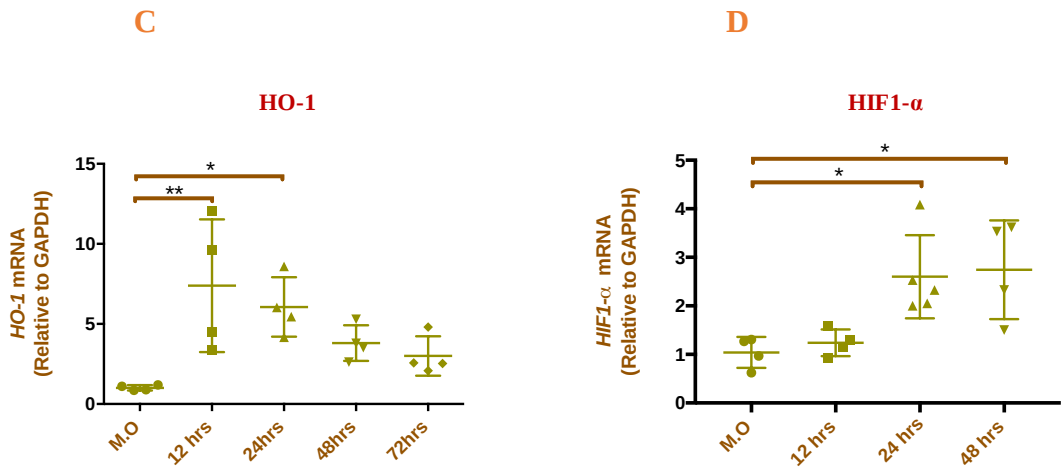

Figure 4-12 **Effect of CCl_4 on GSS** (a), NOS2 (b), HO-1 (c), and HIF1-α (d) expression in mouse liver across the time course of the injury (12–72 h); *n* = 4 per group. Data are presented as the mean ± SD. * P < 0.05, ** P < 0.01, *** P < 0.001, and **** P < 0.0001.

4.4 Discussion

As mentioned above, CCl_4 is a hepatotoxin that has been widely used in animal experiments to induce acute and chronic liver injury. However, the time course of acute CCl_4 injury has not been well defined. Here, I used a single dose of CCl_4 to induce acute liver injury in mice. I then carried out experiments in order to understand the effects of CCl_4 treatment at different time points. The level of liver injury in mice was assessed by the histological examination of liver sections and liver enzyme activity. More specifically, the time course experiments found significant alterations in different biological aspects, such as inflammatory response, oxidative stress, levels of antioxidants, and autophagy activities. The expression profiles were different between the earlier and

later stages of the liver injury following CCl_4 injection. I believe that each time point reflects a specific area of interest and should, therefore, be used as a particular time window to assess the therapeutic function of treatment against liver disease.

Previous studies have reported an increase in liver enzymes with histological damage 24 hours after CCl_4 administration in mice (Zahedi et al., n.d.) and rats (Janakat and Al-Merie, 2002). Our results indicate that, after a single dose of intraperitoneal (IP) CCl_4, there was a significant increase in liver enzymes after 24 hours and 48 hours, the maximum effect being seen after 24 hours. The liver enzymes had recovered somewhat by 72 hours. Liver histology showed massive necrotic areas 24 hours and 48 hours after treatment with CCl_4, with more infiltration of inflammatory cells observed 72 hours after injury. I noted that the effect of CCl_4 administration in mouse liver had fully returned to normal 96 hours after injury.

Leucocyte infiltration is associated with acute liver injury development and prognosis. Here I have demonstrated that inflammatory cells are released during a time course following acute liver injury using CCl_4. The inflammatory response, as measured by CD45 expression, significantly increased after the administration of CCl_4 with a significant increase after 48 hours and 72 hours. Similar findings have been reported by other groups using immunohistochemistry (Karlmark et al., 2009) and flow cytometric analysis (Karlmark et al., 2010). Both studies showed the maximum infiltration rate of leucocytes at 48 hours after treatment with CCl_4; I notably observed in my experiments that the leucocyte infiltrates were differentially distributed, with more cells seen in the portal tracts than in the lobular area. A clear reduction was reported in CD45 expression after 96 hours. Macrophage numbers (F4/80 expression) peaked 72 hours after treatment

by CCl_4 with clear localization around the portal tracts. However, animal models of liver injury have shown some remarkable heterogeneous populations of macrophages with distinct functions (Tacke and Zimmermann, 2014). Thus, future work is needed to determine which macrophage subsets are involved in responses to CCl_4-induced liver injury.

To define the response of inflammatory cytokines or chemokines to liver injury following acute CCl_4 exposure, a time course study was performed to provide insight into how CCl_4 alters the hepatic expression of cytokines or chemokines at different time points. In this study, we used multiplex in particularly because our biological sample (mouse serum) is limiting and we want to measure and screen a wide variety of pro- or anti-inflammatory cytokines. In general, serum cytokine quantification by multiplex arrays offers the potential of evaluating and screen of a wide variety of pro- or anti-inflammatory cytokines over ELISA measurements. Despite potential advantages of this new technology, experience with these techniques is limited, and it has not emerged to date as the gold standard in inflammatory cytokines measurement due to the low specificity and sensitivity. In contrast, Enzyme-linked immunosorbent assay (ELISA), the most widely used and best validated method, is limited by its ability to measure only a single cytokine in each sample and the assay is time consuming and costly.

Due the measurement issues with multiplex assays and data interpretation, we confirmed some parameters using ELISA, In particular TNFα. In case of measuring the TNFα level in mouse serum using ELISA or multiplex, we saw clear variability between the lab techs who were running the samples using multiplex and our ELISA results in serum TNFα

activity. Using ELISA assay, the serum TNFα level was significantly increased 24 and 48 hours after CCl_4 induction.

Furthermore, IL-6 level was significantly increased 24 hours and 48 hours after CCl_4 - induced liver injury. My findings indicate that cytokine levels correlate with hepatocellular damage, as they increased rapidly by 24 hours and, therefore, may have the ability to regulate liver inflammation after CCl_4 injury. In addition, the development of liver injury was significantly correlated with higher expression of chemokines, mainly MCP-1 and IP-10. My study indicates that eotaxin and MIP-1α did not show any alteration in the acute model of liver injury, but they may have a role in chronic liver injury. Further work should consider studying the correlation between these cytokines and the level of oxidative stress and autophagy in the acute liver injury induced by CCl_4.

The present study also illustrates that the rate of hepatocyte proliferation (as measured by Ki-67 IHC) also increased with time after CCl_4 injury. Several studies have reported a strong correlation between hepatocyte proliferation and liver regeneration (Fang et al., 1994). As seen in liver sections stained with Becl-2, the autophagy level increased after 24 hours. This finding indicates that necrosis is related to autophagy expression. In addition, real-time PCR revealed that mRNA expression of P62 in the liver was upregulated at 12 hours and 24 hours after CCl_4 injection, and Beclin-2 reached a peak at 72 hours. This result suggests that P62 activity occurs early in the development of liver injury. However, the acute administration of CCl_4 in mice did not induce clear modifications in the levels of LC3B. The same finding has been reported in different studies in relation to acute liver injury. For example, autophagy was shown to increase with concanavalin A-induced liver hepatitis (Yang et al., 2010). They found that CCl_4 toxicity induced DNA damage after 12 hours and 24 hours, but few cells were observed

in the later points. I believe that the UC-MSC may have some role in DNA repair and possibly whether UC-MSC can trigger autophagy to enhance liver regeneration. Therefore, the above findings indicated a time point to use for my *in vivo* experiment.

Oxidative stress and ROS production play a key role in the progression of the liver damage associated with the induction of CCl_4 in mice. The present study revealed that CCl_4 induction in mice markedly increased the expression of GSS, HO-1, and NOS2 during the time course of liver injury. Remarkably, GSS and NOS2 showed no expression at 12 hours following CCl_4 induction, whereas HO-1 expression significantly increased and reached a peak at 12 hours. Hepatic GSS level increased in a time-dependent manner and significantly increased at 24, 48, and 72 hours after CCl_4 administration. These findings clearly show that oxidative stress induced by CCl_4 was correlated with other aspects explained earlier, such as cytokines, chemokines, and apoptosis.

In agreement with the upregulated gene expression of oxidative stress after CCL_4 administration, hypoxia activity was examined using HIF1-α in the liver across the time course of the injury. I observed an upregulation of HIF1-α expression at 24 hours and 48 hours. In this regard, the culture of MSCs under hypoxia has been shown to have a potential impact on MSC migration and differentiation (Mohyeldin et al., 2010). Accordingly, I suggest that MSCs may play a more important biological function in the hypoxic microenvironment.

In addition, I have reported for the first time a study to evaluate the gene expression of five different antioxidants in an injured liver throughout the time course of the injury. I found that the levels of antioxidant enzymes exhibited significant variation at different time points, with an initial elevation followed by a gradual decline in expression. The

variation trends of SOD and catalase at the various times were different. Across the antioxidant enzymes tested, I observed that they were expressed the highest on the third day, with the greatest reduction observed in catalase and IDH-1 at 12 hours, followed by a slower increase. These two antioxidants could be the ones that contribute most to the nature of the defence against liver injury. In addition, SOD1, SOD2 and SOD3 peaked 48 hours after CCl_4 induction and then gradually declined at 72 hours. This may have resulted from the different factors having different reaction times and secretion peaks, which is in line with prior studies. In parallel observations, a previous report demonstrated a higher expression of antioxidants following an acute liver failure model induced by D-galactosamine/LPS (Gal/LPS) (Zeng et al., 2015). In addition, the same finding was reported in patients undergoing treatment of acute liver injury.

In summary, the future of developing MSC-based therapies for liver diseases lies in understanding the interactions between MSCs and the microenvironment of the injured liver. In this *in vivo* study, I have been able to provide useful evidence of the dynamic cellular changes and disease activities involved in acute CCl_4-induced liver injury over different time points. Following CCl_4 injury, a cascade of cellular changes occurs over the course of an injury, causing destruction of the liver architecture, enhanced apoptosis, oxidative stress, and subsequent infiltration of immune cells to the injured area of the liver. The findings of this chapter have important implications for defining the most effective study endpoints to use for my *in vivo* experiment, which aimed at improving the therapeutic efficacy of mesenchymal stromal cells in liver injury.

CHAPTER 5

THE ANTI-INFLAMMATORY ROLE OF UMBILICAL CORD-DERIVED MESENCHYMAL STROMAL CELLS IN MICE WITH ACUTE LIVER INJURY

5.1 Introduction

Acute liver failure (ALF) is a common cause of mortality and morbidity. The most common aetiologies of ALF are viral hepatitis (B and C) and hepatotoxicity induced by overdose of chemicals such as acetaminophen. The latter has been shown to be the most common cause of acute liver failure in Western Europe (Bernal and Wendon, 2013) .The clinical symptoms of ALF are defined by a rapid loss of hepatocellular function in the absence of pre-existing chronic liver disease. Symptoms include hepatic encephalopathy and the development of failure in multiple organs (Forbes et al., 2015). In order to treat these diseases, liver transplantation is the primary and most effective treatment, however, due to the lack of donor organs and difficulties related to immune rejection, alternative therapies must be comprehensively studied. Cell-based therapies, and in particular MSC therapy, are promising new ways to treat liver diseases.

Stromal cell therapy represents a promising means of treating different liver diseases, and is reported to have special characteristics, potentially including the ability to perform self-renewal, proliferation and differentiation potential compared to more specialised cells (Volarevic et al., 2014). Mesenchymal stromal cells from a variety of tissues have been shown to support and promote liver resolution after acute injury (Christ et al., 2015). In particular, mesenchymal stromal cells derived from human umbilical cord (hUC-MSCs) have been used, both *in vivo* and *in vitro*, as cell therapy for hepatic disease. Human Wharton's jelly-derived mesenchymal stromal cells have been shown to have a significantly higher expression of hepatic-developed markers compared with other sources of MSCs, such as bone marrow and adipose tissue (Buyl et al., 2014). The efficacy of UC-MSCs in liver disease has been studied *in vivo* in a mouse model of partial

hepatectomy, where, a few weeks after transplantation, UC-MSCs were seen to express some hepatic markers, such as albumin and alpha-fetoprotein (AFP). This finding may give more insight towards using UC-MSCs as a potential source for treatment of liver diseases (Campard et al., 2008). Another study looked at the ability of hUC-MSCs to reduce acute liver injury in mice by either the transplantation of hUC-MSCs or adult human hepatocytes (AHHs). In this study, both treatments reduced markers of liver injury, although, as supported by other groups, there was a more significant reduction in inflammatory cytokines with undifferentiated hUC-MSCs (Zhang et al., 2012). hUC-MSCs require further studies to better understand their potential efficacy and associated mechanism of actions in the setting of liver disease.

Given the above evidence for the effectiveness of MSCs in liver diseases, we investigate the possibility of using human umbilical-derived MSCs to repair acute liver injury in mice. As we reported previously in Chapter 4, we developed a mouse model to induce acute hepatotoxic injury using a single dose of CCl_4, and we have successfully investigated a time course study to evaluate the biological changes during the time course of liver injury. In this study, we examined the therapeutic role of UC-MSCs to protect against liver damage caused by CCl_4 induction. In addition, we hypothesize that enrichment approaches are considered to achieve more homogeneous populations of MSCs which may enhance their beneficial effects in liver disease. We used $CD362^+$ (Syndecan-2) marker, which has been identified as a novel marker to select a homogeneous population of MSCs with enhanced immunomodulatory properties and has been recently investigated for its ability to reduce immunogenicity and enhance the immunomodulatory ability in liver inflammation (De Witte et al., 2015; 2017).

Previously, we demonstrated that the expression of $CD362^+$ was more prominent in MSCs isolated from umbilical cord than bone marrow. In addition, we found that the expression of $CD362^+$ in the UC-MSCs was gradually decreased after multiple passages in culture. Furthermore, we demonstrated that $CD362^+$ suppression was stable until about the fifth passage in culture. To our knowledge, no study has specifically investigated a direct comparison of the immunomodulatory properties of unsorted UC-MSCs and $CD362^+$ sorted UC-MSCs *in vivo*. Here, we test the hypothesis that sorting human MSCs with CD362 marker would enhance their anti-inflammatory properties.

5.2 Chapter Aims

In this chapter, we aim to investigate the immunosuppressive characteristics of unsorted/purified human UC-MSCs *in vivo* using the CCl_4 model of acute liver injury. The main aims of this chapter are to:

- Explore the safety and efficacy of MSCs in CCl_4 animal model
- Study the immunomodulatory properties of unsorted (US) UC-MSCs and $CD362^+$ sorted UC-MSC to modulate the number of hepatic infiltrating lymphocytes and monocytes using flow cytometry analysis
- Investigate the antioxidant activities of $CD362^+$ sorted UC-MSCs in the CCl_4 animal model
- Investigate whether UC-MSCs can modulate the autophagy level to improve liver injury *in vivo.*

5.3 Results

5.3.1 Examining the correlation between the number of transplanted MSCs and the resulting liver function

Different animal models have been used to study the therapeutic potential of MSCs in liver diseases. In this chapter, the efficacy of human MSCs was used in acute hepatic injury induced by CCl_4. Previously, our result showed that the peak of inflammation, as reported by hepatic CD45 and F480 expression was 72h after CCl_4 induction of liver injury. Hence, we decided to analyse the data at 72 hours post-infusion. Four hours after CCl_4 treatment (1ml/kg body weight), UC-MSCs (US) were infused systemically via the tail vein and the effects recorded 72 hours after UC-MSCs infusion; animals were sacrificed and blood and liver tissues collected for further investigation (Figure ***5-1***A).

To optimise MSCs treatment in this animal model, a dose-response with varying infusions of unsorted UC-MSCs ($2.5x10^5$, $5x10^5$ and $1x10^6$) was undertaken. The activity of liver enzymes (ALT) was measured for each animal in order to evaluate the liver injury. As shown in Figure ***5-1***B, the serum ALT levels in the injured mice (CCl_4) were clearly increased compared with non-injured group (treatment with mineral oil). There was no significant decrease in ALT level in both $2.5x10^5$ and $1x10^6$ groups but animals appeared to have the same level of improvement. In contrast, the $5x10^5$ showed a variation between animals with increase in ALT in some mice.

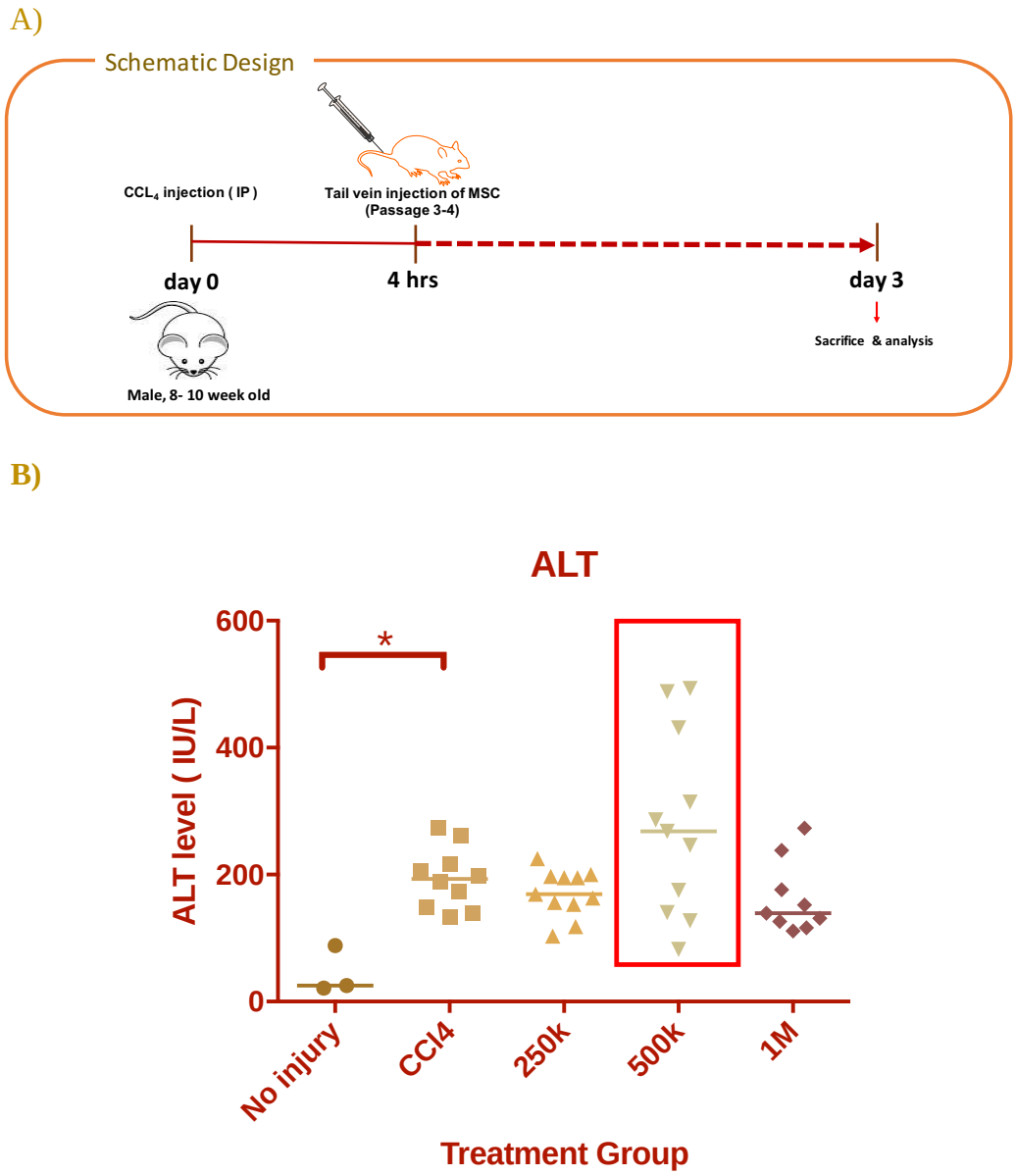

Figure 5-1 Analysis of ALT liver enzyme after infusion of different doses of MSCs (US) in mice with Acute CCl_4. A) Experimental design used in this study, CCl_4 or mineral moil treatment (1ml/kg body weight) were injected to mice, followed by MSCs infusion after four hours. Animals were sacrificed for serum and tissue collection for further study. B) Serum ALT level in normal group with mineral oil (non-injured), injured group (CCl_4), and treatment groups (CCl_4+MSCs). Data are expressed with median value and represent >10 animals/group. ANOVA with post-hoc analysis was performed. Data are presented as the mean ± SD. *P < 0.05, **P < 0.01 and ***P < 0.001.

5.3.2 Unsorted UC-MSC versus CD362^{+} sorted UC-MSC for the treatment of acute liver injury induced by CCl_4 injection

After CCl_4 acute liver injury, unsorted UC-MSC and CD362+ sorted hUC-MSCs were infused at two dose levels - $2.5x10^5$ and $1x10^6$. Liver enzyme (ALT) was measured to evaluate the liver injury in each animal. A significant reduction was observed with $2.5x10^5$ unsorted UC-MSC and CD362+ sorted UC-MSC (Figure ***5-2***). ALT level was reduced after infusion with unsorted UC-MSC and CD362+ sorted MSCs compared with CCl_4 injury only. We also observed a reduction with $1x10^6$ CD362+ sorted UC-MSC, but this did not reach statistical significance. In this study, we also used heat-inactivated MSCs, as control group, by heating human MSCs for 10 minutes to 55^{o}C; cells were then washed with PBS and used for future experiment. Using flow cytometry, all heated MSCs became necrotic and >90% of the cells were dead, as reported in Figure ***5-3***.

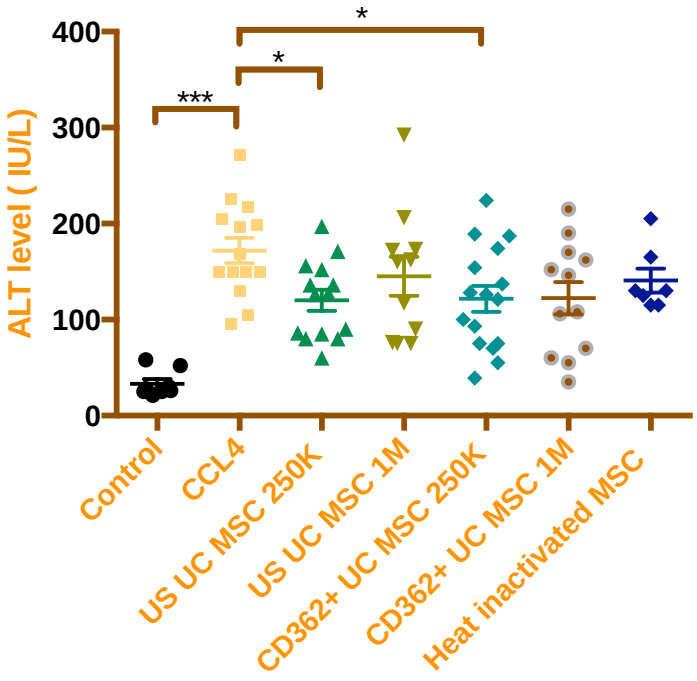

Figure 5-2 Analysis of ALT liver enzyme after infusion of two doses of unsorted hUC-MSCs and CD362+ sorted hUC-MSCs in mice with acute CCl_4 injury. Graph indicates serum ALT level in different groups of mice. Data are expressed with median value and represent >10 animals/group. ANOVA with post-hoc analysis was performed. Data are presented as the mean ± SD. *P < 0.05, **P < 0.01 and ***P < 0.001.

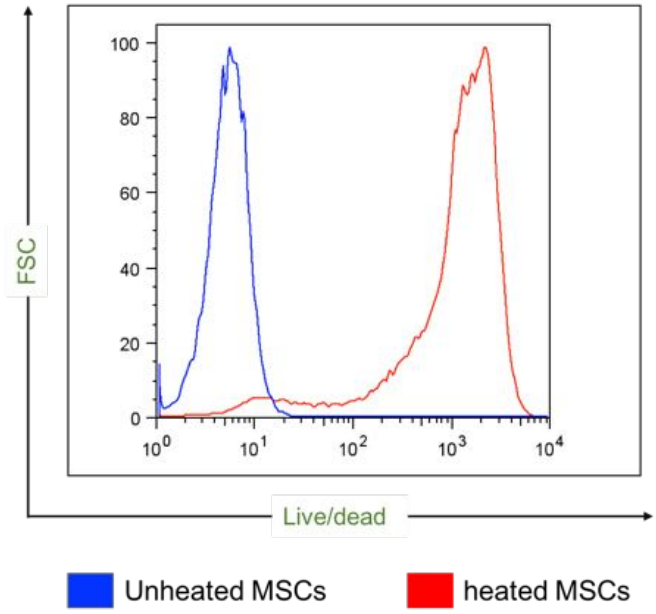

Figure 5-3 Respresentative histogram of APC/CY7 expression on MSCs by flow cytometry. Expression of APC/CY7 of the unheated (blue line) and heated MSCs (red line). Heated MSCs were heated in a heating block for 10 minutes.

Histological examination using H&E staining (Figure ***5-4***) showed a normal structure in the control group (treatment with mineral oil) and an abnormal hepatic injury (extensive area of necrosis) after treatment with CCl4. In comparison with the injured mice, there was less cellular damage in the liver structure with fewer inflammatory cells observed after MSCs administration.

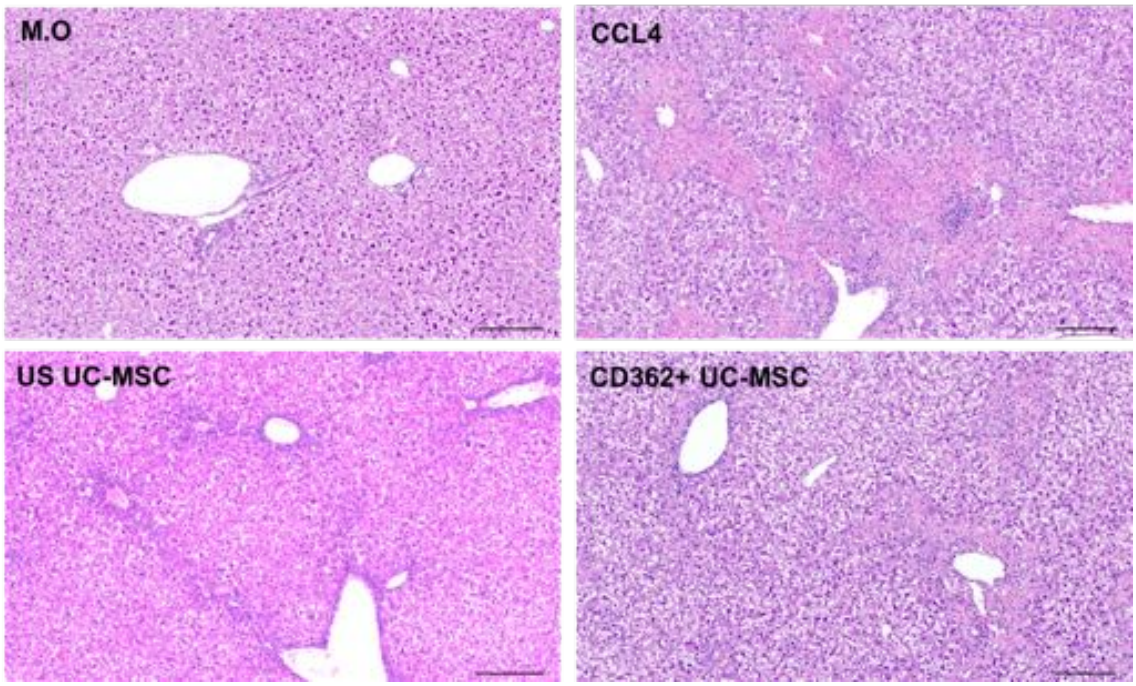

Figure 5-4 H&E staining of liver sections after treatment with $2.5x10^5$ of hUC-MSCs. Represents structure of the liver sections after control mice (M.O). CCl_4-injured mice, and mice undergoing MSCs transplantation following liver injury; a clear improvement of necrotic area was noticed with both MSCs treatment group. Scale bars: 200 μm.

5.3.3 Effect of unsorted and CD362+ sorted UC-MSCs infusion on hepatic lymphocyte and monocyte populations in CCl_4-induced liver injury

The immunosuppressive effect of hUC-MSCs from two populations (unsorted hUC-MSCs and $CD362^+$ sorted hUC-MSCs) on immune cell sub-sets in liver and blood were examined in this chapter.

5.3.3.1 Sorted CD362^{+}UC-MSCs reduce hepatic CD45^{+} immune cells

To examine whether infusion of MSCs could ameliorate liver inflammation of CCl_4-injured mice, we compared the therapeutic potential of unsorted hUC-MSCs and CD362^{+} sorted UC-MSCs after administration of $2.5x10^5$ MSCs by intravenous injection. We analysed expression of CD45^{+} in the liver sections via immunohistochemistry (Figure 5-5A) and found that both unsorted MSCs or CD362^{+} sorted MSCs resulted in a significant reduction in CD45^{+} expression in mice injured with CCl_4 injection (Figure 5-5A). To further show the functionality of transplanted cells, we quantified all CD45 positive immune cells isolated from the liver and the blood using flow cytometry analysis. CD362^{+} sorted UC-MSCs-treated mice exhibited significant reduction in hepatic CD45 positive cells compared to US UC-MSCs-treated mice. However, we found no significant differences in the CD45^{+} positive cells isolated from blood (Figure 5-5B).

A)

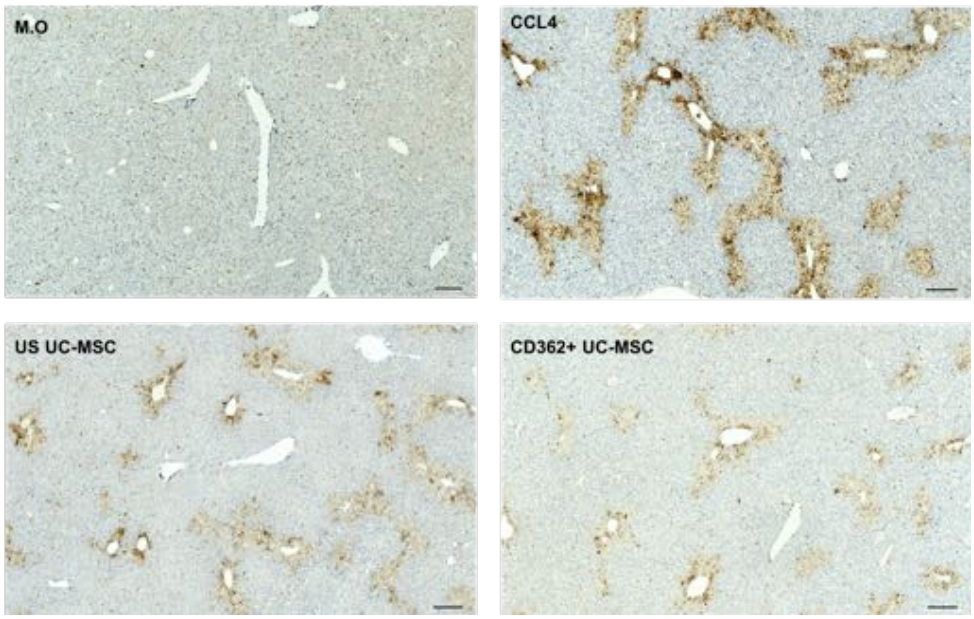

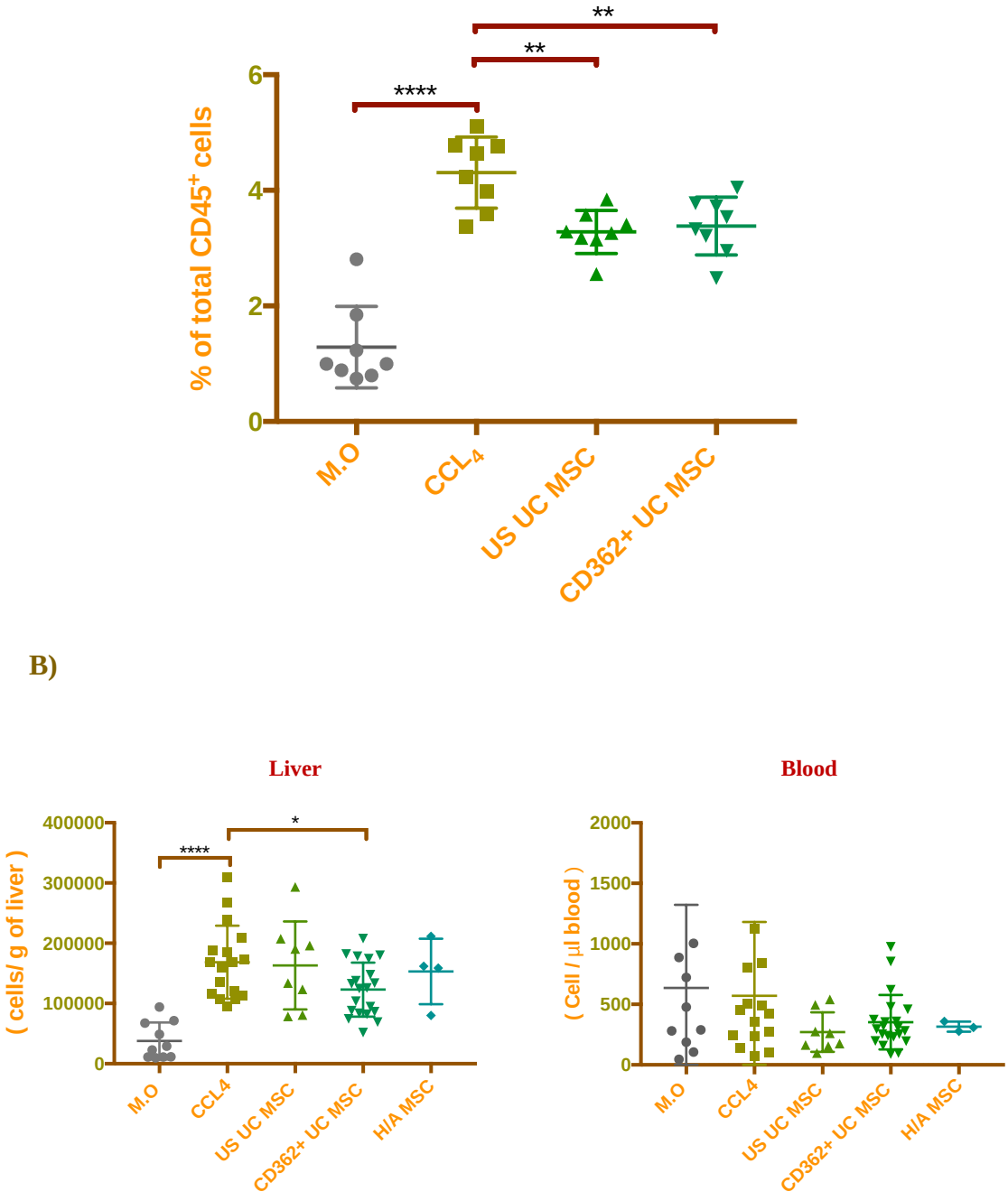

Figure 5-5 CD362^{+}UC-MSCs reduce hepatic CD45^{+} immune cells. A) Representative immunohistochemical (IHC) staining for hepatic CD45^{+} cells expressed as a percentage of the surface area of the field view analysed using ImageJ software (8 animals per group). Scale bars: 200µm. B) cells were gated from live CD45^{+} cells isolated from fresh mice livers and blood. Data are expressed as the number of infiltrating cells per gram of fresh liver tissue and per 1µl of blood (>8 animals per group, 4 animals in the H/A group). Data are presented as the mean ± SD. *P < 0.05, **P < 0.01 and ***P < 0.001.

5.3.3.2 CD362+UC-MSCs reduce total hepatic lymphocytes, non-NK cells, and B cells

Increases of NK, non-NK and B cells can directly contribute to the inflammation associated with acute liver injury in mice (Mehal and Friedman, 2007). I further investigated the influence of MSCs administration on these immune cells across different tissue sources, mainly liver and blood. I show that MSCs transplantation reduces the total number of lymphocytes as shown in (Figure ***5-6***A). In addition, both population of MSCs showed significant reduction in hepatic non-NK ($CD49^-$) and B cell ($CD19^+$) numbers. (Figure ***5-6***A). However, administration of US and $CD362^+$ sorted MSCs did not lead to changes in the hepatic nor circulating number of NK cells (Figure ***5-6***B). These results provide strong evidence that UC-MSCs decrease the number of hepatic non-NK cells as well as B cells.

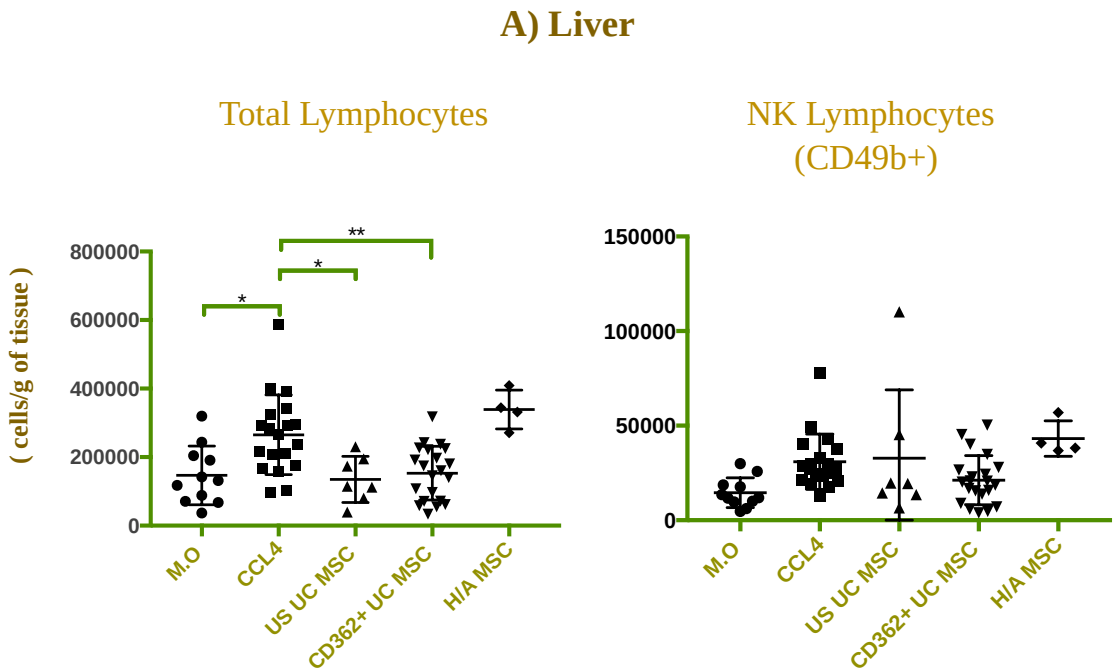

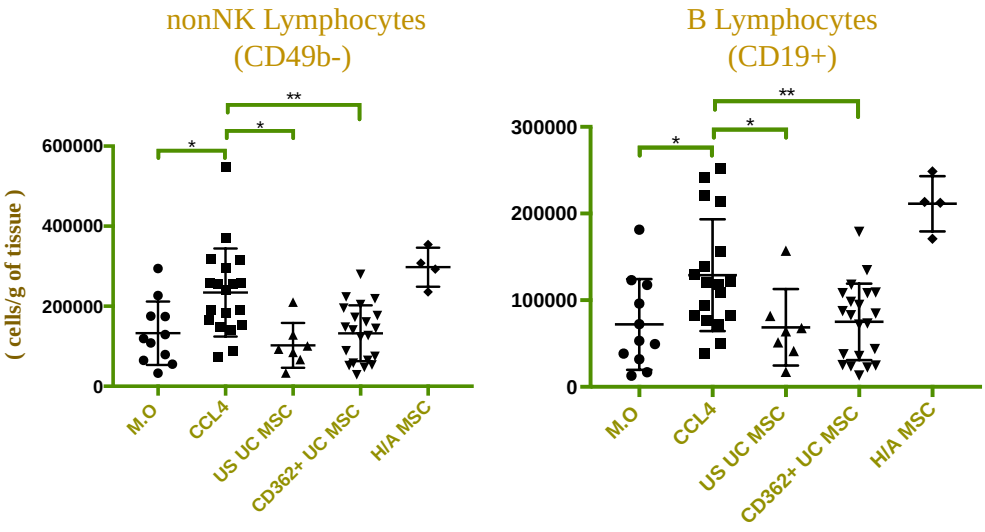
nonNK Lymphocytes
(CD49b-)
B Lymphocytes
(CD19+)
(cells/g of tissue)
600000
400000
200000
0
300000
200000
100000
0
*
**
M.O
CCL4
US UC MSC
CD362+ UC MSC
H/A MSC

B) Blood

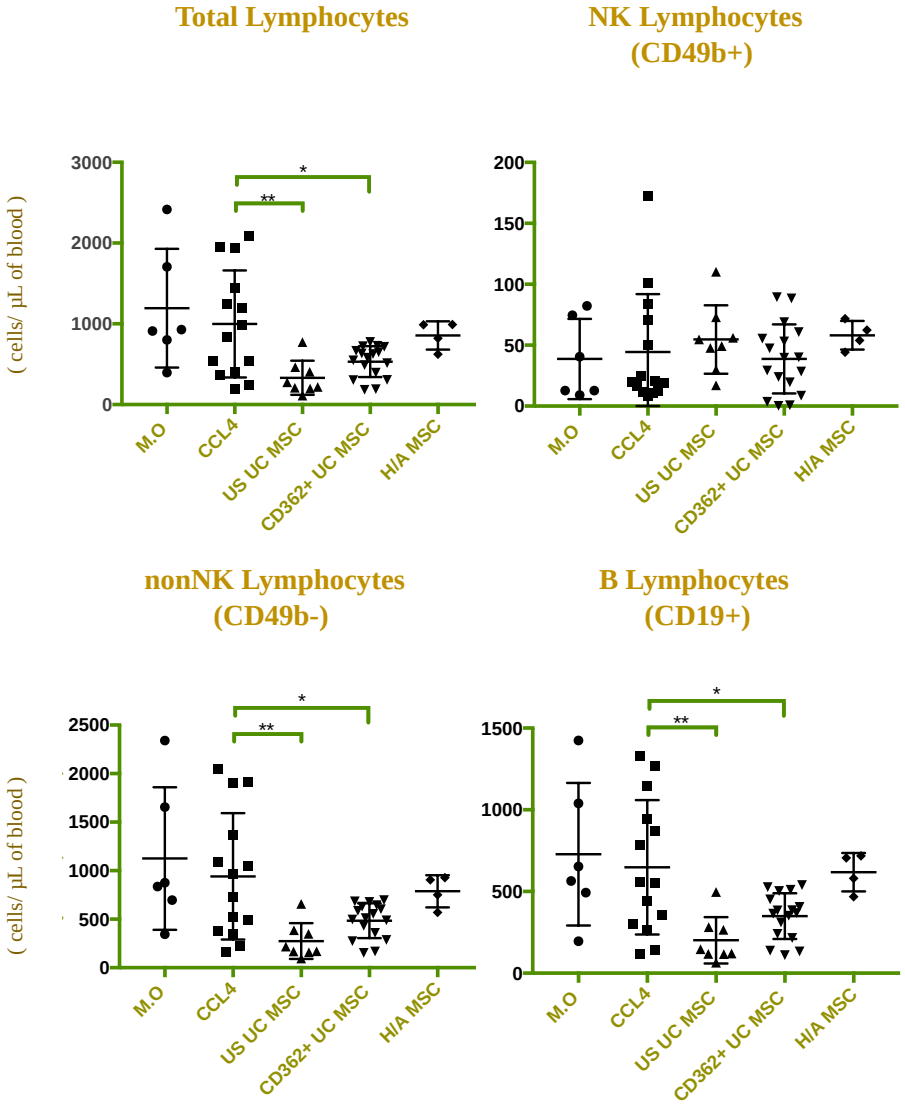
Total Lymphocytes
NK Lymphocytes
(CD49b+)
nonNK Lymphocytes
(CD49b-)
B Lymphocytes
(CD19+)
(cells/ µL of blood)
3000
2000
1000
0
200
150
100
50
2500
1500
500
*
**
M.O
CCL4
US UC MSC
CD362+ UC MSC
H/A MSC

Figure 5-6 Analysis of lymphocyte population using flow cytometry analysis. A) Number of NK, non-NK and B cells represents a different NK, non-NK and B lymphocyte isolated from mouse liver after transplantation with US and CD362 UC-MSCs. Data are expressed by the number of infiltrating cells per gram of fresh liver tissue. B) Number of NK, non-NK and B cells in circulating blood following administration of US and CD362 UC-MSCs. Data are expressed as the number of infiltrating cells per 1µl of blood. (>8 animals per group, 4 animals in the H/A group). Data are presented as the mean ± SD. *P < 0.05, **P < 0.01 and ***P < 0.001.

Having demonstrated by flow cytometry that there was a significant reduction in the number of the non-NK and B cells, I further examined the potential of hMSCs to reduce the number of $CD3^+$, $CD4^+$ and $CD8^+$ cells in CCl_4-injured mice, but I could not observe any significant differences with any of the MSC groups. More importantly, I could not report any significance difference between the healthy and CCl_4-injured groups in this animal model. Interestingly, significant reductions were observed in circulating numbers of $CD3^+$, $CD4^+$ and $CD8^+$ cells 3 days following MSCs treatment, as shown in Figure **5-7**.

Because several studies have reported that MSCs can modulate liver inflammation through the induction of regulatory T cells (Sivanathan et al., 2015), I investigated whether unsorted UC-MSCs and CD362 UC-MSCs could further modulate the suppression of T cells through induction of Treg cells. As shown in Figure ***5-8***, my data reported that none of the MSCs (unsorted and sorted CD362 cells) had a significant impact on hepatic regulatory T cells (Tregs), as reported by expression of $CD3^+$, $CD4^+$, $CD25^+$ and $FOXP3^+$. Overall, my findings indicate that the therapeutic effect of MSCs (US and CD362) on CCl_4 acute liver injury failed to suppress $CD3^+$, $CD4^+$ and $CD8^+$cells,

and to induce the generation of Tregs in the liver. I did however observe an effect of MSC treatment on the numbers of circulating $CD3^+$, $CD4^+$ and $CD8^+$ immune cells.

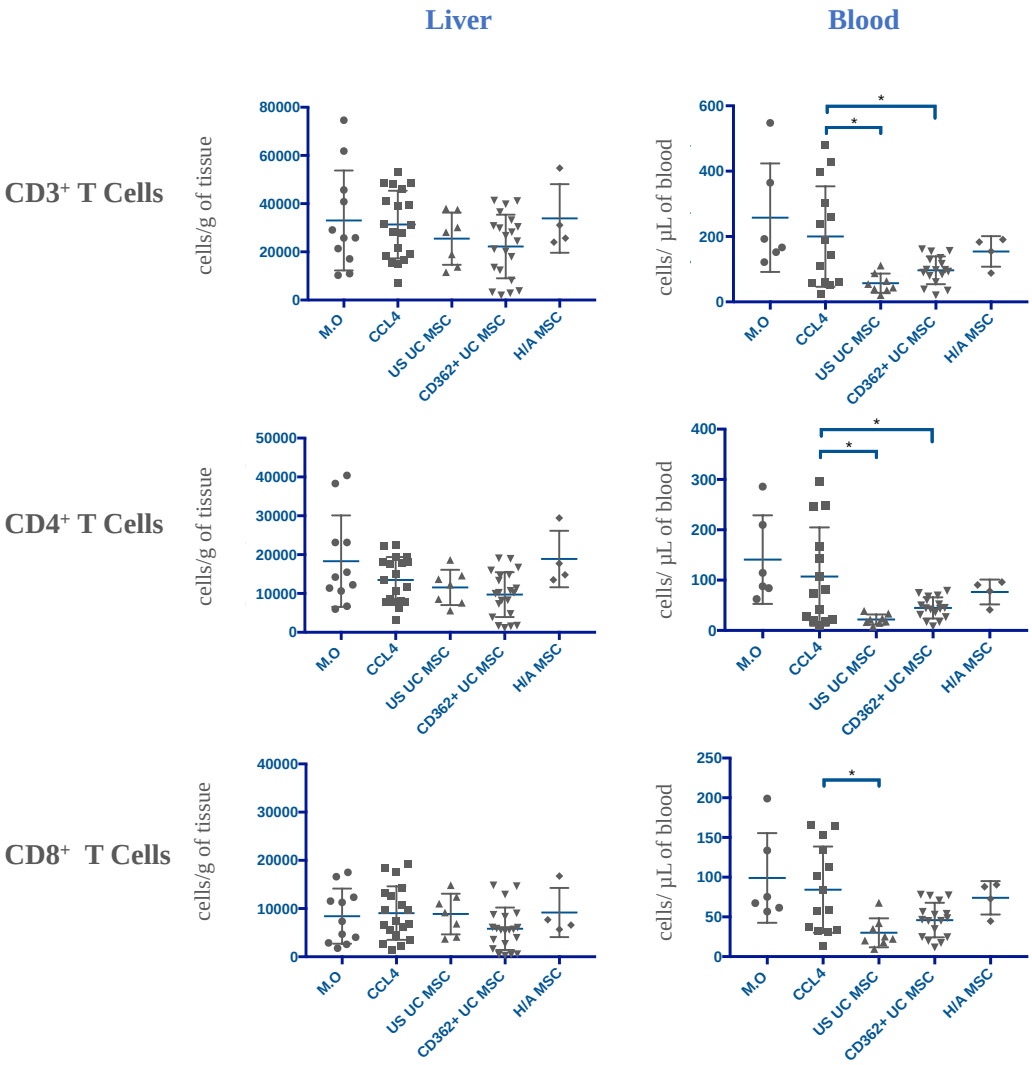

Figure 5-7 The numbers of infiltrating $CD3^+$, $CD4^+$ and $CD8^+$ cells in the livers and blood of CCl_4-injured mice were quantified by flow cytometry three days after treatment with UC-MSCs. All cells were gated from live cells isolated from the fresh mice livers and blood. Data are expressed as the number of infiltrating cells per gram of fresh liver tissue and by the number of infiltrating cells per 1µl of blood. (>8 animals per group, 4 animals in the H/A group). Data are presented as the mean ± SD. *P < 0.05, **P < 0.01 and ***P < 0.001.

A)

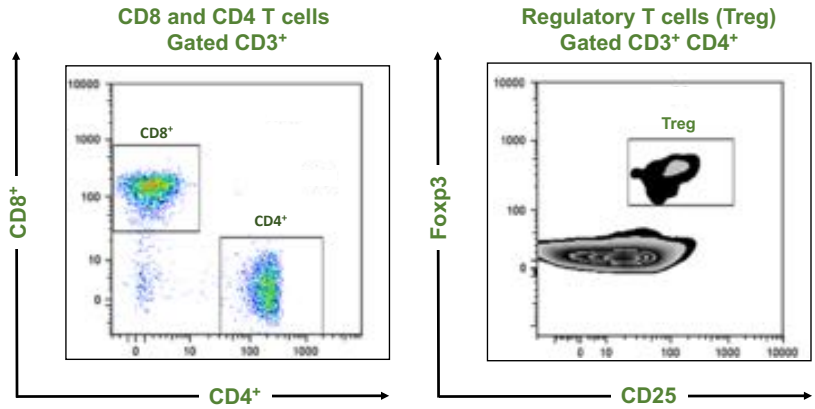

B)

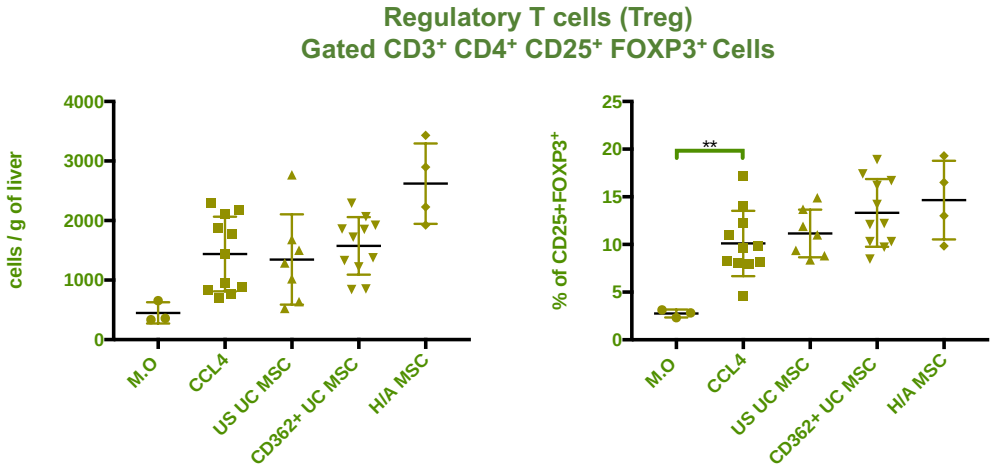

Figure 5-8 The generation of regulatory T cells following UC-MSCs infusion. (A) representative diagram shows the gating strategy used for analysis of Tregs. B) The generation of regulatory T cells in the liver of CCl_4-injured mice was quantified by flow cytometry. All cells were gated from live $CD3^+CD4^+CD25^+FOXP3^+$ cells isolated from the fresh mice livers. Data are expressed as percentages (%) and the number of cells per gram of fresh liver tissue. (>8 animals per group, 4 animals in the H/A group). Data are presented as the mean ± SD. *P < 0.05, **P < 0.01 and ***P < 0.001.

5.3.3.3 Flow cytometric analysis of intrahepatic monocyte sub sets in mice with CCl_4-induced liver injury after treatment with UC-MSCs

Following CCl_4, the number of hepatic infiltrating macrophages peaked at 72 hours (as reported previously in Chapter 4). I further analysed the ability of MSCs to modulate monocyte subsets in mice with acute CCl_4 liver injury. Three days following intravenous administration of MSCs, immune cells were isolated from mouse liver and blood and analysed using flow cytometry. I observed a remarkable increase in the total $CD11^+$ cells and $CD11^+$ $F4/80^+$ in CCl_4-injured mice when compared to the normal mice treated with mineral oil (Figure **5-9**A). In comparison to the CCl_4-injured mice, I reported that US and CD362 MSCs significantly downregulated the number of macrophages ($CD11^+$ $F4/80^+$) in the liver, but did not show any significant observation in circulating monocytes (Figure **5-9**A). Further quantification of F4/80 positive cells on liver section using IHC provided a similar observation, which resulted in a decreased level of macrophages following $CD362^+$ MSCs administration (Figure **5-9**B). Together, these results indicated that $CD362^+$ sorted MSCs reduce the number of hepatic macrophages, suggesting that MSCs could play a role in liver injury through modulation of monocytes and macrophages.

A)

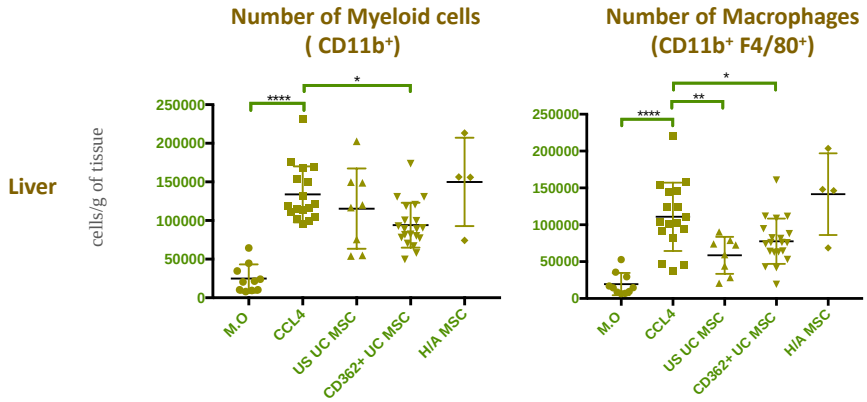

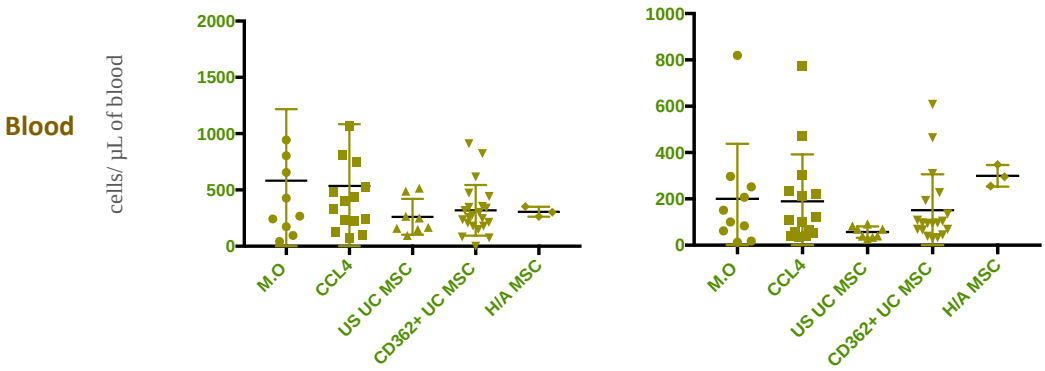
Blood
cells/ µL of blood
2000
1500
1000
500
0
M.O
CCL4
US UC MSC
CD362+ UC MSC
H/A MSC
1000
800
600
400
200
0
M.O
CCL4
US UC MSC
CD362+ UC MSC
H/A MSC

B)

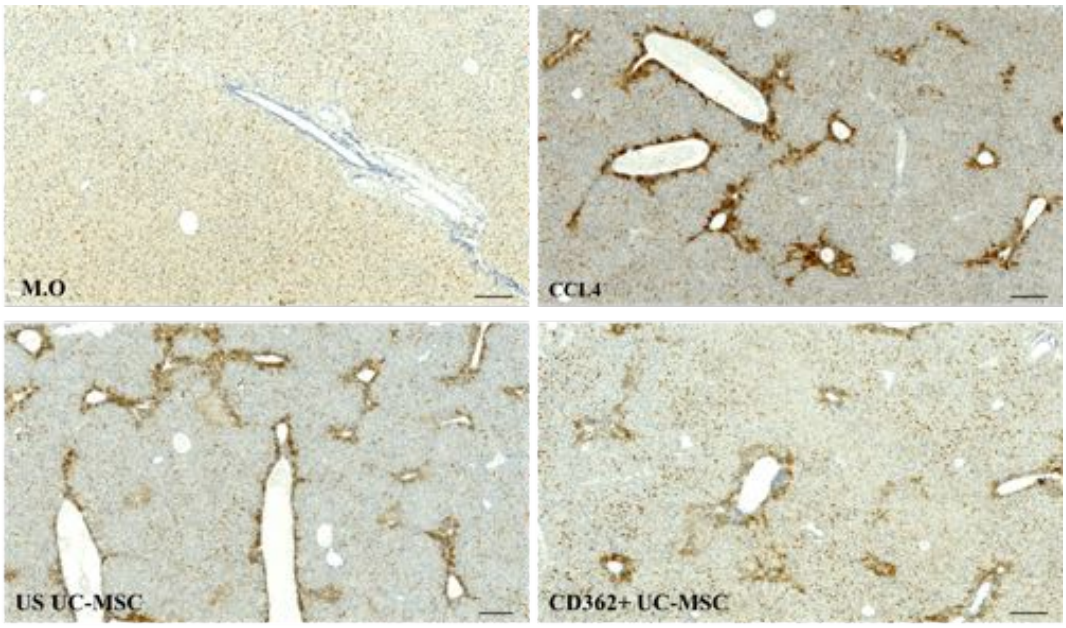
M.O
CCL4
US UC-MSC
CD362+ UC-MSC

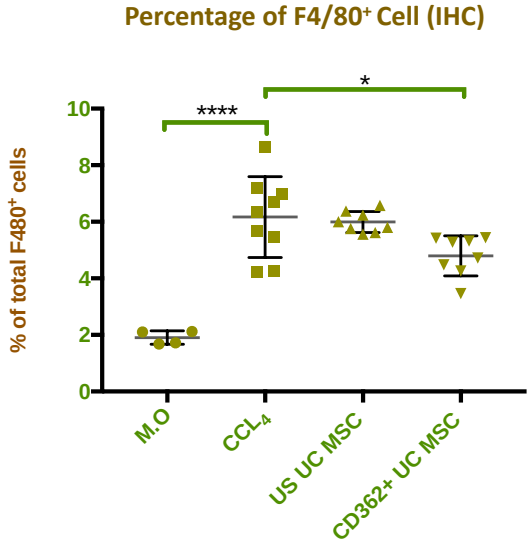
Percentage of F4/80+ Cell (IHC)
% of total F480+ cells
****
*
10
8
6
4
2
0
M.O
CCL4
US UC MSC
CD362+ UC MSC

Figure 5-9 CD362^{+}UC-MSCs reduce hepatic F4/80^{+} immune cells in mice injured with CCl_4 induction. A) Cells were gated from live CD11b^{+} F4/80^{+} cells and isolated from fresh mice livers and blood. Data are expressed by the number of infiltrating cells per gram of fresh liver tissue and per 1µl of blood (>8 animals per group, 4 animals in the H/A group). B) Representative immunohistochemical (IHC) staining for hepatic F4/80^{+} cells expressed as a percentage of the surface area of the field view analysed using imageJ software (8 animals per group). Scale bars: 200µm. Data are presented as the mean ± SD. *P < 0.05, **P < 0.01 and ***P < 0.001.

5.3.3.4 Administration of UC-MSCs fails to induce macrophage polarisation from classically-activated M1-phenotype towards alternatively-activated M2-phenotype in inflamed murine liver.

To further characterise the changes in the infiltrated macrophages, I quantified and phenotyped different macrophage populations using flow cytometry. In the present study, the macrophage markers (F4/80) and (Ly6C) were used to identify two distinct populations of macrophages; CD11b^{+} F4/80 Ly6C^{hi} was used to characterise the pro-inflammatory M1-phenotypes (classical macrophages) whereas CD11b^{+} F4/80 Ly6C^{lo} (Alternative macrophages) was used for anti-inflammatory M2-phenotypes (Figure ***5-10***A). To determine the role of MSCs function in macrophage polarisation, I compared the immunosuppressive ability of US and CD362 UC-MSCs on M1 and M2-like cells isolated from mouse liver. Based on the flow cytometry data, MSCs had no effect on the macrophage phenotype.

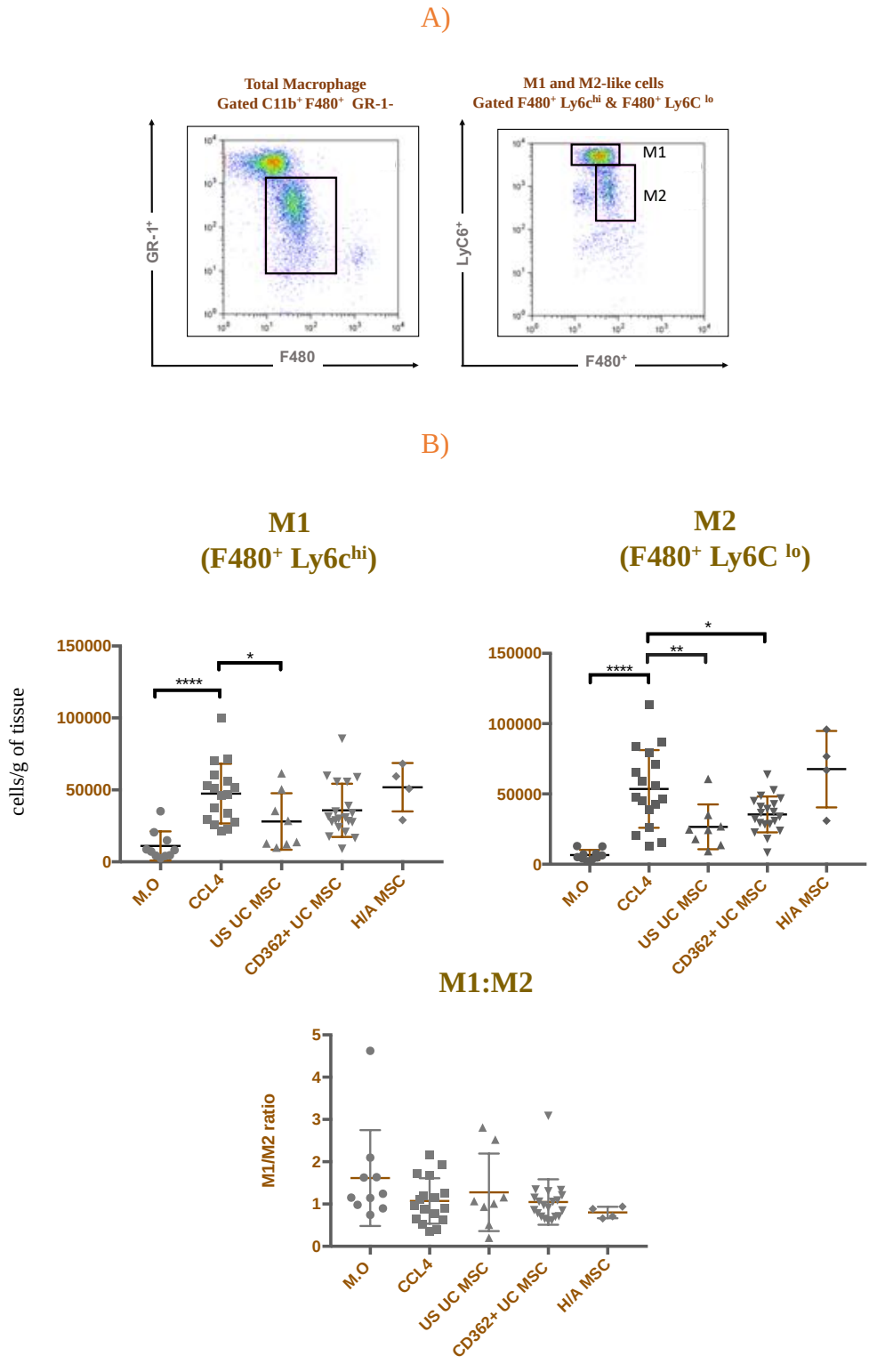

Figure 5-10 The effect of UC-MSCs infusion on the M1 and M2 macrophages. A) Representative diagram shows the gating strategy used for analysis M1 and M2-like cells. B) The total number of CD11b^{+} F4/80 Ly6C^{hi} classically-activated pro-inflammatory M1-phenotypes and CD11b^{+} F4/80 Ly6C^{lo} anti-inflammatory M2-phenotypes in the livers of CCl_4-

injured mice were quantified by flow cytometry analysis. The percentage of M1 cells, M2 cells of fresh liver tissue of CCl_4 mice receiving either 250K US UC MSC or $CD362^+$ UC MSC were quantified and compared to the injured group. M1/M2 ratio expressed the proportion of M1 and M2 cells in the liver tissues. Data are expressed as percentages (%) of fresh liver tissue. (>8 animals per group, 4 animals in the H/A group). Data are presented as the mean ± SD. *P < 0.05, **P < 0.01 and ***P < 0.001.

Next, I further analysed the influence of $CD362^+$ MSCs as well as US MSCs on the levels of neutrophils in liver and blood at 72 hours post-CCl_4 injury. Compared with that in the CCl_4-injured group, the degree of infiltration of $CD11b^+$ $Ly6G^+$ cells (neutrophil) was markedly decreased in both MSCs treatment, but I observed a significant reduction in the number of hepatic neutrophils with US MSCs (Figure ***5-11***).

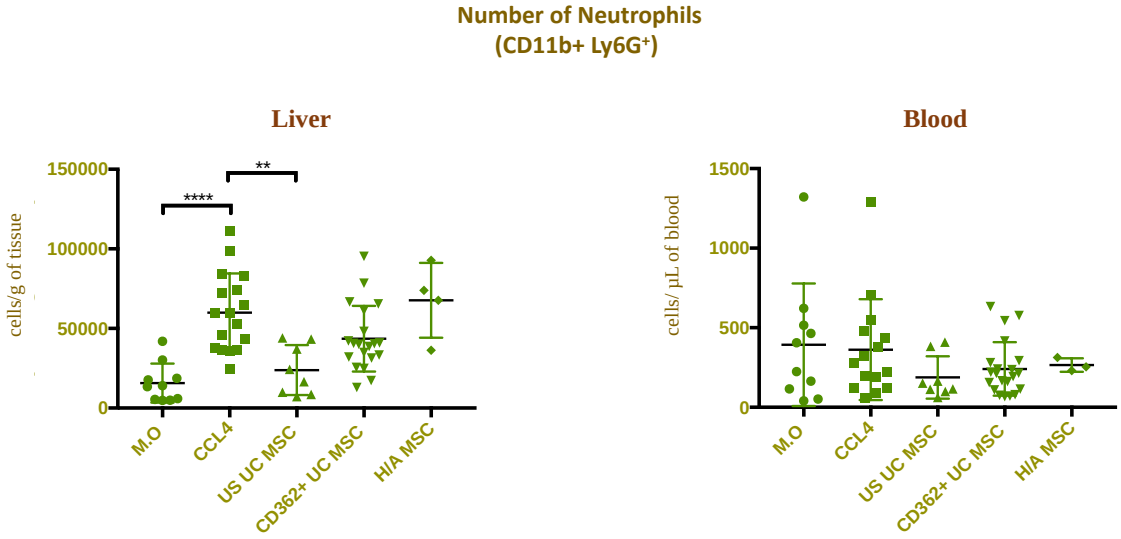

Figure 5-11 The effects of UC and CD362 MSCs on expression of the inflammatory neutrophil in the liver and blood at 72 hours post-CCl_4 treatment. Neutrophils were gated from live $CD11b^{+\text{ and}}$ $Ly6G^+$ cells isolated from the fresh mice livers and blood. Data are expressed by the number of infiltrating cells per gram of fresh liver tissue and per 1µl of blood (>8 animals per group, 4 animals in the H/A group). Data are presented as the mean ± SD. *P < 0.05, **P < 0.01 and ***P < 0.001.

5.3.4 Evaluating the oxidative stress and antioxidant markers in CCl_4 mice undergoing MSC transplantation

Oxidative stress and free radicals are two main observations in the mouse liver following CCl_4 induction. Oxidative stress can be measured by the quantified number of free radicals in the liver. Here, I used the Thiobarbituric acid reactive substances (TBARS) assay to detect the level of oxidative stress using liver lysates from CCl_4-injured liver following MSCs injections. Three days following MSCs administration, a pattern of increase in TBARS contents in the liver samples was observed but did not reach statistical significance (Figure ***5-12***A). Moreover, additional experiments were performed to investigate other markers, such as HO-1, GSS and HIF1-α, in the mouse liver using qPCR. I found that hepatic expression of HO-1 was significantly down regulated following MSCs injections (Figure ***5-12***B). Another contradictory finding was reported in HIF1-α expression, which was shown to have significantly increased with MSCs treatment as compared with the CCl_4-injury mice treated with PBS, as shown in Figure ***5-12***B. GSS gene expression levels were still elevated after 72 hours of CCl_4 treatment and declined slightly after exposure to MSCs infusion.

Antioxidants provide a first line of defence against oxidative stress derived from injured tissue. In this experiment, I examined whether MSCs could modulate oxidative stress through secretion of antioxidants to treat the liver damage caused by CCl_4 induction. In line with my previous findings, I found that antioxidants levels were changed gradually through the time course of the injury, with variation across the different antioxidants tested. Accordingly, I used two time points (24 and 72 hours) to evaluate the correlation between MSCs and antioxidants level in the liver. Data indicated that, after MSCs

administration, the CCl_4-injured mice exhibited different expression profiles of SOD1, SOD2, SOD3, IDH-1, and catalase after 24 hours of MSCs infusion (Figure ***5-13***). No differences were observed between the untreated and MSCs-treated mice at this time point (24 hours). However, expression of IDH-1 gene appeared to have significantly increased after 72 hours of MSCs injection, whereas SOD2 exhibited a pattern of low expression (*p* 0.0684) compared to the untreated group. I did not notice any changes in the expression of SOD1, SOD3 and catalase.

A)

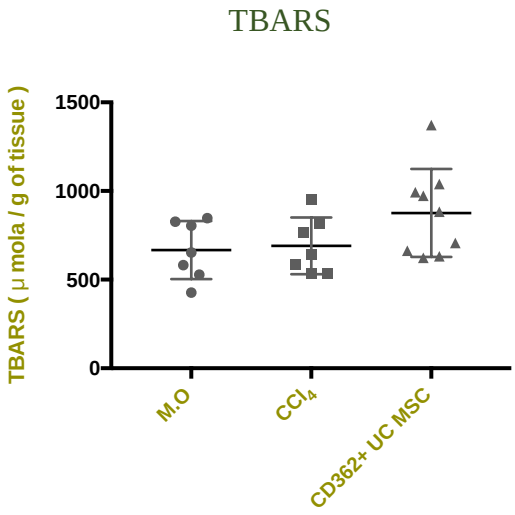

B)

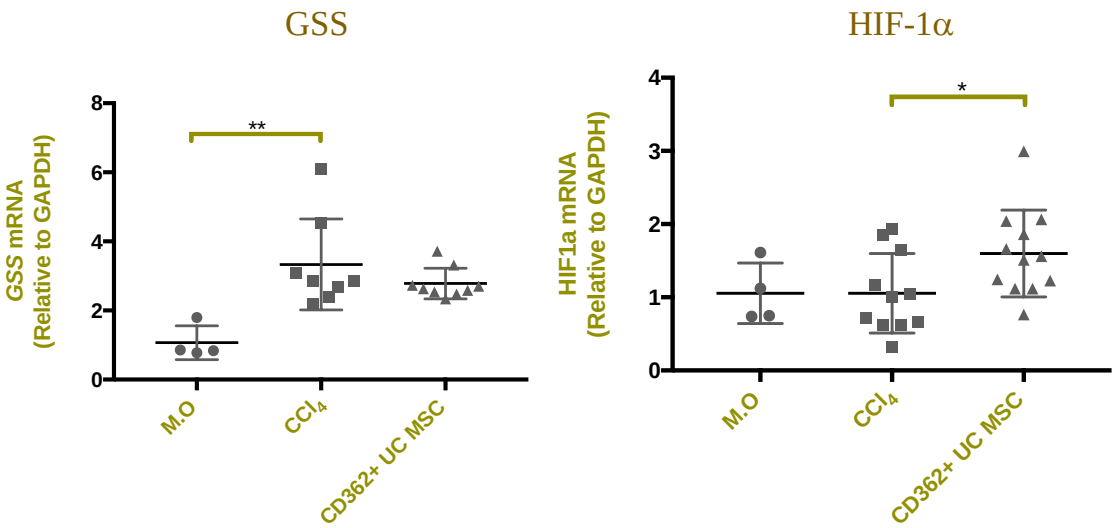

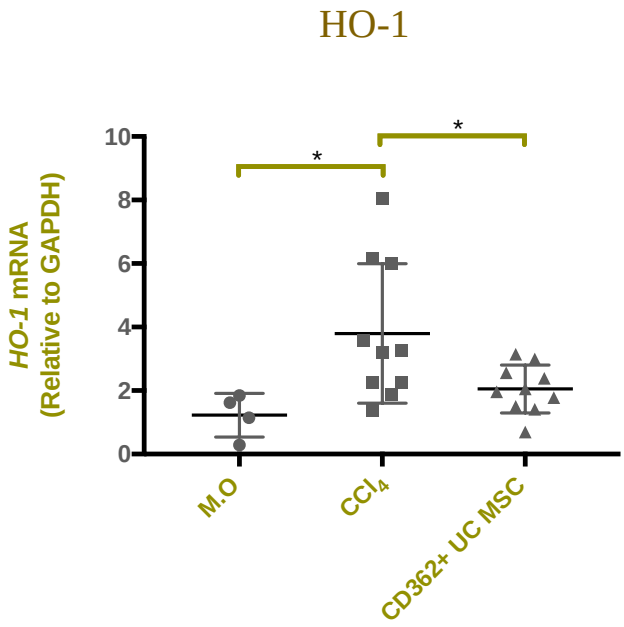

Figure 5-12 Evaluation of *in vivo* oxidative stress in liver samples obtained from mice undergoing MSCs transplantation. A) TBARS levels were measured from liver lysate 72 hours following MSCs administration (7-8 animals per group). Gene expression of GSS, HO-1 and HIF1-α in the liver after MSCs administration in CCl_4-injured mice was measured by qPCR and normalised to GAPDH B. (>8 animals per group, 4 animals in the H/A group). Data are presented as the mean ± SD. *P < 0.05, **P < 0.01 and ***P < 0.001.

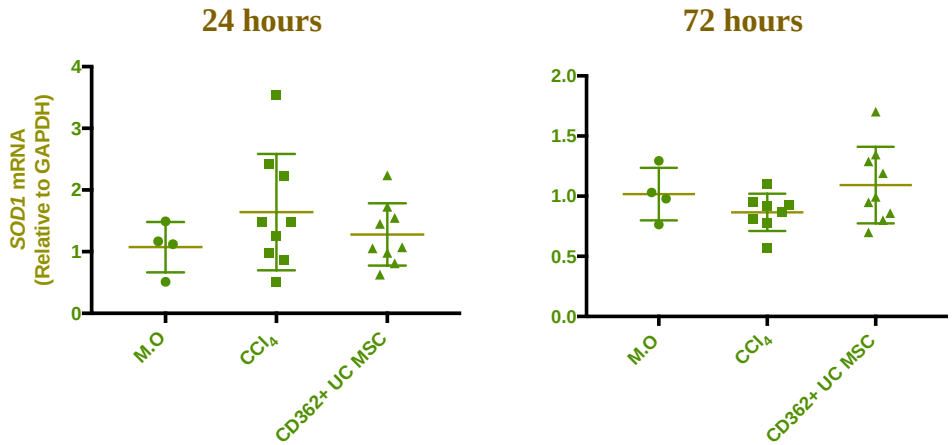

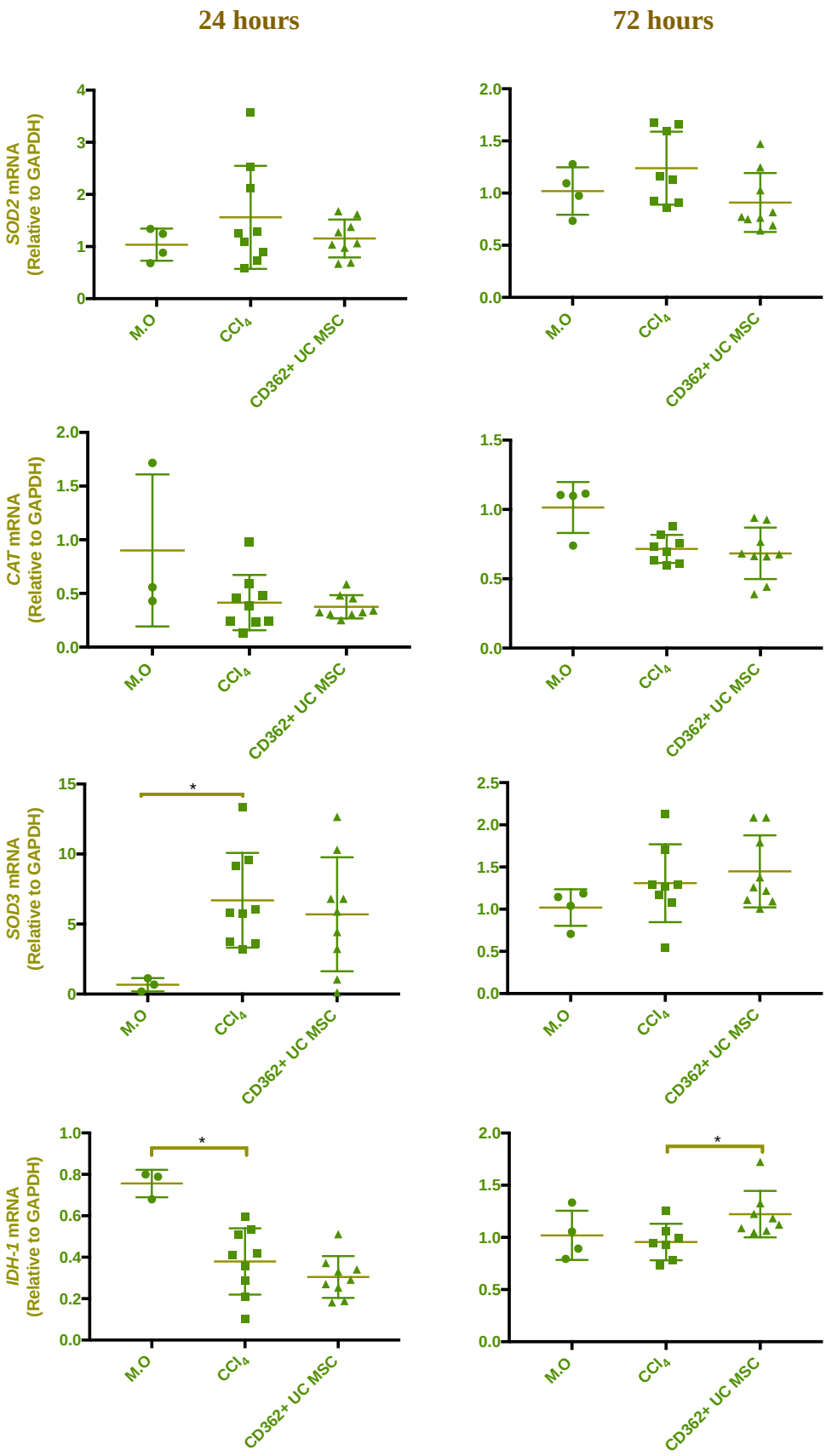
24 hours
72 hours
SOD2 mRNA (Relative to GAPDH)
CAT mRNA (Relative to GAPDH)
SOD3 mRNA (Relative to GAPDH)
IDH-1 mRNA (Relative to GAPDH)
M.O
CCl4
CD362+ UC MSC
*

Figure 5-13 Analysis of gene expression of antioxidant in the liver at 24 and 72 hours following MSCs treatment. Changes in the hepatic gene expression of SOD1, SOD2, SOD3, IDH-1 and catalase in CCl_4-treated mice receiving 250K $CD362^+$ UC MSC quantified by q-PCR (4-8 animals per group). Data are presented as the mean ± SD. *P < 0.05, **P < 0.01 and ***P < 0.001.

5.3.5 Evaluating the anti-apoptotic markers in CCL4 mice undergoing MSC transplantation

I next performed experiments to investigate whether anti-apoptotic markers related to MSCs administration may be critical in these experimental conditions. Figure ***5-14*** presents the qPCR results of Birc5 and Bcl2l1 in mouse liver form both injured as well as the MSCs treatment group. The expression of Birc5 gene was found to be extremely high three days following liver injury induced by CCl_4, whereas Bcl2l1 expression was not found to change. I compared the expression of Birc5 and Bcl2l1 three days following MSCs transplantation, with no difference observed when compared to injured mice treated with PBS (Figure ***5-14***).

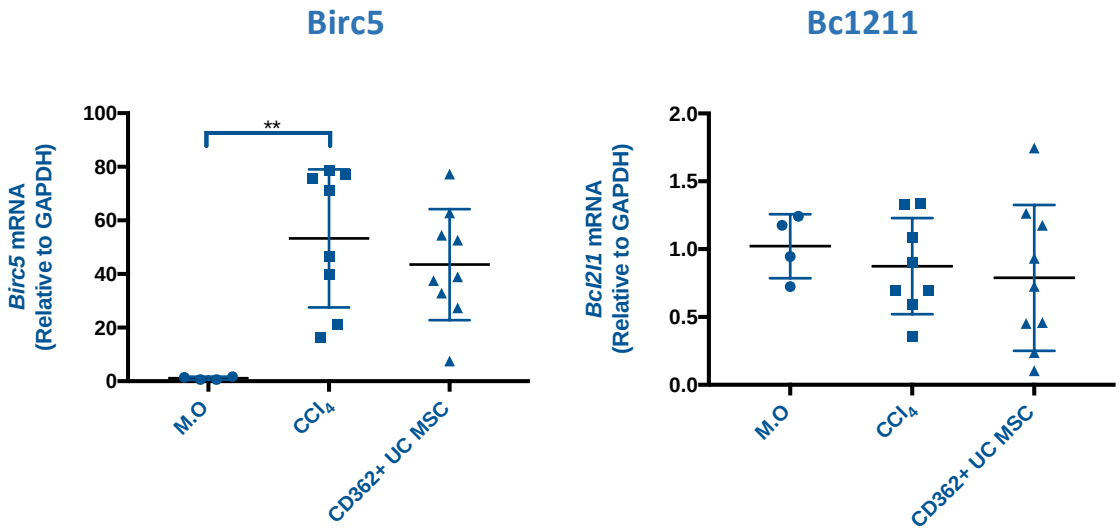

Figure 5-14 Birc5 and Bcl2l1 gene expression in CCl_4-injured liver after treatment with MSCs. (4-8 animals per group). Data are presented as the mean ± SD. *P < 0.05, **P < 0.01 and ***P < 0.001.

5.3.6 Effect of MSC transplantation on the expression of surface adhesion molecules

Two adhesion molecules, in particular, intracellular adhesion molecule (ICAM)-1 and vascular cell adhesion molecule (VCAM)-1, have shown to mediate the immunosuppressive function of MSCs via direct adhesion of MSCs to the immune cells (Chamberlain et al., 2011). To assess whether adhesions molecules were expressed in the hepatic injury induced by CCl_4, I evaluated the expression of ICAM and VCAM markers using qPCR as well as IHC. I found that ICAM and VCAM were highly expressed after 72 hours of CCl_4. More importantly, I explored the role of MSCs transplantation in the level of ICAM and VCAM adhesion molecules 72 hours following MSCs infusion. I observed a similar induction of ICAM (Figure ***5-15***) and VCAM (Figure ***5-16***) in the MSCs-treated mice as compared to CCl_4-injured mice treated with PBS.

A

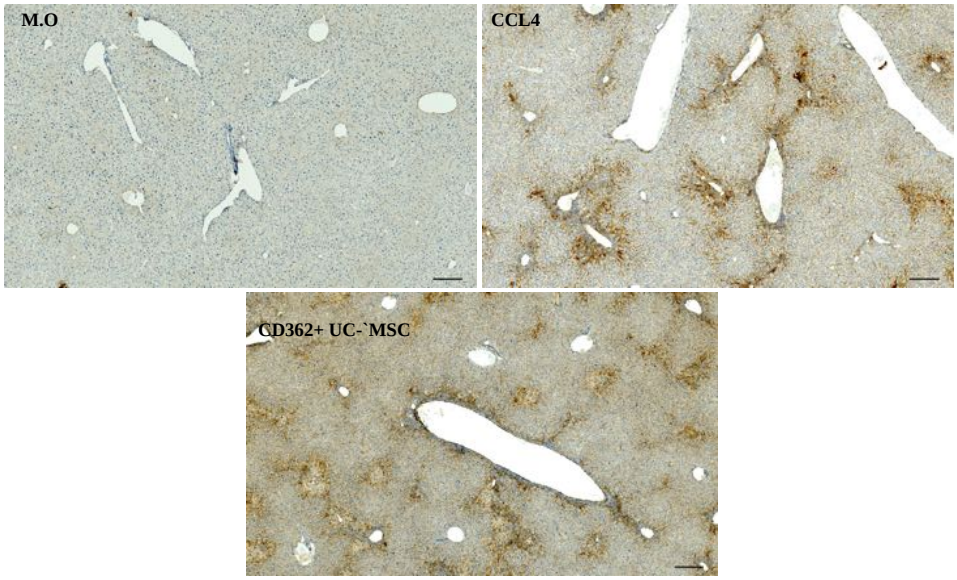

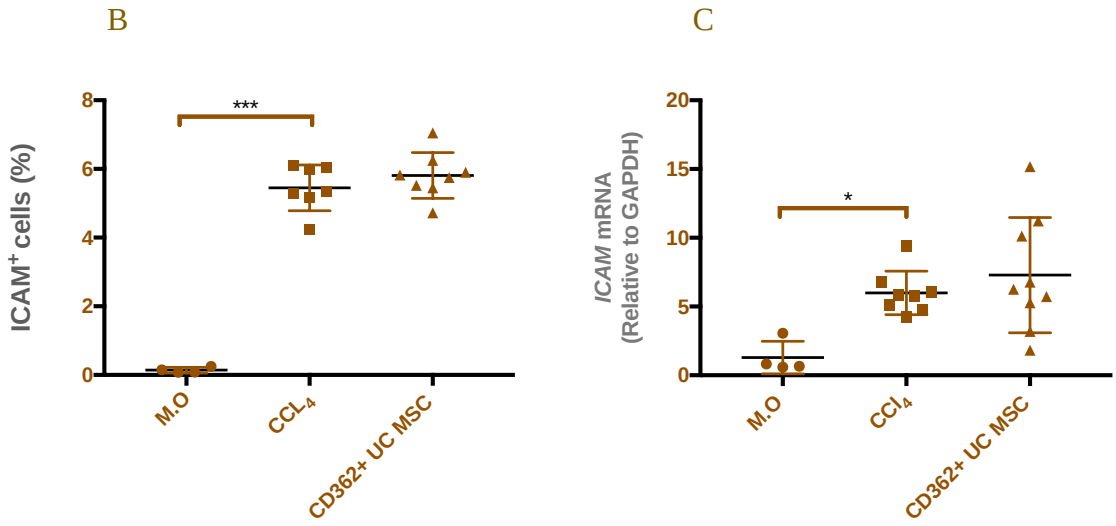

Figure 5-15 Effect of CD362$^+$UC-MSCs treatment on the hepatic ICAM-1 expression in the murine model of acute CCl_4. A) representative immunohistochemical (IHC) staining for hepatic ICAM$^+$ cells. B) quantification of ICAM$^+$ cells expressed as a percentage of the surface area of the field view analysed using imageJ software (8 animals per group). C) Changes in hepatic ICAM-1 mRNA expression in CCl_4-treated mice receiving 250K CD362$^+$ UC MSC quantified by q-PCR (4-8 animals per group). Scale bars: 200µm. Data are presented as the mean ± SD. *P < 0.05, **P < 0.01 and ***P < 0.001.

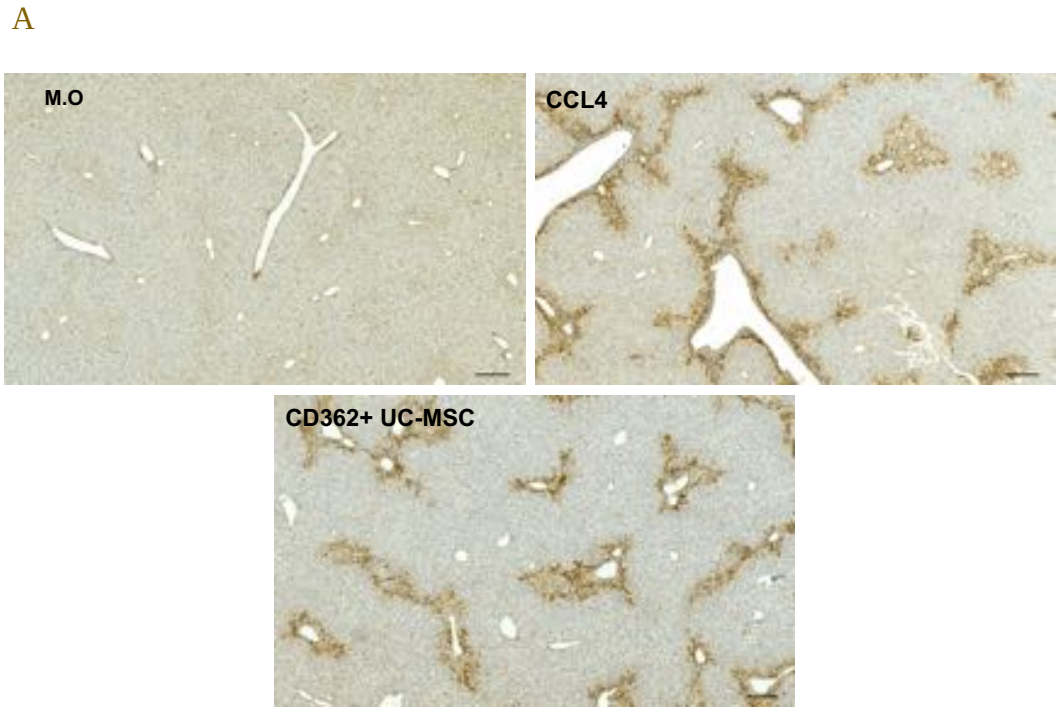

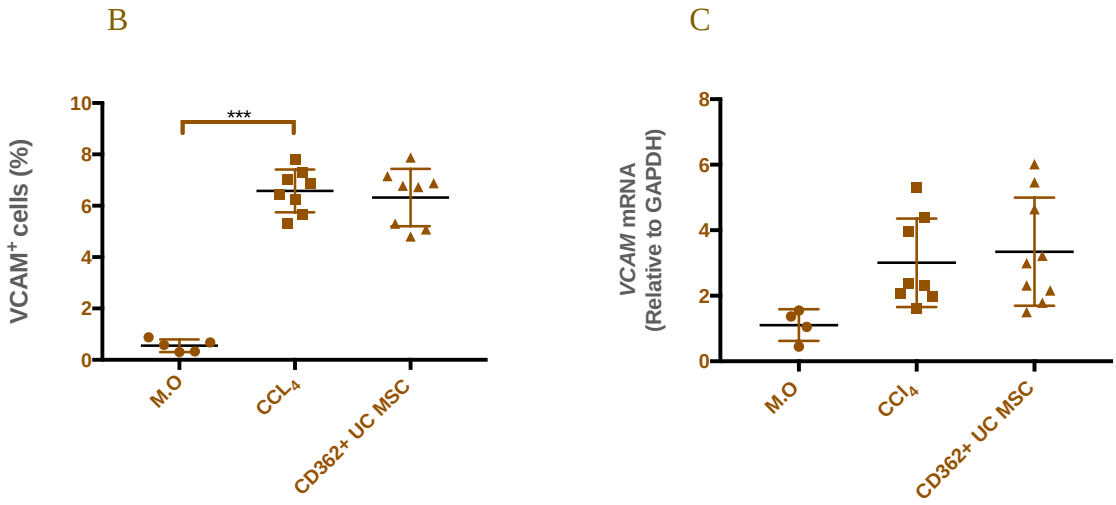

Figure 5-16 Effect of CD362$^+$UC-MSCs treatment on the hepatic VCAM-1 expression in the murine model of acute CCl_4. A) Representative immunohistochemical (IHC) staining for hepatic VCAM$^+$ cells. B) quantification of VCAM$^+$ cells expressed as a percentage of the surface area of the field view analysed using imageJ software (8 animals per group). C) Changes in hepatic VCAM-1 mRNA expression in CCl_4-treated mice receiving 250K CD362$^+$ UC MSC quantified by q-PCR (4-8 animals per group). Scale bars: 200µm. * Data are presented as the mean ± SD. *P < 0.05, **P < 0.01 and ***P < 0.001.

5.4 Discussion

The therapeutic potential of hUC-MSCs has been previously reported, but few studies have reported their effects in different animal models of acute liver injury (Burra et al., 2012; Zhu et al., 2013). These studies reported that transplanted mesenchymal stromal cells migrated to the site of chronic liver injury.

To address whether UC-MSCs have a therapeutic role in liver injury, I used a CCl_4-induced mice model of acute liver injury. Herein, I report the efficacy of the human UC-

MSCs in a liver injury model induced by CCl_4 using $CD362^+$ sorted UC-MSC and unsorted UC-MSCs. In this study, an efficacy dose-response with hUC-MSCs ($2.5x10^5$, $5x10^5$ and $1x10^6$) was assessed in acute CCl_4 liver injury. I observed that both $2.5x10^5$ and $1x10^6$ dose appear to have the same level of improvement, however, the $5x10^5$ dose shows extensive variation between animals, with an increase in ALT in some mice. Accordingly, I excluded the $5x10^5$ dose and used $2.5x10^5$ and $1x10^6$ in my further experiments.

The liver injury, as measured by serum ALT level, was not statistically significant in the dose response study (Figure 5-1), we can claim that it may simply related to using MSCs with late passages or lack of experience which caused technical limitation, especially in the MSCs infusion *in vivo.* We believe we overcome these limitations with more improvement in the technical skills and performed our in vivo experiment using MSCs with low passage number.

According to the above finding, head-to-head comparison between unsorted and $CD362^+$ purified hUC-MSCs was performed using two different doses ($2.5x10^5$ and $1x10^6$). A significant reduction in serum ALT was reported with infusion of $2.5x10^5$ $CD362^+$ UC-MSCs as well as US MSCs. My results indicate that the sorted cells have similar efficacy as unsorted cells in liver injury and that the low dose ($250x10^3$) effectively reduced inflammatory liver injury. In addition, my pathological examination of liver morphology by H&E staining revealed that liver necrosis resulted from CCl_4 injury is reduced after a single dose of UC-MSCs.

According to the above findings, I suggest that MSCs derived from umbilical cord could have immune regulatory properties to reduce the liver injury induced by CCl_4, and I

believe this could be a potential mechanism to further explain. As I have previously shown (Chapter 4), acute liver injury induced by CCl_4 is characterised by increased infiltrating of immune cells in the liver tissue. Here, I further investigated the correlation between the acute liver injury and immune cells using flow cytometric analysis; circulating immune cells were also reported in this study. In response to injury, I found a significant increase in the immune cells, expressed by $CD45^+$ isolated from liver, with no difference reported in the immune cells isolated from the blood. I also found that circulating immune cells did not correlate with the number of $CD45^+$ cells isolated from the liver. I believe that MSCs could have recruited some immune cells from circulation to the inflamed liver.

Recent evidence has shown that MSCs have an immunomodulatory function mediated by an interaction between immune cells in the tissue microenvironment and transplanted MSCs (Shi et al., 2012). The present study was designed to investigate if $CD362^+$ enriched MSC had superior efficacy to unsorted MSC. There was no convincing difference although $CD362^+$ sorted MSCs did not occasion have greater efficacy. This marker was found to play an essential role in immune regulation by reducing the immunogenicity (De Witte et al., 2017; de Witte et al., 2015). It has linked to contribute to modulate T cell biology through regulation of the T- cell receptor (TCR/CD3) complex expression, which can enhance the ability of T cell to response to any stimuli (Rovira-Clavé et al., 2012), and reported to have possible role to control fibrosis by modulate expression of TGF-β in fibroblast cells (Chen et al., 2004). According to the CD45 immunohistochemistry staining, the expression of leukocytes at the injured area of the liver was significantly decreased in the $CD362^+$ MSCs treatment group compared to US MSCs. This was

confirmed by the total of CD45 positive immune cells isolated from the liver using flow cytometry. According to the flow cytometry data, we only observed reduction in the CD45+ with the CD362 sorted MSCs. The reason why the unsorted cells did not reduce the hepatic CD45 positive cells is could be due to the low sample size in the unsorted MSCs treatment group comparing to the CD362+ sorted cells. More interestingly, MSCs in both conditions failed to modulate systemic immune cells.

The improvement in the liver injury following MSCs transplantation in this study could come from the ability of MSCs to modulate the liver inflammation through reduction in NK, non-NK and B cells. I compared the effects of MSCs on T cell lymphocyte obtained from different sources of CCl_4-injured mice (peripheral blood and liver). Three days after systemic perfusion of US and CD362 MSCs, a significant reduction in the non-NK cell as well as B cells was observed, as compared to CCl_4-injured mice treated with PBS. A similar phenomenon has also been reported by several studies, showing that MSCs can inhibit the proliferation and activation B cell as well as differentiation of B cell to plasma cells with immunoglobulin production ability (Corcione et al., 2006). Consistent with this, it has been shown by Ribeiro et al. (2013) that MSCs can indirectly inhibit B cell function by hampering their proliferation and activation. In the normal liver, B cell counting for up to 8% among all the lymphocyte population and get expanded in high number following liver inflammation (Robinson et al., 2016). Although another study reported that B cells were found to accumulate in the liver fibrosis and increased disease progression (Novobrantseva et al., 2005).

The potential cause for the differences observed in intra-hepatic B cells could come from the inhibitory effect of MSCs on B cell proliferation, activation, or ability to differentiate to plasma cells. This suppressive effect on the B cells could be associated with expression of some molecules on MSCs. For example, PD-L1 and CCL2 were reported to MSCs inhibition of B cells (Ribeiro et al., 2013). It is still unknown whether these factors released by MSCs on direct contact with B cells or required activation signal from B cells to enhance their immunoregulatory action. Another interesting point that remains to be studied in the future is the potential of MSCs to induce pro-tolerogenic B cell subsets in the liver microenvironment that have themselves provide immunomodulatory properties.

Furthermore, significant reduction was reported in the same immune cells isolated from peripheral blood. These findings could represent a possible explanation for the capacity of MSCs to reduce inflammation in the liver injury in this murine model. These observations indicative of endocrine or/and paracrine between MSCs and circulated immune cells and vice versa. We believe the changes induced by MSCs in the peripheral blood immune cells are associated with cytokines profiles released after MSCs administration. Abroad spectrum of factors produce by MSCs have been reported in different study, including HGF, EGF, VEGF, stromal cell-derived factor-1, IL-10, and IL-6 (Chao et al., 2014). Further study using UC-MSC-conditioned medium are necessary to confirm that paracrine factors of UC-MSCs alone could enhance the liver injury through several mechanisms. In addition, Use of MSC-derived exosomes or microvesicles in different diseases condition have shown therapeutic potential such as the ability to avoid transfer of apoptotic cells which may have influence in the activation of the local immune system. Also, exosomes or microvesicles are small and circulate easily whereas MSCs are too large to circulate easily through capillaries and many not get to the site of injury.

Concerning the ability of MSCs to immune modulate the T cell subpopulation, MSCs from different sources have been reported to inhibit proliferation of $CD3^+$, $CD4^+$ and $CD8^+$ lymphocyte *in vivo* and *in vitro* (Li et al., 2012; Bernardo and Fibbe, 2013). In line with these previous findings, I evaluated the therapeutic efficacy of MSCs to reduce T cell subpopulations by investigating the effect of US and CD362 sorted MSCs on $CD3^+$, $CD4^+$ and $CD8^+$ T lymphocytes. I showed that the hepatic expression of $CD3^+$, $CD4^+$ and $CD8^+$ were not changed by MSCs treatment, this could be due to the failure of these mice to develop a significant increase in $CD3^+$, $CD4^+$ and $CD8^+$ after inducing CCl_4 injury.

More interestingly, I found that US and CD362 sorted MSCs equally targeted blood circulation of $CD3^+$ and $CD4^+$ causing a significant reduction of their number *in vivo.* This beneficial result could be explained by the fact that UC-MSCs enhanced their anti-inflammatory properties through secretion of chemokines, or could trigger the secretion of angiogenetic factors, such as VEGF, FGF, and CXCL9 (Gu et al., 2017) . Another possible action could come from the fact that that microenvironment of the inflammation could trigger the MSCs to recruit more anti-inflammatory cells or differentiate some immune cells towards a regulatory phenotype to modulate the immunomodulatory function. Another reason might be that $CD362^+$ MSC secreted more cytokines and chemokines compared with US UC-MSCs; these factors could directly promote the recruitment of CD4 and CD3 lymphocyte from circulation to the inflamed liver.

Overall, I believe that MSCs may have a primary paracrine effect, but not through a direct interaction with injured liver cells. Further work needs to be considered to investigate

the therapeutic potential of a cell free condition medium derived from MSCs and confirm the potential of MSCs to act in a paracrine manner. In parallel observations, recent studies have shown that MCSs' paracrine function could be considered as a primary mechanism for the therapeutic effect of MSCs against tissue injury (Ranganath et al., 2012).

Consistent with results obtained in $CD3^+$, $CD4^+$ and $CD8^+$, I did not show any significant differences in the $CD4^+$ $CD25^+$ $FOXP3^+$ Tregs isolated from mouse liver following MSCs treatment, although there were no significant differences in the percentage of the Tregs following administration of US and CD362 sorted MSCs. Together, the above findings clearly demonstrate that in this model MSCs were not able to promote the generation of regulatory T cells and suggests that other regulatory mechanisms are involved in the immunosuppressive properties of the MSCs in the CCl_4 acute liver injury. Therefore, an interesting possibility is that a number of MSCs did not reach the injured site or there is a need to have more cells to enhance the number of regulatory T cells *in vivo*. More interestingly, our group has recently found that using the same type of MSCs with the same dosage was able to significantly improve the expansion of the hepatic Tregs in the MDR2 KO animal model (unpublished data). We further reported whether MSCs treatment has the ability to modulate both the cell numbers as well as the activation state of macrophages *in vivo*.

Within the innate immune system, macrophages have been reported to play an essential role in acute liver injury, and are normally enhanced by cellular components released from necrotic cells and acute tissue damage microenvironment (Luster et al., 2005). In the acute CCl_4 model used in this study, macrophages have clearly contributed to the liver

inflammation induced by CCl_4. In my *in vivo* experiment, flow cytometry data, together with the immunohistochemistry of F4/80, proved that CD362 UC-MSCs treatment decreased the number of macrophages in the liver. In addition, my data showed a decrease in macrophage numbers in the liver of the injured mice upon MSCs treatment with US or CD362 sorted cells. This reduction in macrophages could likely be associated with the ability of MSCs to interact with the innate immune response and improve their immunosuppressive behaviour or by secreted soluble factors which, therefore, promote tissue anti-inflammatory response. I believe that the reduction in macrophage infiltration by MSCs treatment is associated with the liver improvement in this CCl_4 animal model.

On the other hand, my study also demonstrates no changes in the monocyte numbers in the blood circulation following MSCs treatment. In contrast to our previous finding about the ability of MSCs to reduce the circulation of CD3 and CD4 T cells *in vivo*, I believe that UC-MSCs could secrete some factors which could have a specific function to recruit the circulation of lymphoid but not myeloid cells. Furthermore, macrophages polarisation plays an important role in the immunomodulation of several disease conditions (Lawrence and Natoli, 2011). Accordingly, the hepatic population of M1-like cells and M2-like cells was characterised and investigated in this study using flow cytometry. A very interesting finding in this study was that both US and sorted CD362 were unable to convert the M1 macrophages into M2 macrophages. This finding could suggest that one reason for the failure of the MSCs to modulate the macrophage polarisation might be due to the short time frame of the acute liver injury induced by CCl_4. Our group has recently found that UC-MSCs, both sorted and unsorted, were able to polarise the M1-like cells to M2-like cells in a murine model of liver fibrosis MDR2 (unpublished data), which we

believe could be a new mechanism that makes MSCs exhibit more anti-inflammatory properties in the treatment of liver disease. Another possible reason could come from the short observation period in our study; the effect of MSCs to polarise macrophages requires a long time and, therefore, MSCs could have greater potential in macrophages polarisation in chronic injury than in acute injury. In addition, analysis of the infiltrated neutrophil showed a pattern of reduction in the liver following MSCs treatment. In my model, a significant decrease in hepatic neutrophil was observed post-transfusion of US UC-MSCs. In contrast, I could not observe any beneficial effect of MSCs injection on the circulating number of neutrophils.

In addition to the ability of MSCs to reduce acute liver injury via immunosuppressive properties, several studies have reported that MSCs could have another therapeutic potential in different disease conditions through decreasing the generation of reactive oxygen species caused from the damaged tissue. These therapeutic functions could come from the ability of MSCs to secrete some factors with anti-oxidant properties. In order to evaluate the potential of UC-MSCs to reduce oxidative stress released from the liver injury, both TBARS and glutathione oxidised (GSS) states were analysed in the liver following MSCs treatment. My study confirmed that MSCs were unable to modify the intracellular oxidative stress in the liver. However, I observed a remarkable increase in TBARS following MSCs injection.

Given its known pathological nature of ROS production, the finding of upregulation on ROS level post-MSCs infusion could suggest the important role of ROS production in maintaining stromal cell functions (Wang et al., 2013). Furthermore, a very interesting

finding in my study is that HIF-1α was significantly upregulated in UC-MSCs compared with the CCl_4-injured group. This finding may suggest that HIF1-a could be a new mechanism that improves the ability of UC-MSCs to exhibit a more potent anti-inflammatory effect in *in vitro* and *in vivo* studies. Another finding of this study could highlight that hypoxia stress could improve the generation of liver injury. My observations are in agreement with previous reports indicating that MSCs under hypoxic condition can induce expression of HIF-1α.

In addition, my study reported that MSCs were not capable of changing the antioxidant levels, as reported by gene expression. SOD1, SOD2, SOD3 and catalase were the most important antioxidants which mediated the oxidative stress in different disease conditions. *In vivo,* it remains unclear which cellular ratio will be achieved during MSCs and T-cells interactions, as MSCs are in low number *in vivo*. The presence of MSCs at sites of inflammation and injury is well-known, but the relative number and sources of MSC that are mobilised remain to be determined. Interestingly, as an important component of the antioxidant system, the IDH-1 antioxidant enzyme was found to be upregulated in the injured mice treated with MSCs. This is an important metabolic enzyme located in the cytosol and with an important role in the liver to protect against ROS accumulation and suppress liver inflammation (Itsumi et al., 2015). An important paper highlighted a critical role for IDH-1enzyme in the control of liver injury *in vivo* (Itsumi et al., 2015). By using IDH-1 deficient KO mice, greater development in liver injury was shown to increase oxidative stress in hepatocytes and increased serum inflammatory cytokines, such as IL6 and TNFα (Itsumi et al., 2015). This information suggested that IDH-1 plays a role in regulation of the cellular damage related to liver

injury. Future studies are warranted to identify pathways that are regulated by IDH1 and to perform MSCs transduced with IDH-1 to evaluate the biological consequences of MSCs function. Other possible work suggests that MSCs could be genetically modified to overexpress IDH-1 for an effective strategy to enhance the MSCs function during liver injury.

As some studies have reported that acute CCl_4 injury is associated with an accumulation of apoptotic cell death, I hypothesised that MSCs could be effective in acute liver injury through their anti-apoptotic properties. In my studies there were significant differences in the expression of two anti-apoptotic genes, in particular of Birc5 (also known as servivin) and Bcl2l1, between control and CCl_4-treated mice, Birc5 gene expression was upregulated after exposure of mice to CCl_4, as compared to control mice treated with mineral oil. In fact, the higher levels of the anti-apoptotic activities have been reported in different liver injury in response to the MSCs treatment. Daan et al. (Van Poll et al., 2008) demonstrated that MSCs treatment supports the regeneration of liver injury through a reduction in hepatocellular apoptosis. Similarly, another study with bone marrow MSCs showed that they reduced apoptotic cells by 50% in the ischaemic region of the stroke injury 3-24 hours following MSCs administration, and were accompanied by an upregulation of the protein level of Bcl-2 and servivin (van Velthoven et al., 2012). In contrast to the previous studies, three days following systemic infusion of MSCs in CCl_4-injured mice, I failed to confirm an association between MSCs and the anti-apoptotic gene used in this study. These results indicate that administration of MSCs in the very early phase after ischaemic brain injury is neuroprotective and, thereby, improves functional outcome. One of the potential explanations may be that the anti-apoptotic function by the

MSCs could be related to the number of transplanted cells, for example injecting 1×10^6 MSCs rather than 2.5×10^5 may have more potential improvement in the anti-apoptotic efficacy of MSC.

Adhesion molecules promote the close interaction between the movement of T cells and MSCs, which is essential to suppress the immune response. In addition, inflammatory cytokines released in response to inflammation can activate the endothelial cells to secret adhesion molecules (Wilson et al., 2018). Using immunohistochemistry and qPCR, I first found that, compared with the liver from normal animal treated with mineral oil, CCl_4-injured mice showed a significant increase in the expression of ICAM-1and VCAM-1 in the liver. However, in this current study, I confirmed that these two adhesion molecules were not altered following MSCs treatment, as compared to the CCl_4-injured mice. According to this finding, I believe that cell-to-cell contact is essential to enhance the level of adhesion molecules in the microenvironment of the injured cells. In line with these findings, a study by Ren et al. (2010) reported that ICAM and VCAM expression have been shown to increase the interaction between MSCs and T cells, which subsequently enhanced the immunosuppressive function of the MSCs *in vitro* (Ren et al., 2010). Moreover, MSCs have been found to release adhesion molecules after stimulation with inflammatory cytokines (Shi et al., 2012).

In summary, because of their immunomodulatory ability, MSCs administration is a promising candidate for the treatment of liver diseases. Herein, the therapeutic effects of US and sorted CD362 umbilical cord MSCs were reported in CCl_4-induced acute liver injury. I showed that US and CD362 MSCs improve the hepatic injury of acute hepatitis,

following by down-regulation in hepatic $CD45^+$ infiltrating cells, as well as a reduction in non-NK cells and B cells, both in the injured liver and in the circulation. However, macrophage polarisation and induction of Tregs was not altered by MSCs therapy. My data highlights MSCs also increased IDH-1 enzymes, which could have a specific mechanism related to MSCs' immunosuppression functions. Finally, the different therapeutic effects of MSCs can be due to the specific microenvironment in each disease condition as well as the mechanisms which control their biological function in their niche.

CHAPTER 6

IN VIVO EFFICACY OF HUMAN UMBILICAL CORD MSCs IN THE OVA-BIL MOUSE MODEL OF ALLOIMMUNE LIVER INJURY

6.1 Introduction

In an animal model of acute liver injury, I previously investigated the efficacy of human UC-MSCs in acute hepatotoxic liver injury induced by CCl_4. I found that administration of hUC-MSCs had the ability to reduce liver damage, as indicated by a reduction in liver enzymes, as well as modulating hepatic inflammation. Studies have suggested that the mechanisms MSCs use in mediating immunosuppression effects could differ between various animal models of acute liver injury (Christ et al., 2015). Thus, I planned to study another animal model in which MSCs could potentially modulate the immune reaction in acute liver injury.

The model in this study was chosen due to its unique features, where inflammation was developed to target the biliary area in the liver specifically. The Ova-Bil animal model was developed by Buxbaum et al. and was associated with hepatobiliary injury (Buxbaum et al., 2006). In this animal model, Ova-Bil transgenic mice were tolerant to the overexpression of ovalbumin (OVA) antigen in their biliary epithelium and developed normally without any clinical development of hepatic inflammation or injury. However, hepatobiliary injury was induced by the adaptive transfer of splenocytes isolated from OT-I (OVA-specific $CD8^+$ T cells) and OT-II (OVA-specific $CD4^+$ T cells) transgenic mice into male Ova-Bil transgenic mice. Inflammation in the liver was specific without targeting any other organs in the Ova-Bil transgenic mice. In addition, the authors reported that this hepatobiliary inflammation is $CD8^+$ dependent, and no response was reported with $CD4^+$ cells alone. In general, this animal model shows increased damage in the bile duct with more inflammation around the portal area. In this study, we examined

the therapeutic role of UC-MSCs in protecting against liver damage caused by alloimmune liver injury.

6.2 Chapter Aims

In this chapter, I examined the extent of hepatic injury and inflammatory response caused by the adaptive transfer of OT-I and OT-II cells into Ova-Bil transgenic mice. More importantly, to the best of my knowledge, this study was the first to investigate the immunosuppressive potential of unsorted/purified human UC-MSCs *in vivo* using the Ova-Bil model of acute liver injury. The main aims of this chapter were to:

- Explore the safety and efficacy of human UC-MSCs in the Ova-Bil animal model.
- Specifically, study the ability of unsorted UC-MSCs and $CD362^{+}$ sorted UC-MSCs to modulate the number of hepatic infiltrating lymphocytes and monocytes, using flow cytometry analysis.
- Investigate whether UC-MSC administration can modulate activational status of hepatic endothelium *in vivo.*

6.3 Results

6.3.1 Development of biliary inflammation in Ova-Bil transgenic mice

The Ova-Bil mouse strain used for this study was inbred and maintained as heterozygotes on a C57Bl/6 background in our animal unit. Routine genotyping for heterozygous apical sodium-dependent bile acid transporter (ASBT)-membrane-bound ovalbumin (mOVA) in animals was carried out using real-time PCR (Transnetyx, Inc., Tennessee, USA). The OT-II mouse strain was maintained as homozygous and routine genotyping was carried out using real-time PCR (Transnetyx, Inc., Tennessee, USA).

This chapter details how alloimmune hepatobiliary injury was developed by the transfer of T cells from OT-I and OT-II transgenic mice into male Ova-Bil mice. Briefly, 10–12 week-old male OT-I and OT-II mice were sacrificed and their spleens harvested for splenocyte isolation. Splenocytes obtained from these mice were injected intraperitoneally (IP) into Ova-Bil mice. Ten days after OT-I and OT-II T-cell infusion, the animals were sacrificed and their blood and liver tissue collected for further investigation.

6.3.2 ALT level after the adoptive transfer of $10x10^6$ OT-I and/or $10x10^6$ OT-II splenocytes into OVA-BIL mice

To determine the functional consequence of transferring different populations of OT-I and OT-II splenocytes into Ova-Bil transgenic mice, a comparison study was conducted to determine liver injury and hepatic inflammation in Ova-Bil mice following the adaptive

transfer of $10x10^6$ splenocytes from OT-I, OT-II or OT-I and OT-II. Figure ***6-1***A briefly describes the design of this experiment.

As demonstrated (Figure ***6-1***B), the serum level of the ALT enzyme confirmed liver injury as indicated by the adaptive transfer of $10x10^6$ OT-I and OT-II splenocytes or through the induction of a single population of $10x10^6$ OT-I splenocytes, which is consistent with previous published data (Derkow et al., 2007). However, the $10x10^6$ OT-I and OT-II splenocyte group reported more significant injury compared with Ova-Bil mice injected with only $10x10^6$ OT-I splenocytes. In contrast, the adaptive transfer of $10x10^6$ OT-II splenocytes alone demonstrated a similar level of injury when compared with the ALT level in Ova-Bil mice treated with PBS. These findings confirm that OT-I splenocyte transplantation is directly associated with the development of liver injury in this animal model. More interestingly, the induction of OT-I splenocytes together with OT-II splenocytes exhibited the most effective treatment of induced liver injury in Ova-Bil transgenic mice.

A

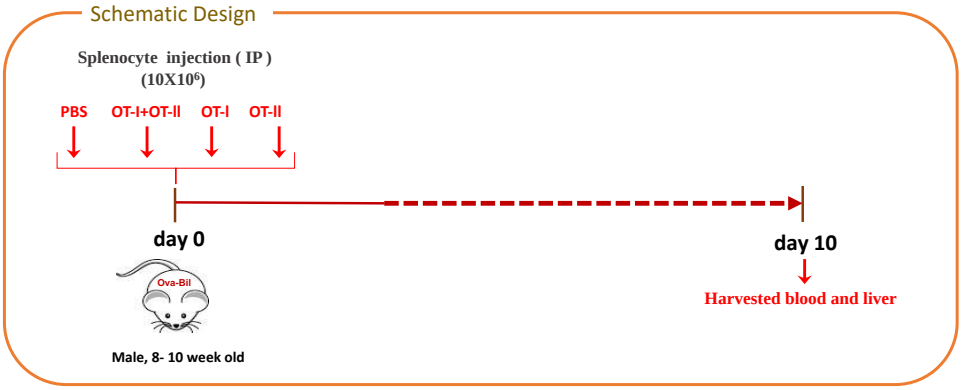

B

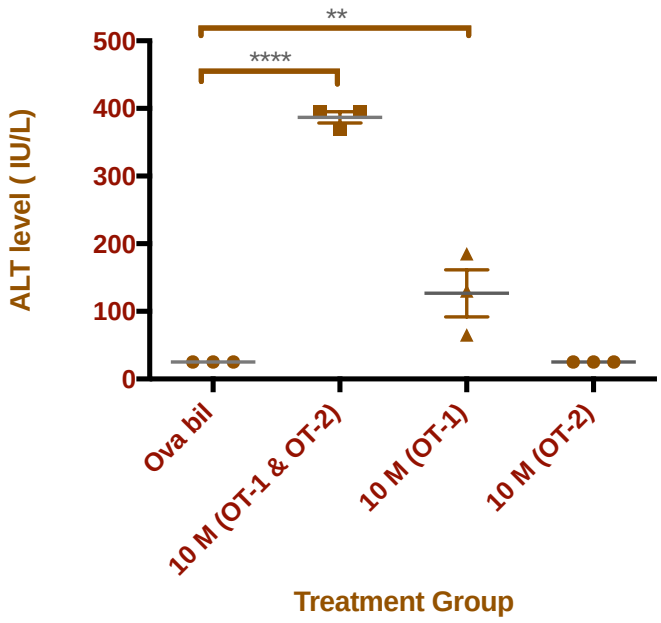

Figure 6-1 Male Ova-Bil mice show variation in liver enzyme activity after the induction of OT-I and OT-II. A) Design of the study. B) In mice that received intraperitoneal injections of $10x10^6$ of OT-I and OT-II, $10x10^6$ of OT-I, and $10x10^6$ of OT-II, serum ALT activities were elevated after 10 days. Representative data (3 mice for each time point). Each value is represented as the mean ± SD. * $P < 0.05$, ** $P < 0.01$, *** $P < 0.001$, and **** $P < 0.0001$.

6.3.3 ALT level after the adoptive transfer of different doses of OT-I and OT-II splenocytes into OVA-BIL mice

To optimize the level of injury in this animal model, a dose response study was performed with varying numbers of OT-I and OT-II splenocytes. I performed an experiment in which Ova-Bil mice were intraperitoneally injected with different doses of OT-I and OT-II splenocytes. Figure ***6-2*** illustrates the three different groups of animals injected with different doses of OT-I and OT-II splenocytes: 1) $10x10^6$ OT-I and $4x10^6$ OT-II

splenocytes (this dose was described by Buxbaum et al. 2006); 2) $15x10^6$ OT-I and $6x10^6$ OT-II splenocytes; and 3) $10x10^6$ OT-I and $10x10^6$ OT-II splenocytes.

As shown in Figure ***6-2***, I noted that injections of $10x10^6$ OT-I and $10x10^6$ OT-II splenocytes demonstrated more hepatic injury, as shown by the increased ALT levels compared with other OT-I and OT-II splenocyte doses. In addition, less variation in ALT levels was reported for the same doses in both female and male mice. These findings demonstrate that the level of liver injury in Ova-Bil mice correlates with the number of OT-I and OT-II splenocytes in a dose-dependent manner.

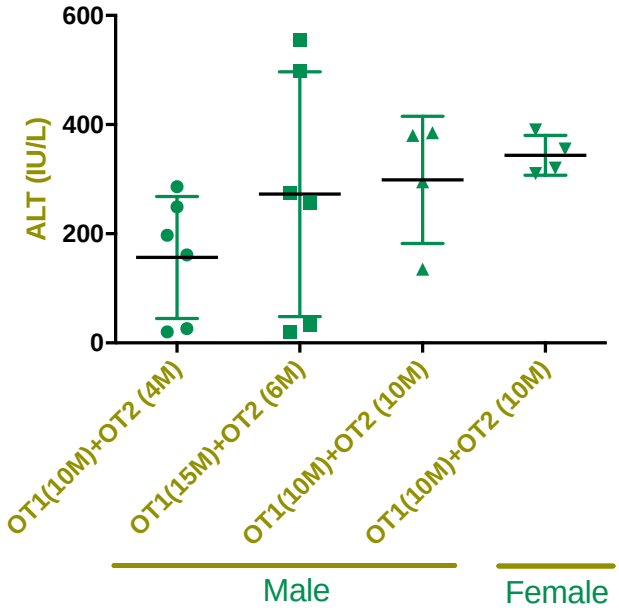

Figure 6-2 Analysis of ALT liver enzymes after infusion of different doses of OT-I and OT-II into Ova-Bil mice. Serum ALT level in Ova-Bil mice treated with different doses of OT-I and OT-II splenocytes (4–5 animals per group). Data are presented as the mean ± SD. * $P < 0.05$, ** $P < 0.01$, and *** $P < 0.001$.

6.3.4 Expression of Vα2 in the liver after the adoptive transfer of OT-I and OT-II splenocytes

As found earlier, liver injury in Ova-Bil mice developed following administration of OT-I and OT-II splenocytes. As reported by the authors who developed this animal model, splenocytes isolated from OT-I and OT-II transgenic mice were reported to express Vα2 on their surface receptors, whereas splenocytes from C57Bl/6 expressed < 2% Vα2 on their surface (Buxbaum et al., 2006). Accordingly, Vα2 monoclonal antibody was used to detect the OT-I and OT-II splenocytes transferred into Ova-Bil mice. Ten days following the adoptive transfer of OT-I and OT-II splenocytes, flow cytometric evaluation was performed to investigate the number of OT-I and OT-II splenocytes found in the liver and to track which population of splenocytes caused the liver injury. Our results indicated that the parentage of $V\alpha2^+$ cells was significantly increased in the Ova-Bil mice adoptively transferred with OT-I and OT-II or with only OT-II splenocytes (Figure 6-3A). However, Ova-Bil recipient mice treated with OT-II splenocytes did not show any Vα2-positive cells in their liver and were similar to the control Ova-Bil mice treated with PBS. These data clearly indicate that the transfer of OT-I splenocytes was shown to have a correlation with an increased expression of $V\alpha2^+$ cells in the liver, and we believe this population (OT-I) triggers the inflammation caused in the Ova-Bil model. In contrast, OT-II splenocytes failed to generate $V\alpha2^+$ cells in the liver, but these cells could be required for inducing hepatobiliary inflammation in Ova-Bil mice.

A

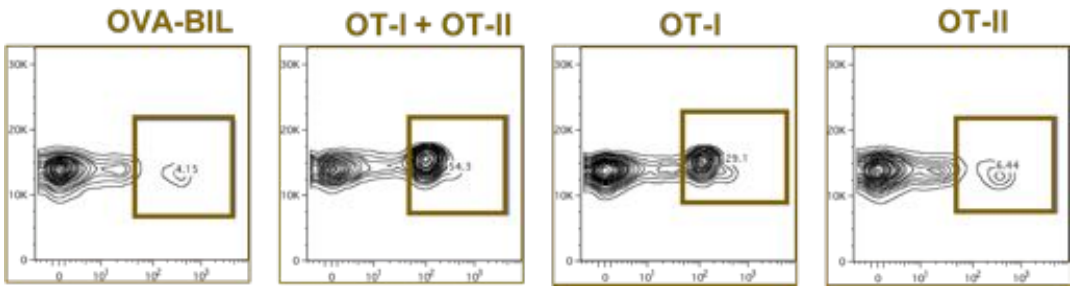

B

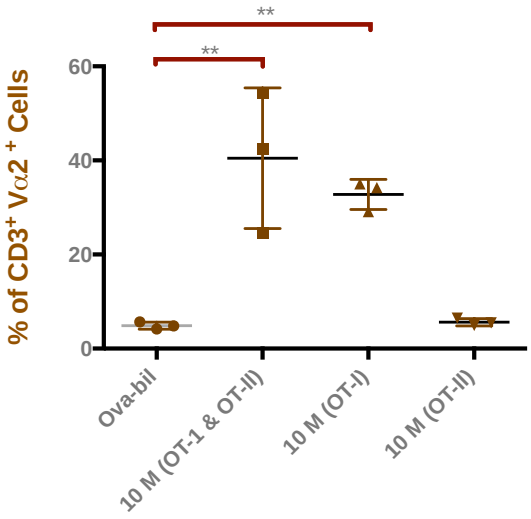

Figure 6-3 Expression of Vα2-positive cells after the adaptive transfer of OT-I and OT-II cells into Ova-Bil mice. (A) Flow cytometry representative diagram showing the percentage of Vα2^{+} cells after the adaptive transfer of OT-I and OT-II. B) The percentage of Vα2 cells in the liver of Ova-Bil mice was quantified by flow cytometry. All cells were gated from live CD3^{+} Vα2 $^{+}$ cells isolated from fresh mouse livers (3 animals per group). Data are presented as the mean ± SD. * P < 0.05, ** P < 0.01, and *** P < 0.001.

6.3.5 Increase in lymphocyte population following the adoptive transfer of OT-I and OT-II splenocytes

To investigate the inflammatory response following the adaptive transfer of OT-I and OT-II splenocytes into Ova-Bil mice, flow cytometry analysis was performed to examine the lymphocytic immune cells isolated from mice with adoptivel transferred OT-I and OT-II splenocytes. Ten days after the induction of OT-I and OT-II in the Ova-Bil mice, I saw a remarkable increase in the number of NK, non-NK and B cells in the liver compared with the control group (Ova-Bil with PBS). Interestingly, I also observed significant differences in NK cells as well as B cells following the adoptive transfer of OT-I splenocytes alone (Figure 6-4A). As expected, I reported no inflammatory response following the adoptive transfer of OT-II cells alone and observed a similar number of inflammatory cells when compared with the control group.

I then further investigated the influence of OT-I and OT-II transfer on $CD3^+$, $CD8^+$, and $CD4^+$ immune cells isolated from the livers of Ova-Bil mice. I clearly showed that the adoptive transfer of OT-I and OT-II splenocytes, as well as OT-I alone, significantly increased the total number of $CD3^+$ and $CD8^+$ lymphocytes in the liver (Figure 6-4B). In addition, OT-I alone was able to enhance the number of hepatic $CD4^+$ cells, compared with the induction of OT-I and OT-II together. However, the transfer of OT-II cells alone did not lead to changes in the number of hepatic $CD3^+$, $CD4^+$ and $CD8^+$ T cells. These observations illustrated that OT-I splenocytes directly contributed to the inflammation associated with acute liver injury in mice. Generally, the hepatic inflammation of this model depended on or required OT-I splenocytes (OVA-specific $CD8^+$ cells).

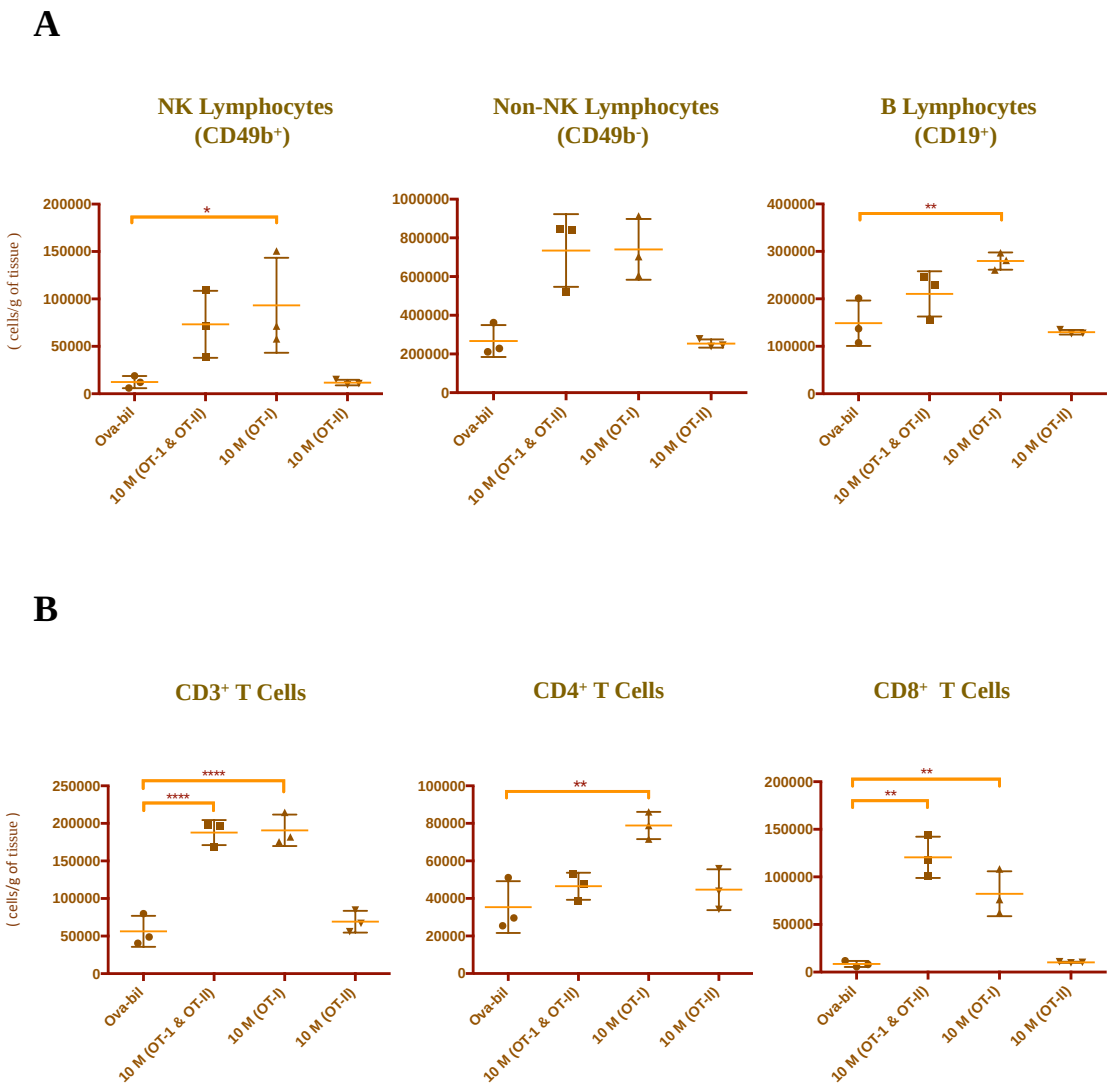

Figure 6-4 Analysis of lymphocyte populations using flow cytometry analysis. A) Represents NK and non-NK B lymphocytes isolated from mouse liver after the adoptive transfer of OT-I and OT-II. B) The numbers of infiltrating $CD3^+$, $CD4^+$ and $CD8^+$ cells in the livers of Ova-Bil mice were quantified by flow cytometry 10 days after the transfer of OT-I and OT-II. Data are expressed as the number of infiltrating cells per gram of fresh liver tissue (3 animals per group). Data are presented as the mean ± SD. * $P < 0.05$, ** $P < 0.01$ and *** $P < 0.001$.

6.3.6 Increase in monocyte populations following the adoptive transfer of OT-I and OT-II splenocytes in Ova-Bil mice

I further analysed the ability of OT-I and OT-II to modulate the monocyte subsets in Ova-Bil mice with liver injury. Ten days after the IP administration of OT-I and OT-ll cells, immune cells were isolated from mouse liver and analysed using flow cytometry. I observed a remarkable increase in the total $CD45^+$ (Figure 6-5A), $CD11^+$ (Figure 6-5B) and $CD11^+$ $F4/80^+$ (Figure 6-5C) cells in Ova-Bil mice in response to the adoptive transfer of OT-I and OT-II splenocytes when compared with the normal mice treated with PBS. In comparison with OT-I and OT-II treated mice, I noticed an increase in $CD45^+$, $CD11^+$ and $CD11^+$ $F4/80^+$ cells following the adaptive transfer of a single population of OT-I splenocytes. Further quantification of neutrophil ($CD11b^+$ $Ly6G^+$) and eosinophil ($CD11b^+$ $Gr\text{-}1^{Lo\text{-}neg}$ SSC^{HI}) cells was also reported in this study. I conducted a similar observation, which resulted in a significant increase in hepatic neutrophil and eosinophil cells in Ova-Bil mice following OT-I and OT-II transplantation (Figure 6-5D and E). In contrast, as found previously, the induction of OT-II cells did not lead to changes in the number of hepatic $CD45^+$, $CD11^+$ and $CD11^+$ $F4/80^+$ cells, nor in neutrophil and eosinophil cells. Together, these results indicate that OT-I and OT-II were shown to induce a significant number of hepatic monocytes significantly, suggesting that hepatic monocyte infiltration of this animal model required OT-I splenocyte (OVA-specific $CD8^+$ cells) as well as OT-II (OVA-specific $CD4^+$ cells) to enhance the inflammatory response.

A

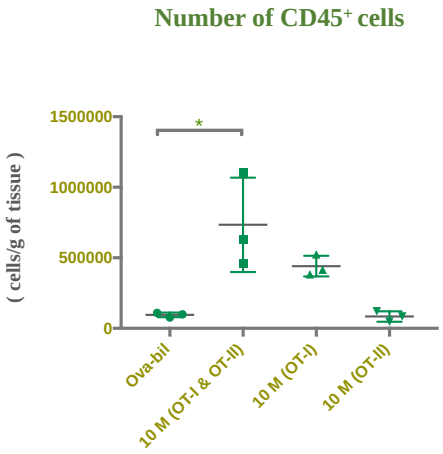
Number of CD45+ cells
(cells/g of tissue)
1500000
1000000
500000
0
*
Ova-bil
10 M (OT-I & OT-II)
10 M (OT-I)
10 M (OT-II)

B

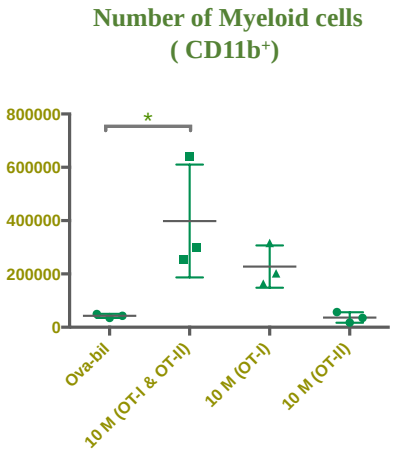
Number of Myeloid cells
(CD11b+)
800000
600000
400000
200000
0
*
Ova-bil
10 M (OT-I & OT-II)
10 M (OT-I)
10 M (OT-II)

C

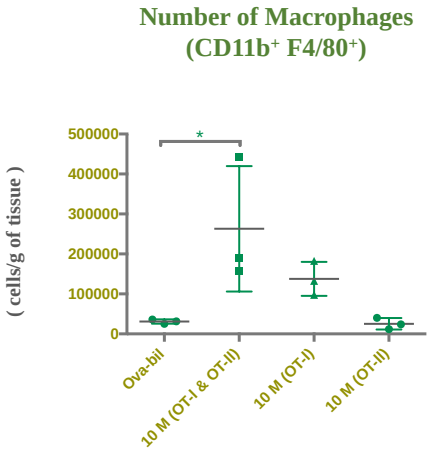
Number of Macrophages
(CD11b+ F4/80+)
(cells/g of tissue)
500000
400000
300000
200000
100000
0
*
Ova-bil
10 M (OT-I & OT-II)
10 M (OT-I)
10 M (OT-II)

D

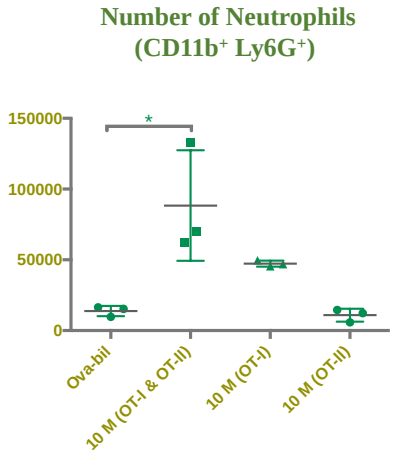
Number of Neutrophils
(CD11b+ Ly6G+)
150000
100000
50000
0
*
Ova-bil
10 M (OT-I & OT-II)
10 M (OT-I)
10 M (OT-II)

E

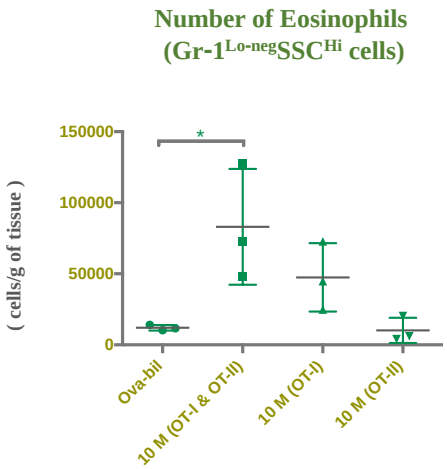
Number of Eosinophils
(Gr-1Lo-negSSCHi cells)
(cells/g of tissue)
150000
100000
50000
0
*
Ova-bil
10 M (OT-I & OT-II)
10 M (OT-I)
10 M (OT-II)

Figure 6-5 Flow cytometry analysis of immune cells following induction of OT-l and OT-ll cells in Ova-Bil mice by day 10. A) Cells were gated from live $CD45^+$ cells isolated from fresh mouse livers. B) Cells were gated from live $CD11b^+$ and $F4/80^+$ cells (C). D) Neutrophils were gated from live $CD11b^+$ and $Ly6G^+$ cells isolated from fresh mouse livers. E) Eosinophils were gated from live $CD11b^+$ $Gr\text{-}1^{Lo\text{-}neg}$ SSC^{HI} cells isolated from fresh mouse livers. All data are expressed as the number of infiltrating cells per gram of fresh liver tissue (3 animals per group). Data are presented as the mean ± SD. * $P < 0.05$, ** $P < 0.01$ and *** $P < 0.00$.

6.3.7 Study of the anti-inflammatory role of human UC-MSCs in the Ova-Bil murine model

As previously demonstrated, UC-MSCs have been found to have a therapeutic effect in a mouse model of acute hepatotoxic liver injury. In this chapter, the efficacy of human MSCs was assessed in an Ova-Bil animal model with acute hepatobiliary inflammation. As stated earlier, this liver injury was developed through the adoptive transfer of OT-I and OT-II splenocytes into Ova-Bil mice. In addition, 4 days after the induction of alloimmune liver damage by the adoptive transfer of OT-I and OT-II into Ova-Bil mice, UC-MSCs were infused intravenously via the tail vein and the mice sacrificed 6 days later. Finally, all mice underwent terminal anaesthesia to allow the collection of blood via cardiac puncture and were then sacrificed (cervical dislocation) to allow harvesting of the liver and other organs for analysis. Figure 6-6 A briefly describes the design of this experiment.

6.3.7.1 Examination of the correlation between the number of transplanted MSCs and the resulting liver function

As I found in the previous CCl_4 animal model, the dose response to MSC injection is essential to optimize the dose for better therapeutic efficacy. Accordingly, a dose response experiment was performed with varying infusions of unsorted UC-MSCs ($2.5x10^5$, $5x10^5$ and $1x10^6$). The activity of liver enzyme (ALT) was measured for each animal in order to evaluate the liver injury. As shown in Figure 6-6B, the serum ALT levels in the injured Ova-Bil mice treated with both $2.5x10^5$ and $1x10^6$ MSCs were not found to show a clear reduction in ALT activity compared with the injured mice treated with PBS. However, animals appeared to show better improvement following an infusion of $5x10^5$ MSCs (Figure 6-6B). Collectively, my data suggest that a $5x10^5$ dose of MSCs could be the optimal dose for improving liver injury in this animal model.

A

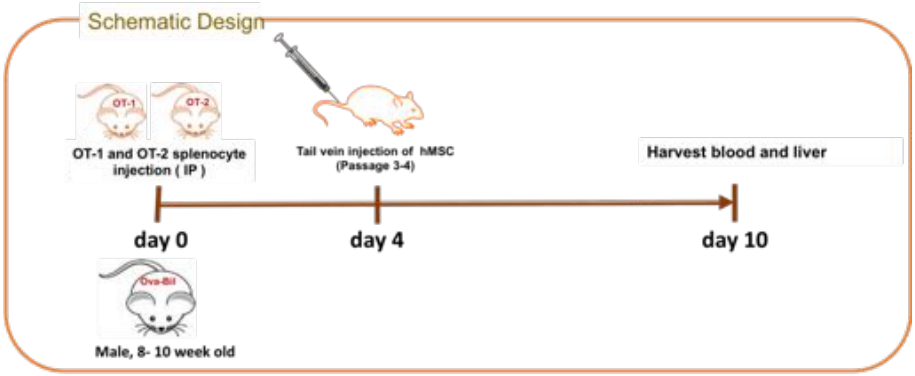

B

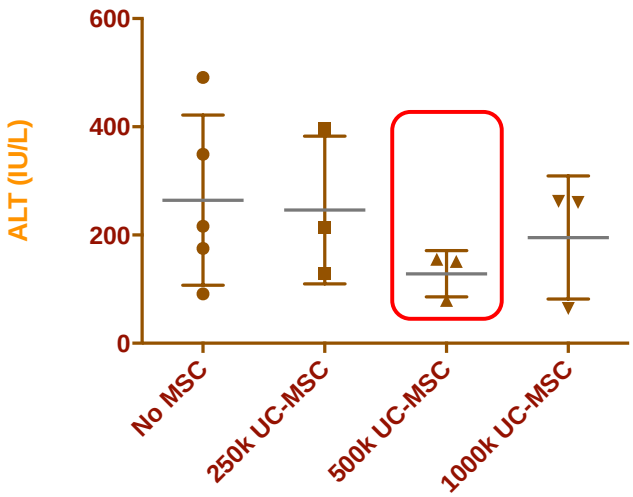

Figure 6-6 Analysis of liver enzymes after the infusion of different doses of MSCs (US) in Ova-Bil mice with hepatobiliary injury. A) Experimental design used in this study. OT-I and OT-II splenocytes were injected into Ova-Bil mice, followed by an IV MSC injection after four days. Animals were sacrificed at day 10 for serum and tissue collection for further study. B) Serum ALT level in Ova-Bil mice treated with different doses of UC-MSCs. Data are expressed as the number of infiltrating cells per gram of fresh liver tissue (5–3 animals per group). Data are presented as the mean ± SD.

6.3.7.2 CD362^{+} sorted UC-MSCs have potential efficacy in treating injury induced in an Ova-Bil model

Following the induction of liver injury in Ova-Bil mice through the adoptive transfer of OT-I and OT-II splenocytes, I examined the functional ability of MSCs to ameliorate liver injury in this animal model. In this study, animals received an intravenous dose of $5x10^5$ human unsorted UC-MSCs or CD362+ sorted UC-MSCs at day 4 following the induction of liver injury in Ova-Bil mice. ALT enzyme activity in the serum at day 10 was measured to evaluate the liver injury in response to MSC treatment. Significant reduction was observed with $5x10^5$ CD362+ sorted UC-MSCs. Interestingly, my data

demonstrated that the ALT level was significantly reduced after the infusion of CD362+ sorted MSCs compared with Ova-Bil injury treated with PBS (Figure 6-7). I also observed a reduction with unsorted UC-MSCs, but this did not reach statistical significance. These data suggest that $CD362^{+}$ sorted MSCs have a potential effect on liver injury in this animal model, and unsorted cells could have a less direct impact on improving liver function in the Ova-Bil animal model.

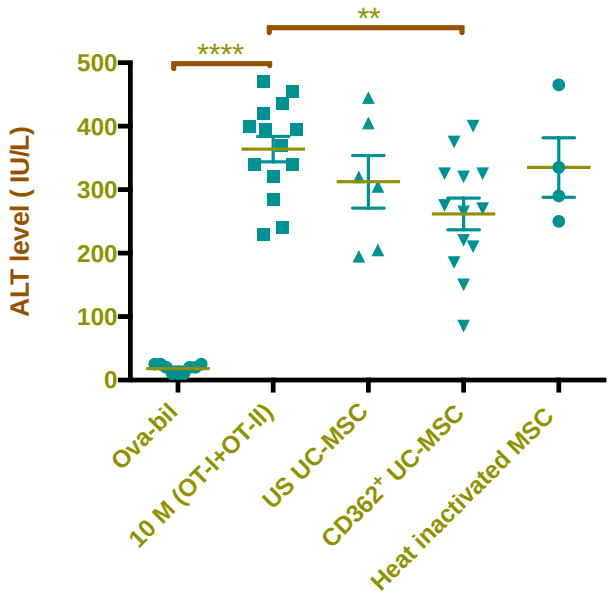

Figure 6-7 Analysis of ALT liver enzymes after infusion of human unsorted UC-MSCs or CD362+ sorted UC-MSCs in Ova-Bil mice. The graph indicates serum ALT levels in different groups of mice treated with unsorted or $CD362^{+}$ sorted UC-MSCs. Data are expressed as the median value and represent > 10 animals/group. Data are presented as the mean ± SD. * $P < 0.05$, ** $P < 0.01$, and ***$P < 0.001$.

Histological examination using H&E staining of Ova-Bil mice by day 10 following the transplantation of OT-I and OT-II showed damage in the bile duct area with more leucocytes infiltrated around the portal area (Figure ***6-8***). In comparison with the injured

mice, less cellular damage was seen in the liver microscopically with fewer inflammatory cells observed after MSC administration.

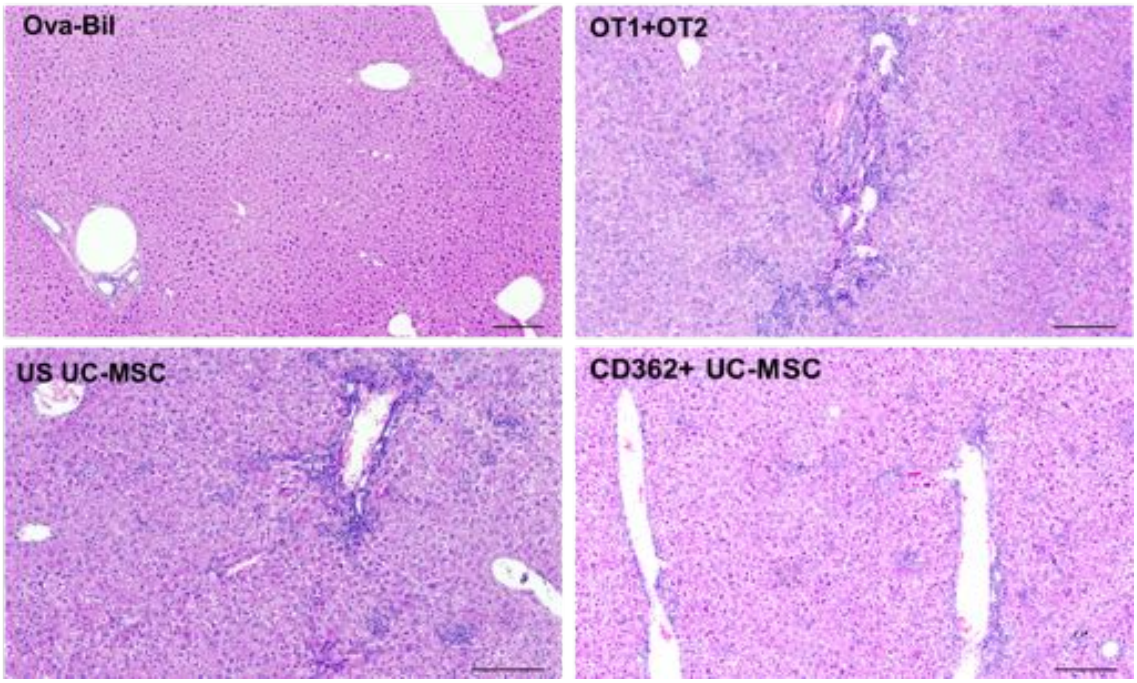

Figure 6-8 H&E staining of liver sections after treatment with different doses of hUC-MSCs. Represents the structure of liver sections of control mice (Ova-Bil), Ova-Bil mice with liver injury induced by OT-I and OT-II and treated with PBS, and mice undergoing MSC administration following Ova-Bil liver injury; a clear improvement in necrosis is seen with the MSC treatment group. Scale bars: 200 μm.

6.3.7.3 Effect of UC-MSC infusion on hepatic lymphocyte and monocyte populations in the Ova-Bil mouse model

In addition to the ability of human UC-MSCs to immunosuppress liver inflammation in acute CCl_4 liver injury, this chapter also examines if human UC-MSCs have a similar feature to modulate the inflammation in the Ova-Bil model. In this chapter, I examine the immunomodulatory function of US UC-MSCs and $CD362^+$ sorted UC-MSCs in the liver

as well as in the circulation and lymphatic tissues, such as the spleen. The lymphocyte and monocyte interaction with MSCs was tested in this study using flow cytometry and immunohistochemistry.

6.3.7.4 Effect of human UC-MSCs on $CD45^+$ immune cells from different tissue sources of Ova-Bil mice

In order to evaluate the ability of human UC-MSCs to modulate liver inflammation in Ova-Bil mice, I assessed the effect of using unsorted hUC-MSCs and $CD362^+$ sorted UC-MSCs through the intravenous injection of $2.5x10^5$ MSCs into Ova-Bil injured mice. I analysed the expression of $CD45^+$ cells isolated from the liver as well as the spleen and blood using flow cytometry analysis. As reported in Figure 6-9A, the unsorted and $CD362^+$ sorted UC-MSC-treated mice exhibited no significant reduction in hepatic $CD45^+$ cells compared with Ova-Bil mice treated with PBS. The same observation was also found in $CD45^+$ cells isolated from the spleen and blood. To further show the functionality of transplanted cells, I quantified $CD45^+$ in the liver sections following treatment of MSCs using immunohistochemistry (Figure 6-9B). I found that administration of $CD362^+$ sorted MSCs resulted in a significant reduction in $CD45^+$ expression in Ova-Bil mice compared with unsorted UC-MSCs. These results show that only $CD362^+$ sorted UC-MSC administration rescued hepatic inflammation in Ova-Bil mice.

A

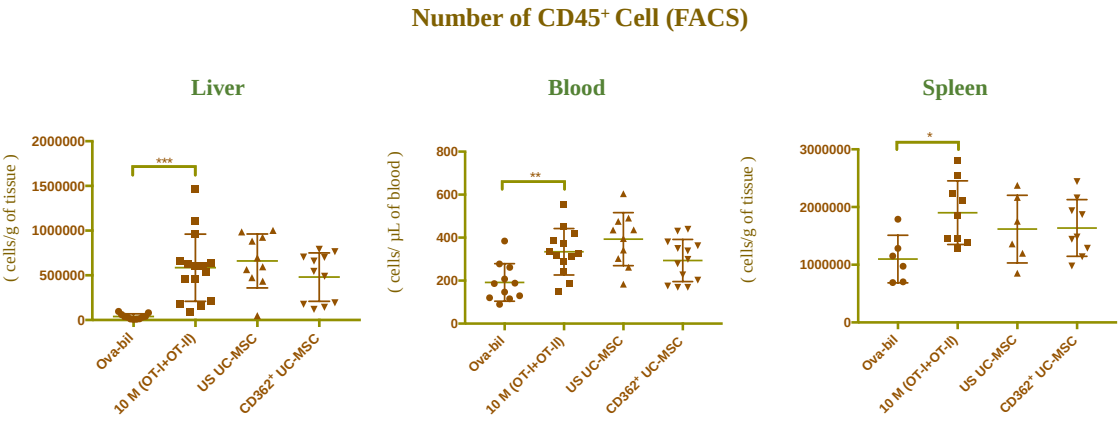
Number of CD45+ Cell (FACS)
Liver
Blood
Spleen
(cells/g of tissue)
(cells/ µL of blood)
(cells/g of tissue)
2000000
1500000
1000000
500000
0
800
600
400
200
3000000
***
**
*
Ova-bil
10 M (OT-I+OT-II)
US UC-MSC
CD362+ UC-MSC

B

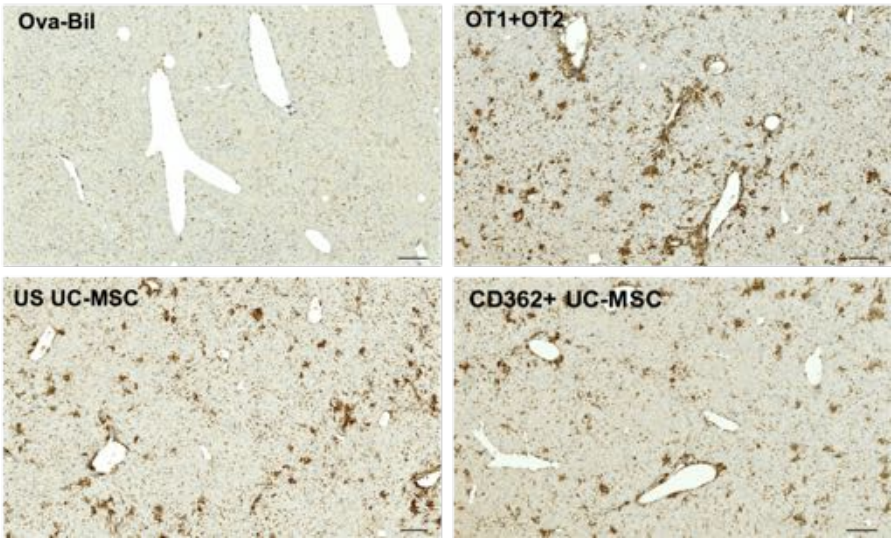
Ova-Bil
OT1+OT2
US UC-MSC
CD362+ UC-MSC

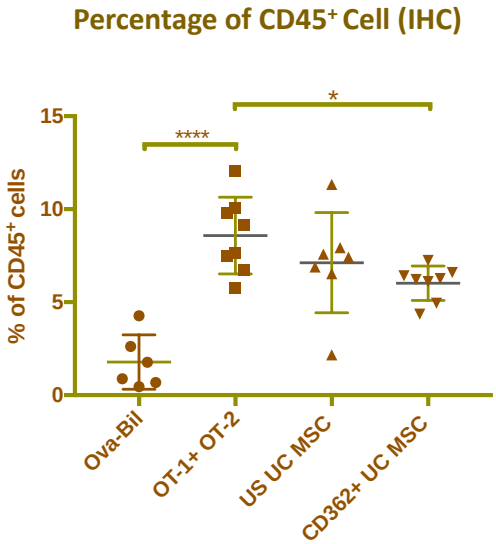
Percentage of CD45+ Cell (IHC)
% of CD45+ cells
15
10
5
0
****
*
Ova-Bil
OT-1+ OT-2
US UC MSC
CD362+ UC MSC

Figure 6-9 Flow cytometry and IHC analysis of CD45$^+$ cells post-MSC infusion into Ova-Bil mice. A) Cells were gated from live CD45$^+$ cells isolated from fresh mouse liver, spleen and blood. Data are expressed as the number of infiltrating cells per gram of tissue (liver and spleen) and per 1 µ of blood (> 8 animals per group). B) Representative IHC staining of hepatic CD45$^+$ cells expressed as a percentage of the surface area of the field view analysed using ImageJ software (8 animals per group). Scale bars: 200 µm. Data are presented as the mean ± SD. * P < 0.05, ** P < 0.01, and *** P < 0.001.

6.3.7.5 Effect of UC-MSC infusion on lymphocyte populations in the Ova-Bil liver injury model

I further investigated the influence of MSC transplantation on NK, non-NK and B lymphocytes from different tissue sources: mainly, liver, spleen, and blood. I clearly show that MSC transplantation from neither population (US or CD362) did not reduce the total number of NK (CD49$^-$) and non-NK (CD49$^-$) cells or B cell (CD19$^+$) lymphocytes (Figure ***6-10*** and Figure ***6-11***). In addition, MSCs showed no significant reduction in the NK, non-NK, and B lymphocytes isolated from spleen and blood compared with the Ova-Bil mice treated with PBS.

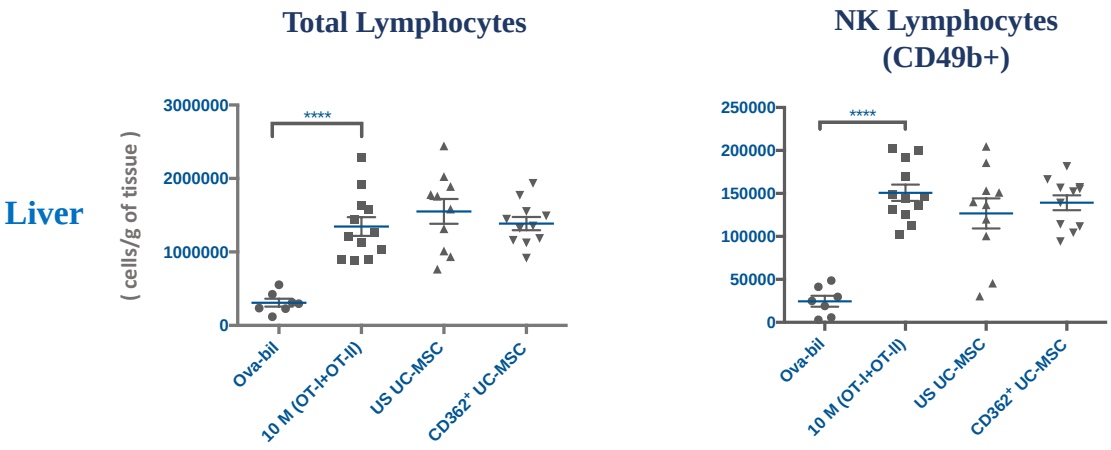

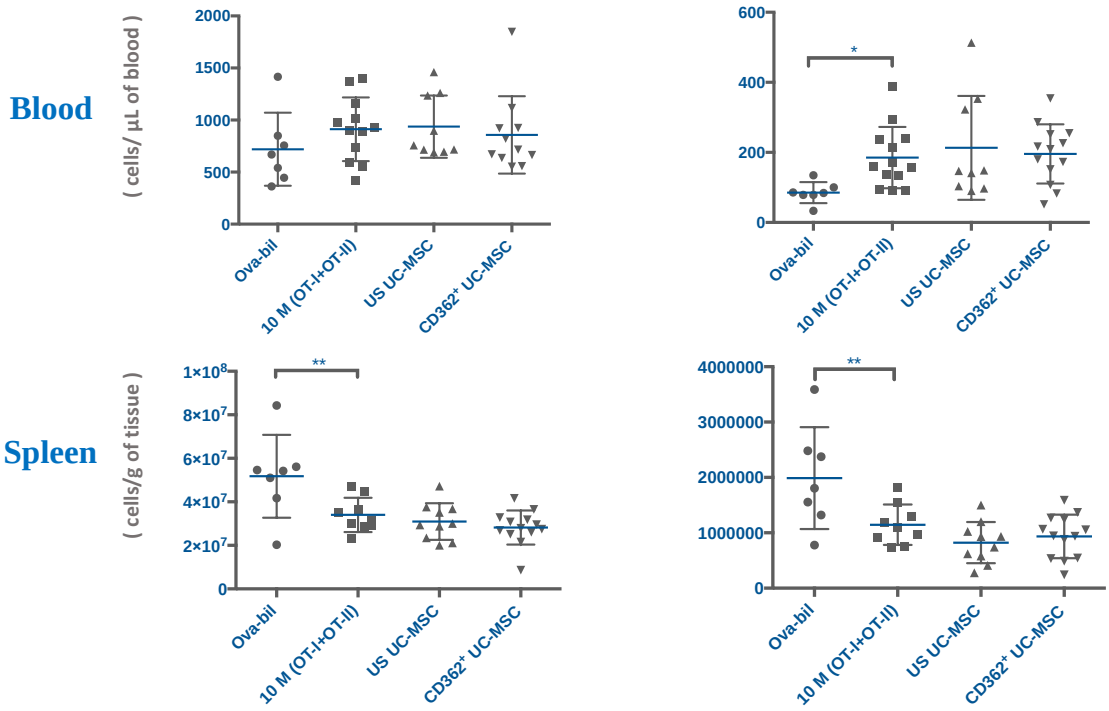

Figure 6-10 Analysis of total lymphocyte and NK-cell populations using flow cytometry assay. Represents the total lymphocytes and NK ($CD49^+$) lymphocytes isolated from the liver, spleen, and blood of Ova-Bil mice after administration of US or CD362 UC-MSCs. Data are expressed as the number of infiltrating cells per gram of liver and spleen tissue or by the number of infiltrating cells per 1 µ of blood (> 8 animals per group). Data are presented as the mean ± SD. * P < 0.05, ** P < 0.01, and *** P < 0.001.

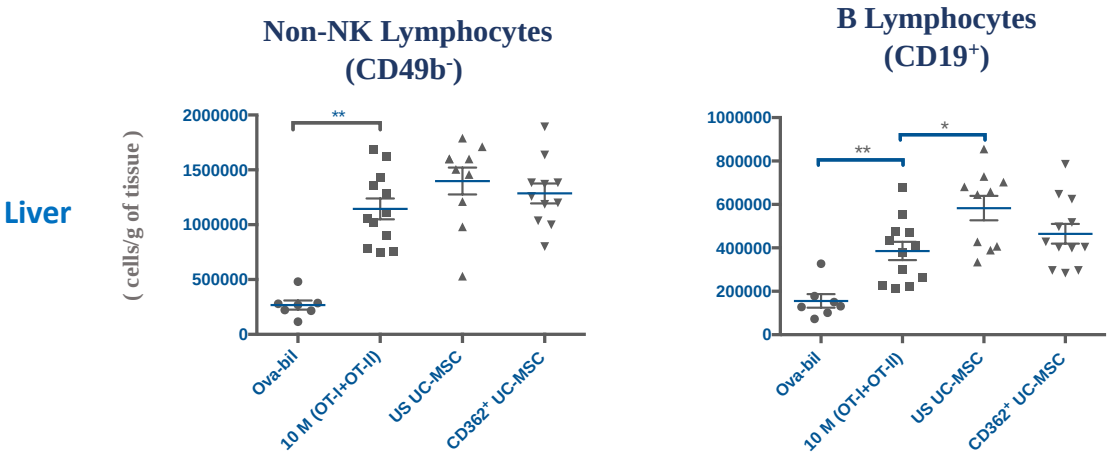

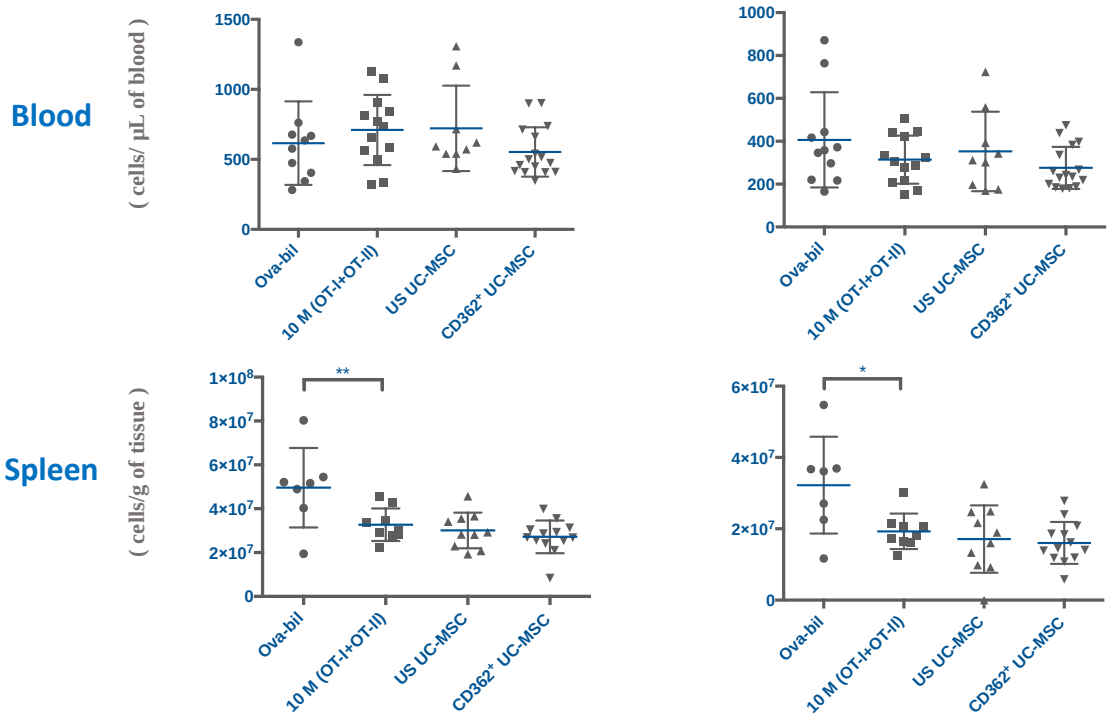

Figure 6-11 Analysis of non-NK cells and B lymphocytes using flow cytometry assay. Represents a difference in non-NK T cells ($CD49^-$) and B lymphocytes ($CD19^+$) isolated from the liver, spleen, and blood of Ova-Bil mice after administration of US or CD362 UC-MSCs. Data are expressed as the number of infiltrating cells per gram of liver and spleen tissue or by the number of infiltrating cells per 1 µ of blood (> 10 animals per group). Data are presented as the mean ± SD. * $P < 0.05$, ** $P < 0.01$, and *** $P < 0.001$.

6.3.7.6 CD362+ UC-MSCs enhance CD4+ expression in the liver of Ova-Bil mice with hepatobiliary inflammation

The potential of MSCs to suppress the proliferation of $CD3^+$, $CD4^+$ and $CD8^+$ T cells was examined in Ova-Bil mice with hepatobiliary injury. The quantification of the hepatic infiltration of $CD3^+$ and $CD8^+$ T cells in the Ova-Bil mice showed no differences between

MSC-treated and untreated Ova-Bil mice. The same finding was reported in $CD3^+$ and $CD8^+$ T cells isolated from spleen and blood (Figure ***6-12***). Interestingly, analysing the number of CD4+ T cells in the liver displayed a significant increase in the presence of MSC treatment. However, my results indicate that US and CD362 sorted MSCs had equal induction effects on hepatic CD4 T cells in Ova-Bil mice compared with the untreated group (Figure ***6-13***). In contrast, I did not observe any efficiency in MSCs in the upregulation of the number of CD4 T cells isolated from blood or spleen.

In accordance with my findings regarding the ability of MSCs to upregulate $CD4^+$ cells in the liver, I investigated whether this observation could relate to the ability of MSCs to induce the generation of regulatory T cells (Tregs). Thus, I further tested whether MSCs could immunosuppress liver inflammation via the induction of Tregs. As shown in Figure ***6-14***, my data reported that neither kind of MSC (unsorted and CD362 sorted cells) transplantation had a significant impact on hepatic Tregs, as reported by the expression of $CD3^+$, $CD4^+$, $CD25^+$ and $FOXP3^+$.

Together, my findings indicate that the therapeutic effect of MSCs (US and CD362) in the Ova-Bil animal model failed to suppress $CD3^+$ and $CD8^+$ cells and induced the generation of Tregs in the liver, as well as in the spleen and blood. In contrast, I found greater efficiency in MSC treatment in upregulating hepatic $CD4^+$ T cells in Ova-Bil mice with hepatobiliary inflammation.

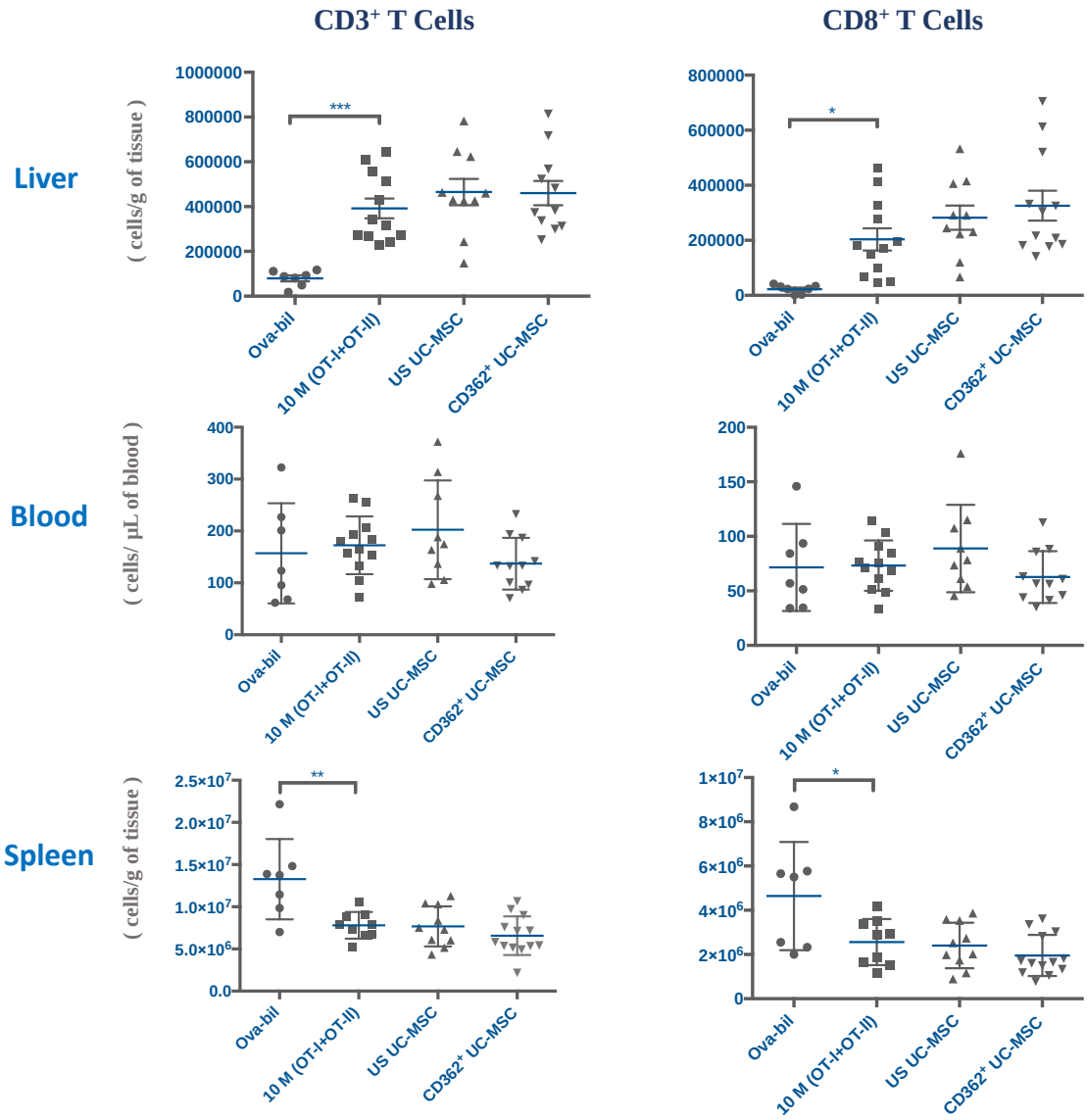

Figure 6-12 Numbers of infiltrated CD3$^+$ and CD8$^+$ cells in the liver, blood and spleen of Ova-Bil injured mice, quantified by flow cytometry. All cells were gated from live cells isolated from fresh mouse livers, spleen, and blood. Data are expressed as the number of infiltrating cells per gram of fresh tissue and by the number of infiltrating cells per 1 µ of blood (> 10 animals per group). Data are presented as the mean ± SD. * $P < 0.05$, ** $P < 0.01$, and *** $P < 0.001$.

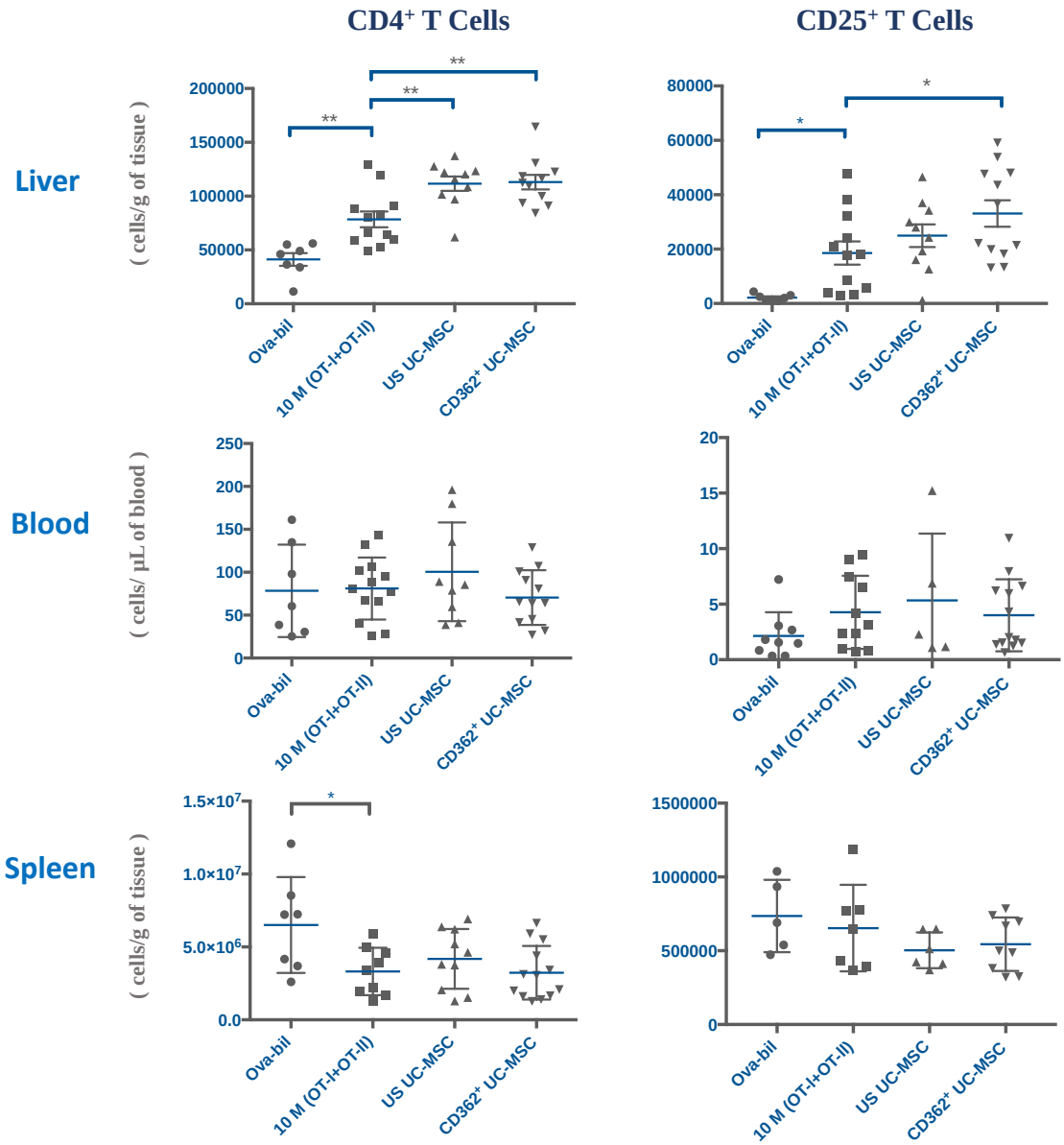

Figure 6-13 Numbers of infiltrated CD4$^+$and CD25$^+$ cells in the liver, blood and spleen of Ova-Bil injured mice, quantified by flow cytometry. All cells were gated from CD3$^+$ cells isolated from fresh mouse liver, spleen and blood. Data are expressed as the number of infiltrating cells per gram of fresh tissue and by the number of infiltrating cells per 1 µ of blood (> 10 animals per group). Data are presented as the mean ± SD. * $P < 0.05$, ** $P < 0.01$, and *** $P < 0.001$.

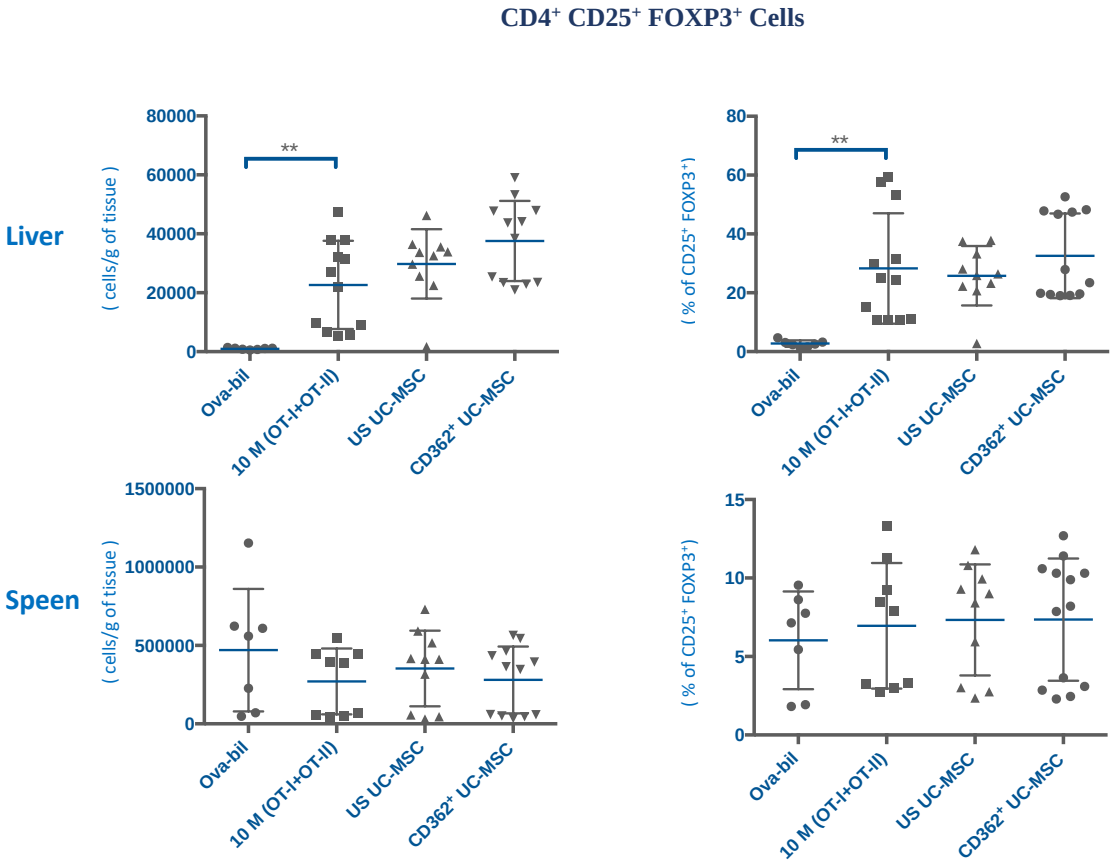

Figure 6-14 Generation of regulatory T cells following UC-MSC infusion. The generation of regulatory T cells in the liver of Ova-Bil mice was quantified by flow cytometry. All cells were gated from live $CD3^+$, $CD4^+$, $CD25^+$ and $FOXP3^+$ cells isolated from fresh mouse liver and spleen. Data are expressed as the number of cells per gram of fresh liver tissue (> 10 animals per group). Data are presented as the mean ± SD. * $P < 0.05$, ** $P < 0.01$, and *** $P < 0.001$.

6.3.8 Flow cytometric analysis of myeloid subsets in mice with Ova-Bil liver inflammation after infusion of UC-MSCs

I further analysed the ability of MSCs to modulate the myeloid immune cells in Ova-Bil injured animals. Following the intravenous administration of MSCs, immune cells were

isolated from mouse tissue and circulation and analysed using flow cytometry. I observed a remarkable increase in the total $CD11^+$ $F4/80^+$ following adoptive transfer of OT-I and OT-II when compared with the control group of Ova-Bil mice. In addition, my flow cytometry data showed that US and CD362 MSCs had no ability to modulate the number of macrophages ($CD11^+$ $F4/80^+$) in liver compared with the Ova-Bil injured mice (Figure ***6-15***A). However, further quantification of $F4/80^+$ cells in liver sections using IHC provided another observation, which showed a decreased level in macrophages following US and $CD362^+$ sorted MSC administration (Figure 6-15B). Together, these results indicated that MSCs were shown to reduce the number of hepatic macrophages infiltrating the liver section, suggesting that MSCs could play a role in liver injury through the modulation of macrophages in the liver.

A

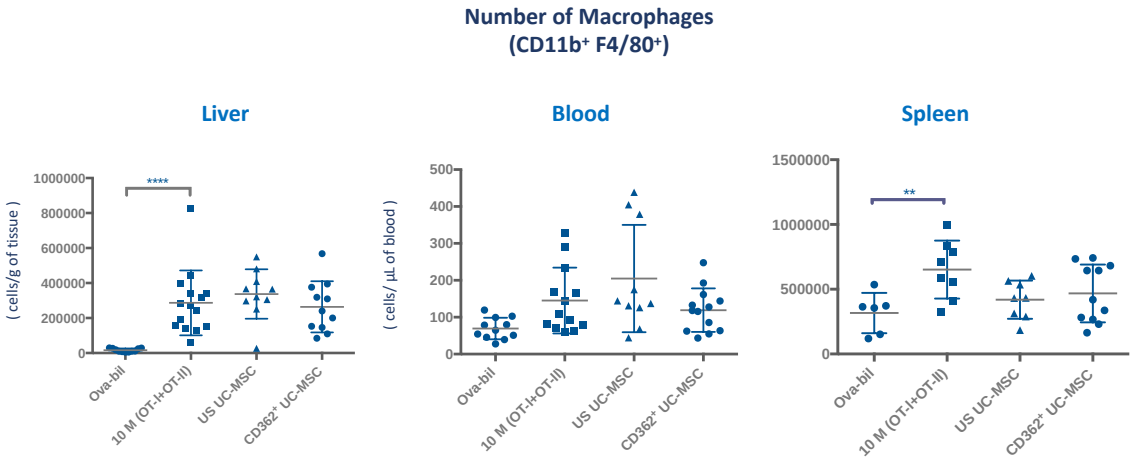

B

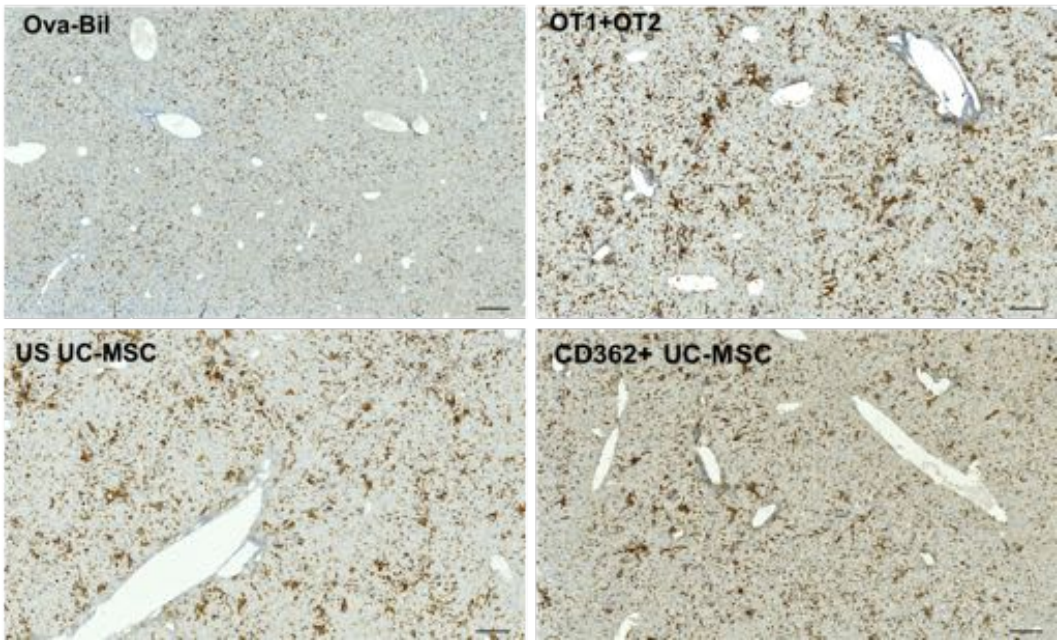

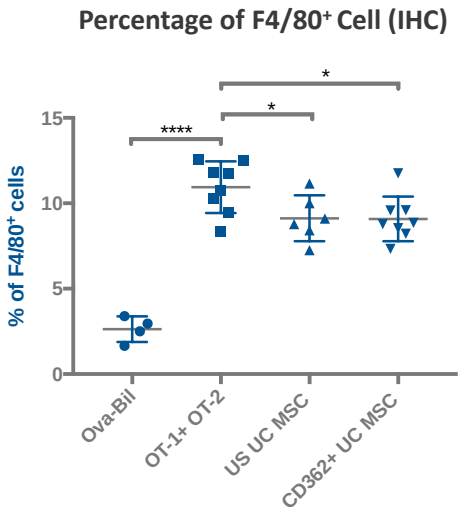

Figure 6-15 CD362$^+$ UC-MSCs reduced hepatic F4/80$^+$ immune cells in Ova-Bil mice with acute liver injury. A) Cells were gated from live CD11b$^+$ F4/80$^+$ cells isolated from fresh mouse liver, spleen and blood. Data are expressed as the number of infiltrating cells per gram of tissue (liver and spleen), and per 1 μ of blood (> 8 animals per group). B) Representative IHC staining of hepatic F4/80$^+$ cells expressed as a percentage of the surface area of the field view analysed using ImageJ software (8 animals per group). Scale bars: 200 μm. Data are presented as the mean ± SD. * $P < 0.05$, ** $P < 0.01$, and *** $P < 0.001$.

In order to fully characterize the different phenotypes of the infiltrated macrophages, I quantified the different populations of macrophages using flow cytometry. As mentioned in the previous chapter, macrophage markers $CD11b^{+}$ F4/80 $Ly6C^{hi}$ and $CD11b^{+}$ F4/80 $Ly6C^{lo}$ were used to identify classical and alternative macrophages, respectively. To investigate the role of MSCs in macrophage polarization, I compared the immunosuppressive ability of US and CD362 UC-MSCs on M1 and M2-like cells isolated from mouse liver. Based on my flow cytometry data, the MSCs did not show any change in macrophage phenotype between M1 and M2-like cells (Figure ***6-16***).

Another population of myeloid cells was investigated in this study. I analysed the influence of $CD362^{+}$ MSCs as well as US MSCs on the levels of neutrophils from different tissue sources (liver and spleen) and the blood of OBA-BIL mice. Compared with the control group, the degree of infiltration of $CD11b^{+}$ $Ly6G^{+}$ cells (neutrophils) did not change in response to either MSC treatment. This result was reported in liver as well as in blood and spleen (Figure ***6-17***).

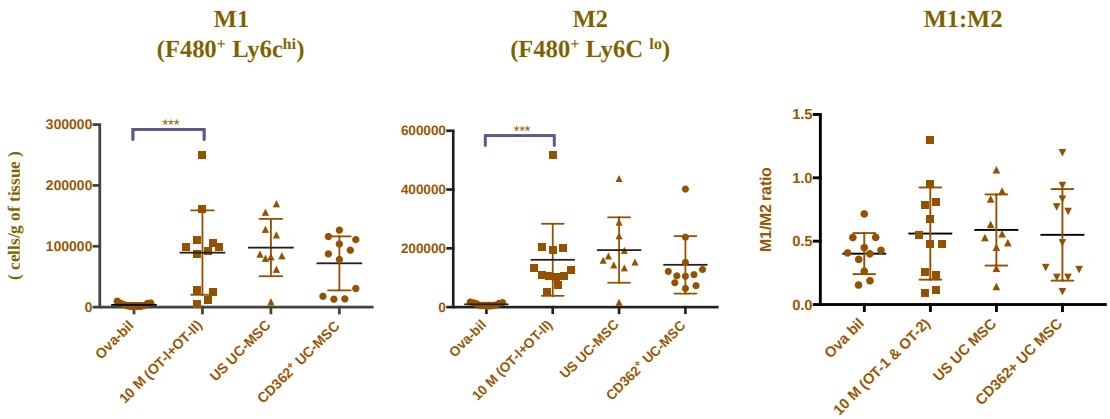

Figure 6-16 Effect of UC-MSC infusion on M1 and M2 macrophages. The total number of $CD11b^+$ F4/80 $Ly6C^{hi}$ classically activated pro-inflammatory M1-phenotypes and $CD11b^+$ F4/80 $Ly6C^{lo}$ anti-inflammatory M2-phenotypes in the livers of Ova-Bil injured mice were quantified by flow cytometry analysis. The percentages of M1 cells and M2 cells in fresh liver tissue of Ova-Bil mice receiving either 250K US UC-MSCs or $CD362^+$ UC-MSCs were quantified and compared with the injured group. The M1/M2 ratio expressed the proportion of M1 and M2 cells in the liver tissues. Data are expressed as percentages (%) of fresh liver tissue (> 8 animals per group). Data are presented as the mean ± SD. * P < 0.05, ** P < 0.01, and *** P < 0.001.

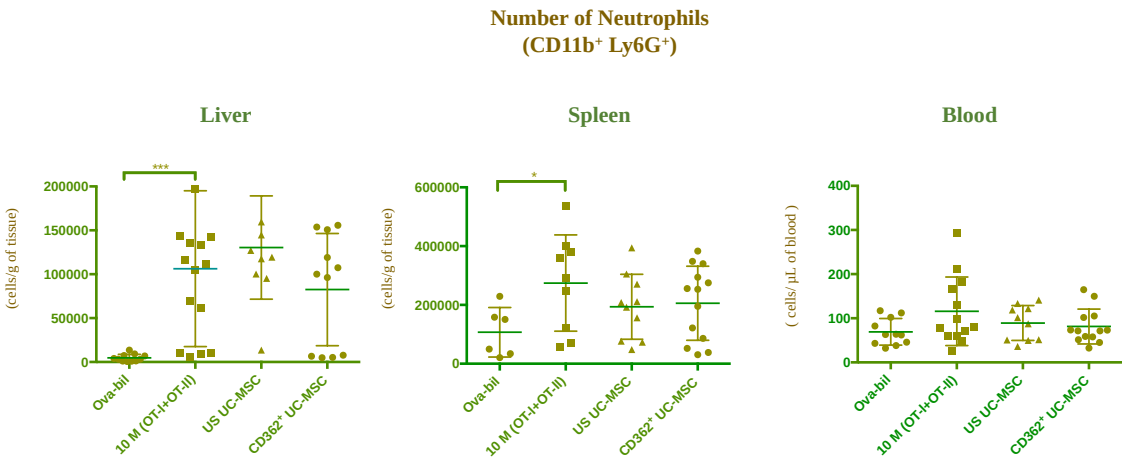

Figure 6-17 Effects of UC and CD362 MSCs on the expression of inflammatory neutrophils in Ova-Bil mice with liver injury. Neutrophils were gated from live $CD11b^+$ and $Ly6G^+$ cells isolated from fresh mouse livers, spleen, and blood. Data are expressed as the number of infiltrating cells per gram of fresh liver tissue and per 1 µ of blood (> 8 animals per group). Data are presented as the mean ± SD. * P < 0.05, ** P < 0.01, and *** P < 0.001.

6.3.9 CD362+ UC-MSC downregulated hepatic endothelial cell activation (expression of ICAM and VCAM) in Ova-Bil mice with liver injury

To assess whether hepatic endothelial cells are activated in the hepatic injury of Ova-Bil mice I studied the expression of ICAM and VCAM in the liver using qPCR as well as IHC. ICAM-1 and VCAM-1 adhesion molecules have been shown to mediate the immunosuppressive function of MSCs through the direct adhesion of MSCs to immune cells (Chamberlain et al., 2011).

In this study, I found that ICAM and VCAM were highly expressed in Ova-Bil mice 10 days after liver injury. To explore the role of MSCs in the modulation of ICAM and VCAM expression *in vivo*, I analysed the level of ICAM and VCAM adhesion molecules using IHC and qPCR 6 days following MSC infusion. Interestingly, I observed a significant reduction in ICAM expression in liver sections of Ova-Bil mice treated with CD362+ MSCs compared with mice treated with PBS (Figure ***6-18***A). Similarly, I found that Ova-Bil mice treated with CD362 MSCs had significantly less expression of VCAM, as demonstrated by the quantification of the percentage of $VCAM^{+}$ cells in mouse liver sections, as shown in Figure ***6-19***A. To further confirm the previous findings, the expression of ICAM and VCAM mRNA in the mouse liver was investigated in the presence of MSC treatments, using qPCR. I confirmed a significant decrease in the expression of ICAM (Figure ***6-18***C) and VCAM (Figure ***6-19***C) in the liver of Ova-Bil mice treated with CD362 MSCs, as measured by qPCR. I observed a trend towards a decline in ICAM and VCAM in OVA-BIL mice treated with US MSCs but without any statistical significance recorded.

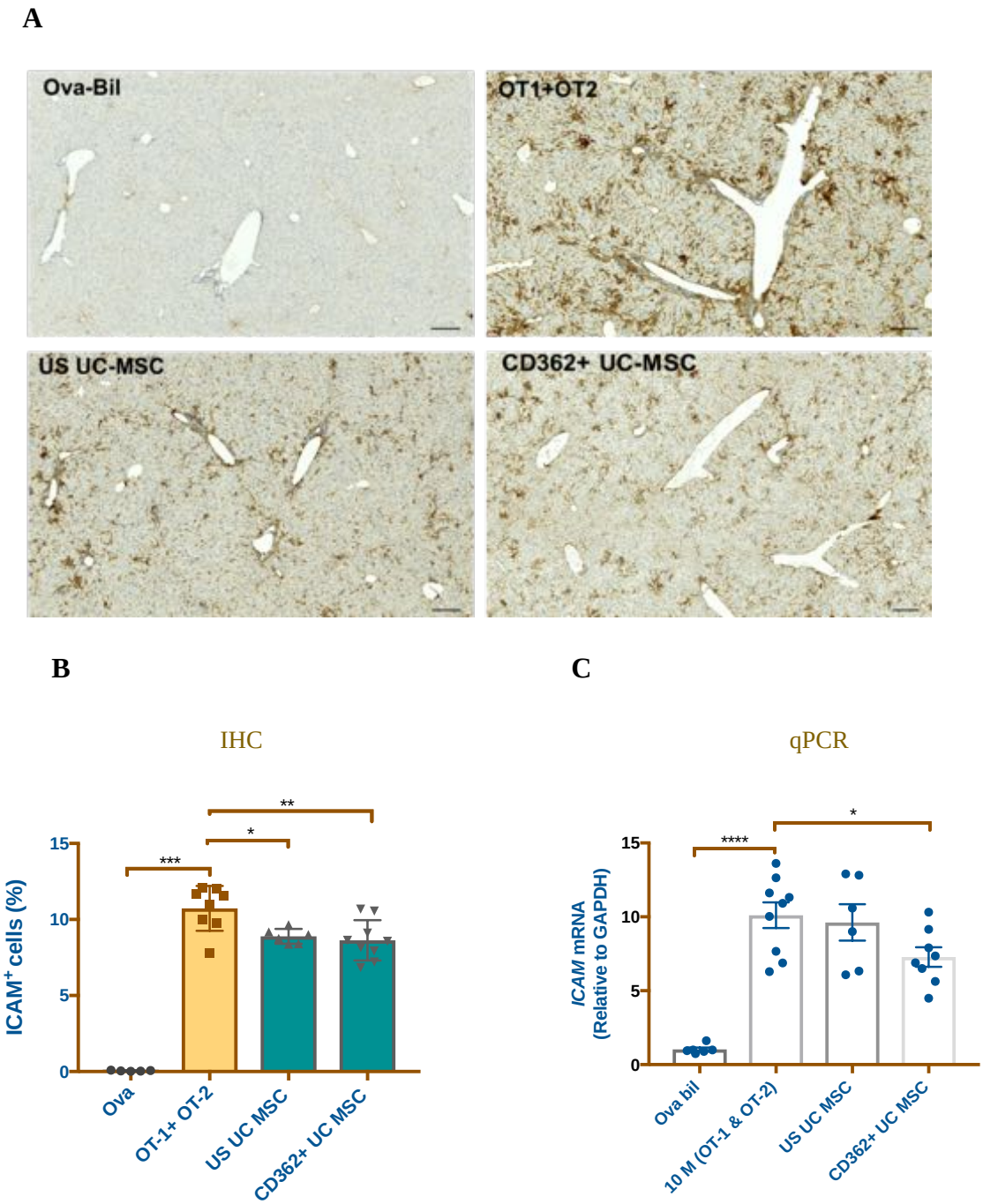

Figure 6-18 Effect of MSC treatment on hepatic ICAM-1 expression in the Ova-Bil murine model. A) Representative IHC staining of hepatic ICAM$^+$ cells. B) Quantification of ICAM$^+$ cells expressed as a percentage of the surface area of the field view analysed using imageJ software (8 animals per group). C) Changes in hepatic ICAM-1 mRNA expression in Ova-Bil mice following injection of US and CD362$^+$ UC-MSCs quantified by qPCR (8 animals per group). Scale bars: 200 µm. Data are presented as the mean ± SD. * $P < 0.05$, ** $P < 0.01$, and *** $P < 0.001$.

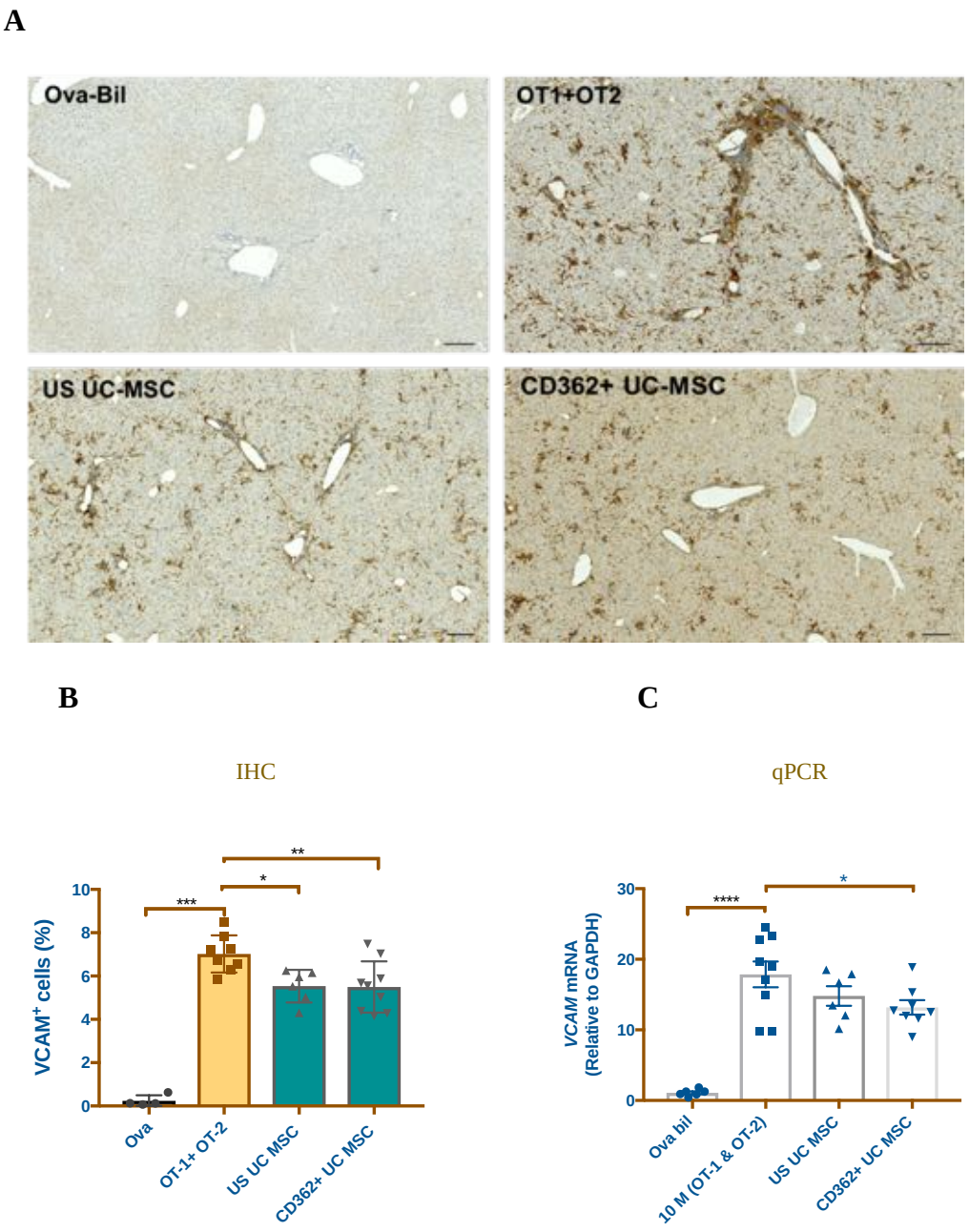

Figure 6-19 Effect of MSC treatment on hepatic VCAM-1 expression in the Ova-Bil murine model. A) Representative IHC staining of hepatic $VCAM^+$ cells. B) Quantification of $VCAM^+$ cells expressed as a percentage of the surface area of the field view analysed using imageJ software (8 animals per group). C) Changes in hepatic VCAM-1 mRNA expression in Ova-Bil mice following injection of US and $CD362^+$ UC-MSC quantified by q-PCR (8 animals per group). Scale bars: 200 μm. Data are presented as the mean ± SD. * $P < 0.05$, ** $P < 0.01$, and *** $P < 0.001$.

6.3.10 Cytokine production following MSC induction in Ova-Bil mice with liver inflammation

Two cytokines, in particular, TNF-α and INF-γ, were shown to have a remarkable upregulation following the adoptive transfer of OT-I and OT-II, as shown in Figure ***6-20***. I further assessed the immunosuppressive function of MSCs in modulating cytokines in the livers of injured mice. I explored the therapeutic role of MSC administration on TNF-α and INF-γ cytokine secretion 6 days following infusion. I observed minimal induction in INF-γ with no difference in TNF-α in the MSC-treated mice when compared with Ova-Bil mice treated with PBS (Figure ***6-20***).

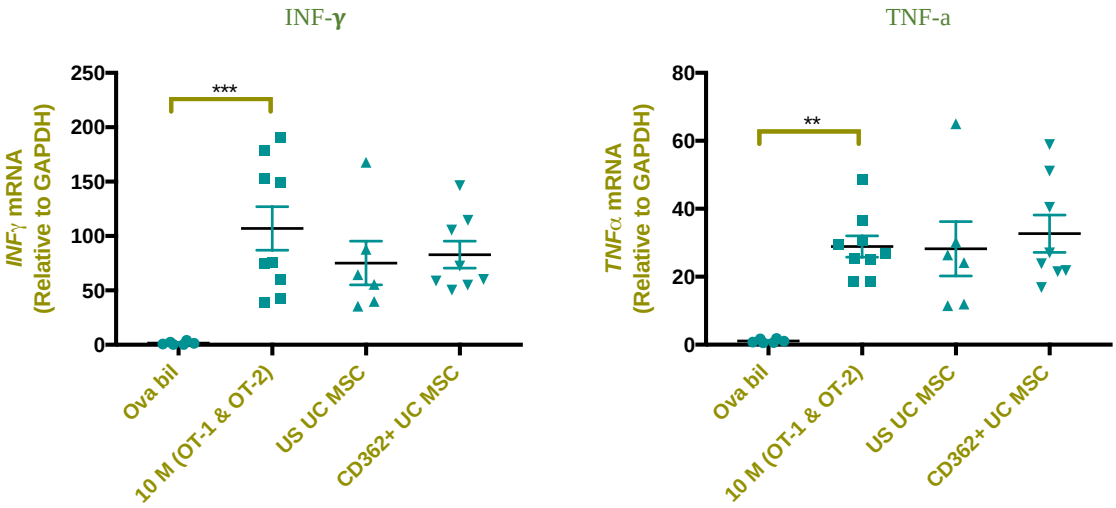

Figure 6-20 Analysis of gene expression of inflammatory cytokine expression in the liver following MSC treatment. Changes in the hepatic gene expression of TNF-α and INF-γ in Ova-Bil mice receiving MSCs, quantified by q-PCR (8 animals per group). Data are presented as the mean ± SD. * $P < 0.05$, ** $P < 0.01$, and *** $P < 0.001$.

6.4 Discussion

The therapeutic potential of human UC-MSCs has been reported in the repair of injured tissue. In some clinical studies, MSCs were found to be safe, with features indicating a potential to treat human diseases (Suk et al., 2016b; Houlihan and Newsome, 2008). There are several ongoing clinical trials to demonstrate the clinical efficacy of MSCs in different disease conditions. Several research groups have reported beneficial effects of MSC infusions in different animal models of acute liver injury (Zhu et al., 2013; Milosavljevic et al., 2017b). I previously reported beneficial effects of MSC infusions in animal models of acute liver injury. To further address whether UC-MSCs have a therapeutic role in liver injury, I used an Ova-Bil model of liver injury with hepatobiliary inflammation. Based on a previously developed animal model (Buxbaum et al., 2006), I developed hepatobiliary injury in Ova-Bil mice by adoptively transferring T cells from OT-I and OT-II transgenic mice. However, the course of the inflammation has not been well defined. Here, I found the most effective dose of OT-I and OT-II to induce liver injury and inflammation. Further experimentation was conducted in order to understand the immune phenotype changes in the liver following the induction of OT-I and OT-II. In this study, I reported the effectiveness of the transplantation of human UC-MSCs into Ova-Bil mice following the adoptive transfer of OT-I and OT-II cells. The most effective dose of MSCs was defined and two populations of MSCs were investigated. The beneficial therapeutic effect of US and $CD362^{+}$ sorted MSCs was found to reduce liver injury in Ova-Bil mice induced by OT-I and OT-II. I demonstrated that the potential effect of MSCs to protect liver injury was mediated by the ability of MSCs to enhance $CD4^{+}$ cells in the injured liver. In addition, it has been reported that CD362 sorted MSCs might enhance the therapeutic effect of MSCs to modulate liver injury through the

downregulation of adhesion molecules. Taken together, these findings provide a promising indication for using MSCs to treat liver diseases, as they were reported to be safe and for their ability to immunomodulate liver inflammation as well as regulate adhesion molecules.

An Ova-Bil animal model of liver injury was developed in which the antigen ovalbumin in hepatocytes (Derkow et al., 2007) or biliary epithelium cells (Buxbaum et al., 2006) is highly expressed. In both studies, inflammation was developed by the adoptive transfer of splenocytes isolated from OT-I and OT-II transgenic mice. This animal model was found specifically to target liver tissue and induce hepatobiliary inflammation. As mentioned above, I used Ova-Bil transgenic mice with overexpression of ovalbumin (OVA) antigens in their biliary epithelium, as described by Buxbaum et al. In agreement with the aforementioned study, Ova-Bil mice were, prior to the induction of OT-I and OT-II, reported to have a normal liver structure without any injury observed, as demonstrated by a normal serum ALT level. The level of injury in Ova-Bil mice has been reported as showing remarkable changes in response to different doses of OT-I and OT-II splenocytes. Initially, I used $10x10^6$ OT-I and $4x10^6$ OT-II splenocytes as described in the previous study. However, I observed clear variations in liver ALT levels between mice, with no inflammatory response observed in some animals. To overcome this issue, I performed an experiment with different doses of OT-I and OT-II splenocytes. I noted that injection of $10x10^6$ OT-I and $10x10^6$ OT-II splenocytes demonstrated more hepatic injury, as shown by increased activity of ALT enzyme, when compared with other doses of OT-I and OT-II splenocytes. This observation demonstrated that the level of liver

injury in Ova-Bil mice is correlated with the number of OT-I and OT-II splenocytes injected in a dose-dependent manner.

Interestingly, I found that liver injury was triggered by the adaptive transfer of OT-I and OT-II splenocytes. On the other hand, the induction of a single population of OT-I splenocytes had the ability to develop liver injury in OVA-VIL mice, whereas OT-II splenocytes alone functioned effectively in developing liver injury in the same animal. This finding is consistent with previously published data (Buxbaum et al., 2006). These and our results confirm that $CD8^+$ specific T cells initiated the liver injury in this animal model.

In addition to their effect on liver injury, I noted that the highest proportion of the cells that migrated to the liver were OT-I cells, as reported by the percentage of $V\alpha2^+$ in the OVA-BIL mice transferred with OT-I and OT-II or with only OT-I splenocytes. Our observations are in line with a previous study, which reported that $CD8^+$ T cells were trapped in the liver and caused hepatitis even in the absence of $CD4^+$ T cells (Derkow et al., 2007). However, I probably observed minor differences with the previous study that are likely to be associated with the different routes of administration of OT-I and OT-II cells, as well as the OT-I and OT-II purified following isolation from the spleen. Collectively, these findings confirm that OT-I splenocyte transplantation is directly associated with the development of liver injury in this animal model. More interestingly, the induction of OT-II splenocytes alongside OT-II splenocytes exhibited more liver injury in Ova-Bil transgenic mice. This suggests that OT-II cells could be required to induce hepatobiliary inflammation in Ova-Bil mice. However, this feature could be

specific to this model, as $CD4^+$ cells have been reported as inducing sufficient liver injury in NOD mice (Irie et al., 2006).

To determine the inflammatory response of this interaction, I examined the different populations of immune cells isolated from the livers of Ova-Bil mice in the presence of OT-I and OT-II splenocytes. As expected, the numbers of hepatic NK, non-NK and B cells in the liver were found to be normal in Ova-Bil mice prior to the induction of OT-I and OT-II. The transfer of OT-II cells alone had a similar inflammation profile to that reported in the control group. Interestingly, I reported an increase in hepatic NK cells as well as B cells following the adaptive transfer of OT-I splenocytes alone. In addition to the previous findings, OT-I alone significantly increased the total number of CD3 and CD8 lymphocytes in the liver. However, the latter cells were further able to enhance the number of hepatic $CD4^+$ cells, compared with the induction of OT-I and OT-II together. However, the induction of OT-II cells did not lead to changes in the number of hepatic CD3, CD4, and CD8 T cells. These observations illustrated that OT-I directly contributed to the inflammation associated with acute liver injury in mice. Generally, the hepatic inflammation in this model was dependent on or required OT-I splenocytes (OVA-specific $CD8^+$ cells), and OT-II splenocytes (OVA-specific $CD4^+$ cells) were not able to induce liver inflammation in Ova-Bil mice. One reason could be the low number of CD^+4 cells reaching the injured liver following IP injection, or this could be due to the lack of MHC-II expression in hepatic antigen-presenting cells (APCs), which could place CD^+4 in a steady state without activation.

In addition to the upregulation of adaptive immune cells in this liver model, I observed a remarkable increase in innate immune cells following OT-I and OT-II transplantation. My data illustrated the total number of hepatic $CD45^+$, $CD11^+$ and $CD11^+$ $F4/80^+$ cells in Ova-Bil mice in response to the adoptive transfer of OT-I and OT-II splenocytes when compared with normal mice treated with PBS. In comparison with OT-I and OT-II treated mice, I noticed an increase in $CD45^+$, $CD11^+$ and $CD11^+$ $F4/80^+$ cells following the adaptive transfer of a single population of OT-I. However, there were significant numbers of hepatic neutrophil ($CD11b^+$ $Ly6G^+$) and eosinophil ($CD11b^+$ $Gr\text{-}1^{Lo\text{-}neg}$ SSC^{HI}) cells in the Ova-Bil mice following OT-I and OT-II transplantation. In contrast, as found previously, the induction of OT-II cells did not lead to changes in the number of $CD45^+$, $CD11^+$ or $CD11^+$ $F4/80^+$ hepatic cells or in neutrophil or eosinophil cells. Together, these results indicate that OT-I and OT-II have been shown to induce a significant number of hepatic monocytes, suggesting that the hepatic monocyte infiltration of this animal model requires OT-I (OVA-specific $CD8^+$ cells) as well as OT-II (OVA-specific $CD4^+$ cells) splenocytes to enhance the inflammatory response. More importantly, this animal model is important in understanding the role of CD8 and CD4 in the development of liver injury, as well as hepatic inflammation. Another feature of this animal model is that it can be used to determine the interaction of CD8 and CD4 with innate immune cells and the underlying mechanisms of liver injury, which opens another area of study.

In the previous chapter, I demonstrated that human UC-MSCs have the ability to improve the hepatic injury of acute hepatitis caused in hepatotoxic acute liver injury induced by CCl_4. To validate whether this efficacy persisted *in vivo*, I further analysed the therapeutic role of UC-MSCs in Ova-Bil mice, which is another murine model of inflammatory liver

disease. As I had previously reported the variation in efficacy of the dose response in the CCl_4 model, I conducted a similar study using varying infusions of hUC-MSC dosages ($2.5x10^5$, $5x10^5$ and $1x10^6$). In this study, the injured Ova-Bil mice treated with both $2.5x10^5$ and $1x10^6$ were not found to have a clear reduction in ALT activity, whereas $5x10^5$ MSCs appeared to show a better improvement in liver injury. Collectively, my data suggest that a $5x10^5$ dose of MSCs could be the most effective dose which is able to improve the liver injury in this animal model. Interestingly, this finding was in contrast with our previous data on CCl_4, as $2.5x10^5$ and $1x10^6$ doses appeared to show more efficient sufficient improvement and a $5x10^5$ dose showed major variation between animals. This finding highlighted that the optimal effective dose depends on understanding each disease condition, as well as the mechanism of MSCs in modulating injury. I believe that a high dose of cells is not required to have greater therapeutic efficacy. I further suggest that a high dose of injected MSCs could enhance the inflammatory and immune responses from the host immune system. In contrast with the above finding, it has been suggested that repeated MSC infusions have the potential for therapeutic outcomes in graft-versus-host disease (GVHD) animals when compared with a single dose of MSCs (Nauta and Fibbe, 2007). Furthermore, another study found that three subsequent doses of MSCs reduced the collagen deposition in a mouse model with liver fibrosis, which could be due to that animal model being chronic, and suggests repeated doses for better treatment (Fiore et al., 2015).

In accordance with the above finding, a comparison study between unsorted and $CD362^+$ purified hUC-MSCs was performed in this study using intravenous doses of $5x10^5$ human unsorted UC-MSCs or CD362+ sorted UC-MSCs at day 4 following the induction of liver

injury in Ova-Bil mice. ALT enzyme activity in the serum at day 10 was measured to evaluate the liver injury in response to MSC treatment. A significant reduction in serum ALT was reported with infusions of $CD362^+$ sorted UC-MSCs. My results indicate that $CD362^+$ sorted cells have more efficacy in liver injury compared with unsorted cells. These data suggest that CD362 sorted MSCs have potential positive effects in liver injury in this animal model and I hypothesize that purifying MSCs may lead to more efficacy in the treatment of liver disease. In addition, my H&E staining of liver morphology revealed that liver preserved a normal structure with fewer leucocytes infiltrated around the portal area after exposing the animal to a single dose of UC-MSCs. In accordance with the above findings, I suggest that MSCs derived from umbilical cord could have immunosuppressive properties to reduce liver injury in OT-I and OT-II induction, and I believe this could be a potential mechanism to further study.

In our previous study in CCl4 model, I found that intravenous injections of human UC-MSCs attenuated the inflammation associated with liver injury induced by CCl_4 treatment. Here, I examined whether human UC-MSCs had a similar feature to modulate inflammation in the Ova-Bil model. Following the inflammation induced by the induction of OT-I and OT-II cells, I analysed the expression of $CD45^+$ cells isolated from the liver, spleen and blood, using flow cytometry analysis. My data found that unsorted and $CD362^+$ sorted UC-MSC-treated mice exhibited no significant reduction in hepatic $CD45^+$ cells compared with Ova-Bil mice treated with PBS. The same findings were reported in $CD45^+$ cells isolated from the spleen and blood. On the other hand, Ova-Bil mice showed specific hepatic expression of $CD45^+$ cells around the portal area, as reported by IHC. Interestingly, in response to CD362 sorted MSCs, we reported a

significant reduction in the number of $CD45^+$ cells in the liver sections of Ova-Bil mice compared with mice treated with unsorted UC-MSCs. These results show that only $CD362^+$ sorted UC-MSC transplantation rescued the hepatic inflammation in the Ova-Bil mice. The high level of expression of the $CD362^+$ marker may have a positive impact on the efficacy of UC-MSCs in liver inflammation associated with the Ova-Bil model, possibly because CD362 may secrete more endogenous cytokines, which promotes the anti-inflammatory function in this animal model.

I conducted further experiments to define the influence of MSC treatment on NK, non-NK and B lymphocytes isolated from different tissue sources, in particular, liver, spleen, and blood. After systemic perfusion of US and CD362 MSCs, I observed no changes in non-NK, NK, and B cells isolated from mouse liver, when compared with Ova-Bil mice treated with PBS. However, my results found that MSCs did not have an effect on immune cells isolated from peripheral blood and spleen. These findings could represent a possible explanation for the capacity of MSCs to reduce inflammation in the liver injury in this murine model. The opposite observation was recorded for CCl_4, as reported by the ability of MSCs to reduce the B and non-NK cells in the liver. This could be explained by the two animal models used in this study having different levels of inflammation, as I believe that CCl_4 is less severe when compared with the OBA-BIL mice. Based on this present study, I suggest research into whether MSCs have equal ability to engraft to injured liver when comparing two animal models following systemic infusion, and to report if MSC engraftments are correlated with the efficacy of MSCs to reduce liver injury in this animal model.

I analysed the translation potential of MSCs to suppress the proliferation of $CD3^+$, $CD4^+$ and $CD8^+$ T cells in Ova-Bil mice with hepatobiliary injury. My data indicate that the hepatic infiltration of $CD3^+$ and $CD8^+$ T cells in Ova-Bil mice showed no differences between treated and untreated MSCs in these animals. A similar finding reported that MSCs isolated from bone marrow had no direct effect on CD8+ cells, but had some influence on the proliferation of T cells (Ramasamy et al., 2008). Interestingly, analysis of the number of CD4+ T cells in the liver showed a significant increase in the presence of MSC treatment. However, my results indicated that US and CD362 sorted MSCs reported equal induction effects on hepatic CD4 T cells in Ova-Bil mice compared with the untreated group. In contrast, I did not observe any ability of MSCs to upregulate the number of CD4 T cells isolated from blood or spleen. It is possible that the increase in CD4 expression could be associated with an increase in IL-10 in the circulation by MSCs. MSCs have been shown to secrete more IL-10 in response to activated T cells when compared with MSCs under normal culture conditions. Several studies have reported that MSC treatment could cause more CD4+ cells to polarize towards Tregs with a positive expression of FOXP3. Accordingly, I assessed if MSCs could immunosuppress liver inflammation via the induction of Tregs. Surprisingly, my data indicate that MSCs had no significant impact on hepatic Tregs in this animal model.

Within the liver, macrophages have a great effect on the pathogenesis of liver diseases, with essential functions in homeostasis and the progression of different liver diseases (Tacke and Zimmermann, 2014). In a previous chapter, I found that MSCs suppressed macrophage activity in mouse liver with hepatotoxic injury but failed to polarize the macrophages towards an anti-inflammatory phenotype. Here, I further analysed the

ability of MSCs to modulate the myeloid immune cells in Ova-Bil injured animals. My flow cytometry data reported that US and CD362 MSCs had no ability to modulate the number of macrophages ($CD11^+$ $F4/80^+$) in the liver. In addition, the circulating macrophages isolated from peripheral blood, as well as spleen, were not shown to change following MSC treatment. In contrast, quantification of $F4/80^+$ cells in liver sections found a decreased level of macrophages following US and $CD362^+$ sorted MSC transplantation. Furthermore, I compared the immunosuppressive ability of US and CD362 UC-MSCs in M1 and M2-like cells isolated from mouse liver. Based on my flow cytometry data, the MSCs did not show any change in the macrophage phenotype between M1 and M2-like cells. This could be due to UC-MSCs lacking secretion of IL-6, which is reported to have a positive impact towards the differentiation of monocytes from macrophages with anti-inflammation phenotypes (Chung and Son, 2014). Another possible factor is the time period that MSCs require for this therapeutic feature. M1-like cells have been found to have early activation within 3 days and later to polarize to M2-like cells by the day following MSC injection (Arnold et al., 2007). In my animal models, my endpoints following MSC administration were 6 days in the Ova-Bil and 3 days in the CCl_4 animal model. Thus, I may have missed the ability of MSCs to have this polarization capacity and suggest considering later time points in future study. In addition, further experiments are suggested to study cell-to-cell contact via the direct culture of immune cells isolated from injured liver and MSCs, as applying exosomes from MSCs to the same cells could answer the paracrine efficacy of MSCs *in vitro*.

ICAM-1 and VCAM-1 adhesion molecules have been shown to mediate the immunosuppressive function of MSCs through the direct adhesion of MSCs to immune

cells (Chamberlain et al., 2011). Using IHC and qPCR, the transfer of OT-I and OT-II cells in Ova-Bil mice clearly promoted the expression of ICAM and VCAM in the liver, when compared with normal Ova-Bil mice. Interestingly, one major advantageous observation in the present study is that, upon MSC infusion, I observed a significant reduction in ICAM and VCAM expression in liver sections from Ova-Bil mice treated with CD362+ MSCs compared with mice treated with PBS. In addition, the above observations were confirmed by a significant decrease in the hepatic mRNA expression of ICAM and VCAM in Ova-Bil mice treated with CD362 MSCs. I observed a trend towards a decline in ICAM and VCAM in Ova-Bil mice treated with unsorted MSCs. My finding shows, for the first time, that human CD362 purified MSCs show superior properties compared with normal MSCs. I could not show a significant therapeutic effect of unsorted UC-MSC transplantation in either of the animal models used in this study. This may relate to biological variation and the need for additional experiments, or it may reflect the inferiority of unsorted MSCs. My results are not in line with our previous ICAM and VCAM data from CCl_4 models, which suggests that MSCs have a multifunctional effect and could relate to the pathophysiology of the disease itself. In the Ova-Bil model, the improvement in liver function following MSC transfusion could be mainly due to a reduction observed on ICAM and VCAM expression in the injured liver. We believe that our findings begin to elucidate how multiple classes of factors releasing by MSC cooperate to promote liver improvement. Additional studies, both in vitro and in vivo, are needed to improve our understanding the mechanisms of action of this potential mechanism. In particular, future work is required to demonstrate if MSC can modulate ICAM and VCAM expression on hepatic T cells or hepatic endothelial cells and the consequence in the therapeutic efficacy of MSC in liver disease. In addition,

understanding the interaction between MSCs and ICAM and VCAM could be one of the major mechanisms of MSC therapy and future study needs to be undertaken to investigate this further.

Finally, two cytokines, in particular, TNF-α and INF-γ, have been shown to be produced following activation of T cells (Ito et al., 2010). In addition, the two cytokines have been found to induce the expression of ICAM in liver injury (Afford et al., 2014). In this model, following the adoptive transfer of OT-I and OT-II, we reported increased expression of TNF-α and INF-γ. In addition, I observed a minimum induction in INF-γ with no difference in TNF-α in MSC-treated mice compared with untreated animals.

In summary, MSC transplantation is a promising candidate for the treatment of liver diseases. In this *in vivo* study, I have provided useful evidence of inflammation activities related to the induction of OT-I and OT-II in Ova-Bil mice. Following the induction of liver inflammation, subsequent infiltration of immune cells to the injured area of the liver was reported. The findings of this chapter provide an important explanation for defining the *in vivo* experiment, which aimed at improving the therapeutic efficacy of mesenchymal stromal cells in liver injury. Here, the therapeutic effects of US and CD362 sorted UC-MSCs were reported in this study in Ova-Bil mice with hepatobiliary inflammation. I showed that CD362 MSCs improved the hepatic injury of Ova-Bil mice with acute inflammation, followed by the downregulation of hepatic $CD45^+$ infiltrating cells, as well as F4/80 macrophages in the liver histology. The capacity of macrophage polarization and the induction of Tregs were not altered by MSC therapy. MSCs also demonstrated a remarkable increase in hepatic CD4+ cells, which could have a specific

mechanism related to MSC immunosuppression functions. Given the immunosuppressive properties of MSCs, it was clearly that purifying MSCs with CD362+ cells would enhance the ability of MSCs to reduce the level of adhesion molecules (ICAM and VCAM), which makes MSCs a more promising candidate in the treatment of liver diseases. Finally, the different therapeutic effects of MSCs could be due to the specific microenvironment in each disease condition, as well as the mechanisms which control their biological function in their particular niche.

CHAPTER 7

IN VIVO TRACKING AND MONITORING OF THE HOMING OF INTRAVENOUS UMBILICAL CORD MESENCHYMAL STROMAL CELLS

7.1 Introduction

MSCs offer great potential for the treatment of different diseases and conditions and could have therapeutic benefits. Moreover, the homing of infused stromal cells has been reported in several studies. For example, several studies have reported that MSCs are trapped in the lung after systemic administration (Lee et al., 2009; Galleu et al., 2017), while others have found that MSCs have the ability to migrate to a site injury and offer therapeutic improvement. In contrast, the route of MSC administration, such as intraperitoneal (IP), intramuscular, subcutaneous (SC) or intrahepatic injections, has been shown to be another important aspect in the literature and seems to have a role in achieving better therapeutic applications (Uccelli et al., 2008; van Velthoven et al., 2012). In addition, a direct comparison between different routes of MSC injection has shown that intramuscular administration results in a prolonged survival of MSCs compared to *in vivo* injection (Braid et al., 2017).

The accurate quantification and determination of numbers of infused stromal cells are still not fully defined. Therefore, many recent researchers have reported different methods for studying the homing of transplanted stem cells *in vivo*. Magnetic resonance imaging (MRI) was reported to be a good technique for tracking infused cells in animals. Sheng Hong Ju et al. successfully studied the migration of labelled bone marrow MSCs (BM-MSCs) to the liver using MRI and found that the labelled cells were localized in the liver after three hours and then showed a gradual reduction after 3, 7 and 14 days (Ju et al., 2007). Another technique that has been used in an animal study is an *in vivo* imaging system (IVIS), which represents a reliable optical system for detecting the migration of infused cells (Eisenblätter et al., 2009). Using this technique, labelled MSCs are infused

by several routes and the cells detected using the IVIS system. The MSCs were found to disappear within a few days following IV injection, but were detected at 3–4 weeks when injected intraperitoneally or subcutaneously (Braid et al., 2017). Another study has determined the homing of MSCs administered by intravenous (IV) injection by testing the DNA expression of human albumin using qPCR. They reported different expressions among different tissues with the greatest expression in the lung (Briquet et al., 2014). More recently, an advanced system was developed that provided very high-resolution images for a whole mouse using CryoViz technology. This device is a fully automatic machine which has the sensitivity to detect a single live cells, and can provide a 3D structure for the whole animal or a specific organ of interest (Roy et al., 2009). In addition, one unique feature of this technique is the ability to quantify the number of live cells *in vivo* after fluorescent labelling of cells prior to injection.

In the present work, I performed a biodistribution study of human MSCs (hMSCs) following injection into an animal model with liver injury. Side-by-side comparison of the homing of MSCs was reported between an Ova-Bil animal model and a CCl_4 animal model. Briefly, $CD362^+$ sorted MSCs were labelled with quantum dots (Q-605) and adoptively infused via the tail vein into mice to investigate their biodistribution at different time points after infusion. Next, I determined the fate of infused labelled cells by using the CryoViz^{TM} system (BioInVision, Cleveland, USA). Here, I showed that studying the cryo-imaging of a whole mouse demonstrated that UC-MSCs infused intravenously were detected in the lung, liver and spleen, and that most of the MSCs were trapped in the lung and rapidly cleared by 24 hours, with few cells remaining in the different organs. I did not notice any liver-specific increase in the number of MSCs.

7.2 Chapter Aims

In the present study, I used UC-MSCs labelled with quantum dots (Qdots) in two mouse models of liver injury to assess the biodistribution as well as the fate of the injected MSCs. In addition, I hypothesized that the homing of MSCs to the site of liver injury was necessary for greater therapeutic efficacy. The aims of this study were to:

- Monitor and track the engraftment of MSCs *in vivo*.
- Quantify and determine the number of infused cells accurately.
- Examine whether infused cells migrated to the site of injury or home to different parts of the body.
- Determine how long transplanted MSCs stay in the body following systemic infusion.
- Establish in which part of the liver injected MSCs can be identified (e.g., the parenchyma or portal).

7.3 Results

7.3.1 Qdots have high labelling efficacy and do not affect the viability or enhance the apoptosis of MSCs

Identification of the distribution of infused UC-MSCs *in vivo* would provide a better understanding of the mechanism of action of these cells and their homing, after systemic infusion. Here, mice received an IV injection of MSCs labelled with Qdots. Qtracker Cell Labelling Kits (Qtracker® 625 Cell Labelling Kit, Invitrogen, A10198) were used to label MSCs for *in vivo* cell tracing (the labelling procedure was reported previously in chapter 2). Briefly, MSCs were incubated with Qdots at 37 °C for 45–60 minutes, and the cells washed twice with complete growth medium and resuspended in normal saline for infusion.

In order to address whether Qdots have an effect on the viability of MSCs, I determined the viability of the MSCs one hour after labelling with Qdots by using flow cytometry. My results demonstrated that the viability of MSCs was about 84% following labelling with Qdots. This result clearly showed that Qdots had no observable effect on the viability of MSCs *in vitro* (Figure **7-1**A). More importantly, it was essential to determine the efficiency of Qdots when labelling MSCs for cell tracking. In order to confirm the efficiency of Qdot-labelled MSCs, I studied the expression of Qdots one hour after staining using flow cytometry. My FACS data showed that > 90% of the MSCs were labelled with Qdots, as shown in Figure **7-1**A. A representative image of MSCs labelled with Qdots is shown in Figure **7-1**B.

A

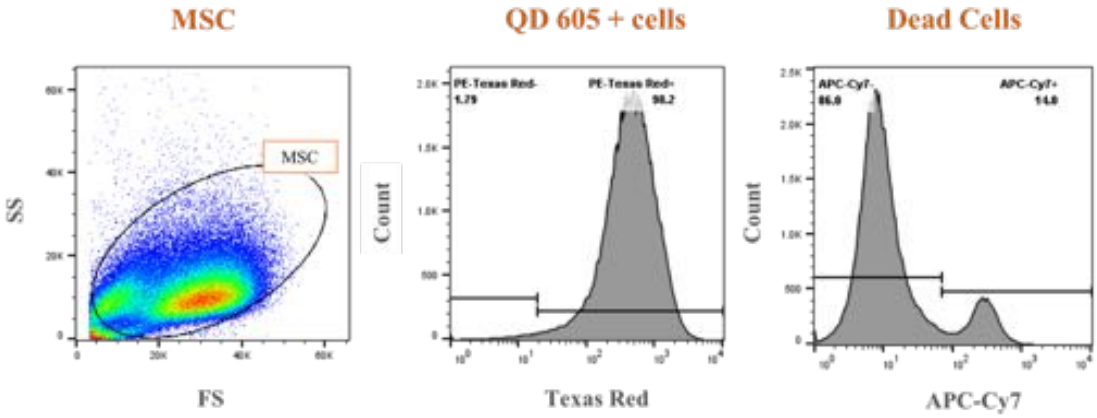

B

QDs labelling of MSCs

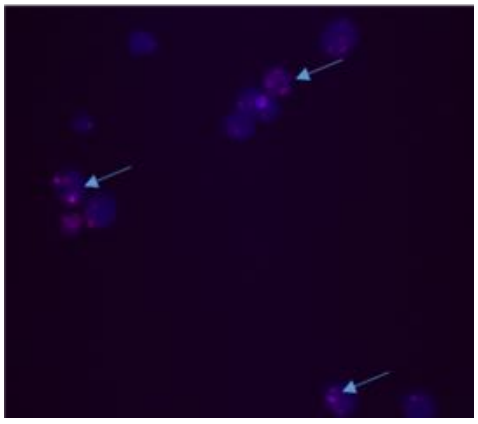

Figure 7-1 Efficacy and cell viability following quantum dot labelling of MSCs. A) Cell viability was measured by flow cytometry of Qdot-labelled MSCs 1 hour after staining. Following the Qdot-labelled MSCs for 1 hour, I observed > 90% of cells were stained with Qdots. B) Representative image of MSCs labelled with Qdots (as indicated by the arrows).

To further optimize the presence of Qdot-labelled MSCs *in vivo*, I directly injected Qdot-labelled MSCs into lung tissue harvested from mice and visualized the cells using the CryoViz™ technique. A large number of Qdot-labelled MSCs were clearly observed in the lung tissue, which indicated that our Qdots were a good labelling dye to use for my further *in vivo* tracking experiments (Figure ***7-2***).

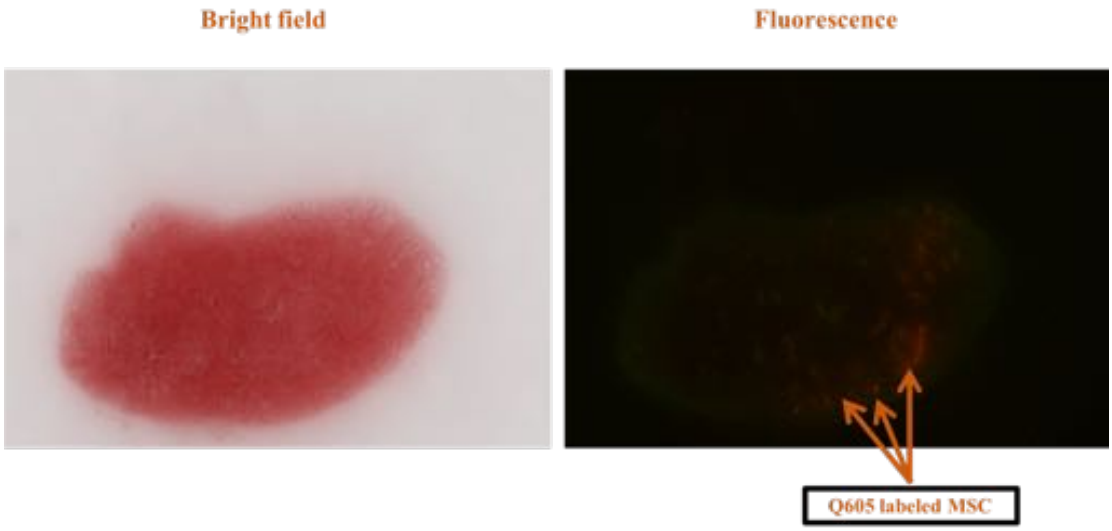

Figure 7-2 Representative image of bright and florescent lung tissue following direct induction of MSCs labelled with Qdots (arrows denote the MSCs labelled with Qdots).

7.3.2 Biodistribution of Q-605-labelled UC-MSCs in CCl_4 and OVA-BIL animal models

7.3.2.1 Study design

Two animal models of liver injury were investigated in this study in order to assess the homing of infused MSCs *in vivo*. The biodistribution of human UC-MSCs labelled with

Qdots was assessed by injecting them intravenously in both CCl_4 and OVA-BIL animal models. Animals were then sacrificed for whole-body imaging at different time points.

In the CCl_4 animal model, UC-MSCs labelled with Qdots were injected 4 hours after the induction of liver injury using CCl_4. Following intravenous injection of $250x10^3$ Qodt-labelled MSCs, the mice were sacrificed at different time points (1 h, 3 h, 1 day, 2 days, 3 days, and 7 days), and whole mouse bodies were snap frozen in optimal cutting temperature (OCT) medium and stored at -80 °C until the day of the analysis. A schematic diagram of the study design is shown in Figure **7-3**A. The other model examined in this chapter to investigate the fate of MSCs post-systemic perfusion was the Ova-Bil animal model. After the induction of liver injury in Ova-Bil mice using OT-I and OT-II cells, a single infusion of Qdot-labelled MSCs was given on day 4 and the mice were sacrificed at 1 hour, 1 day, and 5 days following MSC injection (Figure **7-3**B). In both models, labelled cells were quantified in different organs (lung, liver, and spleen) and the percentage of detected cells was calculated from the global cell count at 1 hour. In addition, whole-body images and 3D fluorescence structures were detected at different time points using the Cryo-Imaging System (BioInVision, Cleveland, USA).

A. CCl_4

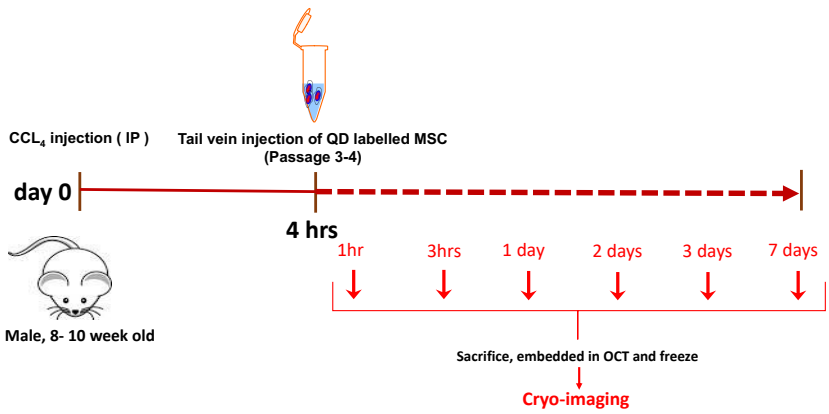

B. OVA-BIL

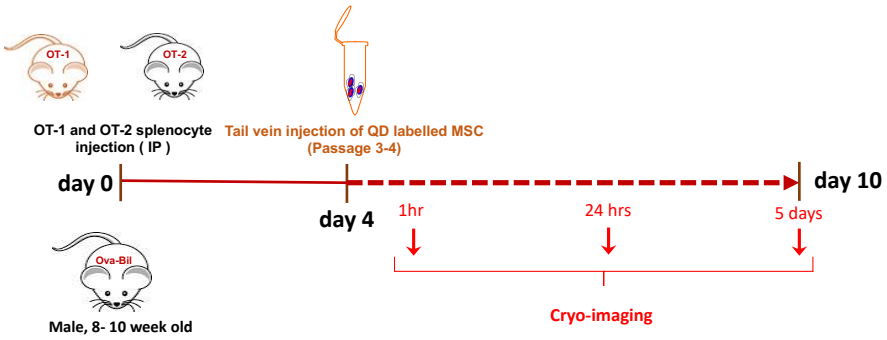

Figure 7-3 A) Illustration of the study design. A) Animals were treated with CCl_4. After 4 hours, mice received an intravenous injection ($250x10^3$) of human MSCs labelled with Qdots. Animals were then sacrificed at different time points (1 h, 3 h, 1 day, 2 days, 3 days, and 7 days) and then snap frozen in OCT medium for further analysis. B) Ova-Bil mice received adaptive transfer of OT-I and OT-II cells. After 4 days, the mice received an intravenous injection ($500x10^3$) of UC-MSCs labelled with Qdots. Animals were then sacrificed at different time points (1 h, 1 day, and 5 days) and then snap frozen in OCT medium for further analysis.

7.3.2.2 Global hMSC retention at different time points following MSC infusion

In the CCl_4 model, the mice received an intravenous injection of $250x10^3$ UC-MSCs and were sacrificed at different time points (3 h, 1 day, 2 days, 3 days, and 7 days). Labelled cells were quantified in different organs, in particular, the lung, liver, and spleen. The percentage of cells detected was calculated from the total global number of live cells found 1 hour after MSC infusion. The global cell retention count in the whole body was found to be 91% within 1 hour of MSC infusion, and then reduced slightly to 70% 3 hours after MSC induction. Interestingly, cell retention was observed to decline massively after

24 hours of infusion such that only 6% of total live cells could be detected. By days 2, 3, and 7, the total live cells reported was < 4%, as shown in Figure **7-4**A.

In addition to the above finding, I considered whether the above observation was seen in another animal model of liver injury. Here, the liver injury in the Ova-Bil mice was developed by the induction of OT-I and OT-II cells. By day 4, the Ova-Bil mice received an intravenous injection of $500x10^3$ UC-MSCs and were sacrificed at different time points (1 h, 1 day, and 5 days). As explained above, the total cell retention was calculated based on the global cell count at 1 hour post infusion. As expected, I detected a similar number of cells *in vivo* at 1 hour with a total of 90%. At 24 hours and 5 days following MSC infusion, the cell retention detected was 8%–4%, respectively (Figure **7-4**B). My observation clearly demonstrated that the injected MSCs were found to have decreased markedly after 24 hours, by approaching 80%, which suggested that the cells could become apoptotic very quickly and/or were targeted by the host immune system.

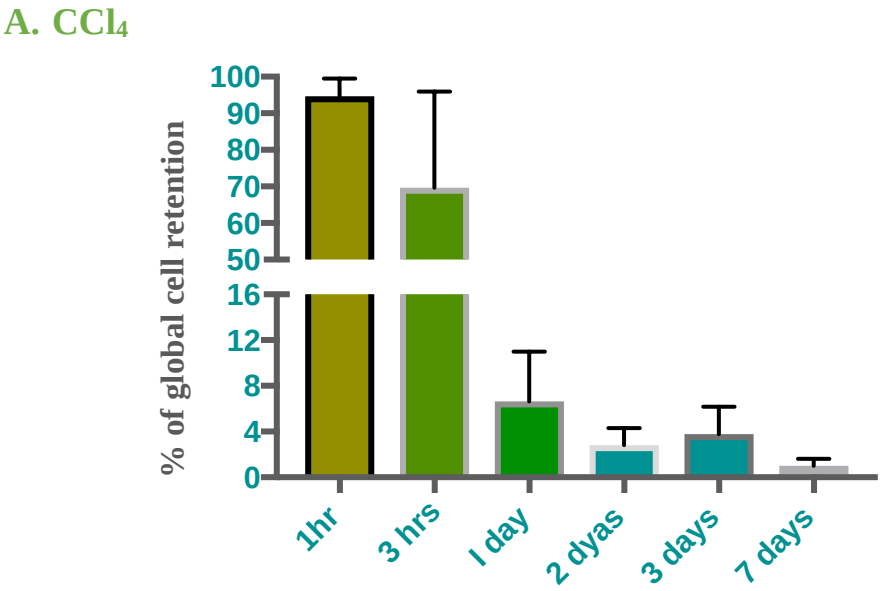

B. Ova-Bil

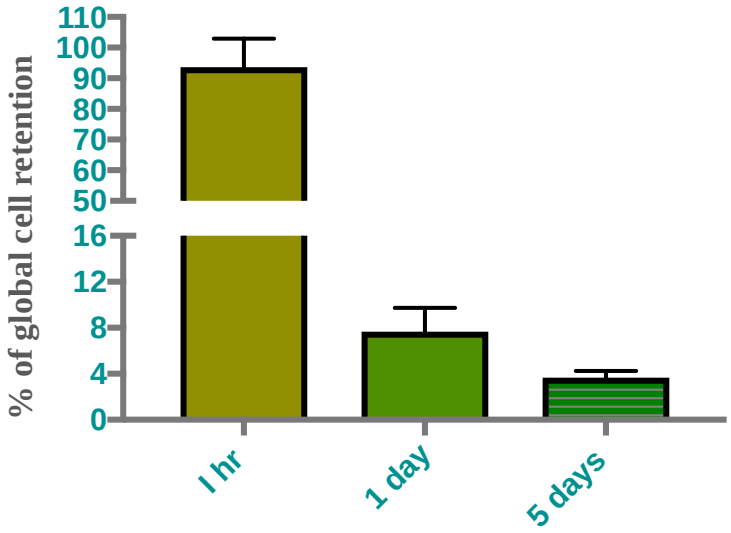

Figure 7-4 Qdot-labelled MSC retention at different time points in CCl_4 and Ova-Bil mouse models of liver injury. A) MSC retention at different time points in the CCl_4 injured mice after IV induction of Qdot-labelled MSCs (n = 3–5/time point). B) MSC retention at different time points in the Ova-Bil injured mice after IV induction of Qdot-labelled MSCs (n = 3 mice in each time point). Data are presented as the mean ± SD. The percentage of cells were calculated and normalized to the global cell number 1 hour after MSC injection.

7.3.2.3 Biodistribution of Qdot-labelled MSCs in the lung, liver, and spleen at different time points following induction of liver injury

Next, I assessed the *in vivo* biodistribution of Qdot-labelled MSCs following systemic induction in two animal models of liver injury. One hour after infusion of MSCs into CCl_4 injured mice, the majority of the live cells detected were found in the lung (> 90%) with a small number of cells observed in the liver (3–4%), as shown in Figure **7-5**A. Furthermore, my data showed that a small percentage of cells were found in the lung 24 hours after MSC treatment (5%) compared with the MSCs detected in the lung at 1 and 3 hours post-MSC infusion. A massive reduction was observed in the number of cells at

subsequent time points (2 days, 3 days, and 7 days); 0.8% of total quantified cells were detected in the whole body after 7 days (Figure **7-5**A).

Interestingly, the distribution pattern of MSCs in the Ova-Bil mice was found to be the same as that reported in the CCl_4 animal model. As shown in Figure **7-5**B, 80% of Qdot-labelled MSCs appeared to home to the lung 1 hour after systemic infusion, with 20% migrating to the liver in the same period. At 24 hours following MSC treatment, more than 90% of the MSCs injected were undetectable. However, I found that 2% of the cells were in the lung and 6% of the live injected cells were detected in the liver. Despite the low number of engrafted cells in the liver after 24 hours, I detected more engraftment of MSCs in the liver compared with the lung at 24 hours. This finding could demonstrate that, in both models, less than 0.5% of MSCs were found in the spleen across all the time points. I found that MSCs were engrafted to the lung at a higher rate within 1 hour of injection. In addition, I did not observe any evidence in this study that injected MSCs showed a higher engraftment rate within the liver (site of injury).

A. CCl_4

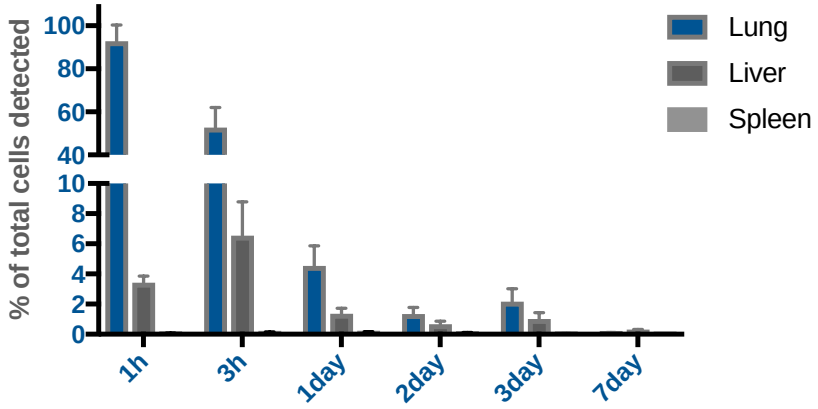

B. Ova-Bil

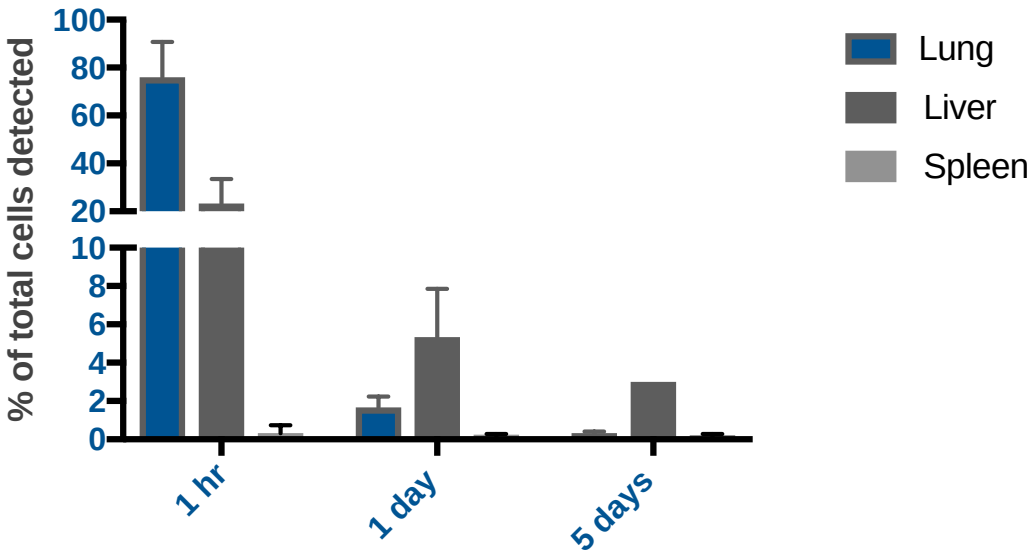

Figure 7-5 Biodistribution of Qdot-labelled MSCs in the lung, liver, and spleen at different time points. A) Number of MSCs homing to the lung, liver, and spleen were quantified after different time points in CCl_4 mice with hepatotoxic injury (3–5 animals per group). B) At 1 hour, 1 day, and 5 days, MSCs homing to the lung, liver, and spleen were quantified in Ova-Bil mice (3 animals per group). The percentage of cells was calculated and normalized to the global cell number 1 hour after MSC injection. Data are presented as the mean ± SD.

7.3.2.4 MSCs do not home to the site of liver injury 24 hours after MSC injection

I compared the engraftment efficiencies of MSCs in healthy mice at 24 hours with animals with liver injury in CCl_4 and Ova-Bil animal models. In the CCl_4 model, my data showed that infused MSCs were reported to have equal distribution patterns between the control animals (M.O) and the injured mice (CCl_4) within the lung, liver, and spleen at 24 hours post-MSC injection (Figure ***7-6***A). In addition, the engraftment of systemic infused MSCs was determined in the Ova-Bil mice at 24 hours. Surprisingly, I observed a remarkable decrease in the number of MSCs detected in the lungs and livers of Ova-Bil mice subjected to OT-I and OT-II cell induction (injured group) compared with the Ova-Bil

healthy mice (Figure ***7-6***B). This pattern of reduction suggested that MSC engraftment in the Ova-Bil mice had a different appearance to that in the CCl_4 mouse model.

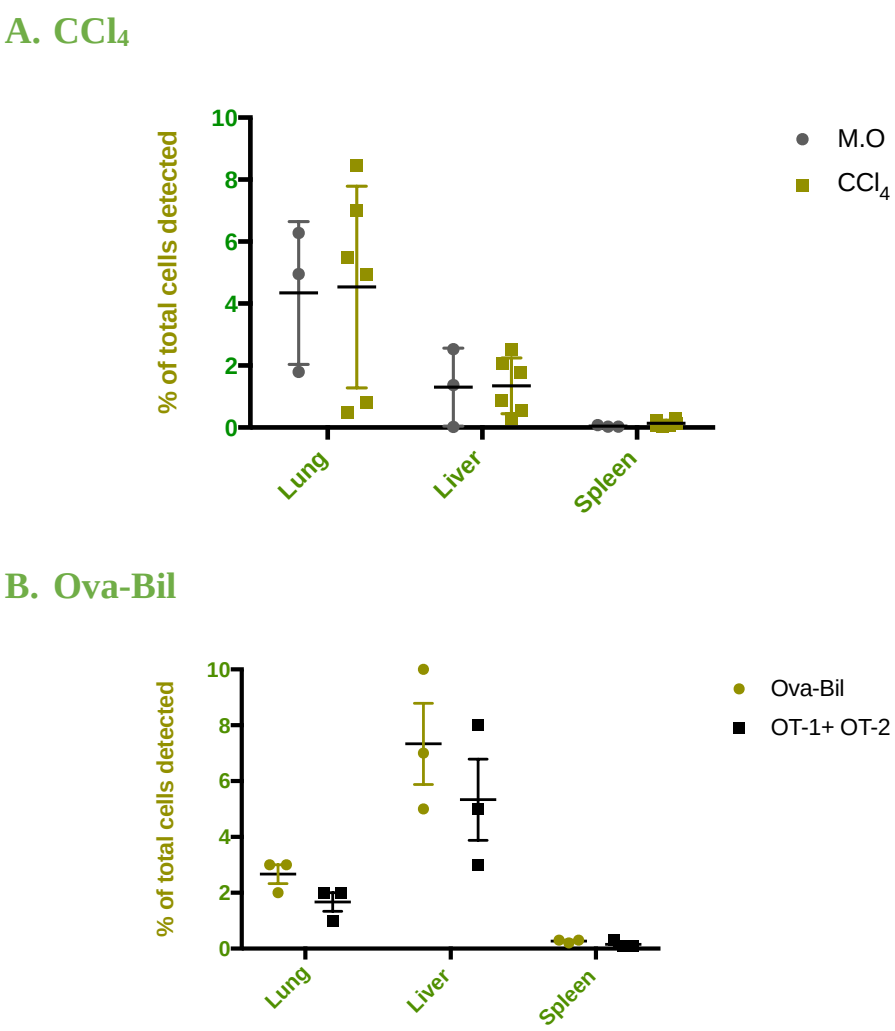

Figure 7-6 Percentage of MSCs detected at 24 hours in different organs of healthy mice and liver-injured mice. A) Number of MSCs homing to the lung, liver, and spleen were quantified at 24 hours and compared between healthy mice and CCl_4 mice with liver injury (3 animals per group). B) At 24 hours, MSCs homing to the lung, liver, and spleen were quantified in Ova-Bil mice with or without OT-I and OT-II induction (3 animals per group). The percentage of cells was calculated and normalized to the global cell number in the lung 1 hour after MSC injection. Data are presented as the mean ± SD.

7.3.2.5 Whole-mouse cross-section images for the in vivo detection of infused MSCs across different organs at different time points

To monitor the fate of infused MSCs over time, whole-body images were evaluated at different time points using the Cryo-Imaging System (Figure 7-7A and B). In both animal models, Qdot-labelled MSCs were detected at different time points in different organs in the mice. As reported in Figure 7-7A and B, the majority of Qdot-labelled MSCs were observed in the lung within one hour of a systemic injection, following by significant reductions across the later time points. I observed the same reduction in both the CCl_4 and Ova-Bil animal models. However, I did not detect more cells migrating to the site of injury or inflammation, which I thought would provide a trigger for MSC migration.

For the further evaluation of MSCs detected *in vivo*, I confirmed the previous finding by using a 3D cryo-imaging system which has the ability to detect Qdot-labelled MSCs injected in mice in different organs at several time points. In Figure **7-8**, the high-resolution 3D fluorescent images show that most of the injected cells accumulated in the lung within one hour of MSC infusion, as reported in the CCl_4 and Ova-Bil animal models. However, I reported more MSCs engrafted in the livers of Ova-Bil mice 1 hour after infusion compared with livers from CCl_4-injured mice (Figure **7-8**A and B). However, my 3D images showed that MSCs were no longer detected in any of the organs 5 and 7 days post infusion. These time points indicated that most MSCs were detected in the lung in the earlier time points and declined with time. I also detected that Ova-Bil mice were able to trigger more MSCs to the site of injury within 1 hour of the injection.

A. CCl_4

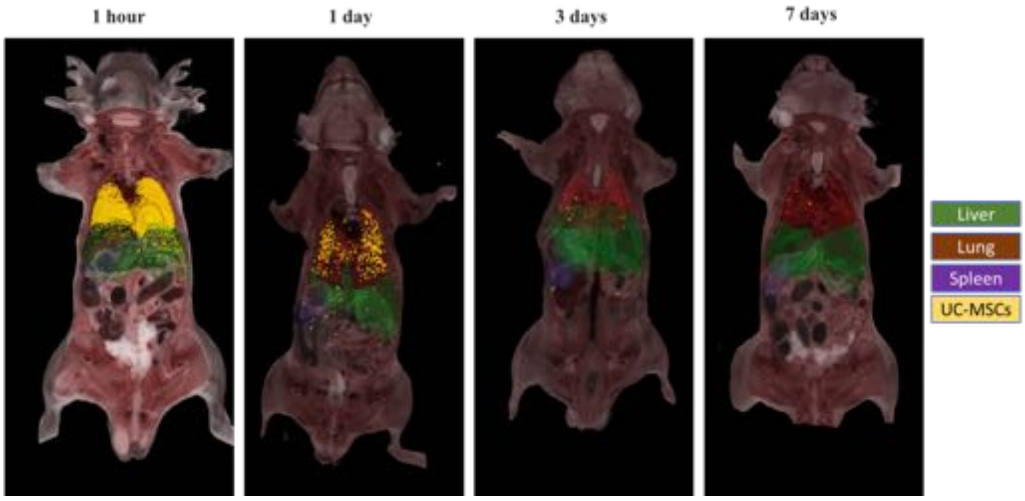

B. Ova-Bil

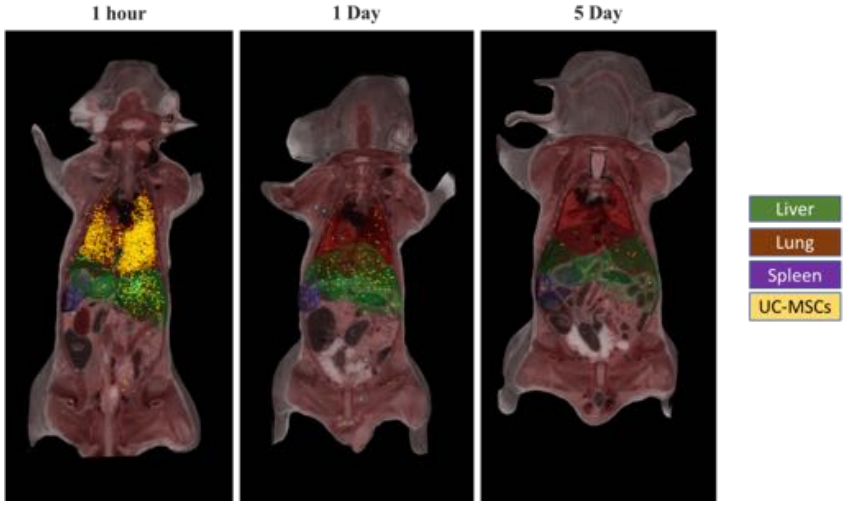

Figure 7-7 Representative images of the biodistribution of intravenously injected MSCs *in vivo* at different time points. A) Visualization of MSC distribution in whole mice after intravenous injection of MSCs at different time points in CCl_4 mice with hepatotoxic injury. B) Representative sections showing whole-body MSC distribution in Ova-Bil mice at 1 hour, 1day, and 5 days post-MSC infusion.

A. CCl_4

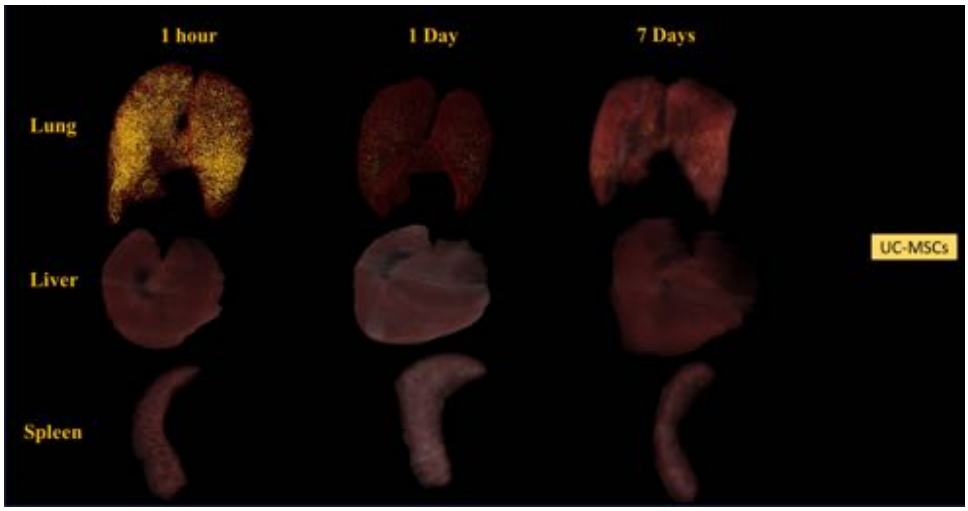

B. Ova-Bil

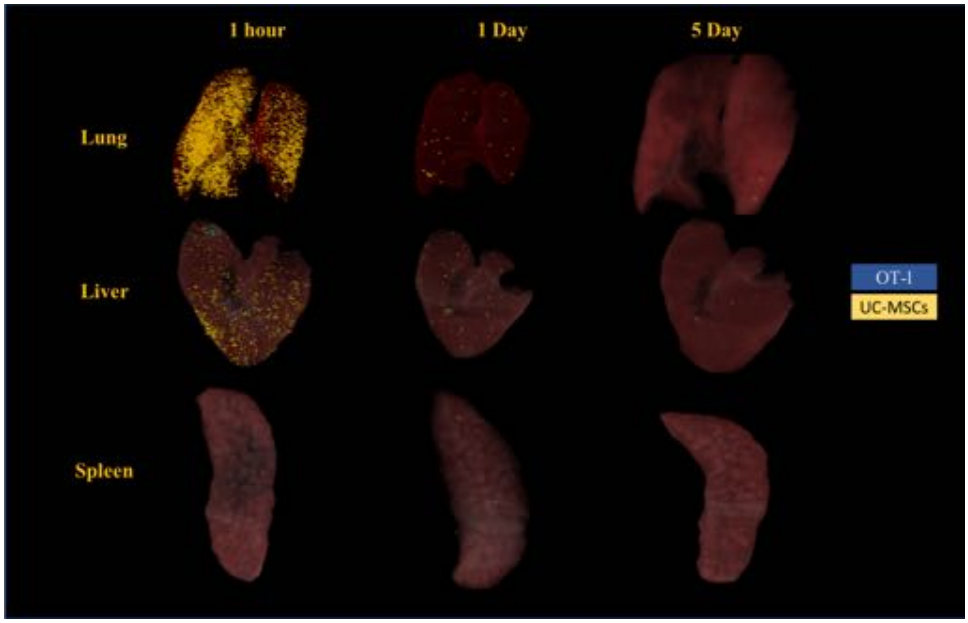

Figure 7-8 3D fluorescent CryoViz™ images of *in vivo* detection of infused Qdot-labelled MSCs in different organs at different time points. A) Visualization of MSC distribution in a 3D bright field in the lung, liver, and spleen after intravenous injection of MSCs at different time points in CCl_4 mice. B) Representative 3D images showing MSC distribution in the lung, spleen, and liver of Ova-Bil mice at 1 hour, 1 day, and 5 days post infusion.

7.3.2.6 Qdot-labelled MSCs localized in the hepatic parenchymal area in the CCl_4 model across time points

To further verify the distribution and localization of Qdot-labelled MSCs in the liver, I performed histological analysis of liver sections using the CryoViz™ imaging system. Representative bright field and fluorescent images of MSCs were detected in liver sections from CCl_4 mice and were noted *in vivo* at different time points post-MSC injection. Interestingly, MSCs were found predominantly near the parenchymal area in the liver sections, as seen in Figure ***7-9***. I did not find that cells migrated specifically to the portal area. In addition, I observed a greater number of MSCs 1 hour after MSC injection, followed by reductions in MSC numbers with time. My data suggest the possibility that MSCs had interacted with hepatocytes as well as with other immune cells that resulted from liver inflammation.

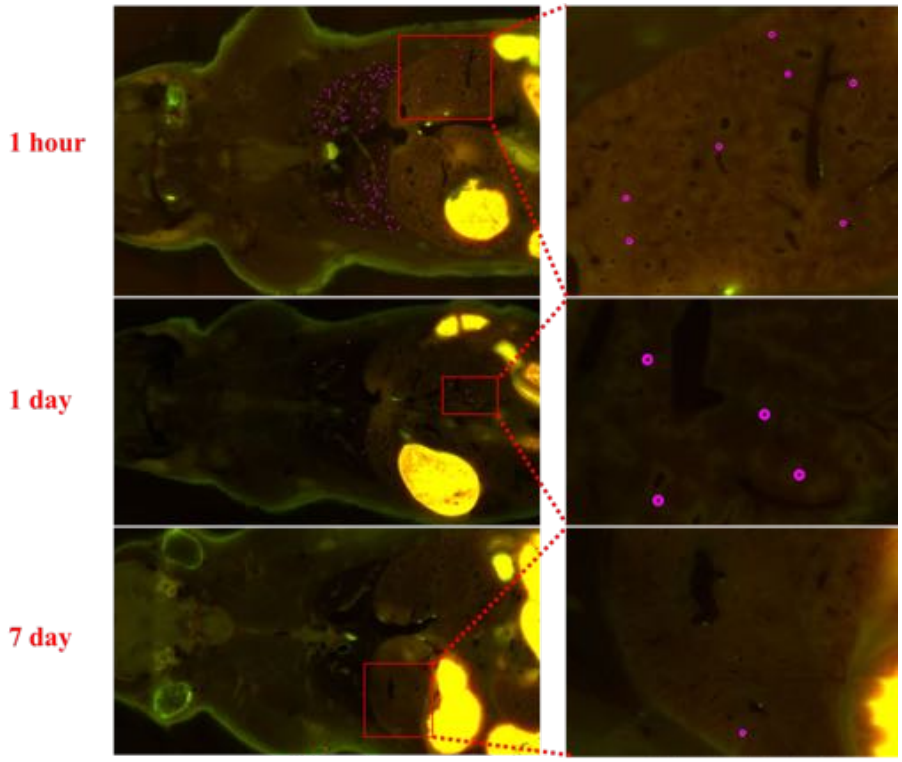

Figure 7-9 Representative bright field and fluorescent images of Qdot-labelled MSCs in the liver sections of mice with CCl_4 injury. Visualization of the presence of MSCs in liver sections after intravenous injection of MSCs at different time points (1 h, 1 day, and 7 days) in CCl_4 mice. Pink circles represent Qdot-labelled MSCs detected in liver sections.

7.3.2.7 Visualizing Qdot-labelled MSCs outside the major organs (lung, liver and spleen) 1 hour after systemic infusion in Ova-Bil mice

Finally, I performed whole-body cryo-imaged mouse sections to further define other specific organs to which MSCs may have engrafted following systemic infusion of MSCs in the Ova-Bil mouse model. As shown in Figure ***7-10***, I found that some MSCs engrafted to different organs in the mouse body, such as the kidney, ribs, and adrenal glands, 1 hour after intravenously infused MSCs.

Figure 7-10 Representative sections showing whole-body MSC distribution to different parts of the body in Ova-Bil mice at 1hour post-MSC infusion. Red circles represent Qdot-labelled MSCs detected in the liver section.

7.4 Discussion

MSCs hold promising therapeutic potential for several clinical applications. However, several barriers in the field of cell therapy have been intensively reported in order to understand the engraftment as well as the viability of cells following *in vivo* induction. In addition, the homing of infused MSCs has been reported in several studies, and different techniques used to quantify the number of cells (Pritchard, 2016). In this study, I investigated the dynamic homing of MSCs by using a new imaging system that has been developed recently and can provide very high-resolution images with a 3D view of a whole mouse (Roy et al., 2009). I used hMSCs isolated from the umbilical cord and systemically infused in two animal models with liver injury. I found that most of the injected MSCs were trapped in the lung within 1 hour and showed a remarkable decline in numbers after 24 hours. My findings are in line with previous results that demonstrated MSC engraftment as well as the quantification observed across time points of the systemic induction of MSCs.

In order to evaluate the homing ability of MSCs *in vivo*, I used Qdots, which are fluorescent nanoparticles with a size range of 2–10 nm (Ferreira et al., 2008). In this study, and prior to the *in vivo* induction of MSCs, I investigated the viability of MSCs following culture with Qdots *in vitro* and assessed the efficiency of MSCs labelled with Qdots. My flow cytometry data reported that MSCs were labelled with Qdots for one hour and resulted in high labelling efficiency (92%), with no effects reported regarding the viability of the MSCs. Similar findings have been reported by other groups, which found that Qdots showed high efficiency in labelling mouse embryonic stem cells (85%) and reported no dead cells detected in response to the Qdot-labelling procedure (Rak-

Raszewska et al., 2012). In contrast, another study reported lower efficiency (70%) following the labelling of hMSCs with Qdots (Auletta et al., 2015). Another report found that MSCs labelled with Qdots decreased after co-culture *in vitro* for 24 hours. Accordingly, in my *in vivo* experiments, the Qdot-labelled MSCs were injected immediately after the one hour labelling procedure and injected intravenously (Muller-Borer et al., 2007). I found Qdots to be a safe and feasible material for cell labelling to track MSCs after infusion *in vivo*. My *in vitro* characterization also led me to hypothesize that Qdots had high labelling efficiency with no direct effect on MSC viability. This demonstrated that Qdots would be a more beneficial and suitable material to use for tracking MSCs *in vivo* in terms of fully understanding their engraftment ability and potential in cell therapy. Future analysis is, however, essential to evaluate the cytotoxicity of Qdots after internalization by MSCs.

In this study, I analysed the fate of MSCs labelled with Qdots after systemic infusion in two animal models of liver injury. Here, I used the CryoViz™ imaging system to monitor the trafficking of MSCs and quantified live MSCs after infusion in mice with liver injury. In the CCl_4 hepatotoxic model, the global cell retention count in the whole body was found to be 91% within 1 hour of MSC infusion and declined massively (6%) 24 hours after infusion. On the other hand, Ova-Bil mice with hepatobiliary injury induced by OT-I and OT-II induction showed retention of 90% of total MSCs injected at 1 hour, followed by a marked reduction in MSCs (8%) at 24 hours post infusion. In line with these findings, using the CryoViz™ imaging system, Schmuck et al. showed that 80% of hMSCs were detected within different organs 1 hour after systemic infusion and this dropped to < 0.06% within 2 days post infusion (Schmuck et al., 2016). In a similar finding, umbilical

cord matrix stem cells were detected after 2 days but no cells were observed 6 and 12 days after infusion (Weiss et al., 2006). In comparison with other studies, Gao et al. have shown that MSCs can be detected in many organs, such as the lung, heart, liver, and kidney, from the first hour to 7 days after intravenous injection of MSCs (Gao et al., 2001). However, the above studies used different techniques (IVIS and MRI), which cannot detect the actual number of live cells and they counted the cells according to the intensity of florescence used to stain the cells. Notably, our data clearly demonstrated that MSCs remained live in the lung for a few hours after infusion and disappeared from the lung after 24 hours, suggesting that MSCs have a short life in the recipient mice. Questions remain with regard to why MSCs are trapped directly to the lung, and why MSCs no longer exist 24 hours after injection.

However, the shortness of MSC viability, as well as their quick disappearance, has no impact on the therapeutic function of MSCs, as reported in several studies. One important finding could come from the idea that MSCs are cleared via lung macrophages; this was reported by the increased expression of the F4/80 marker in the lungs of mice undergoing MSC injection (Hoogduijn et al., 2013). In addition to the clean-up of MSCs by macrophages, a very recent study has demonstrated that MSCs might have the ability to induce the distribution of monocytes and show immunoregulatory ability across the body (de Witte et al., 2018). Furthermore, the same study showed that the majority of MSCs were dead 24 hours after injection with engraftment potential to the lung and liver. It was found that MSCs could change the phenotypic characteristics of monocytes to a non-classical phenotype.

In order to achieve the short-term survival of injected cells, the local transplantation of an injection could provide more efficient therapy in liver disease. In addition, I suggest that another route of administration could be applied to investigate the potential delivery of injected cells to the site of injury. For example, the infusion of MSCs directly into the portal vein may lead to more engraftments to the local liver injury and subsequently improve therapeutic efficacy. The beneficial effect of the direct injection of MSCs into the portal vein has been reported in acute liver injury and was found to have more promising support of liver regeneration (Cao et al., 2012). In contrast, it is important to note that the local injection of MSCs in some organs, such as the brain and heart, is not acceptable clinically and may lead to the development of more invasive complications. Hence, IV delivery is less invasive and would be the most effective form of administration despite the low engraftment rate.

In addition, the biodistribution of Qdot-labelled MSCs was calculated as a percentage of the cells detected at each time point normalized to the global cell count in the lung at 1 hour. In the CCl_4 model, the majority of MSCs were found in the lung after 1 hour (> 90%) and were subsequently depleted 24 hours after injection (< 4%). However, at the same time point, a small number of cells were detected in the liver, with only 4% of injected cells. On the other hand, Ova-Bil mice with hepatobiliary injury induced by OT-I and OT-II showed 80% of MSCs trapped in the lung at 1 hour, whereas 20% of the MSCs were found in the liver. My results indicated that most cells migrated to the lung within 1 hour and declined gradually with time, and less than 0.8% of the total quantified cells were detected in the whole body after 7 days. Interestingly, the findings in this study clearly indicated that more MSCs engrafted to the liver after 24 hours in the Ova-Bil mice

compared with the cells detected in the lung. This observation was in Ova-Bil mice, which indicated that more MSCs engrafted to the site of injury 24 hours after systemic implantation. Based on these findings, I speculate that the observed variations in the engraftment of MSCs between the CCl_4 and Ova-Bil mouse models suggest that different factors affect the recruitment abilities of MSCs, either from the bloodstream or from the tissue environment of the injured site. I also believe that this could be due to the higher number of infused MSCs in Ova-Bil mice compared with the low number injected into the CCl_4 mice. Thus, I anticipate that a greater number of injected MSCs could result in higher engraftment potential to an injured site. In line with the previous finding, a comparison study was conducted to investigate the number of cells injected and the engraftment potential. This study reported that engraftment potential is correlated to a high number of injected cells (Omori et al., 2008).

The therapeutic efficacy of cell therapy could rely on the engraftment of cells to the site of injury. Accordingly, I conducted a comparison study of MSC engraftment between healthy and liver-injured mice using the CryoViz™ imaging system. In the CCl_4 model, my data showed that infused MSCs were reported to have equal distribution patterns between the control animals (M.O) compared with injured mice (CCl_4) within the lung, liver, and spleen at 24 hours post-MSC injection. In addition, the engraftment of systemically infused MSCs was determined in Ova-Bil mice at 24 hours. Surprisingly, 24 hours after systemic MSC injection, I observed a remarkable decrease in the number of MSCs detected in the lungs and livers of Ova-Bil mice subjected to OT-I and OT-II cell induction (injured group) compared with the Ova-Bil healthy mice. This pattern of reduction suggests that MSC engraftment in Ova-Bil mice appears to be different from

that engrafted in the CCl_4 mouse model. Similarly, a recent study reported that MSCs migrated from the circulation to the tumour microenvironment in mice with hepatic tumours, and no MSCs were found in mice with a healthy liver (Xie et al., 2017). Although some studies reported conflicting data about the fate of systemically infused MSCs *in vivo*, they reported that infused cells showed no differences in the migration to the ischemic liver injury compared to mice with normal livers (Eggenhofer et al., 2012).

Following low numbers of infused MSCs showing engraftment within an injured liver, we further investigated the distribution of Qdot-labelled MSCs in the liver microenvironment and the exact location within the tissue. Interestingly, MSCs were found predominantly near the parenchymal area in liver sections but not in the portal area, as reported in the CCl_4 model. My data might demonstrate that MSCs show a possible interaction with hepatocytes as well as with other immune cells resulting from liver inflammation. In addition, these results provide crucial insight that MSCs may exhibit local trophic or paracrine activity that could offer a consequential therapeutic effect in liver diseases.

I reported that IV injection resulted in a small number of injected MSCs reaching the liver. Further routes of administration should be fully considered in future study. I believe that direct injection into the locale of an injured site will promote the homing of cells with more efficient effects. To increase MSC homing to the liver, MSCs could be modified *in vitro* for greater homing efficiency through one of the following strategies: 1) Sorting MSCs to enrich more purified cells with greater homing functionality (Sherman et al., 2017); 2) Priming MSCs with factors such as cytokines and chemokines, which were found to enhance the recruitment of MSCs to the site of injury (Ren et al., 2011); and 3)

Genetic engineering or modification of MSCs has shown beneficial effects in many preclinical studies (Yang et al., 2015). Another important feature that would seem to require more investigation is to check whether the phenotype of engrafted MSCs has changed or remains the same in the physiological and pathological states.

In summary, the homing of infused stromal cells has been found to be important to promote therapeutic regeneration as well as to treat inflammation in liver diseases. I analysed the fate of MSCs labelled with Qdots after systemic infusion in two animal models of liver injury. This study used the CryoViz™ imaging system to monitor the trafficking of MSCs and quantify live MSCs after infusion in mice with liver injury. I found that most injected MSCs were trapped in the lung within 1 hour and had cleared within 24 hours of systemic infusion. In addition, my findings clearly reported that more MSCs engrafted to the liver after 24 hours in the Ova-Bil mice compared with cells detected in the lung. However, I reported variations in the engraftment of MSCs in the liver at 24 hours between the CCl_4 and the Ova-Bil mouse models, which suggests that different factors affect the recruitment abilities of MSCs in both CCl_4 and Ova-Bil mice. The data in this study will help to guide future aspects related to therapy involving the transplantation of MSCs in liver injury. However, I believe there still remains a major lack of understanding of the several mechanisms of how MSCs are engrafted and target specific tissues in disease conditions.

CHAPTER 8

CONCLUSION AND FUTURE WORK

8.1 Conclusion

8.1.1 MSC characterization and CD362+ expression

Mesenchymal stromal cells have been successfully isolated from human umbilical cord and represent an attractive source of MSCs for use in clinical studies. In addition, maintaining heterogeneity within cultured MSCs population have been shown to be important for optimal therapeutic function. In chapter 3, we showed for the first time that unsorted and CD362 sorted MSCs isolated from umbilical cord demonstrated similar expression of MSCs markers as well as the capacity to undergo tri-lineage differentiation *in vitro*. I would appreciate more comparative studies to give use a better understating about the immunomodulatory function of the both population of MSCs as well as the ability to differentiate to some specialized cells such as hepatocytes *in vitro*.

In this study, I addressed the expression of CD362 across different MSC sources (BM and UC) and found that MSCs from different origins expressed CD362 at different levels. I therefore reported that CD362 expression is predominant in umbilical cord and could be highly expressed in MSCs from birth-associated tissues. In addition, I also demonstrated that the expression of CD362 from different donors at the same passage number expressed different levels of CD362. This variation could come from the variation of donor age which I did not assess in my study, this limitation will be addressed in my future studies. More importantly, my results showed a significant decrease in the expression of CD362 by passage 5. These finding support that using late passage MSCs was not appropriate for their therapeutic use and may not be functionally suitable for transplantation. Further and in more depth *in vitro* studies are required to understand the

function of CD362 expression by MSC and the significance of CD362 in the clinical use of MSCs.

8.1.2 Time course of injury post-CCl_4 administration

The future for developing MSC-based therapies for liver diseases lies in understanding the interactions between MSCs and the microenvironment of the injured liver. In this *in vivo* study, I was able to provide useful evidence of the dynamic cellular changes and disease activities involved in acute CCl_4-induced liver injury over different time points. These changes, therefore, are valuable to assess the efficacy of MSCs after infusion according to the peak of the biological parameters that need to be investigated.

In this chapter, I reported that the maximum effect of liver injury was seen after 24 hours with massive necrotic areas in the liver tissue. My findings also indicate that other parameters such as inflammatory cytokines, oxidative stress, and autophagy are correlated with hepatocellular damage, as they increased rapidly by 24 hours. The inflammatory response increase after 48 hours and peaking 72 hours after treatment with CCl_4 with clear localization around the portal tracts. Furthermore, I found that antioxidant enzymes exhibited significant variation at different time points.

The findings of chapter 4 have important implications for defining the most effective study endpoints to use for my *in vivo* experiment, which aimed at improving the therapeutic efficacy of MSCs in liver injury. In addition, this could help to identify specific pathways to target and understand the functional effect of MSCs on the injured tissue microenvironment.

8.1.3 Therapeutic efficacy of unsorted UC-MSCs and CD362^{+} sorted MSCs in mice with liver injury

The therapeutic potential of hUC-MSCs has been reported to repair injured tissue, but few studies have found beneficial effects of MSC infusions in different animal models of acute liver injury. To address whether UC-MSCs have a therapeutic role in liver injury, I used CCl_4 and Ova-Bil mouse models of acute liver injury. As reported in chapter 5 and 6, an efficacy dose-response with varying infusions of hUC-MSC dosages was assessed in animal models. I observed that both $2.5x10^5$ and $1x10^6$ doses appeared to have the same level of improvement in liver injury, whereas the $5x10^5$ dose had superior efficiency in the treatment of liver injury in the Ova-Bil mice. This finding suggests that high doses of cells are not required for greater therapeutic efficacy, and highlights that the optimal effective dose depends on understanding each disease condition, as well as the mechanisms of MSCs in modulating injury.

The therapeutic effect of CD362^{+} sorted UC-MSCs and unsorted UC-MSCs has not yet been studied in literature. Thus, I conducted, for the first time, comparison study to investigate the effect CD362^{+} sorted UC-MSCs and unsorted UC-MSCs in CCl_4 as well as Ova-Bil mouse models. I demonstrated a significant reduction in serum ALT with infusions of CD362^{+} UC-MSCs as well as US MSCs in CCl_4, whereas the liver injury in the Ova-Bil mice found to have improvement with CD362^{+} sorted UC-MSCs. This finding clearly demonstrated that sorted cells have potential positive effects and more efficacy in the treatment of liver diseases.

I studied the hypothesis that MSC transplantation can promote acute liver injury through an immunosuppressive function using UC-MSCs. I showed that transplantation of unsorted MSCs or $CD362^{+}$ sorted MSCs resulted in significant reduction in hepatic $CD45^{+}$ expression as well as a reduction in non-NK cells and B cells in mice injured with CCl_4 induction. In contrast, no significant reduction in hepatic $CD45^{+}$ cells reported in Ova-Bil mice treated with MSCs. In addition, I reported no change in the hepatic expression of $CD3^{+}$, $CD4^{+}$ and $CD8^{+}$ following the treatment of CCl_4 mice with MSCs. Interestingly, analysis of the number of CD4+ T cells in the liver of Ova-Bil mice showed a significant increase in the presence of US and CD362 sorted MSCs treatment. My results indicate that US and CD362 sorted MSCs reported equal induction effects on hepatic CD4 T cells in Ova-Bil mice compared with the untreated group. In addition, I further analyzed the ability of MSCs to modulate the macrophages in both models following treatment with hUC-MSCs. We only observed that CD362 UC-MSC treatment have decreased the number of macrophages in the injured liver of the CCl4 mice and MSCs had no ability to modulate the number of macrophages in the Ova-Bil mice. Further experiments are suggested to study cell-to- cell contact via the direct culture of immune cells isolated from injured liver and MSCs, as applying exosomes from MSCs to the same cells could answer the paracrine efficacy of MSCs *in vivo.* Another interesting point that remains to be studies is the ability of MSCs to induce B cell subsets that could have proved immunomodulatory properties.

In general, our results have demonstrated that MSCs have anti-inflammatory effects in multiple ways that appear to be related to the different microenvironments in each liver

injury as well as the mechanism which control their biological function in their particular niche.

Interestingly, one major advantageous observation in the present study is that, upon MSC infusion, I observed a significant reduction in ICAM and VCAM expression in liver sections from Ova-Bil mice treated with CD362+ MSCs. However, an opposite finding confirmed that these two adhesion molecules were not altered following MSC treatment of CCl_4-injured mice. This finding shows that CD362 purified MSCs show superior properties compared to unsorted MSCs. This could be due to the ability of the CD362 MSCs to promoted tissue repair through the elevation of chemokines and cytokines to modulate the adhesion molecules activities in the local environment on the injured tissue which can promote tissue regeneration. One of the major challenge of MSC- based therapy is to understand the mechanism of action. Indeed, we acknowledge that further elucidation of the role of adhesion molecules in the immunoregulatory function of the MSCs will be an essential area of future study. In addition, Further analysis of the molecular mechanisms in relation to the interactions between MSCs and inflammation will be essential for developing potential therapeutic applications of MSC-based therapies and for improving our understanding of pathological changes related to specific disease condition.

It is necessary to recognize certain limitations in our present study. One limitation is that the study did not assess the long-term effect of MSCs is unclear. We only focused on the short-term effect (3-5 days) of MSC in all our in vivo studies. The long-term effects remain unknown and merit further investigation. Second, although it was reported that

UMSCs can be induced into hepatocytes in vitro, it is still unknown if these cells really transdifferentiate into hepatocytes in vivo. Third, due to time and fund limitation, we were unable to include and explore the effect of MSCs on apoptosis and autophagy have not been explored in detail. Finally, we did not detect and analyze differences in expression level and effect among all the possible secreted therapeutic factors in both animal models after treatment of hUC-MSCs.

8.1.4 Monitoring and tracking the engraftment of MSCs *in vivo*

The homing of infused stromal cells has been found to be important to promote therapeutic regeneration as well as to treat inflammation in liver diseases. In my study, I investigated the dynamic homing of MSCs by using the CryoViz™ imaging system to monitor the trafficking of MSCs labelled with Qdo and quantify live MSCs after infusion in mice with liver injury. I found that most injected MSCs were trapped in the lung within 1 hour and had cleared within 24 hours of systemic infusion. Questions remain with regard to why MSCs are trapped directly to the lung, and why MSCs no longer exist 24 hours after injection. This rapid clearance of infused MSCs could be mediated by phagocytosis by recipient immune cells and subsequently activate the immune responses. The short-term survival of injected MSCs can be achieved by local transplantation of injection which could provide more efficient therapy in liver disease.

In addition, my findings clearly reported that more MSCs engrafted to the liver after 24 hours in the Ova-Bil mice compared with cells detected in the lung. However, I reported variations in the engraftment of MSCs in the liver at 24 hours between the CCl_4 and the

Ova-Bil mouse models, which suggests that different factors affect the recruitment abilities of MSCs in both CCl_4 and Ova-Bil mice, either from the bloodstream or from the tissue microenvironment of the injured tissue. The data in this study will help to guide future aspects related to therapy involving the transplantation of MSCs in liver injury. However, I believe there still remains a major lack of understanding of the several mechanisms of how MSCs are engrafted and target specific tissues in disease conditions.

8.2 Future Work

In this study, I found that UC-MSCs have regulatory abilities to immunomodulate the inflammation associated with acute liver injury. However, it should be noted that there are several outstanding questions that need to be addressed in order to understand the mechanism of action related to the role of MSCs in immunomodulating liver injury *in vivo*. Understanding the mechanism will support further development of the therapeutic potential of MSCs in clinical trials associated with liver injury. Based on the main findings in this study, I highlight below the main areas that I believe require further study.

- The timing as well as the delivery route of MSCs are critical to increasing the potential function of these cells in the treatment of injury to different tissues. Direct or local injection of MSCs may promote the homing of the cells to the site of inflammation. In addition, the dose and duration of MSC treatment needs to be studied further in preclinical experiments as well as in clinical trials. Another challenge for MSC-based therapy is the cell source, which needs to identify whether MSCs from different tissue sources have different effects in response to the various inflammatory immune cells.

- In addition, more advanced delivery vehicles can be applied for more effective treatment with MSCs. For example, exosomes, as well as MSC-derived macrovesicles, could have an effective function, as it has been reported in various studies that MSCs exhibit paracrine function to modulate damaged tissue. The difference between the ability of MSCs to engraft locally and secrete trophic factors is still unclear and needs further investigation.

- There are important steps in manufacturing MSCs *in vitro*, which could improve the diverse phenotypic characterization of these cells. I believe sorting cells based on marker expression may allow for the selection of cells with greater efficacy. In addition, pre-treatment of MSCs using chemokines or cytokines prior to injection is intended to enhance their biological properties for whichever clinical indication is being considered. This may include improvements in MSC immunomodulatory effects, homing to injured organs and/or greater expansion of cells. More importantly, the genetic correction or modification of transplanted MSCs represents a powerful approach in the use of MSCs in regenerative medicine. In addition, future work is required to develop more advanced techniques which could increase the persistence of MSCs following infusion, which could result in greater therapeutic effect.

- One fundamental aspect of the future of cell therapy which could lead to more successful treatments is understanding the biological as well as the genetic abnormalities of the disease to be treated. This could help to identify specific pathways to target and understand if MSCs can be manipulated or genetically modified based on the injured tissue microenvironment. Another question which needs further study is whether the endogenous MSCs found in the injured microenvironment have a similar function to the exogenous MSCs. I believe this needs more advanced work and standardized protocols for identifying specific markers that could help to study MSCs *in vivo*.

- One of the major impacts of MSC research lies in investigating the correlation between MSCs and the metabolic pathways related to liver disease. I believe that

MSCs have a significant role in the regulation of metabolic enzymes related to the glucose homeostasis that is in turn related to different metabolic syndromes associated with liver disease. Another important piece of evidence that could be related to the engraftment of MSCs could come from studying the interaction between MSCs and platelets.

CHAPTER 9

REFERENCES

Kim, M.-D., Kim, S.-S., Cha, H.-Y., et al. (2014) Therapeutic effect of hepatocyte growth factor-secreting mesenchymal stem cells in a rat model of liver fibrosis. *Experimental & Molecular Medicine*, 46(8), e110.

Afford, S.C., Humphreys, E.H., Reid, D.T., et al. (2014) Vascular cell adhesion molecule 1 expression by biliary epithelium promotes persistence of inflammation by inhibiting effector T-cell apoptosis. *Hepatology*, 59 (5): 1932–1943.

Aggarwal, S. and Pittenger, M.F. (2005) Human mesenchymal stem cells modulate allogeneic immune cell responses. *Blood*, 105: 1815–1822.

Alfaifi, M., Eom, Y.W., Newsome, P.N., et al. (2018) Mesenchymal stromal cell therapy for liver diseases. *Journal of hepatology*.

Almalki, S.G., Llamas Valle, Y. and Agrawal, D.K. (2017) MMP-2 and MMP-14 Silencing Inhibits VEGFR2 Cleavage and Induces the Differentiation of Porcine Adipose-Derived Mesenchymal Stem Cells to Endothelial Cells. *STEM CELLS Translational Medicine*, 6 (5): 1385–1398.

Alves, H., van Ginkel, J., Groen, N., et al. (2012) A Mesenchymal Stromal Cell Gene Signature for Donor Age Wagner, W. (ed.). *PLoS ONE*, 7 (8): e42908.

Amer, M.-E.M., El-Sayed, S.Z., El-Kheir, W.A., et al. (2011) Clinical and laboratory evaluation of patients with end-stage liver cell failure injected with bone marrow-derived hepatocyte-like cells. *European Journal of Gastroenterology & Hepatology*, 23 (10): 936–941.

Amin, M.A., Sabry, D., Rashed, L.A., et al. (2013) Short-term evaluation of autologous transplantation of bone marrow-derived mesenchymal stem cells in patients with cirrhosis: Egyptian study. *Clinical Transplantation*, 27 (4): 607–612.

Anderson, P., Souza-Moreira, L., Morell, M., et al. (2013) Adipose-derived mesenchymal stromal cells induce immunomodulatory macrophages which protect from experimental colitis and sepsis. *Gut*, 62: 1131–1141.

Anthony Armson, B., Allan, D.S. and Casper, R.F. (2015) Umbilical Cord Blood: Counselling, Collection, and Banking. *Journal of Obstetrics and Gynaecology Canada*, 37 (9): 832–844.

Antonucci, I., Stuppia, L., Kaneko, Y., et al. (2011) Amniotic fluid as a rich source of mesenchymal stromal cells for transplantation therapy. *Cell Transplantation*. 20 (6) pp. 789–795.

Arias, I.M., Alter, H.J., Boyer, J.L., et al. (2009) *The Liver: Biology and Pathobiology: Fifth Edition*.

Arnold, L., Henry, A., Poron, F., et al. (2007) Inflammatory monocytes recruited after skeletal muscle injury switch into antiinflammatory macrophages to support myogenesis. *The Journal of experimental medicine*, 204 (5): 1057–69.

Auletta, J.J., Eid, S.K., Wuttisarnwattana, P., et al. (2015) Human mesenchymal stromal cells attenuate graft-versus-host disease and maintain graft-versus-leukemia activity following experimental allogeneic bone marrow transplantation. *Stem cells (Dayton, Ohio)*, 33 (2): 601–14.

Baergen, R.N. (2013) Umbilical Cord Pathology. *Surgical Pathology Clinics*. 6 (1) pp. 61–85.

Bailey, S.M. and Cunningham, C.C. (2002) Contribution of mitochondria to oxidative stress associated with alcoholic liver disease. *Free radical biology & medicine*, 32 (1): 11–16.

Bajt, M.L., Knight, T.R., Farhood, A., et al. (2003) Scavenging peroxynitrite with glutathione promotes regeneration and enhances survival during acetaminophen-induced liver injury in mice. *The Journal of pharmacology and experimental therapeutics*, 307 (1): 67–73.

Baksh, D., Yao, R. and Tuan, R.S. (2007a) Comparison of Proliferative and Multilineage Differentiation Potential of Human Mesenchymal Stem Cells Derived from Umbilical Cord and Bone Marrow. *Stem Cells*, 25 (6): 1384–1392.

Baksh, D., Yao, R. and Tuan, R.S. (2007b) Comparison of Proliferative and Multilineage Differentiation Potential of Human Mesenchymal Stem Cells Derived from Umbilical Cord and Bone Marrow. *Stem Cells*, 25 (6): 1384–1392.

Bara, J.J., Richards, R.G., Alini, M., et al. (2014) Concise review: bone marrow-derived mesenchymal stem cells change phenotype following in vitro culture: implications for basic research and the clinic. *Stem cells (Dayton, Ohio)*, 32 (7): 1713–23.

De Bari, C., Dell'Accio, F., Tylzanowski, P., et al. (2001) Multipotent mesenchymal stem cells from adult human synovial membrane. *Arthritis and rheumatism*, 44 (8): 1928–42.

Basu, S. (2003) Carbon tetrachloride-induced lipid peroxidation: Eicosanoid formation and their regulation by antioxidant nutrients. *Toxicology*. 189 (1–2) pp. 113–127.

Battula, V.L., Treml, S., Bareiss, P.M., et al. (2009) Isolation of functionally distinct mesenchymal stem cell subsets using antibodies against CD56, CD271, and mesenchymal stem cell antigen-1. *Haematologica*, 94 (2).

Bensidhoum, M., Chapel, A., Francois, S., et al. (2004) Homing of in vitro expanded Stro-1- or Stro-1+ human mesenchymal stem cells into the NOD/SCID mouse and their role in supporting human CD34 cell engraftment. *Blood*, 103 (9): 3313–3319.

Bernal, W. and Wendon, J. (2013) Acute Liver Failure The Clinic a l Problem. *N Engl J Med*, 26369 (26): 2525–34.

Bernardo, M.E. and Fibbe, W.E. (2013) Cell Stem Cell Mesenchymal Stromal Cells: Sensors and Switchers of Inflammation. *Stem Cell*, 13: 392–402.

Beyth, S., Borovsky, Z., Mevorach, D., et al. (2005) Human mesenchymal stem cells alter antigen-presenting cell maturation and induce T-cell unresponsiveness. *Blood*, 105 (5): 2214–2219.

Bieback, K., Kern, S., Klüter, H., et al. (2004) Critical parameters for the isolation of mesenchymal stem cells from umbilical cord blood. *Stem cells*, 22 (4): 625–634.

Braet, F. and Wisse, E. (2002) Structural and functional aspects of liver sinusoidal endothelial cell fenestrae: A review. *Comparative Hepatology*. 1.

Braid, L.R., Wood, C.A., Wiese, D.M., et al. (2017) Intramuscular administration potentiates extended dwell time of mesenchymal stromal cells compared to other routes. *Cytotherapy*.

Briquet, A., Grégoire, C., Comblain, F., et al. (2014) Human bone marrow, umbilical cord or liver mesenchymal stromal cells fail to improve liver function in a model of CCl4-induced liver damage in NOD/SCID/IL-2R??(null) mice. *Cytotherapy*, 16 (11): 1511–1518.

Burra, P., Arcidiacono, D., Bizzaro, D., et al. (2012) Systemic administration of a novel human umbilical cord mesenchymal stem cells population accelerates the resolution of acute liver injury. *BMC Gastroenterology*, 12 (1): 88.

Buxbaum, J., Qian, P., Khuu, C., et al. (2006) Novel Model of Antigen-Specific Induction of Bile Duct Injury. *Gastroenterology*, 131 (6): 1899–1906.

Buyl, K., De Kock, J., Najar, M., et al. (2014) Characterization of hepatic markers in human Wharton's Jelly-derived mesenchymal stem cells. *Toxicology in Vitro*, 28 (1): 113–119.

Campard, D., Lysy, P.A., Najimi, M., et al. (2008) Native Umbilical Cord Matrix Stem Cells Express Hepatic Markers and Differentiate Into Hepatocyte-like Cells. *Gastroenterology*, 134 (3): 833–848.

Can, A. and Karahuseyinoglu, S. (2007) Concise Review: Human Umbilical Cord Stroma with Regard to the Source of Fetus-Derived Stem Cells. *Stem Cells*, 25 (11): 2886–2895.

Canosa, S., Moggio, A., Brossa, A., et al. (2017) Angiogenic properties of endometrial mesenchymal stromal cells in endothelial co-culture: an in vitro model of endometriosis Can endometrial mesenchymal stromal cells (E-MSCs) differentiate into endothelial cells in an in vitro co-culture sys- tem with hu. *Molecular Human Reproduction Advanced Access publication on*, 23 (3): 187–198.

Cao, H., Yang, J., Yu, J., et al. (2012) Therapeutic potential of transplanted placental mesenchymal stem cells in treating Chinese miniature pigs with acute liver failure. *BMC Medicine*, 10.

Chamberlain, G., Smith, H., Rainger, G.E., et al. (2011) Mesenchymal Stem Cells Exhibit Firm Adhesion, Crawling, Spreading and Transmigration across Aortic Endothelial Cells: Effects of Chemokines and Shear Pesce, M. (ed.). *PLoS ONE*, 6 (9): e25663.

Chambers, S.M., Shaw, C.A., Gatza, C., et al. (2007) Aging hematopoietic stem cells decline in function and exhibit epigenetic dysregulation. *PLoS biology*, 5 (8): e201.

Chao, Y.-H., Wu, H.-P., Wu, K.-H., et al. (2014) An Increase in CD3+CD4+CD25+ Regulatory T Cells after Administration of Umbilical Cord-Derived Mesenchymal Stem Cells during Sepsis Zimmer, J. (ed.). *PLoS ONE*, 9 (10): e110338.

Chen, E., Hermanson, S. and Ekker, S.C. (2004) Syndecan-2 is essential for angiogenic sprouting during zebrafish development. *Blood*, 103 (5): 1710–9.

Chen, K.-D., Huang, K.-T., Lin, C.-C., et al. (2016) MicroRNA-27b Enhances the Hepatic Regenerative Properties of Adipose-Derived Mesenchymal Stem Cells. *Citation: Molecular Therapy—Nucleic Acids*, 5.

Chen, L., Klass, C. and Woods, A. (2004) Syndecan-2 regulates transforming growth factor-beta signaling. *The Journal of biological chemistry*, 279 (16): 15715–8.

Chen, X., Wang, C., Yin, J., et al. (2015) Efficacy of Mesenchymal Stem Cell Therapy for Steroid-Refractory Acute Graft-Versus-Host Disease following Allogeneic Hematopoietic Stem Cell Transplantation: A Systematic Review and Meta-Analysis del Cañizo, M.C. (ed.). *PLOS ONE*, 10 (8): e0136991.

Chenette, D.M., Cadwallader, A.B., Antwine, T.L., et al. (2016) Targeted mRNA Decay by RNA Binding Protein AUF1 Regulates Adult Muscle Stem Cell Fate, Promoting Skeletal Muscle Integrity. *Cell Reports*,

16 (5): 1379–1390.

Christ, B., Brückner, S. and Winkler, S. (2015) The Therapeutic Promise of Mesenchymal Stem Cells for Liver Restoration. *Trends in Molecular Medicine*, 21: 673–686.

Chung, E. and Son, Y. (2014) Crosstalk between mesenchymal stem cells and macrophages in tissue repair. *Tissue Engineering and Regenerative Medicine*, 11 (6): 431–438.

Clasper, S. (1999) Inducible Expression of the Cell Surface Heparan Sulfate Proteoglycan Syndecan-2 (Fibroglycan) on Human Activated Macrophages Can Regulate Fibroblast Growth Factor Action. *Journal of Biological Chemistry*, 274 (34): 24113–24123.

Corcione, A., Benvenuto, F., Ferretti, E., et al. (2006a) Human mesenchymal stem cells modulate B-cell functions. *Blood*, 107 (1): 367–372.

Corcione, A., Benvenuto, F., Ferretti, E., et al. (2006b) Human mesenchymal stem cells modulate B-cell functions. *Blood*, 107.

Das, R., Jahr, H., Van Osch, G.J.V.M., et al. (2010) The Role of Hypoxia in Bone Marrow–Derived Mesenchymal Stem Cells: Considerations for Regenerative Medicine Approaches. *Tissue engineering*, 16.

Delorme, B., Ringe, J., Gallay, N., et al. (2008) *Specific plasma membrane protein phenotype of culture-amplified and native human bone marrow mesenchymal stem cells.* Blood, 111(5) 2631–2635.

Dennis, J.E., Carbillet, J.-P., Caplan, A.I., et al. (2002) The STRO-1+ marrow cell population is multipotential. *Cells, tissues, organs*, 170 (2–3): 73–82.

Derkow, K., Loddenkemper, C., Mintern, J., et al. (2007) Differential priming of CD8 and CD4 T-cells in animal models of autoimmune hepatitis and cholangitis. *Hepatology*, 46 (4): 1155–1165.

Ding, Y., Xu, D., Feng, G., et al. (2009) Mesenchymal stem cells prevent the rejection of fully allogenic islet grafts by the immunosuppressive activity of matrix metalloproteinase-2 and -9. *Diabetes*, 58 (8): 1797–1806.

Dominici, M., Le Blanc, K., Mueller, I., et al. (2006) Minimal criteria for defining multipotent mesenchymal stromal cells. The International Society for Cellular Therapy position statement. *Cytotherapy*, 8 (4): 315–7.

Dong, F., Patnaik, S., Duan, Z.H., et al. (2017) A Novel Role for CAMKK1 in the Regulation of the

Mesenchymal Stem Cell Secretome. *Stem Cells Translational Medicine*, 6 (9): 1759–1766.

Duijvestein, M., Wildenberg, M.E., Welling, M.M., et al. (2011) Pretreatment with interferon-?? enhances the therapeutic activity of mesenchymal stromal cells in animal models of colitis. *Stem Cells*, 29 (10): 1549–1558.

Eggenhofer, E., Benseler, V., Kroemer, A., et al. (2012) Mesenchymal stem cells are short-lived and do not migrate beyond the lungs after intravenous infusion. *Frontiers in Immunology*, 3 (9).

Eisenblätter, M., Ehrchen, J., Varga, G., et al. (2009) In vivo optical imaging of cellular inflammatory response in granuloma formation using fluorescence-labeled macrophages. *Journal of Nuclear Medicine*, 50: 1676–1682.

El-Ansary, M., Abdel-Aziz, I., Mogawer, S., et al. (2012) Phase II trial: undifferentiated versus differentiated autologous mesenchymal stem cells transplantation in Egyptian patients with HCV induced liver cirrhosis. *Stem Cell Rev*, 8 (3): 972–981.

Fang, J.W., Bird, G.L., Nakamura, T., et al. (1994) Hepatocyte proliferation as an indicator of outcome in acute alcoholic hepatitis. *Lancet (London, England)*, 343 (8901): 820–823.

Ferguson, V.L. and Dodson, R.B. (2009) Bioengineering aspects of the umbilical cord. *European Journal of Obstetrics Gynecology and Reproductive Biology*, 144 (SUPPL 1): 108–113.

Ferreira, L., Karp, J.M., Nobre, L., et al. (2008) New opportunities: the use of nanotechnologies to manipulate and track stem cells. *Cell stem cell*, 3 (2): 136–46.

Fiore, E.J., Bayo, J.M., Garcia, M.G., et al. (2015) Mesenchymal Stromal Cells Engineered to Produce IGF-I by Recombinant Adenovirus Ameliorate Liver Fibrosis in Mice. *stem cell and development*, 24 (6).

Forbes, S.J., Gupta, S. and Dhawan, A. (2015) *Cell therapy for liver disease: From liver transplantation to cell factory*. *Journal of hepatology*, 62(1):S157-S169.

Freyman, T., Polin, G., Osman, H., et al. (2006) A quantitative, randomized study evaluating three methods of mesenchymal stem cell delivery following myocardial infarction. *European Heart Journal*, 27 (9): 1114–1122.

Friedenstein, A.J., Petrakova, K. V, Kurolesova, A.I., et al. (1968) Heterotopic of bone marrow. Analysis of precursor cells for osteogenic and hematopoietic tissues. *Transplantation*, 6 (2): 230–247.

Fukuchi, Y., Nakajima, H., Sugiyama, D., et al. (2004) Human Placenta-Derived Cells Have Mesenchymal Stem/Progenitor Cell Potential. *Stem Cells*, 22 (5): 649–658.

Galleu, A., Riffo-Vasquez, Y., Trento, C., et al. (2017) Apoptosis in mesenchymal stromal cells induces in vivo recipient-mediated immunomodulation. *Science Translational Medicine*, 9 (416): 49–57.

Gao, J., Dennis, J.E., Muzic, R.F., et al. (2001) The dynamic in vivo distribution of bone marrow-derived mesenchymal stem cells after infusion. *Cells, tissues, organs*, 169 (1): 12–20.

Glennie, S., Soeiro, I., Dyson, P.J., et al. (2005) Bone marrow mesenchymal stem cells induce division arrest anergy of activated T cells. *Blood*, 105 (7): 2821–2827.

Gordillo, M., Evans, T. and Gouon-Evans, V. (2015) Orchestrating liver development. *Development*.

Gronthos, S., Zannettino, A.C.W., Hay, S.J., et al. (2003) Molecular and cellular characterisation of highly purified stromal stem cells derived from human bone marrow. *Journal of cell science*, 116 (9): 1827–1835.

Gu, W., Hong, X., Potter, C., et al. (2017) Mesenchymal stem cells and vascular regeneration. *Microcirculation*, 24 (1): 1–15.

Haldar, D., Henderson, N.C., Hirschfield, G., et al. (2016) Mesenchymal stromal cells and liver fibrosis: a complicated relationship. *The FASEB Journal*, 30 (12): 3905–3928.

Hamedi-Asl, P., Halabian, R., Bahmani, P., et al. (2012) Adenovirus-mediated expression of the HO-1 protein within MSCs decreased cytotoxicity and inhibited apoptosis induced by oxidative stresses. *Cell stress & chaperones*, 17 (2): 181–90.

Han, X., Yang, Q., Lin, L., et al. (2014) Interleukin-17 enhances immunosuppression by mesenchymal stem cells. *Cell Death and Differentiation*, 21 (11): 1758–1768.

He, S., Gleason, J., Fik-Rymarkiewicz, E., et al. (2017) Human Placenta-Derived Mesenchymal Stromal-Like Cells Enhance Angiogenesis via T Cell-Dependent Reprogramming of Macrophage Differentiation. *STEM CELLS*, 35 (6): 1603–1613.

He, Z., Hua, J., Qian, D., et al. (2016) Intravenous hMSCs Ameliorate Acute Pancreatitis in Mice via Secretion of Tumor Necrosis Factor-α Stimulated Gene/Protein 6. *Scientific Reports*, 6 (1): 38438.

Hiwase, S.D., Dyson, P.G., To, L.B., et al. (2009) Cotransplantation of placental mesenchymal stromal cells enhances single and double cord blood engraftment in nonobese diabetic/severe combined immune

deficient mice. *Stem Cells*, 27 (9): 2293–2300.

Honmou, O., Onodera, R., Sasaki, M., et al. (2012) Mesenchymal stem cells: therapeutic outlook for stroke. *Trends in molecular medicine*, 18 (5): 292–7.

Hoogduijn, M.J., Roemeling-van Rhijn, M., Engela, A.U., et al. (2013) Mesenchymal Stem Cells Induce an Inflammatory Response After Intravenous Infusion. *Stem Cells and Development*, 22 (21): 2825–2835.

Houlihan, D.D. and Newsome, P.N. (2008) Critical Review of Clinical Trials of Bone Marrow Stem Cells in Liver Disease. *Gastroenterology*, 135 (2): 438–450.

Hung, S.C., Pochampally, R.R., Hsu, S.C., et al. (2007) Short-term exposure of multipotent stromal cells to low oxygen increases their expression of CX3CR1 and CXCR4 and their engraftment in vivo. *PLoS ONE*, 2 (5).

Hur, K.Y., So, J.-S., Ruda, V., et al. (2012) IRE1α activation protects mice against acetaminophen-induced hepatotoxicity. *The Journal of Experimental Medicine*, 209 (2): 307–318.

Irie, J., Wu, Y., Wicker, L.S., et al. (2006) NOD.c3c4 congenic mice develop autoimmune biliary disease that serologically and pathogenetically models human primary biliary cirrhosis. *The Journal of experimental medicine*, 203 (5): 1209–19.

Ishige, I., Nagamura-Inoue, T., Honda, M.J., et al. (2009) Comparison of mesenchymal stem cells derived from arterial, venous, and Wharton's jelly explants of human umbilical cord. *International Journal of Hematology*, 90 (2): 261–269.

Ito, H., Hoshi, M., Ohtaki, H., et al. (2010) Ability of IDO to attenuate liver injury in alpha-galactosylceramide-induced hepatitis model. *Journal of immunology (Baltimore, Md. : 1950)*, 185 (8): 4554–60.

Itsumi, M., Inoue, S., Elia, A.J., et al. (2015) Idh1 protects murine hepatocytes from endotoxin-induced oxidative stress by regulating the intracellular NADP +/NADPH ratio. *Cell Death and Differentiation*, 22 (11): 1837–1848.

Iwakiri, Y., Grisham, M. and Shah, V. (2008) "Vascular biology and pathobiology of the liver: Report of a single-topic symposium." In *Hepatology*. 2008. pp. 1754–1763.

Janakat, S. and Al-Merie, H. (2002) Optimization of the dose and route of injection, and characterisation of the time course of carbon tetrachloride-induced hepatotoxicity in the rat. *Journal of Pharmacological*

and Toxicological Methods, 48 (1): 41–44.

Jang, Y.O., Kim, Y.J., Baik, S.K., et al. (2014) Histological improvement following administration of autologous bone marrow-derived mesenchymal stem cells for alcoholic cirrhosis: a pilot study. *Liver international : official journal of the International Association for the Study of the Liver*, 34 (1): 33–41.

Jeschke, M.G., Gauglitz, G.G., Phan, T.T., et al. (2011) Umbilical Cord Lining Membrane and Wharton's Jelly-Derived Mesenchymal Stem Cells: the Similarities and Differences. *The Open Tissue Engineering and Regenerative Medicine Journal*, 4: 21–27.

Ji, S.T., Kim, H., Yun, J., et al. (2017) Promising Therapeutic Strategies for Mesenchymal Stem Cell-Based Cardiovascular Regeneration: From Cell Priming to Tissue Engineering. *Stem cells international*, 2017: 3945403.

Jiang, D., Muschhammer, J., Qi, Y., et al. (2016) Suppression of Neutrophil-Mediated Tissue Damage-A Novel Skill of Mesenchymal Stem Cells. *Stem cells*, 34 (9): 2393–406.

Jin, H.J., Kwon, J.H., Kim, M., et al. (2016) Downregulation of Melanoma Cell Adhesion Molecule (MCAM/CD146) Accelerates Cellular Senescence in Human Umbilical Cord Blood-Derived Mesenchymal Stem Cells. *Stem cells translational medicine*, 5 (4): 427–39.

Ju, S., Teng, G.-J., Lu, H., et al. (2007) In vivo MR tracking of mesenchymal stem cells in rat liver after intrasplenic transplantation. *Radiology*, 245 (1): 206–15.

Karahuseyinoglu, S., Cinar, O., Kilic, E., et al. (2007) Biology of Stem Cells in Human Umbilical Cord Stroma: In Situ and In Vitro Surveys. *Stem Cells*, 25 (2): 319–331.

Karlmark, K.R., Weiskirchen, R., Zimmermann, H.W., et al. (2009) Hepatic recruitment of the inflammatory Gr1+ monocyte subset upon liver injury promotes hepatic fibrosis. *Hepatology*, 50 (1): 261–274.

Karlmark, K.R., Zimmermann, H.W., Roderburg, C., et al. (2010) The fractalkine receptor CX3CR1 protects against liver fibrosis by controlling differentiation and survival of infiltrating hepatic monocytes. *Hepatology*, 52 (5): 1769–1782.

Kehoe, O., Cartwright, A., Askari, A., et al. (2014) Intra-articular injection of mesenchymal stem cells leads to reduced inflammation and cartilage damage in murine antigen-induced arthritis. *Journal of translational medicine*, 12: 157.

Kellow, Z.S. and Feldstein, V.A. (2011) Ultrasound of the placenta and umbilical cord: A review. *Ultrasound Quarterly*. 27 (3) pp. 187–197.

Khan, R.A., Khan, M.R. and Sahreen, S. (2012) CCl4-induced hepatotoxicity: protective effect of rutin on p53, CYP2E1 and the antioxidative status in rat. *BMC complementary and alternative medicine*, 12: 178.

Kharaziha, P., Hellström, P.M., Noorinayer, B., et al. (2009) Improvement of liver function in liver cirrhosis patients after autologous mesenchymal stem cell injection: a phase I–II clinical trial. *European Journal of Gastroenterology & Hepatology*, 21 (10): 1199–1205.

Kim, C.W., Goldberger, O.A., Gallo, R.L., et al. (1994) Members of the Syndecan Family of Heparan Sulfate Proteoglycans Are Expressed in Distinct Cell-, Tissue-, and Development-specific Patterns. *Molecular Biology of the Cell*, 5: 797–805.

Klyushnenkova, E., Mosca, J.D., Zernetkina, V., et al. (2005) T cell responses to allogeneic human mesenchymal stem cells: Immunogenicity, tolerance, and suppression. *Journal of Biomedical Science*, 12 (1): 47–57.

Knockaert, L., Berson, A., Ribault, C., et al. (2012) Carbon tetrachloride-mediated lipid peroxidation induces early mitochondrial alterations in mouse liver. *Laboratory Investigation*, 92 (3): 396–410.

Kovalovich, K., Deangelis, R.A., Li, W., et al. (2000) Increased toxin-induced liver injury and fibrosis in interleukin-6- deficient mice. *Hepatology*, 31 (1): 149–159.

Kuo, T.K., Hung, S., Chuang, C., et al. (2008) Stem Cell Therapy for Liver Disease: Parameters Governing the Success of Using Bone Marrow Mesenchymal Stem Cells. *Gastroenterology*, 134 (7): 2111–2121.

Kusuma, G.D., Carthew, J., Lim, R., et al. (2017) *Effect of the Microenvironment on Mesenchymal Stem Cell Paracrine Signaling: Opportunities to Engineer the Therapeutic Effect*. Stem cells and development, 26(9): 617-631.

Lanthier, N., Lin-Marq, N., Rubbia-Brandt, L., et al. (2017) Autologous bone marrow-derived cell transplantation in decompensated alcoholic liver disease: what is the impact on liver histology and gene expression patterns? *Stem Cell Research & Therapy*, 8 (1): 88.

Latifi-pupovci, H., Kuçi, Z., Wehner, S., et al. (2015) In vitro migration and proliferation (" wound healing ") potential of mesenchymal stromal cells generated from human CD271 + bone marrow mononuclear cells. *Journal of Translational Medicine*, 13: 315–324.

Lawrence, T. and Natoli, G. (2011) Transcriptional regulation of macrophage polarization: enabling diversity with identity. *Nature Reviews Immunology*, 11 (11): 750–761.

Lee, K.-C., Lin, H.-C., Huang, Y.-H., et al. (2015) *Allo-transplantation of mesenchymal stem cells attenuates hepatic injury through IL1Ra dependent macrophage switch in a mouse model of liver disease. Journal of hepatology*, 36(6):1405-1412.

Lee, O.K., Kuo, T.K., Chen, W.-M., et al. (2004) Isolation of multipotent mesenchymal stem cells from umbilical cord blood. *Blood*, 103 (5): 1669–75.

Lee, P.-H., Tu, C.-T., Hsiao, C.-C., et al. (2016) Antifibrotic Activity of Human Placental Amnion Membrane-Derived CD34+ Mesenchymal Stem/Progenitor Cell Transplantation in Mice With Thioacetamide-Induced Liver Injury. *Stem cells translational medicine*, 5 (11): 1473–1484.

Lee, R.H., Pulin, A.A., Seo, M.J., et al. (2009) Intravenous hMSCs Improve Myocardial Infarction in Mice because Cells Embolized in Lung Are Activated to Secrete the Anti-inflammatory Protein TSG-6. *Cell Stem Cell*, 5 (1): 54–63.

LI, C.D., ZHANG, W.Y., LI, H.L., et al. (2005) Mesenchymal stem cells derived from human placenta suppress allogeneic umbilical cord blood lymphocyte proliferation. *Cell Research*, 15 (7): 539–547.

Li, S., Tan, H.-Y., Wang, N., et al. (2015) The Role of Oxidative Stress and Antioxidants in Liver Diseases. *International journal of molecular sciences*, 16 (11): 26087–124.

Li, W., Ren, G., Huang, Y., et al. (2012) Mesenchymal stem cells: A double-edged sword in regulating immune responses. *Cell Death and Differentiation*, 19 (9): 1505–1513.

Lin, B., Chen, J., Qiu, W., et al. (2017) Allogeneic Bone Marrow-Derived Mesenchymal Stromal Cells for HBV-Related Acute-on-Chronic Liver Failure: A Randomized Controlled Trial. *Hepatology*, 17 (3): 127–128.

Linero, I. and Chaparro, O. (2014) Paracrine Effect of Mesenchymal Stem Cells Derived from Human Adipose Tissue in Bone Regeneration Camussi, G. (ed.). *PLoS ONE*, 9 (9): e107001.

Liu, Y., Meyer, C., Xu, C., et al. (2013) Animal models of chronic liver diseases. *AJP: Gastrointestinal and Liver Physiology*, 304 (5): G449–G468.

Luster, A.D., Alon, R. and von Andrian, U.H. (2005) Immune cell migration in inflammation: Present and future therapeutic targets. *Nature Immunology*. 6 (12) pp. 1182–1190.

Luz-Crawford, P., Kurte, M., Bravo-Alegría, J., et al. (2013) Mesenchymal stem cells generate a CD4+CD25+Foxp3+ regulatory T cell population during the differentiation process of Th1 and Th17 cells. *Stem cell research & therapy*, 4 (3): 65.

Ma, H.C., Shi, X.L., Ren, H.Z., et al. (2014) Targeted migration of mesenchymal stem cells modified with CXCR4 to acute failing liver improves liver regeneration. *World Journal of Gastroenterology*, 20 (40): 14884–14894.

Mantena, S.K., King, A.L., Andringa, K.K., et al. (2008) Mitochondrial dysfunction and oxidative stress in the pathogenesis of alcohol- and obesity-induced fatty liver diseases. *Free radical biology & medicine*, 44 (7): 1259–72.

Mattar, P. and Bieback, K. (2015) Comparing the immunomodulatory properties of bone marrow, adipose tissue, and birth-associated tissue mesenchymal stromal cells. *Frontiers in Immunology*, 6 (NOV): 1–8.

Matthay, M.A., Pati, S. and Lee, J.-W. (2017) Concise Review: Mesenchymal Stem (Stromal) Cells: Biology and Preclinical Evidence for Therapeutic Potential for Organ Dysfunction Following Trauma or Sepsis. *STEM CELLS*, 35 (2): 316–324.

Mehal, W.Z. and Friedman, S.L. (2007) "The Role of Inflammation and Immunity in the Pathogenesis of Liver Fibrosis." In *Liver Immunology*. Totowa, NJ: Humana Press. pp. 111–121.

Meisel, R., Zibert, A., Laryea, M., et al. (2004) Human bone marrow stromal cells inhibit allogeneic T-cell responses by indoleamine 2,3-dioxygenase-mediated tryptophan degradation. *Blood*, 103 (12): 4619–4621.

Melief, S.M., Schrama, E., Brugman, M.H., et al. (2013) Multipotent stromal cells induce human regulatory T cells through a novel pathway involving skewing of monocytes toward anti-inflammatory macrophages. *Stem Cells*, 31 (9): 1980–1991.

Melief, S.M., Zwaginga, J.J., Fibbe, W.E., et al. (2013) Adipose tissue-derived multipotent stromal cells have a higher immunomodulatory capacity than their bone marrow-derived counterparts. *Stem cells translational medicine*, 2 (6): 455–63.

Meng, F., Rui, Y., Xu, L., et al. (2014) *Aqp1 Enhances Migration of Bone Marrow Mesenchymal Stem Cells Through Regulation of FAK and b-Catenin. Stem cells and development*,23(1): 66-75.

Miki, T., Lehmann, T., Cai, H., et al. (2005) Stem cell characteristics of amniotic epithelial cells. *Stem cells*, 23 (10): 1549–59.

Milosavljevic, N., Gazdic, M., Markovic, B.S., et al. (2017) Mesenchymal stem cells attenuate acute liver injury by altering ratio between IL-17 producing and regulatory NKT cells. *Liver Transplantation*, (4): 1040–1050.

Mitchell, C., Robin, M.A., Mayeuf, A., et al. (2009) Protection against hepatocyte mitochondrial dysfunction delays fibrosis progression in mice. *American Journal of Pathology*, 175 (5): 1929–1937.

Modrowski, D., Orosco, A., Thévenard, J., et al. (2005) *Syndecan-2 overexpression induces osteosarcoma cell apoptosis: Implication of syndecan-2 cytoplasmic domain and JNK signaling. Bone*, 37(2): 180-189.

Mohamadnejad, M., Alimoghaddam, K., Bagheri, M., et al. (2013) Randomized placebo-controlled trial of mesenchymal stem cell transplantation in decompensated cirrhosis. *Liver international : official journal of the International Association for the Study of the Liver*, 33 (10): 1490–6.

Mohamadnejad, M., Alimoghaddam, K., Mohyeddin-Bonab, M., et al. (2007) Phase 1 trial of autologous bone marrow mesenchymal stem cell transplantation in patients with decompensated liver cirrhosis. *Archives of Iranian Medicine*, 10 (4): 459–466.

Mohyeldin, A., Garzón-Muvdi, T. and Quiñones-Hinojosa, A. (2010) Oxygen in stem cell biology: A critical component of the stem cell niche. *Cell Stem Cell*, 7 (2): 150–161.

Muller-Borer, B.J., Collins, M.C., Gunst, P.R., et al. (2007) Quantum dot labeling of mesenchymal stem cells. *Journal of Nanobiotechnology*, 5: 9.

Mylotte, L.A., Duffy, A.M., Murphy, M., et al. (2008) Metabolic Flexibility Permits Mesenchymal Stem Cell Survival in an Ischemic Environment. *Stem Cells*, 26 (5): 1325–1336.

Najar, M., Raicevic, G., Boufker, H.I., et al. (2010) Mesenchymal stromal cells use PGE2 to modulate activation and proliferation of lymphocyte subsets: Combined comparison of adipose tissue, Whartonâ€™s Jelly and bone marrow sources. *Cellular Immunology*, 264: 171–179.

Najar, M., Raicevic, G., Jebbawi, F., et al. (2012) Characterization and functionality of the CD200–CD200R system during mesenchymal stromal cell interactions with T-lymphocytes. *Immunology Letters*, 146: 50–56.

Nanaev, A.K., Kohnen, G., Milovanov, A.P., et al. (1997) Stromal differentiation and architecture of the human umbilical cord. *Placenta*, 18 (1): 53–64.

Nasir, G.A., Mohsin, S., Khan, M., et al. (2013) Mesenchymal stem cells and Interleukin-6 attenuate liver fibrosis in mice. *Journal of translational medicine*, 11: 78.

Nassir, F. and Ibdah, J.A. (2014) Role of mitochondria in alcoholic liver disease. *World Journal of Gastroenterology*, 20 (9): 2136–2142.

Nauta, A.J. and Fibbe, W.E. (2007) Immunomodulatory properties of mesenchymal stromal cells. *Blood*, 110 (10): 3499-3506.

Nicola, M. Di, Carlo-Stella, C., Magni, M., et al. (2002) Human bone marrow stromal cells suppress T-lymphocyte proliferation induced by cellular or nonspecific mitogenic stimuli. *Blood*, 99 (10): 3838–3843.

Nitzsche, F., Müller, C., Lukomska, B., et al. (2017) Concise Review: MSC Adhesion Cascade—Insights into Homing and Transendothelial Migration. *Stem Cells*, 35 (6): 1446–1460.

Noguchi, T., Kuo-Lan Fong, Lai, E.K., et al. (1982) Specificity of a phenobarbital-induced cytochrome P-450 for metabolism of carbon tetrachloride to the trichloromethyl radical. *Biochemical Pharmacology*, 31 (5): 615–624.

Novobrantseva, T.I., Majeau, G.R., Amatucci, A., et al. (2005) Attenuated liver fibrosis in the absence of B cells. *The Journal of clinical investigation*, 115 (11): 3072–82.

Ogata, Y., Mabuchi, Y., Yoshida, M., et al. (2015) Purified Human Synovium Mesenchymal Stem Cells as a Good Resource for Cartilage Regeneration Wagner, W. (ed.). *PLOS ONE*, 10 (6): e0129096.

Omori, Y., Honmou, O., Harada, K., et al. (2008) Optimization of a therapeutic protocol for intravenous injection of human mesenchymal stem cells after cerebral ischemia in adult rats. *Brain Research*, 1236: 30–38.

Ortiz, L.A., Gambelli, F., McBride, C., et al. (2003) Mesenchymal stem cell engraftment in lung is enhanced in response to bleomycin exposure and ameliorates its fibrotic effects. *Proceedings of the National Academy of Sciences*, 100 (14): 8407–8411.

Packer, J.E., Slater, T.F. and Willson, R.L. (1978) Reactions of the carbon tetrachloride-related peroxy free radical (CCl3O2.) with amino acids : Pulse radiolysis evidence. *Life Sciences*, 23 (26): 2617–2620.

Park, J.S., Suryaprakash, S., Lao, Y.-H., et al. (2015) Engineering mesenchymal stem cells for regenerative medicine and drug delivery. *Methods*, 84: 3–16.

Peng, L., Xie, D., Lin, B.-L., et al. (2011) Autologous bone marrow mesenchymal stem cell transplantation in liver failure patients caused by hepatitis B: short-term and long-term outcomes. *Hepatology*, 54 (3): 820–8.

Pietilä, M., Lehtonen, S., Tuovinen, E., et al. (2012) CD200 Positive Human Mesenchymal Stem Cells Suppress TNF-Alpha Secretion from CD200 Receptor Positive Macrophage-Like Cells Panepucci, R.A. (ed.). *PLoS ONE*, 7 (2): e31671.

Polchert, D., Sobinsky, J., Douglas, G., et al. (2008) IFN-gamma activation of mesenchymal stem cells for treatment and prevention of graft versus host disease. *European journal of immunology*, 38 (6): 1745–55.

Poli, G. (2000) Pathogenesis of liver fibrosis: role of oxidative stress. *Molecular aspects of medicine*, 21 (3): 49–98.

Van Poll, D., Parekkadan, B., Cho, C.H., et al. (2008) Mesenchymal stem cell-derived molecules directly modulate hepatocellular death and regeneration in vitro and in vivo. *Hepatology*, 47 (5): 1634–1643.

Possamai, L.A., Thursz, M.R., Wendon, J.A., et al. (2014) Modulation of monocyte/macrophage function: a therapeutic strategy in the treatment of acute liver failure. *Journal of hepatology*, 61 (2): 439–45.

Pourgholaminejad, A., Aghdami, N., Baharvand, H., et al. (2016) The effect of pro-inflammatory cytokines on immunophenotype, differentiation capacity and immunomodulatory functions of human mesenchymal stem cells. *Cytokine*, 83: 51–60.

Prevosto, C., Zancolli, M., Canevali, P., et al. (2007) Generation of CD4+ or CD8+ regulatory T cells upon mesenchymal stem cell-lymphocyte interaction. *Haematologica*, 92 (7): 881–888.

Pritchard, W.R. (2016) *Biodistribution and Clearance of Human Mesenchymal Stem Cells by Quantitative Three-Dimensional Cryo-Imaging After Intravenous Infusion in a Rat Lung Injury Model*., pp. 75–86.

Promotes, H., Stromal, M.B. and Formation, T. (2003) Hypoxia Promotes Murine Bone-Marrow-Derived Stromal Cell Migration and Tube Formation. *Stem Cell*, 21 (3): 337–347.

Racanelli, V. and Rehermann, B. (2006) The liver as an immunological organ. *Hepatology*. 43 (1).

Rahman, T.M. and Hodgson, H.J. (2000) Animal models of acute hepatic failure. *International journal of experimental pathology*, 81 (2): 145–57.

Rak-Raszewska, A., Marcello, M., Kenny, S., et al. (2012) Quantum dots do not affect the behaviour of

mouse embryonic stem cells and kidney stem cells and are suitable for short-term tracking Linden, R. (ed.). *PLoS ONE*, 7 (3): e32650.

Ramasamy, R., Tong, C.K., Seow, H.F., et al. (2008) The immunosuppressive effects of human bone marrow-derived mesenchymal stem cells target T cell proliferation but not its effector function. *Cellular Immunology*, 251: 131–136.

Ranganath, S.H., Levy, O., Inamdar, M.S., et al. (2012) Harnessing the mesenchymal stem cell secretome for the treatment of cardiovascular disease. *Cell stem cell*, 10 (3): 244–58.

Rasmusson, I., Le Blanc, K., Sundberg, B., et al. (2007) Mesenchymal stem cells stimulate antibody secretion in human B cells. *Scandinavian Journal of Immunology*, 65 (4): 336–343.

Redondo-Castro, E., Cunningham, C., Miller, J., et al. (2017) Interleukin-1 primes human mesenchymal stem cells towards an anti-inflammatory and pro-trophic phenotype in vitro. *Stem cell research & therapy*, 8 (1): 79.

Ren, G., Roberts, A.I. and Shi, Y. (2011) Adhesion molecules: key players in Mesenchymal stem cell-mediated immunosuppression. *Cell adhesion & migration*, 5 (1): 20–2.

Ren, G., Zhang, L., Zhao, X., et al. (2008) Mesenchymal stem cell-mediated immunosuppression occurs via concerted action of chemokines and nitric oxide. *Cell stem cell*, 2 (2): 141–50.

Ren, G., Zhao, X., Zhang, L., et al. (2010) Inflammatory cytokine-induced intercellular adhesion molecule-1 and vascular cell adhesion molecule-1 in mesenchymal stem cells are critical for immunosuppression. *Journal of immunology*, 184 (5): 2321–8.

Rivera, P., Pastor, A., Arrabal, S., et al. (2017) Acetaminophen-Induced Liver Injury Alters the Acyl Ethanolamine-Based Anti-Inflammatory Signaling System in Liver. *Frontiers in Pharmacology*, 8: 705.

Robinson, M.W., Harmon, C. and O 'farrelly, C. (2016) Liver immunology and its role in inflammation and homeostasis. *Cellular & Molecular Immunology*, 13 (10): 267–276.

Rosova, I., Dao, M., Capoccia, B., et al. (2008) Hypoxic Preconditioning Results in Increased Motility and Improved Therapeutic Potential of Human Mesenchymal Stem Cells. *Stem Cells*, 26 (8): 2173–2182.

Rovira-Clavé, X., Angulo-Ibáñez, M., Noguer, O., et al. (2012) Syndecan-2 can promote clearance of T-cell receptor/CD3 from the cell surface. *Immunology*, 137 (3): 214–25.

Roy, D., Steyer, G.J., Gargesha, M., et al. (2009) 3D cryo-imaging: a very high-resolution view of the

whole mouse. *Anatomical record (Hoboken, N.J. : 2007)*, 292 (3): 342–51.

Sah, S.K., Park, K.H., Yun, C.-O., et al. (2016) Effects of Human Mesenchymal Stem Cells Transduced with Superoxide Dismutase on Imiquimod-Induced Psoriasis-Like Skin Inflammation in Mice. *Antioxidants & Redox Signaling*, 24 (5): 233–248.

Saiman, Y. and Friedman, S.L. (2012) The role of chemokines in acute liver injury. *Frontiers in Physiology*, 3 JUN (June): 1–12.

Salama, H., Zekri, A.R.N., Medhat, E., et al. (2014) Peripheral vein infusion of autologous mesenchymal stem cells in Egyptian HCV-positive patients with end-stage liver disease. *Stem Cell Research and Therapy*, 5 (3).

Sarugaser, R., Lickorish, D., Baksh, D., et al. (2005) Human Umbilical Cord Perivascular (HUCPV) Cells: A Source of Mesenchymal Progenitors. *Stem Cells*, 23 (2): 220–229. doi:10.1634/stemcells.2004-0166.

Sato, K., Ozaki, K., Oh, I., et al. (2007) *Nitric oxide plays a critical role in suppression of T-cell proliferation by mesenchymal stem cells.*, 109: 228–234.

Schioppa, T., Uranchimeg, B., Saccani, A., et al. (2003) Regulation of the chemokine receptor CXCR4 by hypoxia. *The Journal of experimental medicine*, 198 (9): 1391–402.

Schmuck, E.G., Koch, J.M., Centanni, J.M., et al. (2016) Biodistribution and Clearance of Human Mesenchymal Stem Cells by Quantitative Three-Dimensional Cryo-Imaging After Intravenous Infusion in a Rat Lung Injury Model. *STEM CELLS Translational Medicine*, 5 (12): 1668–1675.

Secco, M., Zucconi, E., Vieira, N.M., et al. (2008) Multipotent stem cells from umbilical cord: cord is richer than blood! *Stem cells (Dayton, Ohio)*, 26 (1): 146–50.

Sherman, S.E., Kuljanin, M., Cooper, T.T., et al. (2017) High Aldehyde Dehydrogenase Activity Identifies a Subset of Human Mesenchymal Stromal Cells with Vascular Regenerative Potential. *Stem Cells*, 35 (6): 1542–1553.

Shi, J., Aisaki, K., Ikawa, Y., et al. (1998) Evidence of hepatocyte apoptosis in rat liver after the administration of carbon tetrachloride. *The American journal of pathology*, 153 (2): 515–25.

Shi, J., Aisaki, K., Ikawa, Y., et al. (1998) Evidence of hepatocyte apoptosis in rat liver after the administration of carbon tetrachloride. *The American journal of pathology*, 153 (2): 515–25.

Shi, M., Zhang, Z., Xu, R., et al. (2012) Human Mesenchymal Stem Cell Transfusion Is Safe and Improves

Liver Function in Acute-on-Chronic Liver Failure Patients. *STEM CELLS Translational Medicine*, 1 (10): 725–731.

Shi, Y., Su, J., Roberts, A.I., et al. (2012) How mesenchymal stem cells interact with tissue immune responses. *Trends in Immunology*. 33 (3) pp. 136–143.

Shi, Y., Su, J., Roberts, A.I., et al. (2012) How mesenchymal stem cells interact with tissue immune responses. *Trends in immunology*, 33 (3): 136–43.

Shiels, M.S., Chernyavskiy, P., Anderson, W.F., et al. (2017) Trends in premature mortality in the USA by sex, race, and ethnicity from 1999 to 2014: an analysis of death certificate data. *The Lancet*, 389: 1043–1054.

Shimizu, I., Shimamoto, N., Saiki, K., et al. (2012) "Lipid Peroxidation in Hepatic Fibrosis." In *Lipid Peroxidation*.

Shuai, Z., Leung, M.W., He, X., et al. (2016) Adaptive immunity in the liver. *Cellular & molecular immunology*, 13 (3): 354–68.

Sivanathan, K.N., Rojas-Canales, D.M., Hope, C.M., et al. (2015) Interleukin-17A-Induced Human Mesenchymal Stem Cells Are Superior Modulators of Immunological Function. *Stem Cells*, 33 (9): 2850–2863.

Slater1, T.F., Cheeseman1, K.H. and Ingold, K.U. (1985) Carbon Tetrachloride Toxicity as a Model for Studying Free-Radical Mediated Liver Injury. *Philosophical Transactions of the Royal Society of London. Series B, Biological Sciences Philosophical Transactions of the Royal Society of London. Series B Phil. Trans. R. Soc. Lond. B*, 3111881287 (311): 633–645.

Sobrevals, L., Enguita, M., Quiroga, J., et al. (2016) Insulin-Like Growth Factor I (IGF-I) Expressed from an AAV1 Vector Leads to a Complete Reversion of Liver Cirrhosis in Rats Glorioso, J.C. (ed.). *PLOS ONE*, 11 (9): e0162955.

Sotiropoulou, P.A., Perez, S.A., Gritzapis, A.D., et al. (2006) Interactions Between Human Mesenchymal Stem Cells and Natural Killer Cells. *Stem Cells*, 24 (1): 74–85.

Suk, K.T., Yoon, J.-H., Kim, M.Y., et al. (2016) Transplantation with autologous bone marrow-derived mesenchymal stem cells for alcoholic cirrhosis: Phase 2 trial. *Hepatology*, 64 (6): 2185–2197.

Suto, E.G., Mabuchi, Y., Suzuki, N., et al. (2017) *Prospectively isolated mesenchymal stem/stromal cells*

are enriched in the CD73 + population and exhibit efficacy after transplantation., (May): 1–10.

Szabo, G. and Petrasek, J. (2015) Inflammasome activation and function in liver disease. *Nature Reviews Gastroenterology & Hepatology*, 12 (7): 387–400.

Tacke, F. and Zimmermann, H.W. (2014) Macrophage heterogeneity in liver injury and fibrosis. *Journal of hepatology*, 60 (5): 1090–6.

Talele, N.P., Fradette, J., Davies, J.E., et al. (2015) Stem Cell Reports Expression of a-Smooth Muscle Actin Determines the Fate of Mesenchymal Stromal Cells. *Stem Cell Reports*, 4: 1016–1030.

Taub, R. (2004) Liver regeneration: from myth to mechanism. *Nature Reviews Molecular Cell Biology*, 5 (10): 836–847.

Teixé, T., Nieto-Blanco, P., Vilella, R., et al. (2008) Syndecan-2 and -4 expressed on activated primary human CD4+ lymphocytes can regulate T cell activation. *Molecular Immunology*, 45 (10): 2905–2919.

Tilg, H., Kaser, A. and Moschen, A.R. (2006) How to modulate inflammatory cytokines in liver diseases. *Liver International*, 26 (9): 1029–1039.

Tipnis, S., Viswanathan, C. and Majumdar, A.S. (2010) Immunosuppressive properties of human umbilical cord-derived mesenchymal stem cells: role of B7-H1 and IDO. *Immunology and cell biology*, 88 (8): 795–806.

Troyer, D.L. and Weiss, M.L. (2008) Concise Review: Wharton's Jelly-Derived Cells Are a Primitive Stromal Cell Population. *Stem Cells*, 26 (3): 591–599.

Tsai, C.-C., Su, P.-F., Huang, Y.-F., et al. (2012) Oct4 and Nanog Directly Regulate Dnmt1 to Maintain Self-Renewal and Undifferentiated State in Mesenchymal Stem Cells. *Molecular Cell*, 47: 169–182.

Tsang, W.P., Shu, Y., Kwok, P.L., et al. (2013) CD146+ Human Umbilical Cord Perivascular Cells Maintain Stemness under Hypoxia and as a Cell Source for Skeletal Regeneration. *PLoS ONE*, 8 (10).

Tsubokawa, T., Yagi, K., Nakanishi, C., et al. (2010) Impact of anti-apoptotic and anti-oxidative effects of bone marrow mesenchymal stem cells with transient overexpression of heme oxygenase-1 on myocardial ischemia. *American journal of physiology. Heart and circulatory physiology*, 298 (5): H1320-9.

Tuñón, M.-J., Alvarez, M., Culebras, J.-M., et al. (2009) An overview of animal models for investigating the pathogenesis and therapeutic strategies in acute hepatic failure. *World journal of gastroenterology*, 15

(25): 3086–98.

Uccelli, A., Moretta, L. and Pistoia, V. (2008) Mesenchymal stem cells in health and disease. *Nat Rev Immunol*, 8 (9): 726–736.

Ulrich, C., Abruzzese, T., Maerz, J.K., et al. (2015) Human Placenta-Derived CD146-Positive Mesenchymal Stromal Cells Display a Distinct Osteogenic Differentiation Potential. *Stem Cells and Development*, 24 (13): 1558–1569.

Varin, A., Pontikoglou, C., Labat, E., et al. (2013) CD200R/CD200 Inhibits Osteoclastogenesis: New Mechanism of Osteoclast Control by Mesenchymal Stem Cells in Human Ivanovic, Z. (ed.). *PLoS ONE*, 8 (8): e72831.

van Velthoven, C.T., Kavelaars, A. and Heijnen, C.J. (2012) Mesenchymal stem cells as a treatment for neonatal ischemic brain damage. *Pediatric ReseaRch*, 71 (4).

Volarevic, V., Nurkovic, J., Arsenijevic, N., et al. (2014) Concise Review: Therapeutic Potential of Mesenchymal Stem Cells for the Treatment of Acute Liver Failure and Cirrhosis. *STEM CELLS*, 32 (11): 2818–2823.

Wang, K., Zhang, T., Dong, Q., et al. (2013) Redox homeostasis: the linchpin in stem cell self-renewal and differentiation. *Cell death & disease*, 4 (3): e537.

Wang, K.H., Kao, A.P., Chang, C.C., et al. (2015) Upregulation of Nanog and Sox-2 genes following ectopic expression of Oct-4 in amniotic fluid mesenchymal stem cells. *Biotechnology and Applied Biochemistry*, 62 (5): 591–597.

Wang, L., Han, Q., Chen, H., et al. (2014) Allogeneic Bone Marrow Mesenchymal Stem Cell Transplantation in Patients with UDCA-Resistant Primary Biliary Cirrhosis. *Stem Cells and Development*, 23 (20): 2482–2489.

Wang, L., Li, J., Liu, H., et al. (2013) A pilot study of umbilical cord-derived mesenchymal stem cell transfusion in patients with primary biliary cirrhosis. *Journal of Gastroenterology and Hepatology*, 28: 85–92.

Wehr, A., Baeck, C., Heymann, F., et al. (2013) Chemokine Receptor CXCR6-Dependent Hepatic NK T Cell Accumulation Promotes Inflammation and Liver Fibrosis. *The Journal of Immunology*, 190 (10): 5226–5236.

Wei, N., Yu, S.P., Gu, X., et al. (2013) Delayed intranasal delivery of hypoxic-preconditioned bone marrow mesenchymal stem cells enhanced cell homing and therapeutic benefits after ischemic stroke in mice. *Cell Transplantation*, 22 (6): 977–991.

Weiss, M.L., Anderson, C., Medicetty, S., et al. (2008) Immune Properties of Human Umbilical Cord Wharton's Jelly-Derived Cells. *Stem Cells*, 26 (11): 2865–2874.

Weiss, M.L., Medicetty, S., Bledsoe, A.R., et al. (2006) Human Umbilical Cord Matrix Stem Cells: Preliminary Characterization and Effect of Transplantation in a Rodent Model of Parkinson's Disease. *Stem Cells*, 24 (3): 781–792.

Williams, R., Alexander, G., Aspinall, R., et al. (2017) Health Policy New metrics for the Lancet Standing Commission on Liver Disease in the UK Executive summary. *The Lancet*, 389: 2053–2080.

Wilson, J.J., Foyle, K., Foeng, J., et al. (2018) Redirecting adult mesenchymal stromal cells to the brain: a new approach for treating CNS autoimmunity and neuroinflammation? *Immunology & Cell Biology*.

de Witte, S.F.H., Franquesa, M., Baan, C.C., et al. (2015) Toward Development of iMesenchymal Stem Cells for Immunomodulatory Therapy. *Frontiers in immunology*, 6: 648.

de Witte, S.F.H., Luk, F., Sierra Parraga, J.M., et al. (2018) Immunomodulation By Therapeutic Mesenchymal Stromal Cells (MSC) Is Triggered Through Phagocytosis of MSC By Monocytic Cells. *Stem Cells*.

De Witte, S.F.H., Merino, A.M., Franquesa, M., et al. (2017) Cytokine treatment optimises the immunotherapeutic effects of umbilical cord-derived MSC for treatment of inflammatory liver disease. *Stem Cell Research & Therapy*, 8.

Wu, G.D., Nolta, J.A., Jin, Y.-S., et al. (2003) Migration of mesenchymal stem cells to heart allografts during chronic rejection. *Transplantation*, 75 (5): 679–685.

Wu, J., Sun, Z., Sun, H.S., et al. (2008) Intravenously administered bone marrow cells migrate to damaged brain tissue and improve neural function in ischemic rats. *Cell Transplantation*, 16 (10): 993–1005.

Xie, C., Yang, Z., Suo, Y., et al. (2017) Systemically Infused Mesenchymal Stem Cells Show Different Homing Profiles in Healthy and Tumor Mouse Models. *STEM CELLS Translational Medicine*, 6 (4): 1120–1131.

Xingwei, P., Zhang, Y.-N., Lie, P.-C., et al. (2009) Differentiation of mesenchymal stromal cells derived

from umbilical cord Wharton's jelly into hepatocyte-like cells. *Cytotherapy*, 11 (5): 548–558.

Yañez, R., Lamana, M.L., García-Castro, J., et al. (2006) Adipose tissue-derived mesenchymal stem cells have in vivo immunosuppressive properties applicable for the control of the graft-versus-host disease. *Stem cells (Dayton, Ohio)*, 24 (11): 2582–91.

Yang, J.-X., Zhang, N., Wang, H.-W., et al. (2015) CXCR4 receptor overexpression in mesenchymal stem cells facilitates treatment of acute lung injury in rats. *The Journal of biological chemistry*, 290 (4): 1994–2006.

Yang, M.C., Chang, C.P. and Lei, H.Y. (2010) Endothelial cells are damaged by autophagic induction before hepatocytes in Con A-induced acute hepatitis. *International Immunology*, 22 (8): 661–670.

Yu, J., Yin, S., Zhang, W., et al. (2013) Hypoxia preconditioned bone marrow mesenchymal stem cells promote liver regeneration in a rat massive hepatectomy model. *Stem Cell Research and Therapy*, 4 (4).

Yu, Y., Liao, L., Shao, B., et al. (2017) Knockdown of MicroRNA Let-7a Improves the Functionality of Bone Marrow-Derived Mesenchymal Stem Cells in Immunotherapy. *Molecular Therapy*, 25 (2): 480–493.

Zagoura, D.S., Roubelakis, M.G., Bitsika, V., et al. (2012) Therapeutic potential of a distinct population of human amniotic fluid mesenchymal stem cells and their secreted molecules in mice with acute hepatic failure. *Gut*, 61 (6): 894–906..

Zahedi, K., Barone, S.L., Xu, J., et al. (2012) *Hepatocyte-specific ablation of spermine/spermidine-N 1 -acetyltransferase gene reduces the severity of CCl 4 -induced acute liver injury*. *Am J Physiol Gastrointest Liver Physio.*

Zeng, W., Xiao, J., Zheng, G., et al. (2015) Antioxidant treatment enhances human mesenchymal stem cell anti-stress ability and therapeutic efficacy in an acute liver failure model. *Scientific reports*, 5: 11100.

Zhang, J., Lingling Hou, B., Xiaoyan Wu, B., et al. (2016) Inhibitory effect of genetically engineered mesenchymal stem cells with Apoptin on hepatoma cells in vitro and in vivo. *Molecular and Cellular Biochemistry*, 416: 193-203.

Zhang, S., Chen, L., Liu, T., et al. (2012) Human umbilical cord matrix stem cells efficiently rescue acute liver failure through paracrine effects rather than hepatic differentiation. *Tissue engineering. Part A*, 18 (13–14): 1352–64.

Zhang, T., Li, X.-H., Zhang, D.-B., et al. (2017) *Repression of COUP-TFI Improves Bone Marrow- Derived*

Mesenchymal Stem Cell Differentiation into Insulin-Producing Cells. 8: 220-231.

Zhang, X., Huang, W., Chen, X., et al. (2017) CXCR5-Overexpressing Mesenchymal Stromal Cells Exhibit Enhanced Homing and Can Decrease Contact Hypersensitivity. *Molecular Therapy*, 25 (6): 1434–1447.

Zhang, Z., Lin, H., Shi, M., et al. (2012) Human umbilical cord mesenchymal stem cells improve liver function and ascites in decompensated liver cirrhosis patients. *Journal of Gastroenterology and Hepatology (Australia)*, 27 (2): 112–120.

Zhang, Z. and Wang, F.-S. (2013) Stem cell therapies for liver failures and cirrhosis. *Journal of Hepatology*, 59: 183–185.

Zhu, X., He, B., Zhou, X., et al. (2013) Effects of transplanted bone-marrow-derived mesenchymal stem cells in animal models of acute hepatitis. *Cell and Tissue Research*, 351 (3): 477–486.

Zuk, P. a, Zhu, M., Mizuno, H., et al. (2001) Multilineage cells from human adipose tissue: implications for cell-based therapies. *Tissue engineering*, 7 (2): 211–228.